Fraunhofer-Institut für Zelltherapie
und Immunologie, Institutsteil
Bioanalytik und Bioprozesse IZI-BB

Identification and Functional Characterization of Aptamers Targeting Human Urokinase and NDM-1 for Therapeutic and Diagnostic Applications

Nico Dreymann

Kumulative Dissertation

zur Erlangung des akademischen Grades
"doctor rerum naturalium"
(Dr. rer. nat.)
in der Wissenschaftsdisziplin Molekularbiologie

eingereicht an der
Mathematisch-Naturwissenschaftlichen Fakultät
Institut für Biochemie und Biologie
der Universität Potsdam

angefertigt am
Fraunhofer-Institut für Zelltherapie und Immunologie (IZI)
Institutsteil Bioanalytik und Bioprozesse (IZI-BB),
Potsdam-Golm

Potsdam,
April 2023

This work is protected by copyright and/or related rights. You are free to use this work in any way that is permitted by the copyright and related rights legislation that applies to your use. For other uses you need to obtain permission from the rights-holder(s).
https://rightsstatements.org/page/InC/1.0/?language=en

Erstgutachterin: Prof. Dr. Katja Arndt
Institut für Biochemie und Biologie
Universität Potsdam
Karl-Liebknecht-Straße 24-25
14476 Potsdam

Zweitgutachterin: Prof. Dr. Katja Hanack
Institut für Biochemie und Biologie
Universität Potsdam
Karl-Liebknecht-Straße 24-25
14476 Potsdam

Drittgutachterin: Prof. Dr. Susanne Füssel
Klinik und Poliklinik für Urologie
Universitätsklinikum Carl Gustav Carus Dresden
Fetscherstraße 74
01307 Dresden

Mitglieder der Prüfungskommission:

Prof. Dr. Elke Dittmann (Vorsitz)
Prof. Dr. Ria Baumgrass
Prof. Dr. Frank Bier

Ort und Tag der Disputation: Potsdam, 28.09.2023

Published online on the
Publication Server of the University of Potsdam:
https://doi.org/10.25932/publishup-61291
https://nbn-resolving.org/urn:nbn:de:kobv:517-opus4-612919

Acknowledgement

I would like to express my sincere gratitude to all the people who accompanied and supported me during the course of my doctoral thesis. First, I would like to thank Dr. Marcus Menger for the opportunity to conduct my doctoral thesis in his research group at the Fraunhofer IZI-BB. Thank you for the confidence in my work, the freedom in the design of my research, the insights beyond my dissertation, and for always having an open door.

I would like to thank Prof. Dr. Katja Arndt for the supervision from university side, the discussion about my work and the review of my thesis. At the same time, I would like to thank Prof. Dr. Katja Hanack and Prof. Dr. Susanne Füssel for the willingness to review my thesis. Many thanks to Prof. Dr. Elke Dittmann for being the chair of the examination committee, and to Prof. Dr. Ria Baumgrass and Prof. Dr. Frank Bier for being a part of my examination board.

A big thank you goes to Julia Wünsche for her work in the selection of the uPA aptamers, which made it possible to revive this project and to Dr. Dana Vu Van and Prof. Dr. Susanne Füssel for their work in the evaluation of potential biomarkers.

I am dearly grateful to Wiebke Sabrowski for the great teamwork, the joyful days in the lab, the discussion about experimental designs, proofreading papers, emails, and everything else. And last but not least, for the friendship that has developed outside the working context, for an always open ear and for keeping my head up at every time. My sincere thanks go to Anja Möller and Denise Czepluch for the introduction to almost all methods used in our laboratory, for helping me out with scientific questions and for the performance of SPR and NGS experiments. Thanks to my current and former colleagues, especially to Felix Pfisterer and Tobias Gerling, who lightened up every workday and made it fun with silly conversations during the lunch breaks. Thank you to Jennifer Danso for her support in the sandwich assay evaluation and SELEX against other targets as part of her internship and bachelor thesis.

And last but not least, a big thank you to my family and friends. To my parents, my sister and my grandma for their support during this time and as always. To my girlfriend for her support and especially for bearing with me during this time and during the last weeks of preparing my thesis. And to my friends for their support with an always cold beer in hand. Here’s to more cool times and awesome evenings.

Summary

Aptamers are single-stranded DNA (ssDNA) or RNA molecules that can bind specifically and with high affinity to target molecules due to their unique three-dimensional structure. For this reason, they are often compared to antibodies and sometimes even referred to as “chemical antibodies”. They are simple and inexpensive to synthesize, easy to modify, and smaller than conventional antibodies. Enzymes, especially hydrolases, are interesting targets in this context. This class of enzymes is capable of hydrolytically cleaving various macromolecules such as proteins, as well as smaller molecules such as antibiotics. Hence, they play an important role in many biological processes including diseases and their treatment. Hydrolase detection as well as the understanding of their function is therefore of great importance for diagnostics and therapy. Due to their various desirable features compared to antibodies, aptamers are being discussed as alternative agents for analytical and diagnostic use in various applications. The use of aptamers in therapy is also frequently investigated, as the binding of aptamers can have effects on the catalytic activity, protein-protein interactions, or proteolytic cascades. Aptamers are generated by an *in vitro* selection process. Potential aptamer candidates are selected from a pool of enriched nucleic acid sequences with affinity to the target, and their binding affinity and specificity is investigated. This is one of the most important steps in aptamer generation to obtain specific aptamers with high affinity for use in analytical and diagnostic applications. The binding properties or binding domains and their effects on enzyme functions form the basis for therapeutic applications.

In this work, the binding properties of DNA aptamers against two different hydrolases were investigated. In view of their potential utility for analytical methods, aptamers against human urokinase (uPA) and New Delhi metallo-β-lactamase-1 (NDM-1) were evaluated for their binding affinity and specificity using different methods. Using the uPA aptamers, a protocol for measuring the binding kinetics of an aptamer-protein-interaction by surface plasmon resonance spectroscopy (SPR) was developed. Based on the increased expression of uPA in different types of cancer, uPA is discussed as a prognostic and diagnostic tumor marker. As uPA aptamers showed different binding sites on the protein, microtiter plate-based aptamer sandwich assay systems for the detection of uPA were developed. Because of the function of urokinase in cancer cell proliferation and metastasis, uPA is also discussed as a therapeutic target. In this regard, the different binding sites of aptamers showed different effects on uPA function. *In vitro* experiments demonstrated both inhibition of uPA binding to its receptor as well as the inhibition of uPA catalytic activity for different aptamers. Thus, in addition to their specificity and affinity for their targets, the utility of the aptamers for potential diagnostic and therapeutic applications was demonstrated. First, as an alternative inhibitor of human urokinase for therapeutic purposes, and second, as valuable recognition molecules for

the detection of urokinase, as a prognostic and diagnostic marker for cancer, and for NDM-1 to detect resistance to carbapenem antibiotics.

Zusammenfassung

Aptamere sind einzelsträngige DNA- oder RNA-Moleküle, die aufgrund ihrer charakteristischen dreidimensionalen Struktur spezifisch und mit hoher Affinität an Zielmoleküle binden. Häufig werden sie mit Antikörpern verglichen und als „chemische Antikörper“ bezeichnet. Sie sind einfach und kostengünstig zu synthetisieren, leicht zu modifizieren und kleiner als herkömmliche Antikörper. Enzyme, insbesondere Hydrolasen, sind hierbei unter anderem interessante Zielmoleküle. Diese Klasse von Enzymen ist in der Lage verschiedene Makromoleküle wie z.B. Proteine, aber auch kleinere Moleküle, wie z.B. Antibiotika, hydrolytisch zu spalten. Sie spielen in vielen biologischen Prozessen und somit auch in Erkrankungen und deren Behandlung eine wichtige Rolle. Daher ist ihre Detektion, sowie das Verständnis ihrer Funktion für die Diagnostik und Therapie von hoher Bedeutung. Durch ihre Vorteile gegenüber Antikörpern werden Aptamere als Alternativen für den analytischen und diagnostischen Einsatz in verschiedenen Applikationen diskutiert. Der Einsatz von Aptameren in der Therapie wird ebenfalls häufig untersucht, da die Bindung der Aptamere Auswirkungen auf die katalytische Aktivität, Protein-Protein-Interaktionen oder proteolytische Kaskaden haben kann. Aptamere werden mittels *in vitro* Selektion generiert. Aus einem Pool angereicherter Nukleinsäuren mit Affinität zum Zielmolekül werden anschließend potentielle Aptamerkandidaten identifiziert und ihre Bindung zum Zielmolekül untersucht. Dies ist einer der wichtigsten Schritte in der Aptamergenerierung, um spezifische Aptamere mit hoher Affinität für den späteren Einsatz in analytischen und diagnostischen Applikationen zu erhalten. Die Bindungseigenschaften einschließlich der Bindedomänen und deren Auswirkungen auf die Funktion des Zielmoleküls stellen die Grundlage für spätere therapeutische Anwendungen dar.

In dieser Arbeit wurden die Bindungseigenschaften von DNA Aptameren gegen zwei verschiedene Hydrolasen untersucht. Für den potentiellen Nutzen in analytischen Methoden wurden Aptamere gegen die humane Urokinase (uPA), sowie gegen die New-Delhi metallo-β-lactamase-1 (NDM-1) mittels molekularbiologischer Methoden auf deren Bindungsaffinität und Spezifität untersucht. Anhand der uPA-Aptamere wurde ein Protokoll für die Messung der Bindungskinetik einer Aptamer-Protein-Bindung mittels Oberflächenplasmonenresonanz Spektroskopie (SPR) entwickelt. Durch die erhöhte Expression von uPA in vielen Krebserkrankungen, wird dieser als prognostischer und diagnostischer Tumormarker diskutiert. Die in dieser Arbeit untersuchten Aptamere gegen die Urokinase zeigten unterschiedliche Bindestellen, wodurch Aptamer-basierte Sandwich Assay Systeme auf Mikrotiterplattenbasis für die Detektion von uPA etabliert werden konnten. Durch die Funktion der Urokinase in der Zellproliferation und Metastasierung in Krebserkrankungen wird uPA ebenfalls als therapeutisches Zielprotein diskutiert. Hierbei zeigten die unterschiedlichen

Bindestellen der Aptamere verschiedene Auswirkungen auf die Funktion von uPA. Mittels *in vitro* Experimenten konnte die Inhibierung der Bindung von uPA zu ihrem Rezeptor, sowie die Inhibierung der katalytischen Aktivität von uPA mit Hilfe verschiedener Aptamere nachgewiesen werden. Somit wurde für die Aptamere, neben ihrer Spezifität und Affinität zu ihren Zielmolekülen, der Nutzen für potentielle diagnostische und therapeutische Anwendungen gezeigt. Zum einen als alternativer Inhibitor der Urokinase für therapeutische Zwecke, als auch als wertvolle Erkennungsmoleküle für den Nachweis von Urokinase, als prognostischer und diagnostischer Marker für Krebserkrankungen, sowie für NDM-1, zum Nachweis der Resistenz gegen Carbapenem-Antibiotika.

List of Abbreviations

aa	Amino acids
ASCO	American Society of Clinical Oncology
ATF	Amino-terminal fragment
BLI	Bio-layer interferometry
BSA	Bovine serum albumin
CD	Circular dichroism
DNA	Deoxyribonucleic acid
ds DNA	Double stranded DNA
EDTA	Ethylenediaminetetraacetic acid
ELISA	Enzyme-linked immunosorbent assay
EMSA	Electrophoretic mobility shift assay
FLAA	Fluorescent-dye linked aptamer assay
GFD	Growth factor domain
HMW-uPA	High molecular weight uPA
HRP	Horseradish peroxidase
IC_{50}	Half maximal inhibitory concentration
ITC	Isothermal titration calorimetry
k_a	Association rate
KD	Kringle domain
K_D	Dissociation constant
k_d	Dissociation rate
LFD	Lateral flow device
LMW-uPA	Low molecular weight uPA
LNA	Locked nucleic acid
LOD	Limit of detection
LOQ	Limit of quantification
MST	MicroScale thermophoresis
NDM-1	New-Delhi metallo-β-lactamase 1
NGS	Next generation sequencing
NMR	Nuclear magnetic resonance
nt	Nucleotides
Oxa-23	Oxacilinase 23
PAGE	Polyacrylamide gel electrophoresis
PAI-1	Plasminogen activator inhibitor-1
PAI-2	Plasminogen activator inhibitor-2

PCR	Polymerase chain reaction
PLAU	Gene name of urokinase-type plasminogen activator
pro-uPA	Zymogen of urokinase-type plasminogen activator
RNA	Ribonucleic acid
RT-	Reverse transcription
RU	Response unit
SA-beads	Streptavidin coated magnetic beads
SDS	Sodium dodecyl sulfate
SELEX	Systematic Evolution of Ligands by EXponential enrichment
SPD	Serine protease domain
SPR	Surface plasmon resonance
ssDNA	Single stranded DNA
TMB	3,3’,5,5’-Tetramethylbenzidin
tPA	Tissue-type plasminogen activator
uPA	Urokinase-type plasminogen activator (active two-chain enzyme)
uPAR	Urokinase-type plasminogen activator receptor
VEGF	Vascular endothelial growth factor
VEGFR 1/2	Vascular endothelial growth factor receptor 1/2
WHO	World Health Organization

Table of Contents

Acknowledgement I
Summary II
Zusammenfassung IV
List of Abbreviations VI
Table of Contents VIII

1. Preface 1
2. General Introduction 2
   2.1 Nucleic Acid Aptamers 2
   2.2 Aptamer Generation Process 3
   2.3 Aptamer Characterization 5
      2.3.1 Surface Plasmon Resonance Spectroscopy – the Gold Standard in Kinetic Characterization 6
      2.3.2 Microscale Thermophoresis – an Immobilization-free Approach in Binding Characterization 7
   2.4 Aptamers in Therapy 8
      2.4.1 Urokinase-type Plasminogen Activator – a Serine Protease with Therapeutic and Diagnostic Potential 10
   2.5 Aptamers as Recognition Molecules in Immunoassays 12
      2.5.1 Urokinase-type Plasminogen Activator as a Tumor Marker in Cancer 14
      2.5.2 New-Delhi Metallo-β-Lactamase 1 as an Antibiotic Resistance Marker 16
   2.6 Aim of the work 17
3. Results 18
   3.1 Manuscript I 18
   3.2 Manuscript II 41
   3.3 Manuscript III 55
   3.4 Manuscript IV 73
4. General Discussion 85
   4.1 Aptamer Characterization for Identification of Aptamers with Therapeutic and Diagnostic Potential 87
   4.2 Use of Aptamers Targeting uPA for Therapeutic Purposes in Cancer 90
   4.3 Use of Aptamers in Immunoassays for Detection of uPA 93
   4.4 Conclusion and Outlook 95
5. Literature 97

6. List of Figures 107
7. Eidesstattliche Erklärung 108
8. Appendix 109
8.1 Supplementary Information to Manuscript III 109
8.2 Supplementary Information to Manuscript IV 112
8.3 Parameters of the SELEX for HMW-uPA 120
8.4 Parameters of the SELEX for LMW-uPA 121
8.5 Overview of the Different Sandwich Assay Combinations for Detection of HMW- and/or LMW-uPA 122
8.6 Individual Author Contributions to the Publications 125
8.7 Patent Descriptions 127
8.7.1 DNA Aptamers and their use in (pre)diagnosis of cancer 127
8.7.2 DNA aptamers inhibiting binding of Urokinase type plasminogen activator (uPA) with Urokinase type plasminogen activator receptor (uPAR) and inhibiting uPA activity 129

1. Preface

Since their discovery, research on aptamers has increased strongly over the last decades. Due to their high specificity and affinity for their targets, they are comparable to antibodies and can be used in a variety of applications. The ease of synthesis and modification makes aptamers attractive alternatives as recognition elements for basic research analysis, diagnostic applications, and as effective agents for therapeutic approaches. My doctoral thesis focuses on the identification and characterization of aptamers targeting enzymes and on the evaluation for their use as analytical or therapeutic agents. In this context, characterization of binding properties is a prerequisite for their use in these areas, and determination of binding affinities and specificities is essential to identify highly affine and specific aptamers with potential effects on target function.

This cumulative thesis comprises three different peer-reviewed research articles, which are published in international scientific journals and one book chapter published in the series “Methods in Molecular Biology”. They deal with the identification and characterization of binding properties of aptamers targeting human urokinase (uPA) (manuscript I) and New-Delhi metallo-β-lactamase-1 (manuscript IV). Urokinase aptamers were additionally evaluated in *in vitro* experiments for their therapeutic value (manuscript I) and their use in analytical assays for diagnostic approaches whereby an aptamer-based sandwich assay for detection of uPA was developed (manuscript III). The book chapter describes in a detailed protocol how kinetic parameters of an aptamer-protein interaction can be measured using surface plasmon resonance spectroscopy (manuscript II). To underline my own input to each manuscript, a declaration of my individual contribution is given in each results section. The general introduction provides an overview of the different topics that are part of my work with further background information for a deeper scientific understanding and outlines the aims of this thesis. The discussion connects and highlights the results of all manuscripts with critical considerations on the methods used in these studies, the use of the aptamers for diagnostic or therapeutic purposes, a comparison with already known aptamers and an outlook on further perspectives.

2. General Introduction

2.1 Nucleic Acid Aptamers

Aptamers are synthetic single-stranded oligonucleotides (ssDNA, RNA, or nucleic acids with other chemistries) that can bind to specific target molecules due to their unique three-dimensional structure (Ellington and Szostak 1990). They were first discovered in 1990 by Craig Tuerk and Larry Gold who described RNA ligands to a bacteriophage T4 DNA polymerase (Tuerk and Gold 1990). Independently and very shortly after, Andrew D. Ellington and Jack W. Szostak described an *in vitro* selection of RNA molecules that bind small organic dyes (Ellington and Szostak 1990). Since then, a variety of several thousand aptamers have been generated and described in the literature. The target molecules of aptamers range from metal ions such as Cu^{2+}, Pb^{2+}, Zn^{2+} and As^{2+} (Guo et al. 2021), small molecules as for example the hormones 17β-estradiol and cortisol or antibiotics like kanamycin A or streptomycin (Pfeiffer and Mayer 2016), peptides and proteins (Tabarzad and Jafari 2016), viruses (Sánchez-Báscones et al. 2021) and even whole organisms like bacteria (Trunzo and Hong 2020) or protozoan parasites (Ospina-Villa et al. 2018). Aptamers - named from the Latin "aptus", meaning "to fit" and the Greek “meros”, meaning "the part" (Ellington and Szostak 1990) – usually consist of 20–100 nucleotides (Röthlisberger and Hollenstein 2018) and are sometimes even referred to as “chemical antibodies” because of their comparable binding properties to antibodies (Shigdar et al. 2013). Their unique secondary and tertiary structures are influenced by certain conditions such as ionic strength, ph and temperature. Upon formation of their structure, they are able to bind their targets specifically and with high affinity, similar to the key-and-lock principle by forming specific binding pockets (Hianik 2018). Structural motifs of aptamers such as hairpins, stem-loops, helix-duplexes, and G-quadruplexes (Chan et al. 2022; Gelinas et al. 2016) play an important role in the binding and stability of aptamers (Nagatoishi et al. 2011). Aptamers bind to their targets via hydrogen bonding, electrostatic interactions, the hydrophobic effect, π-π stacking, van der Waals forces, or a combination of these binding forces (Cai et al. 2018). Compared to antibodies, aptamers have desirable properties, such as easy generation, simple and cost-effective chemical synthesis, low batch-to-batch variability, reversible folding properties, small size and low immunogenicity (Dunn et al. 2017). Therefore, they are suitable for use as tools in a variety of applications, like in diagnostics, in environmental and food analysis, in biosensors (so-called aptasensors), in bio-imaging, or even as therapeutic agents (Song et al. 2012).

2.2 Aptamer Generation Process

Aptamers are selected by the Systematic Evolution of Ligands by EXponential enrichment (SELEX) technology (Ellington and Szostak 1990). In this iterative *in vitro* selection process a chemically produced random oligonucleotide library consisting of approximately 10^{13} - 10^{15} different nucleotide sequences is screened for affinity to the specific target (Klug and Famulok 1994). The oligonucleotide library usually consists of a central random region of about 20-80 nucleotides (nt) flanked by constant regions of about 18-21 nt that function as primer binding sites for PCR amplification (Stoltenburg et al. 2007). The *in vitro* selection is followed by amplification of binding sequences (Stoltenburg et al. 2007). The initial random ssDNA- or RNA-library is incubated with the target and binding sequences are separated from unbound or weakly bound oligonucleotides. In the case of proteins as target molecules, it can be useful to immobilize them on a solid matrix material for an effective separation of bound and unbound sequences. For example, magnetic beads can serve as a matrix material. They can be functionalized to bind proteins directly via various coupling chemistries. For an indirect binding, streptavidin coated magnetic beads (SA-beads) can be used for binding of biotinylated targets, as they are easy to handle and require only a small amount of target (Darmostuk et al. 2015; Stoltenburg et al. 2005).

After separation, target-bound sequences can be eluted from the target for example by heat, high salt solutions like urea, ethylenediaminetetraacetic acid (EDTA), detergents like sodium dodecyl sulfate (SDS) or a combination of those (Niazi et al. 2008; Stoltenburg et al. 2005). Afterwards, the DNA or RNA is precipitated and amplified by PCR (in case of DNA-SELEX) or reverse transcription (RT-) PCR (in case of RNA-SELEX). To obtain a new pool of single-stranded oligonucleotides, the double-stranded DNA (dsDNA) produced by PCR is separated into ssDNA (DNA-SELEX) or, to obtain RNA, an *in vitro* transcription followed by purification is performed (RNA-SELEX). Separation of dsDNA into ssDNA can be performed, for example, by exonuclease digestion of the antisense strand (Null et al. 2000), alkaline denaturation (Wochner et al. 2007), asymmetric PCR, biotin-streptavidin separation or size separation using denaturing urea PAGE (Marimuthu et al. 2012). The enriched pool of single-stranded oligonucleotides then serves as the pool of oligonucleotides for incubation with the target in the next selection round (Stoltenburg et al. 2007). Depending on the target and the respective SELEX strategy, the conditions are adjusted individually in each selection round in order to increase the stringency over the course of the selection. This can be achieved by changing the incubation time, the incubation volume or the number of washing steps, or by using lower amounts of the target molecule in later selection rounds (Marshall and Ellington 2000). A schematic illustration of the SELEX process using a ssDNA library and a target molecule immobilized on magnetic beads is represented in Figure 1.

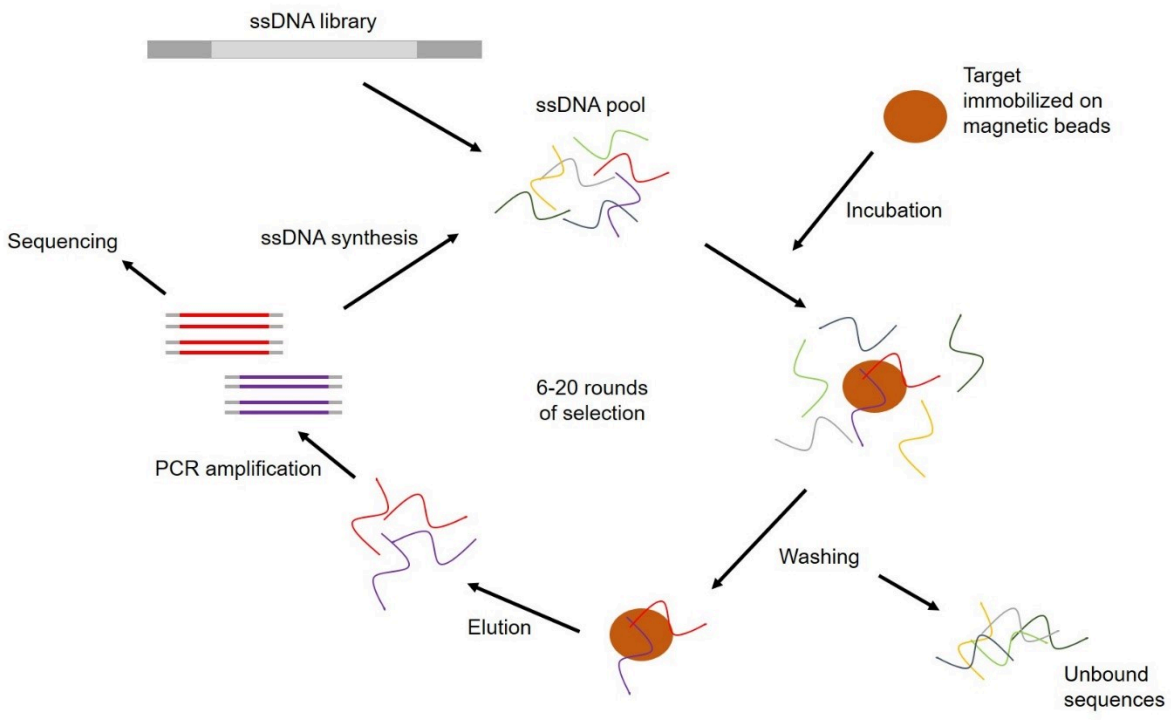

Figure 1: Schematic illustration of the SELEX process with a ssDNA library. SELEX starts with a highly diverse ssDNA library, which is incubated with the target that can be immobilized on magnetic beads. Non-binding sequences are washed away and binding sequences are eluted and amplified by PCR. SsDNA is synthesized from the PCR product, to obtain a new pool of enriched oligonucleotides that can be used for the next selection round. After approximately 6-20 selection rounds, a preferably enriched nucleic acid pool with affinity to the target molecule can be sequenced by NGS.

Several SELEX adjustments can be used over the course of selection (Stoltenburg et al. 2007). The most commonly used modifications are the introduction of negative-selection and counter-selection steps. These preselection steps are introduced to remove unwanted oligonucleotides from the pool and to increase the specificity of selected aptamer candidates. For negative-selection steps, incubation with the selection matrix is introduced to remove unwanted matrix binding sequences. In case of counter-selection, incubation with target-related structures or proteins is used to remove sequences that bind target molecules with similar structures and thus cannot distinguish them from related structures (Zhuo et al. 2017). Mostly, 6-20 selection cycles are required for the selection of target-specific and affine aptamer candidates (Stoltenburg et al. 2007). The number of selection cycles depends on many factors, such as the nature of the target and its isoelectric point (pI), target composition and concentration, the ratio of target to oligonucleotides, selection conditions, and efficiency of the partitioning method of bound and unbound sequences (Stoltenburg et al. 2007).

In the best case, enrichment of binding sequences occurs at the end of a SELEX so that sequence analysis can be performed. Whereas in the past the PCR product was cloned to obtain individual aptamer clones, which were then sequenced by Sanger sequencing, nowadays the enriched pool can be sequenced by next generation sequencing (NGS) (Schütze et al. 2011). NGS data show the number of enriched sequences in the oligonucleotide pool and sequences can be selected for specific characterization. NGS can also show the enrichment of specific sequences over the course of the SELEX by sequencing all or part of the selection rounds. Other methods like real-time PCR, fluorescent labeling of the nucleic acid pool or melting curve analysis can also be used to observe the progression over the course of the SELEX (Mencin et al. 2014). After sequencing, selected oligonucleotide sequences can be used to synthesize aptamer candidates in order to test their binding and to characterize their binding properties.

2.3 Aptamer Characterization

In view of their further application, a step of major importance is to characterize the binding properties of the selected and potential aptamer candidates. Various biochemical and biophysical methods can be used to investigate the binding properties of aptamers to their related targets. These methods can be used to detect binding to the target qualitatively and to quantify the aptamers binding affinity and specificity. Here, determination of basic binding parameters like binding affinity and kinetics of the aptamer-target binding are of particular importance to find the best kinetics depending on the field of application and to determine the interaction strength between the aptamer and its target.

After aptamer selection, potential aptamer candidates are screened for binding to the target molecule. Methods that can be used for suitable detection of binding differ depending on the nature of the target molecule. In the case of macromolecules like proteins as targets, an electrophoretic mobility shift assay (EMSA) or a fluorescent-dye linked aptamer assay (FLAA) can be appropriate to test the different aptamer candidates for target binding in a simple, rapid and inexpensive manner. In an EMSA, a mixture of the target protein and the aptamer candidate is subjected to gel electrophoresis under native conditions through a polyacrylamide gel (Hellman and Fried 2007). Afterwards, the gel is stained with a nucleic acid intercalating fluorescent dye (e.g. ethidium bromide) and samples are visualized under UV-light. Because free nucleic acid migrates faster than a protein-nucleic acid complex, a no-target-control (the aptamer alone) is compared to the mixture of the aptamer candidate and its target protein. If band shifting is detected in the gel, aptamers-target binding is indicated (Hellman and Fried 2007). EMSA is a label- and immobilization-free method for qualitative

detection of target binding in a cost-effective way. Another fast-screening approach of potential aptamer candidates is the FLAA. Here, the target is immobilized on the surface of a microtiter plate. Wells without immobilized target are used as no-target-controls. Aptamer candidates are incubated with the immobilized target and the no-target-control wells. Subsequently, wells are washed and incubated with a fluorescent dye that intercalates into the ssDNA or RNA and fluorescence signals can be measured (Wochner and Glökler 2007).

The signal strength in EMSA and FLAA usually serves as a reference as to which aptamers show affinity and specificity to their related target and can therefore be considered for further characterization. In this context, biophysical methods, such as surface plasmon resonance spectroscopy (SPR), microscale thermophoresis (MST), isothermal titration calorimetry (ITC), bio-layer interferometry (BLI) or SwitchSENSE® technology can be used to determine the non-covalent molecular interaction between the aptamer and its target and to quantify the kinetic parameters (like association [k_a] and dissociation rate [k_d]) or the dissociation constant (K_D) of a binding event (Plach and Schubert 2020). Dissociation constants for the aptamers characterized in this work were determined label-free by SPR and immobilization-free by MST.

2.3.1 Surface Plasmon Resonance Spectroscopy – the Gold Standard in Kinetic Characterization

Surface plasmon resonance spectroscopy serves as the gold standard to characterize non-covalent molecular interaction in real-time without the need of labels. Surface plasmon resonance describes the biophysical phenomenon when a photon of polarized light strikes a metal surface. At a specific angle of incidence, light energy is transferred to the electrons on the metal layer of a sensor surface. These electrons – so called plasmons – are excited and then move parallel to the metal surface in a longitudinal electronic oscillation (Wing Fen and Mahmood Mat Yunus 2013). This causes the intensity of the reflected light to be reduced at a specific angle, which is the so-called SPR-angle. A change in the refractive index near the sensor surface due to molecules binding to the sensor surface results in a change in the SPR angle. This change in SPR angle is directly proportional to mass concentration of the material which is bound to the sensor surface. The change of the SPR angle can then be plotted in real-time in a sensogram with the SPR response given in response units (RU) over time whereas one RU corresponds to an angle shift of 10^{-4} degrees (Nguyen et al. 2015). This indicates approximately 1 pg of protein per mm^2 on a Biacore™ CM5 biosensor chip. For SPR measurements, one binding partner is immobilized on the surface of a biosensor chip (the ligand) while the other interacting partner is injected with a continuous flow and concentration over the sensor surface (the analyte). If the analyte binds to the immobilized ligand, the

refractive index at the sensor surface increases, resulting in a change of SPR angle and a SPR-response is recorded as the association rate (k_a). After injection of the analyte, running buffer flows over the sensor surface of the biosensor chip which allows monitoring of the dissociation of the analyte from the ligand in real-time (dissociation rate, k_d). Several optical biosensors use this phenomenon to define binding parameters of molecular interaction. One well-known optical biosensor is the Biacore™ SPR technology which was used in this work for determination of kinetic parameters.

One important parameter of binding events is the equilibrium dissociation constant (K_D). The K_D is used to assess the binding affinity and strength of a molecular interaction. The determination of association and dissociation rate constants between analyte A and ligand B using the 1:1 Langmuir binding model is given as follows:

$$A + B \underset{k_d}{\overset{k_a}{\rightleftarrows}} AB \tag{1}$$

Where: k_a is the association rate constant [$M^{-1}s^{-1}$]

and k_d is the dissociation rate constant [s^{-1}]

The equilibrium dissociation constant (K_D [M]) is calculated by

$$K_D = \frac{k_d}{k_a} \tag{2}$$

This means that the lower the K_D value, the greater the binding affinity of the ligand to its analyte.

2.3.2 Microscale Thermophoresis – an Immobilization-free Approach in Binding Characterization

While SPR is a label-free technique, microscale thermophoresis is an immobilization-free, thermodynamic related technique to analyze and quantify binding events in solution. Thermophoresis describes the phenomenon of directed movement of molecules in a temperature gradient. The thermophoretic mobility of biomolecules is thereby influenced by the size, charge, and hydration shell of a molecule in a liquid phase. The binding of two interaction partners changes at least one of these factors and binding can be measured

through the change in the thermophoretic mobility of the complex (Jerabek-Willemsen et al. 2011). A microscopic, local temperature gradient is typically created by an infrared laser. One binding partner, which is fluorescently labeled, moves either alone or in complex with its unlabeled target. The fluorescent dye, which is coupled to one binding partner, allows the fluorescence-based tracking of the molecules in the temperature gradient. Titration of the unlabeled binding partner allows for the calculation of dissociation constants. In MST, kinetic parameters like k_a or k_d are usually not assessed. Here, the equilibrium dissociation constant is calculated as follows:

$$K_D = \frac{B * L}{BL} \tag{3}$$

Where: B is the concentration of free binding sites of the fluorescent molecule

L is the concentration of free ligand

And BL is the concentration of complexes of B and L

2.4 Aptamers in Therapy

Antibodies, peptides and small molecules can be used as drugs by targeting specific proteins of therapeutic interest. While small molecules may be toxic and often show lower specificity, peptides and antibodies are often highly specific for their target molecule. However, they can provoke immune responses in patients. Due to likewise high affinity and specificity and paired with low- to no immune responses, aptamers are considered effective alternatives for use in therapy. Aptamers are also known for targeting specific proteins of therapeutic interest while some aptamers even have the ability to inhibit their function (Blank and Blind 2005). In addition to direct inhibition of protein function, inhibition of protein-protein interaction, such as receptor-ligand binding, is described for many therapeutic aptamers (Keefe et al. 2010). This is also the case for the first approved therapeutic aptamer, called Pegaptanib, which was approved by the US food and drug administration (FDA) in December 2004 for the treatment of age-related macular degeneration (AMD). Pegaptanib, sold under the trade name Macugen®, is a modified 27 nt long RNA aptamer targeting the vascular endothelial growth factor (VEGF). Due to binding to VEGF, the interaction between VEGF with its receptor VEGFR 1 and VEGFR 2 is inhibited with an IC_{50} value of 49 pM (Ruckman et al. 1998). This prevents the aberrant angiogenesis responsible for AMD, which leads to loss of visual acuity. A variety of other aptamers for therapeutic use are described in the literature. Some of which

have undergone pre-clinical trials, while others have already undergone pre-clinical and clinical trials (Kanwar et al. 2015).

Among these therapeutically active aptamers, a variety of blood coagulation factor specific aptamers offer interesting inhibition potential in order to treat hematological disorders and cancer. Most coagulation factors are extracellular serine proteases and therefore readily accessible to aptamers (Dupont et al. 2011). Blood coagulation factors are a set of mainly proteins, which are responsible for blood clotting. The great interest in inhibitors of blood coagulation factors is primarily due to the interest in finding new anticoagulants for hematological disorders that are safer to use than the classic ones such as warfarin, heparin and thrombin inhibitors that can lead to bleeding side effects and require routine anticoagulant monitoring (Favaloro and Lippi 2012). Besides blood disorders, it is known that coagulation factors play a major role in cancer. Abnormalities are found in a variety of coagulation factors, which also play an important role in overall tumor progression such as tumor growth, tumor angiogenesis and metastasis (Ünlü and Versteeg 2014). In addition to the coagulation factors that are necessary for blood clotting, there are so-called plasminogen activators: urokinase-type plasminogen activator (urokinase, uPA) and tissue-type plasminogen activator (tPA), which are necessary for lysis of these fibrin clots, which are the product of coagulation. Both proteins are serine proteases that play an important role in the fibrinolytic system because they convert the inactive form plasminogen to the catalytically active form plasmin, which then cuts the fibrin for fibrinolysis (Cesarman-Maus and Hajjar 2005). While tPA is primarily involved in thrombolysis, uPA-dependent plasminogen activation is primarily function within physiological and pathological tissue degradation and remodeling processes, including cancer invasion. (Danø et al. 2005). Urokinase is therefore a much-discussed target for therapeutic approaches in cancer treatment (Ulisse et al. 2009).

2.4.1 Urokinase-type Plasminogen Activator – a Serine Protease with Therapeutic and Diagnostic Potential

Urokinase is the key serine protease of the fibrinolytic system. It converts the inactive form plasminogen to the catalytically active form plasmin on cell surfaces. Urokinase was first discovered as a novel “unnamed” protein in human urine in 1947 by MacFarlane and Pilling (MacFarlane and Pilling 1947). Later, Sobel and co-authors named it urokinase in 1952 (Mahmood et al. 2018). It is produced by the epithelial cells of the renal tubules and circulates in the bloodstream to convert plasminogen to plasmin (Vassalli et al. 1991). A schematic illustration of the domain structure of uPA is shown in Figure 2. It is secreted as a single polypeptide, glycosylated zymogen pro-uPA that consists of 411 amino acid residues. The N-terminal A-chain contains the growth factor domain (GFD, amino acids (aa) 1-49) and the kringle domain (KD, aa 50-131), while the C-terminal B-chain contains the catalytically active serine protease domain (SPD, aa 159-411). Between the N-terminal A-chain and the C-terminal B-chain is a linker domain of 27 aa (aa 132-158). Cleavage of the peptide bond between Lys_{158} and Ile_{159} of pro-uPA by different proteases results in the production of the 54 kDa catalytically active two-chain high-molecular-weight uPA (HMW-uPA) linked by a disulfide bond (Mahmood et al. 2018). Besides other proteases, plasmin itself converts pro-uPA to catalytically active uPA most effectively (Schmitt et al. 1991). HMW-uPA can be cleaved a second time in the linker sequence between Lys_{135} and Lys_{136} by different proteases to the 33 kDa catalytically active low-molecular-weight uPA (LMW-uPA) containing the serine protease domain and in an inactive amino-terminal fragment (ATF) that contains the GFD and the KD. Binding of pro-uPA and HMW-uPA to the glycolipid-anchored uPA receptor (uPAR) activates the conversion of plasminogen to plasmin on cell surfaces, which leads to extracellular proteolysis. Here, HMW-uPA is the main activator of plasmin, while it is 250-fold more potent in converting plasminogen to plasmin (Petersen et al. 1988). The catalytic activity of uPA is naturally inhibited by the serine protease inhibitors plasminogen activator inhibitor-1 and -2 (PAI-1 and PAI-2) which makes plasminogen activation a highly controlled event. Here, PAI-1 serves as the major inhibitor. PAI-1 and uPA form a covalently linked complex, which is absorbed together with uPAR through endocytosis. Through degradation of the uPA-PAI-1 complex, free uPAR is released to the extracellular region (Dupont et al. 2009).

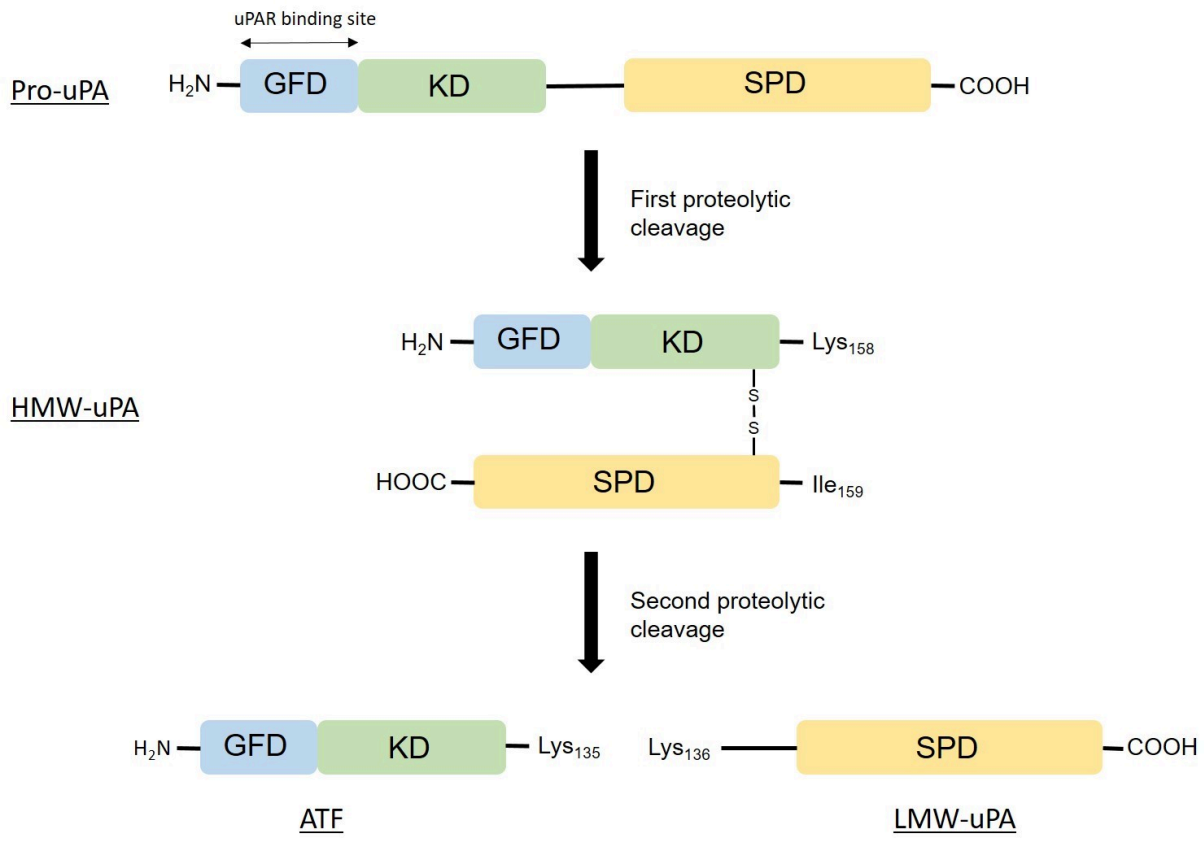

Figure 2: Domain structure of pro-uPA and uPA. Urokinase is secreted as a single polypeptide, glycosylated zymogen pro-uPA containing the growth factor domain (GFD), the kringle domain (KD) and the serine protease domain (SPD). Cleavage of the peptide bond between Lys_{158} and Ile_{159} generates the two-chain, active form of uPA (HMW-uPA) linked by a disulfide bond. A second proteolytic cleavage between Lys_{135} and Lys_{136} results in the generation of catalytically active low molecular weight uPA (LMW-uPA) and the inactive amino terminal fragment (ATF), which contains the GFD and KD. Figure design based on Su et al. (2016) and Mahmood et al. (2018).

Binding of uPA to its receptor uPAR occurs via the GFD of uPA. This makes plasminogen activation not only an event localized on cell surfaces, but also plays a key role in signal transduction (Li Santi et al. 2021). Binding of uPA to uPAR and the conversion of plasminogen to plasmin then in turn activates promatrix metalloproteases. This leads to degradation of extracellular matrix components and basement membrane and releases various growth factors, which allow the formation of new matrix (Su et al. 2016). The uPA-receptor alone or uPA in complex with uPAR also interact with several adhesion molecules such as vitronectin and integrins, proteins of the extracellular matrix and cellular receptors to activate intracellular signaling, which promotes cell proliferation, chemotaxis, apoptosis, adhesion, and migration (Mekkawy et al. 2014). All these processes are necessary for tumorigenesis and cancer progression, as cancer is characterized by the uncontrolled

proliferation of malignant cells, metastasis, and invasion of healthy tissue. Therefore, binding of uPA to its receptor and thereby activating plasminogen to plasmin on cell surfaces is a major process for tumorigenesis and cancer progression. Especially, it enables tumor angiogenesis, malignant cell proliferation, invasion of surrounding tissue, and metastasis (Masucci et al. 2022).

Elevated uPA concentrations have been found in many cancer types, supporting its function in cancer. In cancer cells the expression of the gene (PLAU) encoding uPA is increased by several folds compared to normal cells, where the expression is usually minimal (Mahmood et al. 2018). PLAU transcription is activated by extracellular components e.g., different types of growth factors, cytokines and hormones, which are often elevated during cancer explaining the elevated uPA expression in cancer cells (Irigoyen et al. 1999). As uPA appears to play a crucial role in cancer development, it is an attractive target for cancer therapy. There are two mechanisms by which therapeutics can act. Firstly, by inhibition of uPAs catalytic activity and secondly by inhibition of the uPA-uPAR interaction. Several different studies have investigated inhibitory properties of specific antibodies, small molecules, or aptamers for their potential therapeutic approach by inhibition of uPA activity or uPA receptor binding (Masucci et al. 2022). In this work, uPA specific ssDNA aptamers were tested for their function as inhibitors of uPA catalytic activity and uPA-uPAR interaction.

2.5 Aptamers as Recognition Molecules in Immunoassays

Due to the specific recognition of target molecules, aptamers can be used in various analytical methods. One of the most used analytical methods in clinical laboratories is the immunoassay. It is a powerful and sensitive technology for the detection and quantification of target molecules. Specifically, tumor markers are usually detected and quantified by immunoassays (Yin et al. 2010; Wu et al. 2007). Tumor markers are mostly proteins that are produced by cancer cells and can be found in tissue, blood or other body fluids of cancer patients (Poon and Johnson 2001). In immunoassays, antibodies are typically used for detection of an antigen in solution. Binding of the antigen and its related antibody results in a measurable signal mediated by a reporter moiety coupled to the antibody.

One of the most popular immunoassays for laboratory use is the enzyme-linked immunosorbent assay (ELISA). It is the gold standard for detection and determination of antigen concentrations in physiological samples. There are several different configurations using antibodies in ELISA experiments, which are traditionally carried out on polystyrene microtiter plates (Crowther 2008). One possible configurations is the direct ELISA, in which the antigen is immobilized to the surface of a microtiter plate and an enzyme-conjugated antibody

specific for the antigen is used as a recognition element. Another configuration is the indirect ELISA method, in which the antigen is immobilized on a microtiter plate and a primary unconjugated antibody is used for binding of the antigen. Detection is facilitated by a secondary enzyme-conjugated antibody specific for the primary antibody. A third configuration is the sandwich-ELISA. Here a so-called capture antibody is immobilized on the microtiter plate. The antigen binds to the capture antibody and the captured antigen is detected by another antigen-specific detection antibody. This could be done either using a directly enzyme-conjugated antibody as in the direct ELISA or using a secondary enzyme-conjugated antibody binding to the detection antibody as in the indirect ELISA. Enzymes for the detection of binding can be Horseradish peroxidase (HRP), alkaline phosphatase or β-D-galactosidase (Kumari and Dhir 2003; Liu et al. 2000). The most frequently used enzyme is HRP. Here, the addition of the substrate 3,3‘,5,5‘-Tetramethylbenzidine (TMB) results in a change of color, which can be measured spectrophotometrically. By using a dilution series with known concentration as a calibration curve, the concentration of antigen in the unknown sample can be determined (Herman et al. 2008).

As aptamers can be used as specific recognition molecules and because of their various desirable features, they are conceivable as a replacement for antibodies in ELISAs. In comparison to aptamers, production of monoclonal antibodies often shows batch-to-batch variations and production of antibodies against non-immunogenic molecules is difficult. In contrast, aptamers are simple and inexpensive to produce, easy to modify, and are more chemically stable. In this work, a partial and full replacement of antibodies by aptamers was tested in different sandwich assay formats using previously selected uPA-specific aptamers. Different configurations of the sandwich assays are shown in Figure 3. Here, three different combinations of aptamers and/or antibodies were established for detection of human urokinase and for discrimination of HMW- and LMW-uPA: (a) aptamer-target-aptamer, (b) aptamer-target-antibody and (c) antibody-target-aptamer.

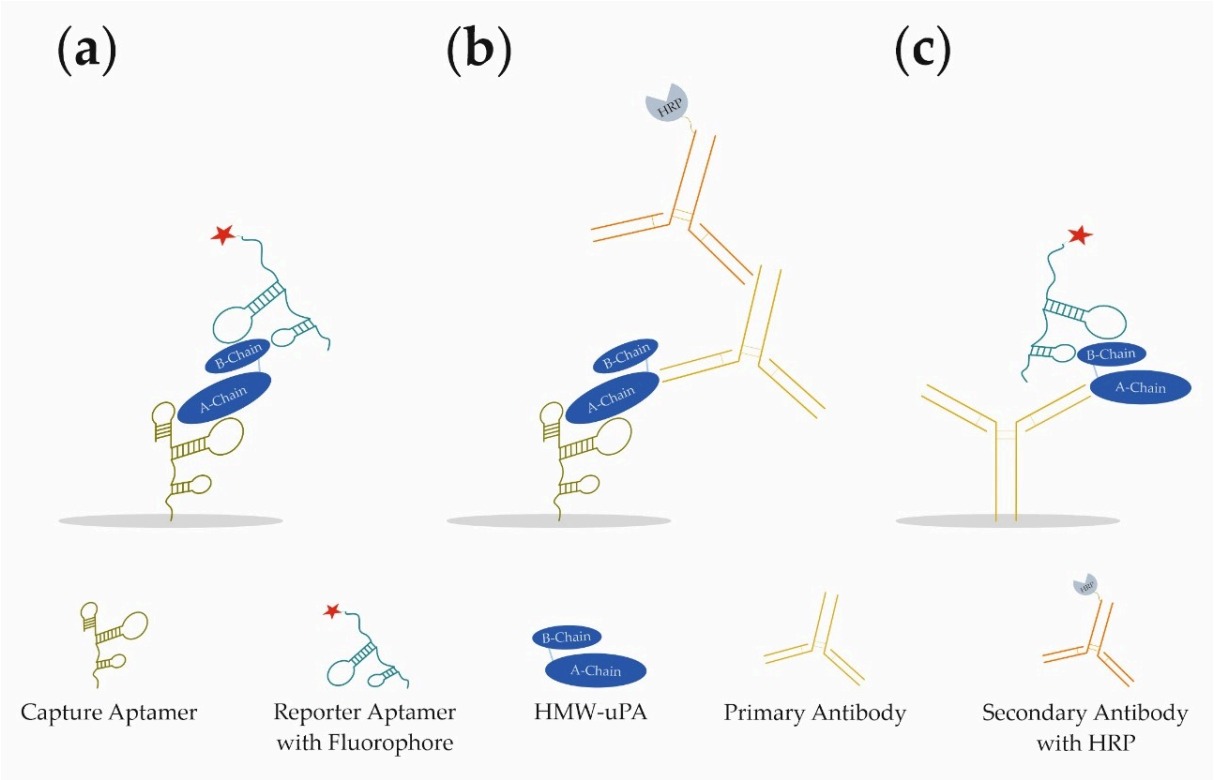

Figure 3: Schematic illustration of the three different sandwich assay formats developed for the detection of human urokinase. (a) Aptamer-target-aptamer, (b) aptamer-target-antibody, and (c) antibody-target-aptamer. Schematic illustration from Dreymann et al. (2022).

2.5.1 Urokinase-type Plasminogen Activator as a Tumor Marker in Cancer

In addition to its therapeutic value and due to its increased concentrations in various types of cancer, uPA is widely discussed as a potential tumor marker for prognosis and diagnosis of cancer (Madunić 2018). Elevated expression of uPA is mainly correlated with poor prognosis and can be found in various cancer types for example breast (Foekens et al. 2000), prostate (Shariat et al. 2007), cervical (Kobayashi et al. 1994), endometrial (Koelbl et al. 1988), colorectal (Yang et al. 2000; Herszényi et al. 2008), lung (Salden et al. 2000) and bladder cancer (Span et al. 2008). The best known example is breast cancer, as the first studies were conducted for this type of cancer. Already in 1985, O'Grady and co-authors identified elevated uPA activity in malignant breast tumors compared to benign ones (O'Grady et al. 1985). Three years later, Duffy et al. (1988) showed that tumor size and metastasis can be associated with uPA activity in primary breast tumors. Since then, numerous studies have been conducted to measure uPA concentrations in various physiological samples for different types of cancer. Using a cohort of 2,780 patients with breast cancer, it was shown that uPA and PAI-1 concentrations can serve as independent prognostic markers for overall and relapse-free

survival (Foekens et al. 2000). As further studies showed that uPA and PAI-1 can serve as a good biomarkers after estrogen receptor and HER2 and are among the ones that attain level-of-evidence 1 in breast cancer, the American Society of Clinical Oncology (ASCO) recommended the determination of uPA/PAI-1 by ELISA as prognostic markers for recurrence and survival in node negative breast cancer patients and to determine if adjuvant chemotherapy could be beneficial (Harris et al. 2007). In most of these studies, elevated uPA levels were measured directly in the affected tissue.

Moreover, increased uPA concentrations were also detected in blood or urine of cancer patients. A recent study showed that uPA can be used alongside other biomarkers as a prognostic marker in the blood of patients with metastatic breast cancer (Banys-Paluchowski et al. 2019). In another study, high levels of uPA in plasma of prostate cancer patients correlated with increased aggressiveness, postoperative diseases progression and metastasis (Shariat et al. 2007; Shariat et al. 2011). Increased uPA levels in blood were also detected for colorectal cancer patients. Here, uPA was suggested as an idependent prognostic marker for patients' survival and metastasis (Yang et al. 2000) and proved to be a better prognostic marker than the commonly used biomarkers CEA and CA 19-9 (Herszényi et al. 2008). Urokinase was also detected in plasma of bladder cancer patients (Shariat et al. 2003b). Recent studies showed that uPA concentrations in plasma have the potential as a predictor for worse survival outcomes and aggressiveness of cancer. Plasma concentrations were associated with recurrence-free and cancer-specific survival (Schuettfort et al. 2021). Elevated uPA concentrations were also found in urine samples of bladder cancer patients (Casella et al. 2002) and were used as a diagnostic biomarker to predict bladder cancer in addition to cytology and other biomarkers (Shariat et al. 2003a).

Hence, the detection and quantification of uPA for prognosis and diagnosis of cancer is of great interest. Detection and concentration measurements are conventionally performed using antibody-based ELISAs. Since aptamers can be used in immunoassays and represent alternative recognition molecules, they were tested as promising capture and detection molecules in microtiter plate-based immunoassays.

2.5.2 New-Delhi Metallo-β-Lactamase 1 as an Antibiotic Resistance Marker

Besides cancers, antibiotic resistance is an increasing worldwide problem that leads to severe and deadly bacterial infections (Talebi Bezmin Abadi et al. 2019). Especially the increase in carbapenem-resistant *Enterobacteriaceae* poses challenges for the health care system, as carbapenem antibiotics serve as the last resort in the treatment of infections with multidrug-resistant bacteria (Kelly et al. 2017). Nevertheless, resistance against carbapenem antibiotics already exists. In order to prevent the spread of resistance and to enable appropriate treatment, carbapenem resistance must be identified. Carbapenem resistance is mediated by carbapenemases. One prominent and hazardous carbapenemase is the New-Delhi metallo-β-lactamase-1 (NDM-1) which was first discovered in 2008 in a strain of *Klebsiella pneumoniae* derived from a patient that traveled to India and contracted a urinary tract infection there (Yong et al. 2009). Since then, NDM-1 containing *Enterobacteriaceae* were found in many countries around the world. One of the reasons for this is that the gene encoding NDM-1 is located on a transmissible resistance-mediating genetic element, which also harbors various other resistance factors (Moellering 2010). That genetic element can be easily transferred to other *Enterobacteriaceae* via horizontal gene transfer allowing rapid spread of this health-hazardous carbapenemase. Therefore, NDM-1 could already been detected in other *Enterobacteriaceae* like *Escherichia coli*, or other klebsiella or enterobacter species (Hammerum et al. 2016). NDM-1 belongs to the Amber class B β-lactamases and is able to hydrolyze carbapenem antibiotics. It is a metallo-β-lactamase that can hydrolyze all β-lactam antibiotics except for Aztreonam which makes the treatment options very limited (Shakil et al. 2011). The detection and differentiation from other carbapenemases is therefore crucial for effective treatment and limitation of further spread. Recently used methods to detect carbapenemases include the detection of carbapenemase encoding genes by PCR or whole genome sequencing. Cabapenemases can further be detected through activity tests, like the Modified Hodge Test or variant of the Carba NP test. (Lutgring and Limbago 2016). Finally, immunoassays can be used for specific detection of carbapenemases via antibody-antigen recognition. Here, the use of antibodies allows the detection and differentiation between different carbapenemase types (Boutal et al. 2017). As already mentioned in section 2.5, aptamers offer a range of desirable features as specific recognition elements and can thus be used for the detection of carbapenemases.

2.6 Aim of the work

The aim of this work was the identification and functional characterization of DNA aptamers against different forms of human urokinase (uPA) for their potential use in diagnostic and therapeutic applications. For this purpose, previously selected DNA aptamers were screened for binding to uPA by an electrophoretic mobility shift assay (EMSA) and a fluorescent dye-linked aptamer assay (FLAA). Here, binding to high-molecular weight uPA (HMW-uPA) and low-molecular weight uPA (LMW-uPA) was investigated to determine potential different binding sites of the aptamers. Using surface plasmon resonance spectroscopy (SPR) and micro scale thermophoresis (MST), binding to the different uPA forms was validated and kinetic parameters were determined. Binding experiments with related proteins were used to demonstrate the specificity of the best uPA aptamer (Manuscript I).

Using an example measurement of an uPA aptamer, a detailed protocol for the measurement and determination of the kinetic parameters of an aptamer-protein interaction using Biacore™ SPR technology was elaborated. In particular, tips and pitfalls that should be taken into account during a measurement were addressed (Manuscript II).

Since uPA is a much-discussed target for cancer therapy, aptamers were functionally characterized and evaluated for their therapeutic value. Here, it was tested in *in vitro* experiments whether the aptamers can inhibit the catalytic activity of uPA and are able to inhibit the binding of uPA to its receptor uPAR (Manuscript I).

Based on the demonstrated binding of the different aptamers to different forms of uPA (Manuscript I) and the consequent assumption of different binding sites, aptamers were tested for their diagnostic utility in microtiter plate-based sandwich assays for the detection of uPA. For this purpose, aptamers were tested for their use in three different sandwich assay formats: (a) aptamer-target-aptamer, (b) aptamer-target-antibody, and (c) antibody-target-aptamer to develop aptamer-based sandwich assay systems with different combinations of aptamers or a combination of aptamer and antibody (Manuscript III).

Determination of the binding parameters of aptamers and their related targets is an important step in the aptamer generation process and is essential for the identification of aptamers with high specificity and affinity to their targets. Therefore, in a further study, the binding parameters of a New Delhi metallo-β-lactamase-1-specific aptamer were investigated using SPR. This NDM1-specific aptamer can be used as a potential detection probe in analytical or diagnostic applications (Manuscript IV).

3. Results

3.1 Manuscript I

Inhibition of Human Urokinase-Type Plasminogen Activator (uPA) Enzyme Activity and Receptor Binding by DNA Aptamers as Potential Therapeutics through Binding to the Different Forms of uPA

Nico Dreymann [1,2], Julia Wuensche [3], Wiebke Sabrowski [1,4], Anja Moeller [1,3], Denise Czepluch [1], Dana Vu Van [5], Susanne Fuessel [5] and Marcus M. Menger [1,3,*]

[1] Fraunhofer Institute for Cell Therapy and Immunology (IZI), Branch Bioanalytics and Bioprocesses (IZI-BB), D-14476 Potsdam, Germany
[2] Institute for Biochemistry and Biology, University of Potsdam, D-14476 Potsdam, Germany
[3] RiNA GmbH, D-12489 Berlin, Germany
[4] Institute of Chemistry and Biochemistry-Biochemistry, Freie Universität Berlin, D-14195 Berlin, Germany
[5] Department of Urology, Technische Universität Dresden, D-01307 Dresden, Germany
[*] Correspondence: marcus.menger@izi-bb.fraunhofer.de; Tel.: +49-331-58187-316

Contributions:

- Designed and planned the study supervised by Marcus M. Menger
- Designed and conducted most of the experiments
    - Target preparation
    - Characterization of isolated DNA aptamers by EMSA and FLAA
    - Parts of K_D-value determination by SPR
    - Detection of the inhibitory effect on uPA-uPAR binding by the aptamers and determination of IC_{50}-values using SPR
    - Detection of the inhibition of the proteolytic activity of uPA by several aptamers
- Analyzed, evaluated and interpreted the experiments mentioned above
- Designed all figures in this manuscript
- Wrote the manuscript

Published in International Journal of Molecular Sciences,

April 28, 2022

DOI: 10.3390/ijms23094890

International Journal of
Molecular Sciences

MDPI

Article

Inhibition of Human Urokinase-Type Plasminogen Activator (uPA) Enzyme Activity and Receptor Binding by DNA Aptamers as Potential Therapeutics through Binding to the Different Forms of uPA

Nico Dreymann [1,2], Julia Wuensche [3], Wiebke Sabrowski [1,4], Anja Moeller [1,3], Denise Czepluch [1], Dana Vu Van [5], Susanne Fuessel [5] and Marcus M. Menger [1,3,*]

[1] Fraunhofer Institute for Cell Therapy and Immunology (IZI), Branch Bioanalytics and Bioprocesses (IZI-BB), D-14476 Potsdam, Germany; nico.dreymann@izi-bb.fraunhofer.de (N.D.); wiebke.sabrowski@izi-bb.fraunhofer.de (W.S.); anja.moeller@izi-bb.fraunhofer.de (A.M.); denise.czepluch@izi-bb.fraunhofer.de (D.C.)
[2] Institute for Biochemistry and Biology, University of Potsdam, D-14476 Potsdam, Germany
[3] RiNA GmbH, D-12489 Berlin, Germany; julia@wundratsch.de
[4] Institute of Chemistry and Biochemistry-Biochemistry, Freie Universität Berlin, D-14195 Berlin, Germany
[5] Department of Urology, Technische Universität Dresden, D-01307 Dresden, Germany; dana.vuvan@uniklinikum-dresden.de (D.V.V.); susanne.fuessel@uniklinikum-dresden.de (S.F.)
* Correspondence: marcus.menger@izi-bb.fraunhofer.de; Tel.: +49-331-58187-316

Abstract: Urokinase-type plasminogen activator is widely discussed as a marker for cancer prognosis and diagnosis and as a target for cancer therapies. Together with its receptor, uPA plays an important role in tumorigenesis, tumor progression and metastasis. In the present study, systematic evolution of ligands by exponential enrichment (SELEX) was used to select single-stranded DNA aptamers targeting different forms of human uPA. Selected aptamers allowed the distinction between HMW-uPA and LMW-uPA, and therefore, presumably, have different binding regions. Here, uPAapt-02-FR showed highly affine binding with a K_D of 0.7 nM for HMW-uPA and 21 nM for LMW-uPA and was also able to bind to pro-uPA with a K_D of 14 nM. Furthermore, no cross-reactivity to mouse uPA or tissue-type plasminogen activator (tPA) was measured, demonstrating high specificity. Suppression of the catalytic activity of uPA and inhibition of uPAR-binding could be demonstrated through binding with different aptamers and several of their truncated variants. Since RNA aptamers are already known to inhibit uPA-uPAR binding and other pathological functions of the uPA system, these aptamers represent a novel, promising tool not only for detection of uPA but also for interfering with the pathological functions of the uPA system by additionally inhibiting uPA activity.

Keywords: biomarker; cancer; cancer therapy; DNA aptamer; microscale thermophoresis (MST); SELEX; surface plasmon resonance spectroscopy (SPR); uPA; uPAR; urokinase

check for updates

Citation: Dreymann, N.; Wuensche, J.; Sabrowski, W.; Moeller, A.; Czepluch, D.; Vu Van, D.; Fuessel, S.; Menger, M.M. Inhibition of Human Urokinase-Type Plasminogen Activator (uPA) Enzyme Activity and Receptor Binding by DNA Aptamers as Potential Therapeutics through Binding to the Different Forms of uPA. *Int. J. Mol. Sci.* **2022**, *23*, 4890. https://doi.org/10.3390/ijms23094890

Academic Editor: Antonio Lucacchini

Received: 12 April 2022
Accepted: 26 April 2022
Published: 28 April 2022

Publisher's Note: MDPI stays neutral with regard to jurisdictional claims in published maps and institutional affiliations.

Copyright: © 2022 by the authors. Licensee MDPI, Basel, Switzerland. This article is an open access article distributed under the terms and conditions of the Creative Commons Attribution (CC BY) license (https://creativecommons.org/licenses/by/4.0/).

1. Introduction

Urokinase-type plasminogen activator (urokinase, uPA) is a serine protease that plays an important role in the fibrinolytic system by converting the inactive-form plasminogen into the catalytically active-form plasmin. Human uPA is produced and secreted as a single polypeptide, glycosylated zymogen pro-uPA, consisting of 411 amino acids with an N-terminal A-chain containing a growth factor domain (GFD, amino acids (aa) 1–49), a kringle domain (KD, aa 50–131) and a C-terminal B-chain containing the catalytically active serine protease domain (SPD, aa 159–411). Between the N-terminal A-chain and the C-terminal B-chain is a linker domain (aa 132–158) [1].

Due to different proteases, pro-uPA undergoes cleavage of the peptide bond between Lys158 and Ile159 to produce the 54 kDa catalytically active two-chain high-molecular-weight uPA (HMW-uPA) linked by a disulfide bond. HMW-uPA can be cleaved a second

time in the linker sequence between Lys135 and Lys136 by various proteases into a catalytically active low-molecular-weight uPA of 33 kDa (LMW-uPA) with a serine protease domain and an inactive amino-terminal fragment (ATF) that contains the GFD and the KD. Binding of pro-uPA and HMW-uPA through the GFD to the glycolipid-anchored uPA receptor (uPAR) activates the conversion of plasminogen to plasmin on cell surfaces [1].

While pro-uPA has more limited enzymatic activity compared to the two-chain HMW-uPA, it is still able to induce plasmin activation, presumably through conformational change of pro-uPA via binding to uPAR [2]. The two-chain HMW-uPA that binds to uPAR is 250-fold more potent in converting plasminogen to plasmin and the main activator of plasmin leading to extracellular proteolysis [3]. This mediates several physiological and pathological pathways by activating growth factors and promatrix metalloproteases, degrading extracellular matrix components and basement membrane and allowing the formation of new matrix, which are all involved in various processes that are necessary for tumorigenesis and cancer progression [4]. In particular, pathophysiological mechanisms such as tumor angiogenesis, malignant cell proliferation, invasion of surrounding tissues, cell extravasation and tumor progression and metastasis are supported by uPA binding to its receptor uPAR [5].

Inhibition of the catalytic activity of uPA is naturally caused by the serine protease inhibitors plasminogen activator inhibitor-1 and-2 (PAI-1 and PAI-2). Here, PAI-1 is the major inhibitor, which makes the conversion to plasmin a highly controlled event. PAI-1 and uPA form a covalently linked complex, which is absorbed together with uPAR through endocytosis. This leads to degradation of the uPA-PAI-1 complex and releases free uPAR to the extracellular region [6].

Independent of proteolytic activity, the uPA-uPAR complex plays a key role in signal transduction by interacting with several adhesion molecules like integrins and vitronectin, cellular receptors and proteins of the extracellular matrix, to control cell proliferation, apoptosis, chemotaxis, adhesion and migration [7]. Several independent studies showed that uPA is widely discussed as a prognostic and diagnostic marker for human malignancies [8] since the elevated expression of uPA in many different cancer types is mainly correlated with a poor prognosis [5,9].

In addition to its diagnostic and prognostic value, uPA is a potential target for cancer therapies by direct inhibition of its proteolytic activity or by inhibition of the uPA-uPAR interaction, which has been shown to suppress tumor growth, tumor invasion and metastasis in animal models [10]. Blocking of the catalytic domain and thereby the catalytic activity was achieved by specific antibodies [11], overexpression of the endogenous inhibitors PAI-1 [12] and small-molecule inhibitors [13]. The serine protease inhibitor Mesupron (WX-671) resulted in reduced metastatic spread and an extended lifespan in clinical trials on pancreatic and breast cancer patients [14]. To inhibit the downstream actions of the uPA-uPAR complex, another strategy is to block binding of uPA to its receptor. Inhibition of the uPA-uPAR complex by human uPA-ATF as an antagonist of uPA-uPAR interaction might be a promising anti-invasion and anti-metastasis strategy by displacing uPA from its cognate receptor [15]. Urokinase-derived cyclic peptides that were synthesized similarly to the GFD of uPA that binds to uPAR showed promising results in hampering tumor growth and metastasis in animal models [16].

In addition to all these strategies, nucleic acid aptamers targeting proteases are suggested as a promising alternative not only for recognition but also as inhibitors of enzymatic and regulatory mechanisms [17,18]. Aptamers recognize their targets with high specificity and affinity corresponding to K_D values in the picomolar to low nanomolar range, and therefore, are comparable to antibodies. Several effective aptamers against proteases are known today [17,18]. Specifically for uPA, Dupont et al. [19] were the first to identify 2′-F-pyrimidine-modified RNA aptamers binding near to the GFD domain. These aptamers were able to block binding of uPA to its receptor uPAR with low nM IC_{50} values. Botkjaer et al. [20] were able to select 2′-fluoro-pyrimidine-modified RNA aptamers binding to the catalytic domain of pro-uPA. The only DNA aptamers known today are reported

for pro-uPA, where a pool of DNA aptamers was selected after 12 selection rounds and a similar group of sequences was revealed with increased affinity to pro-uPA compared to the initial library pool [21].

Here, we present novel, highly affine and specific DNA aptamers of up to 82-nt long that can bind to different forms of human uPA. Single-stranded DNA (ssDNA) aptamers were isolated by systematic evolution of ligands by exponential enrichment (SELEX) from a 42-nt random ssDNA-library with a theoretical diversity of 1.9×10^{25} different sequences. Binding of aptamers was characterized for its affinity and specificity by various assays, including a fluorescent dye-linked aptamer assay (FLAA), electrophoretic mobility shift assay (EMSA), surface plasmon resonance (SPR) spectroscopy and microscale thermophoresis (MST). Selected aptamers could discriminate between HMW- and LMW-uPA. Therefore, we assume that our aptamers bind either in the region of the amino-terminal fragment or the serine protease domain. We also found that aptamer binding inhibited the binding of uPA to its receptor uPAR and suppressed the catalytic activity of uPA. Given the worldwide increase in cancer, the early detection and therapy of cancer are among the most important tasks in today's medicine. Due to the ease of synthesis and modification, selected aptamers represent interesting agents for basic research analysis and diagnostic applications besides other uPA-targeting agents like small molecules, peptides or antibodies. Due to the small size of aptamers, together with their polyanionic nature, which results in good tissue penetration and rapid blood clearance, they may also be promising agents for therapeutics, while showing no immunoreactivity and low-to-no toxicity [22]. Although previous research identified modified RNA aptamers that targeted uPA and inhibited binding of uPA to uPAR [19], to our best knowledge, no aptamers that can inhibit uPA activity have been reported to date. Therefore, our aptamers could be used for potential inhibition of both the functionally important interactions of uPA with its receptor and the catalytic activity of uPA in different types of cancer.

2. Results

2.1. Characterization of Isolated DNA Aptamers to Human Urokinase Revealed Binding Sequences by EMSA and FLAA

After 11 selection rounds for HMW-uPA and 12 selection rounds for LMW-uPA, enriched DNA pools were sequenced using NGS. Analysis of the sequences in the different SELEX pools after selection against HMW-uPA and LMW-uPA showed the number of enriched sequences in the respective DNA pool. After comparing and analyzing the data and sequences in each DNA pool, sequences that showed specific enrichment and were present in both DNA pools were selected to test them for binding to HMW-uPA and LMW-uPA by EMSA and FLAA. Sequences that showed binding against both uPA forms or only against HMW-uPA by EMSA and FLAA are reported in Table 1. Sequences are named as uPA aptamers: uPAapt-xx.

Table 1. Sequences of the variable region of the aptamers binding uPA. Each 41−nt and 42−nt long variable region is flanked by the constant regions of the 20−nt long forward− (5′−AGGTAGAGGAGCAAGCCATC−3′) and reverse− (5′−GATGCGTGATCGAACCTACC−3′) primer binding sites.

Name	Variable Region (5′−3′)
uPAapt−01	ATGGTAACATGCACTAGGTCGCGATGGTTCCGTCTGATCGCT
uPAapt−02	CAAGCGGGGGTGAGAGATCTGTCAGTACGAGCTGGGTTTGCG
uPAapt−03	ACGGAGGCAGAGGGTGAGAGATCTGTTAGTACTAGCCCATGT
uPAapt−06	GGGTGGGTGGGTGGGTGATGGCTCGACTCTACCCTGGCGCTG
uPAapt−08	CAGCGGTAGGGGTTATATAGCTGCGCCATAGGGTACTCGTG
uPAapt−21	GGAGGTACTCACCGACGCTGAACTCCATAGAATGTGGTGATG
uPAapt−26	ATCCGTGGCGTGGTTGGTGGGGGAGGTGGGCGGGTAGACGGT
uPAapt−27	ATGGGGTGTTATGGGGGGGGCTTATTGCGGTCAGGGGACGAT

2.1.1. Gel Shift Experiments (EMSA)

Binding analysis for aptamers was qualitatively validated by gel shift experiments. Band shifting was observed for HMW-uPA with all aptamers, while band shifting for LMW-uPA was only observed for uPAapt-01, uPAapt-02 and uPAapt-03 compared to the no-target control (NTC). An example of band-shifting for uPAapt-02 and uPAapt-21 is shown in Figure 1. For detailed data on the gel shift experiment results for all full-length aptamers, see Table A1.

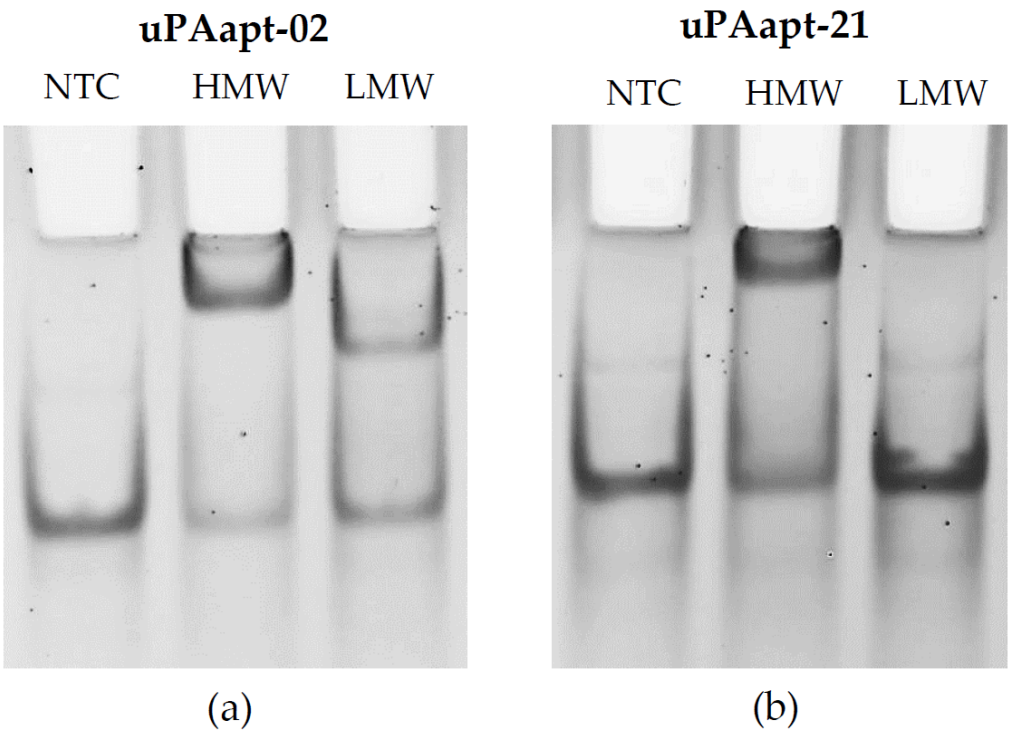

Figure 1. Binding of aptamers to HMW−uPA and LMW−uPA by EMSA. Gel shift experiments for (**a**) uPAapt−02 and (**b**) uPAapt−21. While uPAapt−02 demonstrated binding to both HMW−uPA and LMW−uPA, uPAapt−21 showed only binding to HMW−uPA when compared to the no-target control. NTC = no-target control, HMW = HMW−uPA, LMW = LMW−uPA.

2.1.2. Fluorescent-Dye Linked Aptamer Assay (FLAA)

In FLAA experiments, the highly diverse ssDNA-library used as a control showed a low binding signal to HMW-uPA, which indicates slight, non-specific binding of DNA sequences. However, compared to the ssDNA-library and the no-target control, all aptamers showed higher signals, which indicates binding of aptamers to HMW-uPA. Binding to LMW-uPA was also identified for aptamers uPAapt-01, uPAapt-02, uPAapt-03, uPAapt-06 and uPAapt-27 by FLAA (Figure 2a). Additionally, several sequences were truncated by the forward-primer binding site (uPAapt-xx-F), reverse-primer binding site (uPAapt-xx-R) and both primer binding sites (uPAapt-xx-FR). Truncated aptamers were used to test whether primer binding regions are important to form the secondary structure binding uPA or whether the variable region alone is responsible for the uPA-binding structure. Binding to the different uPA-forms was still detected for truncated variants of aptamers uPAapt-02 and uPAapt-27. Here, high signals were detected for truncated versions of uPAapt-02 for HMW- and LMW-uPA and truncated variants of uPAapt-27 for HMW-uPA (Figure 2b).

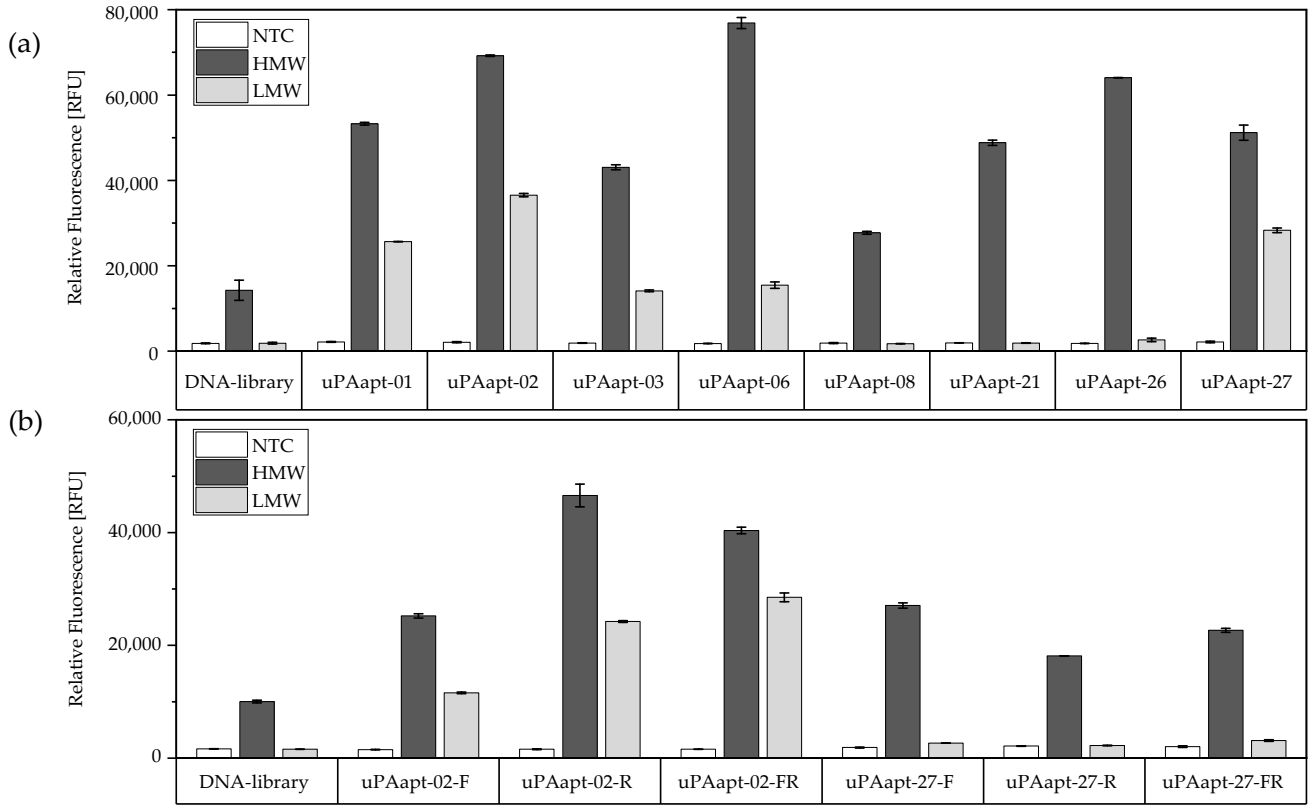

Figure 2. Binding of aptamers to HMW−uPA and LMW−uPA by FLAA. (**a**) Full−length−aptamers and (**b**) truncated versions of aptamers showed binding either to HMW−uPA or to both HMW−uPA and LMW−uPA when compared to their no-target control and the DNA-library. The relative fluorescence unit (RFU) for each sample is shown as the mean value of technical replicates. Error bars represent the range of measured values. NTC = no-target control, HMW = HMW−uPA, LMW = LMW−uPA. Number of records n = 2.

2.2. Aptamers Showed High Affinity to uPA with up to pM K_D Values

Subsequently, identified uPA-binding aptamers (Table 1) and several truncated variants were used for SPR experiments. Injection of uPA dilution series allowed for calculation of kinetic data such as the association and dissociation rates (k_a and k_d) and resulting dissociation constants (K_Ds) of the binding event. For calculation, signals derived from the reference channel were subtracted. Obtained sensograms were fitted to a 1:1 Langmuir binding model using Biacore™ Evaluation Software (version 3.2, GE Healthcare Bio-Sciences AB, Uppsala, Sweden). While binding to HMW-uPA was detected for each aptamer with a K_D in a pM-nM range, binding to LMW-uPA could only be detected for aptamers uPAapt-01, uPAapt-02, uPAapt-02-R, uPAapt-02-FR and uPAapt-21 in an nM-range. While uPAapt-01 showed binding to LMW-uPA, no binding was detected for its truncated variant uPAapt-01-FR, which bound only to HMW-uPA. An example of fitted sensograms for binding of uPAapt-02-FR to HMW-uPA and LMW-uPA is shown in Figure 3.

For the binding of uPAapt-02-FR to HMW-uPA, the association rate was determined as 2.42×10^5 M^{-1} s^{-1} and the dissociation rate was determined as 1.72×10^{-4} s^{-1}. A K_D value of 7.08×10^{-10} M was obtained based on the kinetic data. For binding of uPAapt-02-FR to LMW-uPA, the k_a was 2.47×10^4 M^{-1} s^{-1} and the k_d was 5.30×10^{-4} s^{-1}. The calculated K_D value for binding to LMW-uPA was 2.14×10^{-8} M. The chi^2, a standard statistical method that shows the closeness of a fit, was 1.80 for HMW-uPA and 0.02 for LMW-uPA. For detailed data of the on and off rates, including the chi^2 and calculated dissociation constants of selected aptamers, see Table A2.

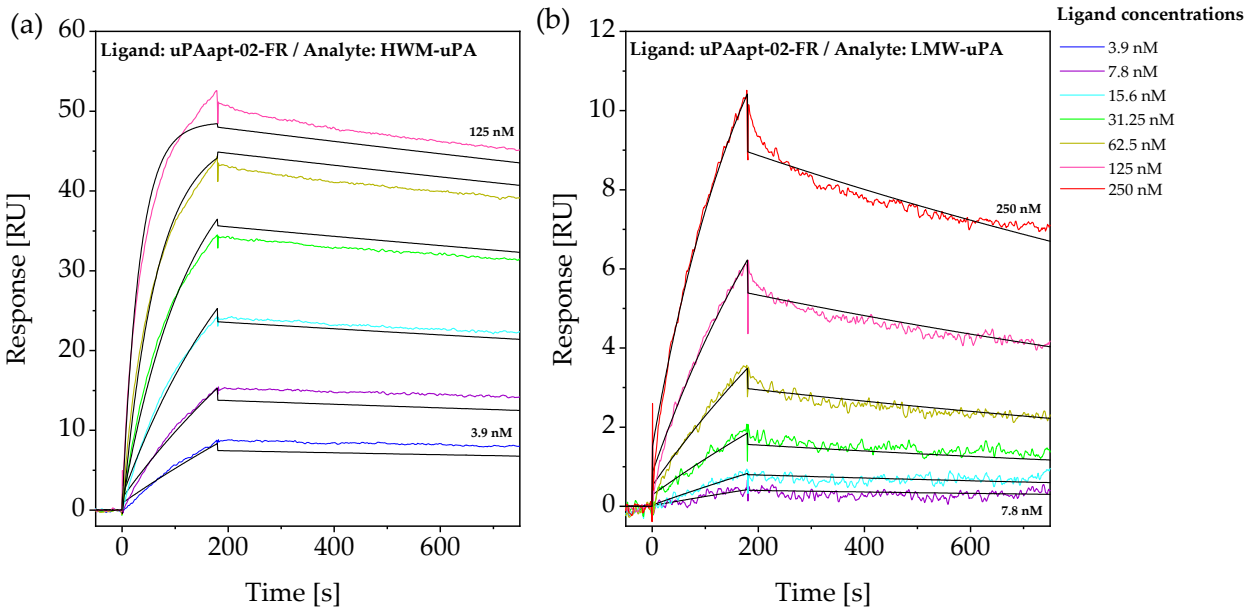

Figure 3. SPR sensograms of uPAapt−02−FR with (**a**) HMW−uPA and (**b**) LMW−uPA. The sensograms show each response unit (RU) over the time (s) of six different urokinase concentrations (for HMW−uPA, 3.9, 7.8, 15.6, 31.25, 62.5 and 125 nM, and for LMW−uPA, 7.8, 15.6, 31.25, 62.5, 125 and 250 nM) overlaid and globally fitted to a 1:1 binding model, to obtain values for the rate and equilibrium constants.

2.3. uPA Aptamer uPAapt-02-FR Demonstrated High Specificity for Human uPA

In addition to SPR, MST was used as an immobilization-free method to determine binding and associated K_D values when both binding partners are free in solution. Detection of binding events is enabled by one binding partner being fluorescently labeled. Here, uPAapt-02-FR was used as a representative for further characterization, as uPAapt-02-FR can bind both uPA forms with high binding affinities and K_D values in the low nM range. Besides binding to HMW- and LMW-uPA, cross-reactivity with pro-uPA, mouse uPA and tPA was tested for uPAapt-02-FR by MST (Table 2).

Table 2. Dissociation constants (K_D) including the K_D confidence from MST measurements for uPAapt−02−FR and uPAapt−21 with HMW−uPA and LMW−uPA, and additionally, for uPAapt−02−FR with pro−uPA, mouse−uPA and tPA.

Aptamer	Target	K_D (M)	K_D Confidence (M)
5′−Cy5−uPAapt−02−FR	HMW−uPA	6.69×10^{-9}	$\pm 1.55 \times 10^{-9}$
	LMW−uPA	9.40×10^{-9}	$\pm 3.10 \times 10^{-9}$
	pro−uPA	1.40×10^{-8}	$\pm 0.65 \times 10^{-8}$
	mouse uPA	-*	-*
	tPA	-*	-*
5′−Cy5−uPAapt−21	HMW−uPA	2.08×10^{-7}	$\pm 0.63 \times 10^{-7}$
	LMW−uPA	1.41×10^{-6}	$\pm 0.45 \times 10^{-6}$

Note: -*, no binding detected.

K_D values determined using MST were comparable to those calculated from SPR data with a K_D value of 6.69×10^{-9} M for HMW-uPA and 9.40×10^{-9} M for LMW-uPA. Furthermore, binding to pro-uPA was detected at a K_D value of 1.40×10^{-8} M. No binding, and therefore, no cross-reactivity was detected for uPAapt-02-FR with mouse uPA and tPA. Examples for binding and no-binding curves of uPAapt-02-FR are shown in Figure 4.

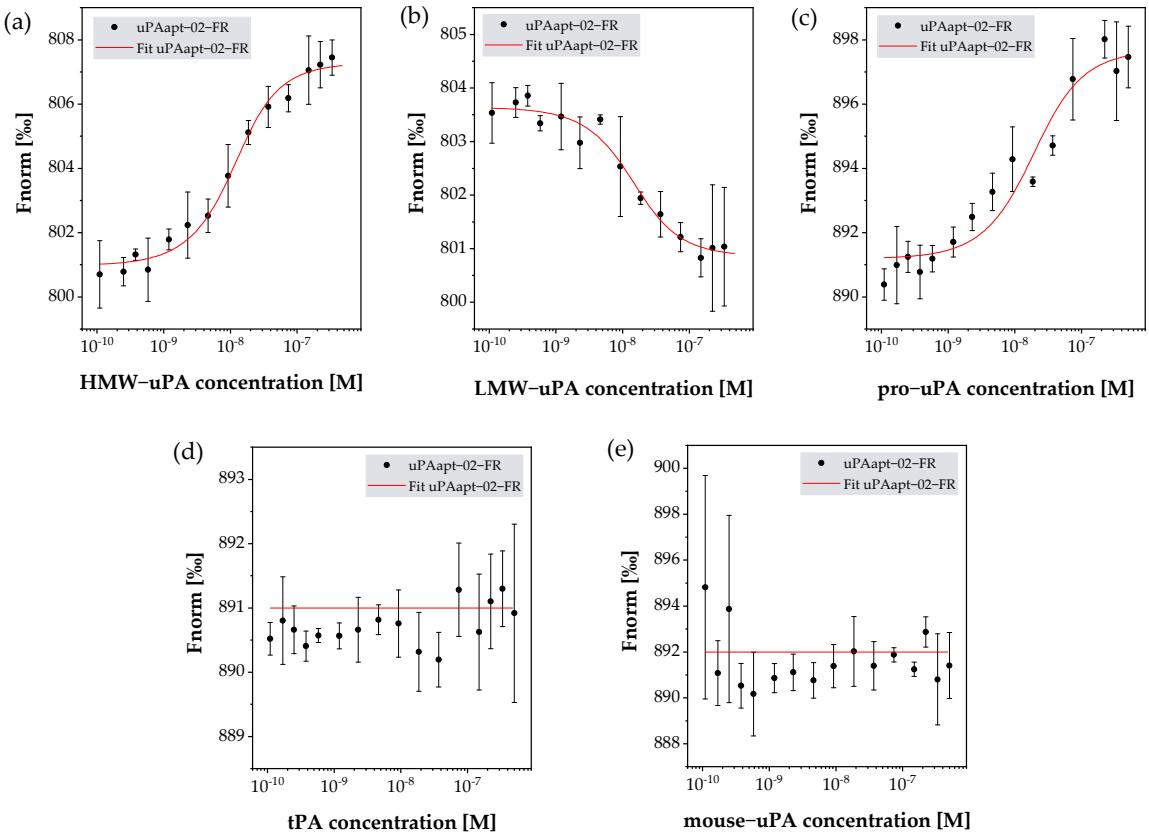

Figure 4. Binding analysis for uPAapt−02−FR with (**a**) HMW−uPA, (**b**) LMW−uPA, (**c**) pro−uPA, (**d**) tPA and (**e**) mouse−uPA using MST. MST measurements were carried out with 5′−Cy5−uPAapt−−02−FR and varying concentrations of the different targets (for HMW− and LMW−uPA, from 0.1 nM to 333 nM, and for pro−uPA, tPA and mouse−uPA, from 0.1 nM to 500 nM). Each plot shows the normalized fluorescence Fnorm (‰) vs. the concentration (M) of the given target. While uPAapt−02−FR showed binding curves for HMW−uPA, LMW−uPA and pro−uPA, no binding was detected for tPA or mouse−uPA. The Fnorm for each sample is shown as the mean value of independent experiments. Error bars represent the standard deviation. Red lines represent the fit of data points using the law of mass action. Number of records $n = 3$.

In addition, uPAapt-21 was also tested for binding to HMW- and LMW-uPA. Here, uPAapt-21 was used as a representative that binds only the HMW-uPA form since it showed binding only to HMW-uPA in EMSA and FLAA. However, in SPR, uPAapt-21 showed binding to both HMW-uPA and LMW-uPA (Table A2). Since, for this aptamer, some techniques showed binding only to HMW-uPA, while others showed binding to both HMW-uPA and LMW-uPA, MST was used to verify its LMW-uPA binding potential with another highly sensitive method. Here, binding of uPAapt-21 could be confirmed with a K_D value of 2.08×10^{-7} M for HMW-uPA and 1.41×10^{-6} M for LMW-uPA. Dissociation constants (K_Ds) including the K_D confidence of a binding event between uPAapt-02-FR or uPAapt-21 and used proteins are shown in Table 2.

2.4. Various Aptamers Reveal an Inhibitory Effect toward Binding of uPA to uPAR with up to nM IC_{50} Values

All full-length aptamers as well as selected, truncated variants were screened for their ability to inhibit uPA-uPAR binding, where several aptamers were able to inhibit binding of uPA to uPAR. Although they differed in the strength of inhibition, the following aptamers showed an inhibitory effect, beginning with the aptamer that showed the best inhibitory effect: uPAapt-21, uPAapt-26, uPAapt-08, uPAapt-02, uPAapt-01, uPAapt-02-R, uPAapt-02-F, uPAapt-02-FR, uPAapt-03, uPAapt-27 and uPAapt-06. Besides some aptamers that showed

no inhibitory effect (uPAapt-01-FR, uPAapt-08-FR, uPAapt-27-FR, uPAapt-27-R and uPAapt-27-F), the DNA-library used for aptamer selection as well as the sequence-unrelated control aptamer Con also showed no inhibitory effect. For the SPR sensogram of the screening of aptamers inhibiting uPA-uPAR binding, see Figure A1. The aptamers that showed the best inhibitory effect (uPAapt-21, uPAapt-26 and uPAapt-08) were used for IC_{50} calculation. The control aptamer Con was also included in IC_{50} calculation to verify sequence-specific IC_{50} values. Binding of uPA to immobilized uPAR on the sensor surface in the presence of increasing concentrations of the different aptamers is shown in Figure 5.

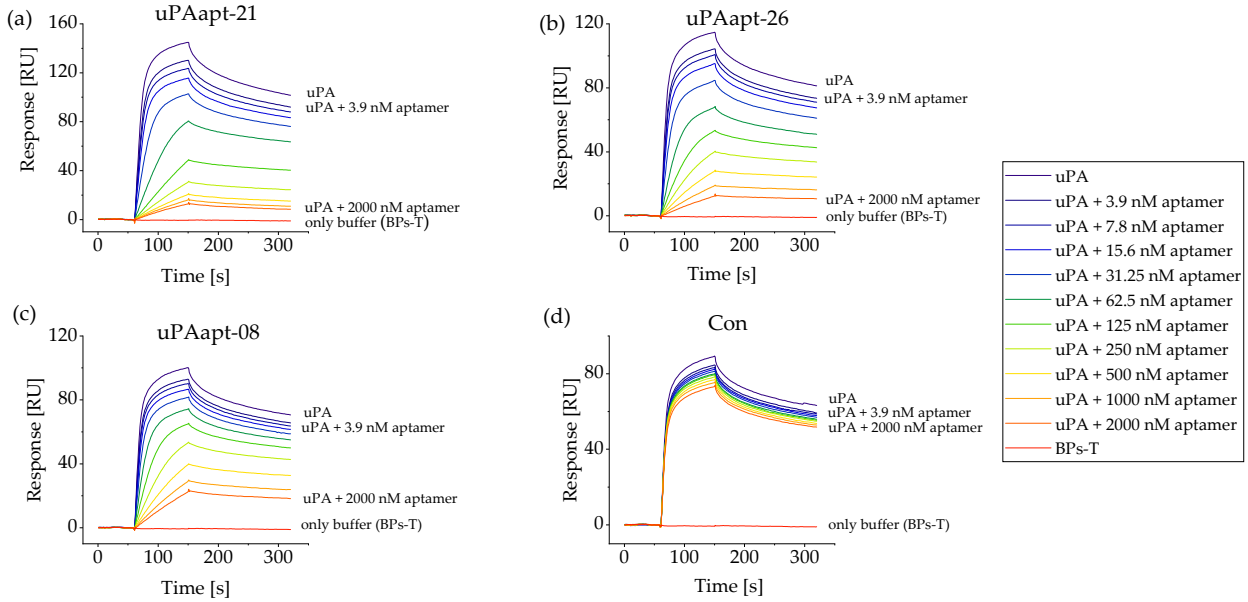

Figure 5. Inhibition of uPA binding to uPAR by selected aptamers. SPR sensograms show the capture of 20 nM human uPA (injected from 60 to 150 s) on a sensor surface with immobilized human uPAR in the presence of increasing concentrations of aptamers. Sensograms display each response unit (RU) over the time (s) for uPA alone or in complex with different aptamer concentrations (3.9, 7.8, 15.6, 31.3, 62.5, 125, 250, 500, 1000 and 2000 nM). (**a**) uPAapt−21, (**b**) uPAapt−26, (**c**) uPAapt−08 and (**d**) Con. While uPAapt−21, uPAapt−26 and uPAapt−08 showed a dose-dependent effect on the inhibition of uPA binding to uPAR, the sequence-unrelated control aptamer Con showed no inhibitory effect.

While uPAapt-21, uPAapt-26 and uPAapt-08 showed a dose-dependent effect on the inhibition of uPA binding to uPAR on the sensor surface, the sequence-unrelated control aptamer Con showed no inhibitory effect. A slight decrease in the reported response values for Con can be attributed to repeated regenerations after each sample injection, which leads to a decrease in uPA-uPAR binding. No binding of aptamers (125–2000 nM) to uPAR could be detected. Response units of uPA in complex with different concentrations of each aptamer were plotted as a function of aptamer concentrations relative to the response of uPA without an aptamer (Figure 6).

As repeated regeneration steps were conducted, binding of uPA to the sensor surface immobilized with uPAR reduced over the measurements. To include this in IC_{50} calculation, uPA was injected before each concentration series of the different aptamers and the loss of the signal was fitted using a polynomial regression model. Each uPA-aptamer-complex response was reduced by the calculated loss of signal. Based on these data, IC_{50} values were estimated by a nonlinear regression analysis, fitting the data to a dose-response function. IC_{50} values with their standard error for the inhibition of uPA-uPAR binding by the different aptamers are shown in Table 3.

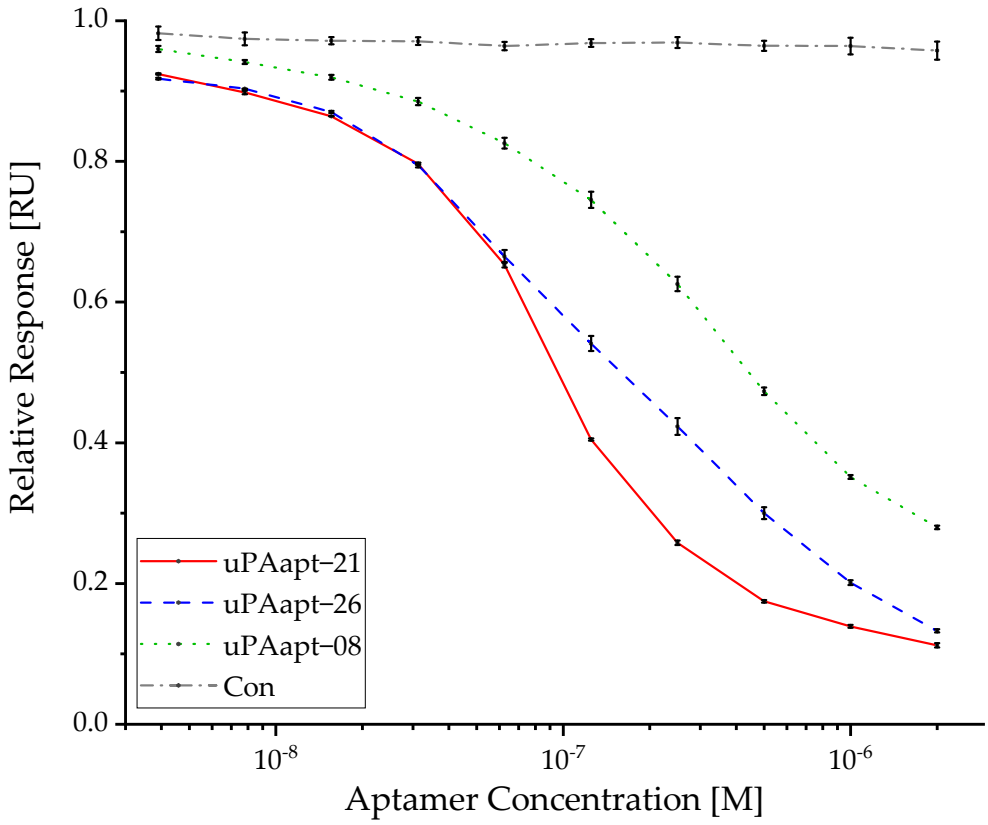

Figure 6. Reported uPA capture level after injection of each sample was plotted as a function of the aptamer concentration (3.9–2000 nM) relative to the response of 20 nM uPA alone for uPAapt−21, uPAapt−26, uPAapt−08 and the sequence-unrelated control aptamer Con. For the calculated IC_{50} values, see Table 3. The relative response (RU) for each sample is shown as the mean value of independent experiments. Error bars represent the range of measured values. Number of records $n = 2$.

Table 3. IC_{50} values of selected aptamers for inhibition of interaction between uPA and its receptor uPAR. IC_{50} values were estimated by nonlinear regression analysis, fitting the data to a dose-response function.

Aptamer	IC_{50} (±Standard Error) (M)
uPAapt−21	8.70×10^{-8} ($\pm 0.40 \times 10^{-8}$)
uPAapt−26	1.65×10^{-7} ($\pm 0.16 \times 10^{-7}$)
uPAapt−08	2.98×10^{-7} ($\pm 0.17 \times 10^{-7}$)
Con	-*

Note: -*, no inhibition could be detected.

2.5. Proteolytic Activity of uPA Can Be Inhibited by Several Aptamers

All full-length aptamers and various truncated variants were screened for their ability to inhibit the proteolytic activity of uPA using the uPA inhibition assay. Although the various aptamers showed only partial inhibition of the proteolytic activity of uPA, uPAapt-01, uPAapt-02-F, uPAapt-02-R, uPAapt-02-FR and uPAapt-03 showed inhibition of uPA activity compared to uPA alone. Moreover, uPAapt-27 showed a very small effect on uPA activity. In particular, uPAapt-01, uPAapt-02-F, uPAapt-02-R and uPAapt-02-FR could inhibit the proteolytic activity of uPA by at least 35% (uPAapt-01: 44%, uPAapt-02-F: 38%, uPAapt-02-R: 45%, uPAapt-02-FR: 42%, uPAapt-03: 15%, uPAapt-27: 6%). For the calculation, uPA without an aptamer was taken as 0% inhibition. All other tested aptamers and several truncated variants, as well as the ssDNA library used as a control, showed no effect on uPA activity compared to uPA alone (Figure 7).

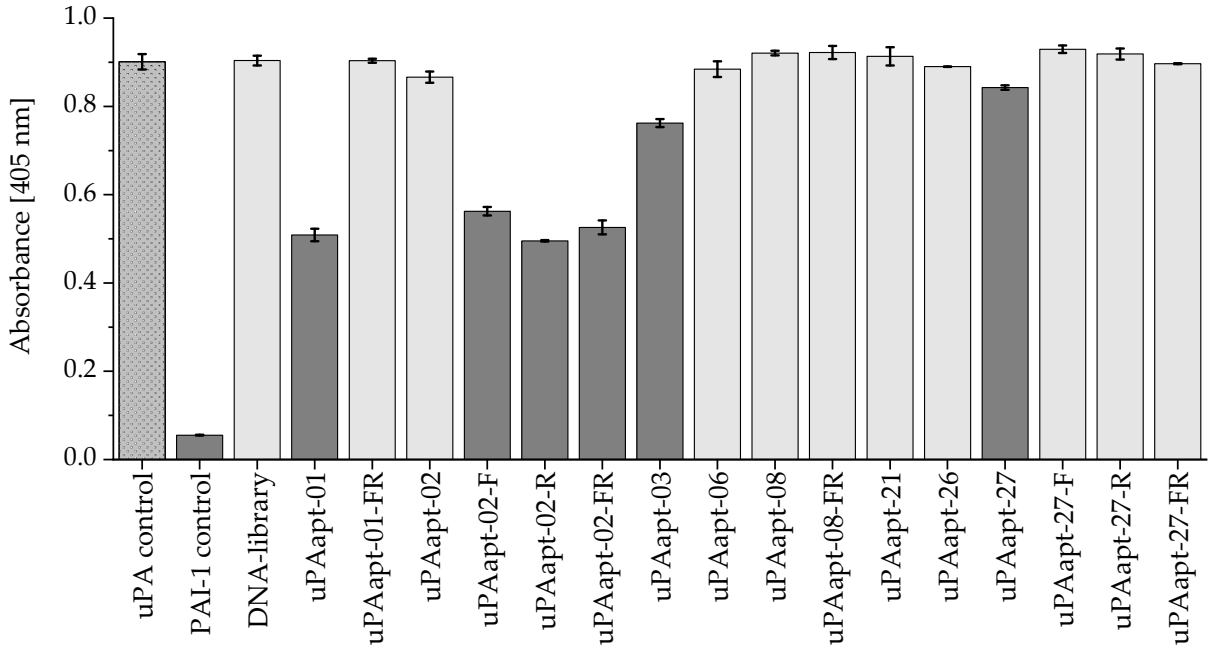

Figure 7. uPA inhibition assay for various aptamers. uPA activity was detected by hydrolysis of the chromogenic substrate. The absorbance was measured at 405 nm after 4 h at 37 °C for uPA (120 pmol) alone (uPA control) or incubated with various aptamers (600 pmol). Incubation with PAI−1 was carried out as a positive control for the specific inhibition of uPA. The DNA-library was used as a control to demonstrate sequence-dependent inhibition. The PAI−1 control and aptamers that showed inhibition of the uPA activity are highlighted in dark grey. The absorbance, for each sample, is shown as the mean value of technical replicates. Error bars represent the range of measured values. Number of records $n = 2$.

To verify whether there was statistically significant inhibition of uPA activity by uPAapt-01 and the truncated variants of uPAapt-02, two additional independent experiments were performed for uPAapt-01, uPAapt-02-F, uPAapt-02-R and uPAapt-02-FR to achieve a total of three independent experiments. Again, uPA alone, uPA incubated with PAI-1 or the DNA-library were included as controls. Statistically significant inhibition ($p < 0.01$) of uPA activity could be demonstrated for uPAapt-01, uPAapt-02-F, uPAapt-02-R and uPAapt-02-FR compared to uPA alone (Figure 8). Significance was determined by Welch's *t*-test.

As several aptamers showed similar inhibitory effects, uPAapt-02-FR was selected for further characterization. As a representative aptamer, uPAapt02-FR showed a dose-dependent effect on the inhibition of uPA activity with a substantial reduction in the conversion of the chromogenic peptide substrate in the range of 0.09 to 46.25 µM. Here, the highest concentration of uPAapt-02-FR (46.25 µM) corresponded to a 100-fold excess of aptamer (Figure 9).

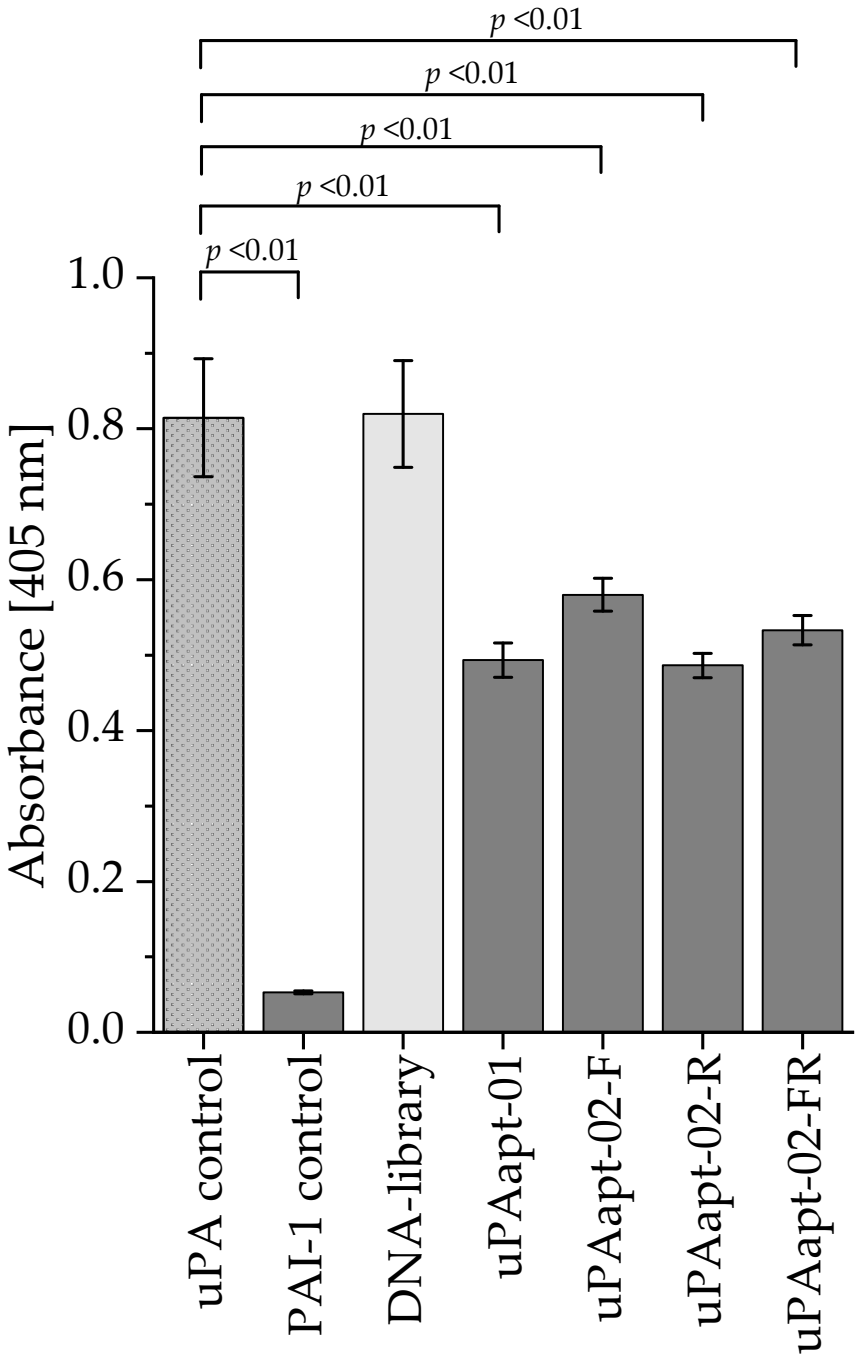

Figure 8. uPA inhibition assay for uPAapt−01 and truncated versions of uPAapt−02 (uPAapt−02−F, uPAapt−02−R and uPAapt−02−FR). uPA activity was detected by hydrolysis of the chromogenic substrate. The absorbance was measured at 405 nm after 4 h at 37 °C for uPA (120 pmol) alone (uPA control) or incubated with aptamers (600 pmol). Incubation with PAI−1 was carried out as a positive control for specific inhibition of uPA. The DNA-library was used as a control to demonstrate sequence-dependent inhibition. PAI−1 control and tested aptamers showed significant inhibition of the uPA activity (p <0.01). The absorbance for each sample is shown as the mean value of three independent experiments (number of records n = 3). Error bars represent the standard deviation. p-values were determined by Welch's t-test.

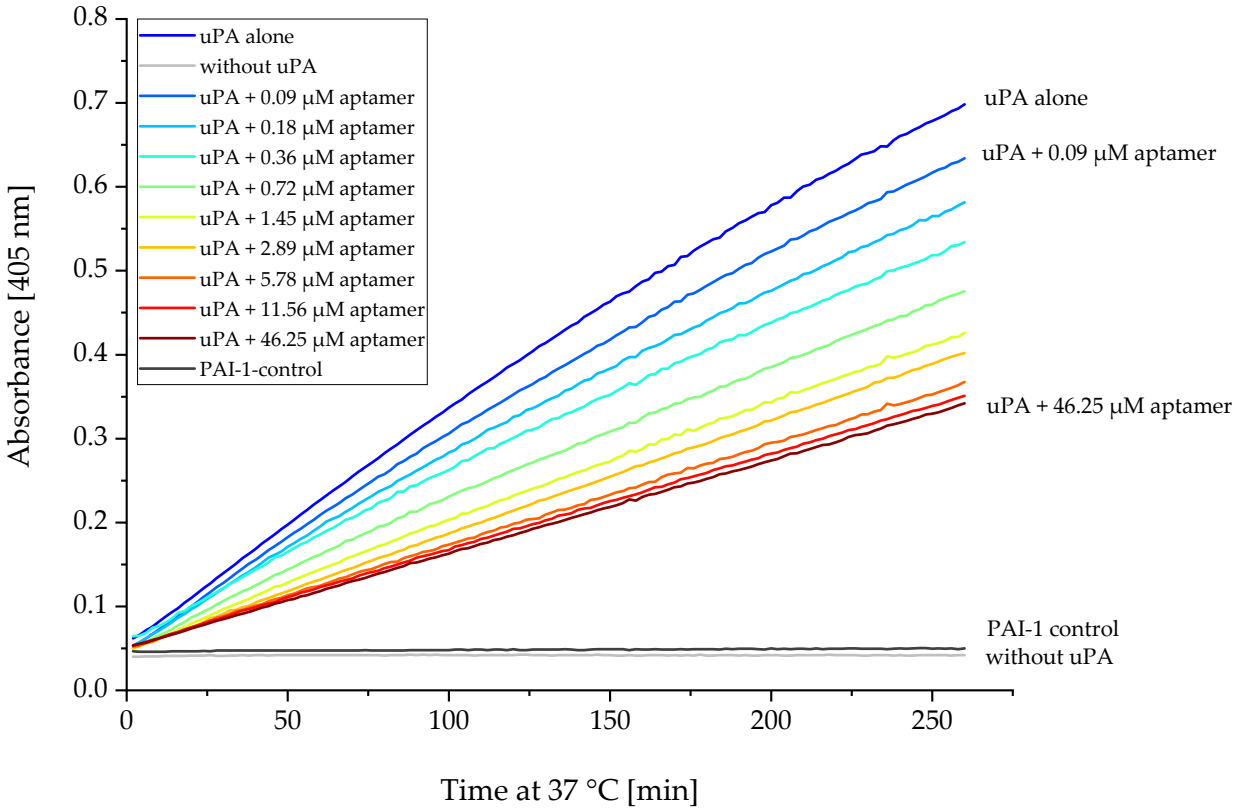

Figure 9. uPA activity inhibition by uPAapt−02−FR. uPA activity was measured by the hydrolysis of the chromogenic substrate. Absorbance was measured at 405 nm over 2 h 20 min at 37 °C in the presence of increasing concentrations of uPAapt−02−FR (0.09, 0.18, 0.36, 0.72, 1.45, 2.89, 5.78, 11.56 and 46.25 μM). Here, uPAapt−02−FR showed a dose-dependent effect on the inhibition of uPA activity, with a substantial reduction in the conversion of the chromogenic peptide substrate. While samples added with PAI−1 served as a positive control, uPA (0.46 μM) alone was used as a negative control. Samples that did not contain uPA were also included as controls. The absorbance for each sample is shown as the mean value of technical replicates. Number of records $n = 2$.

3. Discussion

In this study, we present novel ssDNA aptamers that can not only target different uPA forms and block the interaction of uPA with its receptor but also inhibit the proteolytic activity of uPA. To the best of our knowledge, no other aptamers that can bind in the region of the SPD and inhibit uPA activity have been reported to date. Dupont et al. [19] demonstrated that a 2′-F-pyrimidine-modified RNA aptamer with high affinity and specificity can inhibit the accumulation of uPA-catalyzed plasminogen activation on cell surfaces by binding to the GFD of uPA and thereby blocking uPA-uPAR interaction. None of their selected aptamers were reported to bind near to or at the serine protease domain and thereby block uPA activity [19]. Through binding of the 2′-fluoro-pyrimidine-modified RNA aptamers upanap-126 and upanap-231 from Botkjaer et al. [20] to the catalytic domain of pro-uPA, the proteolytic conversion of pro-uPA to the active two-chain HMW-uPA form was inhibited, but no inhibition of plasminogen activation could be achieved. This suggests that binding inhibited pro-uPA activation rather than direct uPA-mediated plasminogen activation. However, upanap-126 significantly affected tumor cell intravasation and dissemination in vivo due to the inhibition of pro-uPA activation, competing with the binding of pro-uPA to uPAR and preventing the binding of the pro-uPAR/uPAR complex to the glycoprotein vitronectin [20].

We selected novel ssDNA aptamers against HMW- and LMW-uPA that—in addition to binding to the ATF of uPA, which is already known from other aptamers—also bind

in the region of the catalytic domain. Several different aptamers were identified that showed binding either to HMW-uPA or to both uPA forms using different characterization methods [23]. Hence, we assumed that aptamers must have different binding sites. However, results for some aptamers vary based on the method used to determine binding characteristics, and therefore, are not explicit for every aptamer. EMSA is a label- and immobilization-free method to detect binding to protein targets in a cost-effective, easy and quick way. However, this qualitative method tends to detect only binders with high affinity to their target. According to the manufacturer, the fluorescent dye Invitrogen™ Quant-iT™ OLIGREEN™ (Thermo Fisher Scientific Inc., Waltham, MA, USA), which was used in the FLAAs, exhibits significant base selectivity. Therefore, intercalation of the fluorescent dye is primarily sequence-dependent. Additionally, the structure of aptamers will probably also influence the intercalation of the dye. This must be accounted for when evaluating these methods since the sequence of an aptamer and its associated structure play a very important role in binding to the target. Here, it may be that some aptamers stain particularly well, while others do not, which seems to be independent of binding strength to the target. As a result, well-binding sequences may be lost in FLAAs.

Therefore, other quantitative methods like SPR or MST, which are more sensitive, were used. However, quantitative methods also have limitations. In SPR experiments, aptamers are immobilized preferably on the sensor surface, which can affect the access to the aptamer binding site and the aptamer structure. Both can be influenced, for example, by the coupling position of the aptamer (5′- or 3′-end or any internal position), additionally used spacer molecules or non-specific interactions with the matrix surface. While uPAapt-03 and uPAapt-27 showed binding to LMW-uPA in FLAA experiments, no binding was detected in SPR. Loss of binding may indicate that immobilization of the aptamer impacts the binding activity of uPAapt-03 and uPAapt-27 to LMW-uPA. The proposal that aptamers can bind LMW-uPA by various methods may be confirmed by their ability to inhibit uPA activity. In particular, uPAapt-01, uPAapt-02 and uPAapt-03 showed binding to LMW-uPA in the region of the serine protease domain, which was confirmed by the inhibitory effect on the uPA activity. In addition, uPAapt-27 showed a very small effect on the catalytic activity, which confirms that it likely binds near the catalytic domain and affects enzymatic cleavage through steric hindrance. In addition to classical competitive inhibition, binding between the aptamer and target protein can affect protein folding itself, resulting in a type of non-competitive inhibition. Interestingly, uPAapt-01 showed binding to LMW-uPA, while its truncated version uPAapt-01-FR only bound to HMW-uPA and no longer inhibited uPA activity. This is a good example of how the constant primer regions of aptamers may affect the structure and thus also the binding properties. Here, the part that also binds to LMW-uPA might have been cut off. The structure of an aptamer is in a chemical equilibrium of the most energetically favorable conformation. Therefore, an aptamer can form different structures whereby one structure is usually predominant in a buffer solution. This could be another explanation, i.e., that the LMW-uPA binding structure can likely no longer be formed since different structures are formed within one sequence. Accordingly, uPAapt-03 and uPAapt-27 showed no further binding to LMW-uPA in SPR since the sequences have a certain orientation due to immobilization on the sensor surface, and thus, also a certain structure.

Although uPAapt-21 also showed binding to both uPA-forms by various methods, it could not inhibit uPA activity. Interestingly, uPAapt-21 showed the best inhibitory effect on uPA-uPAR binding. While we were unable to determine a specific binding site, we hypothesize that binding of uPAapt-21 results in a steric hindrance near the GFD on HMW-uPA, which is responsible for binding to uPAR. Previously, the size and shape of an aptamer and the domain organization of a multi-domain protein like uPA were shown to provide the basis for extensive sterical interference with protein-ligand interactions [24,25]. Dupont et al. showed that the effect of an aptamer does not always depend on the binding site, which can be somewhere else [24,25]. Here, epitope mapping of the different aptamers by microarray or X-ray crystallography and NMR-spectroscopy

could provide information on different binding epitopes or different structural formations of the aptamer-uPA complex [26]. Aptamers such as uPAapt-08 and uPAapt-26, which showed distinct binding only to HMW-uPA and were, therefore, assumed to bind to ATF, showed an inhibitory effect on uPA-uPAR binding.

Overall, we could select novel ssDNA aptamers with different binding behaviors and inhibitory effects either attributable to the binding regions or the structure that binds to uPA. Inhibition of uPA activity and the mere binding of uPA to its receptor uPAR is an important task to prevent tumor growth, invasion and metastasis [4,5]. While some aptamers showed no inhibitory effect or only inhibited uPA-uPAR binding, all aptamers inhibiting uPA activity showed additional inhibition of the formation of the uPA-uPAR complex, even if not as strong as those that can only inhibit uPA-uPAR binding. A uPA-directed inhibitor that blocks formation of the uPA-uPAR complex and uPA activity is of great advantage as it has been shown that most blocking agents serve as antagonists to uPA-uPAR interaction by binding to uPAR, which still induces the downstream interactions of the uPA-uPAR complex [19]. Using synthetic or naturally occurring inhibitors like aptamers with low molecular weight is also a more cost-effective and feasible approach than the use of antibodies, and expression of PAI-1 is hampered by poor pharmacokinetics and pharmacodynamics [8]. Since our selected aptamers showed different properties affecting uPA, they may serve as promising agents in therapeutics as they interfere with the pathological function of the uPA system.

However, our studies were only performed in situ and inhibition of uPA activity was tested only with an artificial chromogenic substrate. Looking ahead, it would be interesting to determine whether the aptamers can also prevent plasminogen activation in solution, as well as cell surface-associated plasminogen activation, and whether they inhibit binding of uPA to uPAR on cell surfaces to inhibit associated downstream processes. To see if the use of these aptamers inhibits tumor cell invasion in vitro and in vivo would also be of great interest. In addition, many new questions arise: whether the aptamers also affect uPA-PAI-1 binding or plasmin-catalyzed pro-uPA activation, or if aptamers can block receptor-mediated endocytosis of the uPA-PAI-1 complex. However, since DNA is susceptible to nucleases, before in vitro or in vivo use, it may be expedient to stabilize the aptamers against nuclease degradation, for example, by chemical modification [27]. In addition to their use in therapy, they could also be of interest for analytics due to their simple synthesis and modifications, as uPA is also used as a prognostic and diagnostic marker. Since aptamers showed different binding sites, their use in different assay formats—especially in a sandwich assay format for detecting uPA—would be of particular interest.

4. Materials and Methods

4.1. Target Preparation

Native high-molecular-weight uPA (HMW-uPA) isolated from human urine was purchased from ProSpec-Tany TechnoGene Ltd. (Ness-Ziona, Israel). To select aptamers against both uPA forms, the low-molecular-weight form of uPA (LMW-uPA) was obtained by autocatalytic conversion [28]. For this purpose, HMW-uPA was dissolved in PBS at a concentration of 1.0 µg/µL and incubated at 37 °C for a minimum of 32 days. To obtain 33 kDa LMW-uPA, the sample was purified and concentrated using a Nanosep® Centrifugal Device with Omega™ Membrane 30 K (Pall Corporation, New York, NY, USA). Complete conversion and purity of LMW-uPA were determined by SDS-gel electrophoresis [29] (Figure A2). For further use, both uPA forms were biotinylated separately using EZ-Link™ Sulfo-NHS-SS-Biotin (Thermo Fisher Scientific Inc., Waltham, MA, USA) according to the manufacturer's instructions.

4.2. Oligonucleotides and Semiautomatic In Vitro Selection

A single-stranded DNA oligonucleotide library with a theoretical diversity of 1.9×10^{25} was used as a precursor pool for aptamer selection. A 42-nt random sequence was flanked by a constant 20-nt primer region on each side (5′-AGGTAGAGGAGCAAGCCATC-(N42)-

GATGCGTGATCGAACCTACC-3′). Aptamers were selected using a semiautomatic process as previously described [30]. Before selection, ssDNA was refolded. To do so, the ssDNA-library was heated to 90 °C for 3 min and then slowly (for about 30 min) cooled to 25 °C in binding buffer BPs-T (50 mM Bis-Tris/HCl pH 6.5, 110 mM NaCl, 5 mM $MgCl_2$, 1 mM $CaCl_2$, 1 mM KCl, 0.05% *v/v* Tween® 20, Carl Roth GmbH + Co. KG, Karlsruhe, Germany). The ssDNA library was obtained from three different providers (Noxxon Pharma AG, Berlin, Metabion GmbH, Planegg, AptaIT GmbH; Planegg, Germany). A molar mixture from these three different providers (25% from Noxxon Pharma AG, 25% from Metabion GmbH and 50% from AptaIT GmbH) was used for the first round of selection to work with an optimized equal base distribution on every randomized base position. To select aptamers against HMW- and LMW-uPA, selection was carried out separately for each uPA form. To do so, the refolded ssDNA was incubated separately with the biotinylated uPA forms for 60 min at room temperature in BPs-T. After incubation, biotinylated LMW- or HMW-uPA with the bound ssDNA was coupled with streptavidin-coated magnetic beads (Dynabeads M-280 streptavidin, Invitrogen Dynal AS, Oslo, Norway) to transfer them automatically for several washing steps. From selection round six, remaining streptavidin moieties were blocked with 20 µM biotin in BPs-T. To simplify the selection of matrix binders, preselection steps with uncoupled streptavidin beads (from selection round two) and biotin-blocked streptavidin beads (from selection round six) were carried out before uPA incubation. Extensive washing steps with the same buffer were performed after coupling to streptavidin-coated beads (and after blocking with biotin) to remove non-binding oligonucleotides. To observe specific enrichment of uPA-binding DNA sequences, uncoupled streptavidin beads were included in certain rounds of selection as a control. The uncoupled beads were treated separately under the same SELEX conditions. DNA sequences binding to the beads were eluted non-specifically with 8 M urea in BPs-T for 30 min at 65 °C and 900 rpm using a thermoshaker. From selection round six, an additional specific elution step was introduced—with 500 mM dithiothreitol (DTT) in BPs-T for 60 min—before unspecific elution, to reduce the disulfide bond of the EZ-Link™ Sulfo-NHS-SS-Biotin linked to the uPA-forms. Eluted fractions were precipitated with 2-propanol at −20 °C overnight. Precipitated DNA was amplified by PCR with 5′-AGG TAG AGG AGC AAG CCA TC-3′ used as the forward primer and 5′-biotin-C6-GGT AGG TTC GAT CAC GCA TC-3′ used as the reverse primer, which allowed for the subsequent purification of the aptamer strand by alkali denaturation on streptavidin magnetic beads [30]. Finally, after up to 12 selection rounds with the two uPA forms, enriched DNA pools of different selection rounds were sequenced using the next-generation sequencing (NGS) technique by GATC Biotech (Ebersbach, Germany), and the following sequence analysis was performed with COMPAS analysis software (AptaIT GmbH, Planegg, Germany).

4.3. Electrophoretic Mobility Shift Assay (EMSA)

To detect binding between the aptamer and target protein, an electrophoretic mobility shift assay [31] was carried out under native conditions on a 12% polyacrylamide gel (native PAGE) containing 0.5 x Tris-borate buffer (without EDTA) and 1 mM $MgCl_2$. Aptamers were refolded in BPs-T as described above. For interaction analysis of each uPA-form and aptamer, 45 pmol of each uPA form was incubated with 15 pmol of aptamer (for a 3:1 ratio) in a total volume of 15 µL BPs-T for 60 min at 300 rpm and 23 °C on a thermoshaker. Each aptamer (15 pmol), alone without protein, in a total volume of 15 µL BPs-T was carried along as a control. The aptamer alone and the aptamer-protein mixture were subjected to electrophoresis. To detect the difference between the free nucleic acid that migrates faster than the corresponding mixture if a protein-nucleic acid complex is formed, the polyacrylamide gel was stained with ethidium bromide and samples were visualized under UV light.

4.4. Fluorescent Dye-Linked Aptamer Assay (FLAA)

Fluorescence-based binding assays were carried out on a black Pierce™ streptavidin-coated high-capacity plate (Thermo Fisher Scientific Inc., Waltham, MA, USA) as previously described [32]. Before immobilization and between incubation steps, wells were washed three times with 300 µL BPs-T for 90 s at 300 rpm in a thermoshaker. The different biotinylated uPA forms (35 pmol) were immobilized in 100 µL BPs-T for 60 min in different wells. Subsequently, wells were incubated with 50 µM biotin in 200 µL BPs-T for 30 min to block remaining biotin-binding residues and provide the same surface structure as in the selection procedure on magnetic beads. Biotin-blocked wells without uPA were used as a no-target control (NTC). Before application, aptamers were refolded as previously described, and 32 pmol of refolded ssDNA in a total volume of 100 µL BPs-T was added to each well and incubated for 60 min at 23 °C. After washing for 90 s at 300 rpm, 100 µL of a 1:200 dilution of Invitrogen™ Quant-iT™ OLIGREEN™ (Fisher Scientific GmbH, Schwerte, Germany) in BPs-T was added to each well. Following an incubation step of 12 min, fluorescence (excitation 485 nm, emission 535 nm) was measured by multimode microplate reader Mithras^2 LB 943 Monochromator Multimode Reader (Berthold Technologies GmbH & Co. KG, Bad Wildbad, Germany). Due to space limitations, binding of the aptamers was tested using different microtiter plates. Therefore, signals of the DNA-library used as a control in each experiment were averaged from all experiments, and all aptamers were presented in one diagram. All aptamers were tested as duplicates.

4.5. Surface Plasmon Resonance Spectroscopy

Surface plasmon resonance (SPR) spectroscopy experiments [23] were performed using a Biacore™ T200 (GE Healthcare Bio-Sciences AB, Uppsala, Sweden)) at an operating temperature of 25 °C. To analyze the binding characteristics of aptamers to uPA forms and determine dissociation constants (K_Ds), biotinylated aptamers were immobilized as ligands on the sensor chip surface, while uPA forms served as analytes. Neutravidin was immobilized on an EDC/NHS-activated HC200M SPR Sensor Chip (XanTec bioanalytics GmbH, Düsseldorf, Germany) using a Biacore™ immobilization wizard at a flow rate of 20 µL/min. For this purpose, 0.2 M EDC and 0.1 M NHS were dissolved in 50 mM MES (2-(N-morpholino) ethane sulfonic acid) pH 5 and injected for 3 min. After activation, 20 µg/mL neutravidin dissolved in 10 mM acetate buffer pH 5.5 was injected for 2 min, followed by washing with double-distilled water (ddH_2O) for 10 min. Subsequently, remaining binding sites were blocked with 1 M ethanolamine for 7 min. To determine association and dissociation rates, as well as K_Ds of aptamer-uPA complexes, 5′-biotinylated aptamers were immobilized on neutravidin-coated HC200M sensor surfaces to a level of approximately 100 RU. For this, biotinylated aptamers (100 nM) were prepared in running buffer (BPs-T containing 0.005% *v/v* Tween® 20 instead of 0.05% Tween® 20, Carl Roth GmbH + Co. KG, Karlsruhe, Germany) and refolded as previously described. Each flow channel was immobilized with a different biotinylated aptamer, respectively, while channel one served as a reference channel without an aptamer. A sequence-unrelated control oligonucleotide (Con) with the sequence 5′-GGG AAT TCG AGC TCG GTA CCG TAC AGT ACT GCA TAT CTC ATA CTT CCT AGA TAC CAT CCC TGC AGG CAT GCA AGC TTG G-3′ was additionally analyzed for comparison and to demonstrate sequence-dependent binding. Remaining biotin-binding sites on charged channels and the reference channel were blocked with excess biotin (40 µM) for 2 min. Both uPA-forms, HMW- and LMW-uPA, were diluted in running buffer and concentrations ranging from 3.9 to 1 µM were applied on each flow channel at a flow rate of 30 µL/min with 3 min injections and a 5-min delay. The chip surface was regenerated by applying 20 mM Na_2CO_3 for 30 s at a flow rate of 10 µL min.

The uPA-uPAR inhibitory activity of the aptamers in SPR experiments was determined as previously described [19]. Here, human uPAR (human uPAR/CD87 protein, Sino Biological Inc., Beijing, China) was immobilized on an EDC/NHS-activated HC200M SPR Sensor Chip (XanTec bioanalytics GmbH, Düsseldorf, Germany) to approximately 500 RU

using a Biacore™ immobilization wizard at a flow rate of 10 µL/min. The reference surface and remaining binding sites were blocked with 1 M ethanolamine for 7 min. Human uPA (HMW-uPA) alone (20 nM) or together with refolded aptamers in different concentrations (3.9–2000 nM) was prepared in BPs-T and passed over the sensor surfaces at a flow rate of 30 µL/min for 90 s and a 3-min delay. Aptamers alone (125–2000 nM) were injected as well, to exclude the binding of aptamers to uPAR. The chip surface was regenerated with 100 mM acetic acid (pH 2.8) containing 0.5 M NaCl for 15 s at a flow rate of 20 µL/min. Before determination of IC_{50} values, all aptamers were screened for uPA-uPAR inhibitory activity by injecting uPA alone (20 nM) or together with individual aptamers (500 nM) over the sensor surface. All interactions were analyzed using Biacore™ BIAevaluation software (version 3.2, GE Healthcare Bio-Sciences AB, Uppsala, Sweden). Aptamers that showed the best results for inhibition of uPA binding to uPAR were selected for IC_{50} calculation. Response values of uPA in complex with different concentrations of each aptamer were plotted as a function of aptamer concentrations relative to the response of uPA without an aptamer. As repeated regeneration steps were conducted, binding of uPA to the sensor surface immobilized with uPAR reduced over the measurements. To include this in IC_{50} calculation, uPA was injected before each concentration series of the different aptamers, and loss of the signal was fitted using a polynomial regression model. Each uPA-aptamer-complex response was reduced by the calculated loss of signal. IC_{50} values were estimated by a nonlinear regression analysis, fitting the data to a dose-response function using OriginPro 2021 software (OriginLab Corporation, Northampton, MA, USA). The sequence-unrelated control oligonucleotide Con was analyzed for comparison and to demonstrate sequence-dependent inhibition. Two independent experiments were performed. The mean values of the relative response with the respective standard deviation were used for IC_{50} value determination.

4.6. Microscale Thermophoresis

Microscale thermophoresis (MST) experiments were performed on a Monolith NT.115 (NanoTemper Technologies, Munich, Germany) using standard capillaries. Measurements were performed at an MST power of 60% and excitation power ranging from 20 to 60%. In our work, 5′-cyanine 5-labeled aptamers were diluted to 20 nM in BPsT, refolded as previously described and used as the fluorescently labeled binding partner at a constant concentration. Serial dilutions of HMW- and LMW-uPA ranging from 0.1 to 333 nM were prepared in BPs-T. For pro-uPA (BioVision Inc., Milpitas, USA), mouse uPA (Abcam plc, England) and tissue-type plasminogen activator (tPA, EMD Millipore Corp., Burlington, VT, USA) concentrations ranged from 0.1 to 500 nM. In the research, 10 µL of refolded aptamer and protein dilutions was mixed and incubated for 30 min. Samples were measured by the Monolith NT.115. The recorded fluorescence was normalized to the Fnorm per mill and fitted utilizing the K_D formula derived from the law of mass action by MO Affinity Analysis software (NanoTemper Technologies GmbH, Munich, Germany) version 2.3 [33,34]. All measurements were performed as triplicates.

4.7. uPA Inhibition Assay

Inhibition of uPA activity was tested using a Chemicon® PAI Activity Assay Kit (Merck KGaA, Germany) according to the manufacturer's specifications with some modifications. Here, 10x BPs-T (500 nM Bis-Tris/HCl pH 6.5, 1.1 M NaCl, 50 mM $MgCl_2$, 10 mM $CaCl_2$, 10 mM KCl, 0.5% *v/v* Tween® 20, Carl Roth GmbH + Co. KG, Karlsruhe, Germany) was used as the assay buffer (15 µL for the aptamer samples and 20 µL for control samples). Individual aptamers were tested in a five-fold excess for inhibition of enzyme activity to obtain a ratio (aptamer:target) of 5:1. For each well, 600 pmol of aptamer was refolded in 50 µL BPs-T. Then, 10 µL 0.65 µg/µL uPA from the assay kit (equivalent to 120 pmol), alone or in the presence of individual refolded aptamers, was preincubated for 30 min at 23 °C and 350 rpm in a microtiter plate. DdH_2O was added to each sample to reach a total volume of 180 µL before preincubation. For the control (uPA alone), the aptamer solution

was replaced by 50 µL ddH_2O. For the uPA negative control, uPA was replaced by 10 µL ddH_2O. Activated plasminogen activator inhibitor (PAI-1) was prepared as described in the manufacturer's protocol and was used as a positive control. Here, the aptamer solution was replaced by 40 µL activated PAI-1 solution and 10 µL ddH_2O. To test inhibition by uPAapt-02-FR at various concentrations over time, a serial dilution of refolded uPAapt-02-FR ranging from 0.36 to 185 µM was prepared in BPs-T, and 50 µL of each dilution (equivalent to 18–9250 pmol) was preincubated with 10 µL uPA (0.5 µg/µL) from the assay kit (equivalent to 92.5 pmol) as previously described. Afterward, 20 µL of the chromogenic substrate (2.5 µg/µL tripeptide with a p-nitroanilide (pNA) group) was added to each well and hydrolysis was monitored by measuring the absorbance at 405 nm using the EnVision® 2105 multimode plate reader (PerkinElmer® Inc., Waltham, MA, USA). Samples were measured after incubation at 37 °C for 4 h or every 2 min at 37 °C over 4 h 20 min. Significant inhibition of the uPA activity by the different aptamers compared to uPA alone was tested by Welch's unequal variances t-test. Samples were tested as duplicates.

5. Conclusions

In this study, we demonstrated the selection of novel, highly affine and specific DNA aptamers up to 82-nt long by a semi-automatic in vitro selection process (SELEX), which can bind to different forms of human urokinase. Since they bind to different uPA forms, we can differentiate between high-molecular-weight uPA (HMW-uPA) and low-molecular-weight uPA (LMW-uPA). Therefore, we assume that our aptamers bind to different regions of uPA. High affinity and specificity for human uPA, as well as for the zymogen pro-uPA, was demonstrated by surface plasmon resonance (SPR) and microscale thermophoresis (MST). Furthermore, we found that aptamer binding inhibited the binding of uPA to its receptor uPAR and the proteolytic activity of uPA. Since uPA is a much-discussed marker for prognosis and diagnosis in various types of cancer, as well as a target for cancer therapies, our aptamers represent a promising tool for diagnostic applications and could serve as promising agents in therapeutics.

6. Patents

All aptamers used in this manuscript are protected by pending patents.

Author Contributions: Conceptualization, N.D. and M.M.M.; validation, N.D., J.W., W.S. and A.M.; formal analysis, N.D.; investigation, N.D., J.W., W.S., A.M. and D.V.V.; writing—original draft preparation, N.D.; writing—review and editing, N.D., W.S., A.M., D.C., S.F. and M.M.M.; visualization, N.D.; supervision, M.M.M.; project administration, M.M.M.; funding acquisition, S.F. and M.M.M. All authors have read and agreed to the published version of the manuscript.

Funding: This work was supported by the German Federal Ministry of Education and Research (BMBF) through the funding program SME Innovative (grant numbers 16SV6072 to M.M.M. and 16SV6070 to S.F.) and the German state of Brandenburg's Ministry for Science, Research and Culture (MWFK) through the funding program StaF (Strengthening Technological and Applied Research in Scientific Institutions, grant number 85017631 to M.M.M.). The APC was supported by the publishing fund of the Fraunhofer Society.

Institutional Review Board Statement: Not applicable.

Informed Consent Statement: Not applicable.

Data Availability Statement: The datasets for the current study are available from the corresponding author on request.

Conflicts of Interest: The authors declare no conflict of interest.

Appendix A

Table A1. Results of electrophoretic mobility shift assay (EMSA) for HMW−uPA and LMW−uPA.

Aptamer	EMSA	
	HMW−uPA	**LMW−uPA**
uPAapt−01	+	+
uPAapt−02	+	+
uPAapt−03	+	(+)
uPAapt−06	+	-
uPAapt-08	+	-
uPAapt−21	+	-
uPAapt−26	+	-
uPAapt−27	+	-

Note: + = binding, - = no binding, (+) = only light shift detected.

Table A2. On- and off-rates (k_a and k_d) including chi^2 and dissociation constants (K_Ds) from SPR measurements.

Aptamer	Target	k_a [M^{-1} s^{-1}]	K_d [s^{-1}]	K_D [M]	Chi^2
uPAapt−01	HMW−uPA	6.83×10^5	5.15×10^{-4}	7.54×10^{-10}	1.48
	LMW−uPA	7.24×10^4	1.57×10^{-3}	2.17×10^{-8}	0.02
uPAapt−01−FR	HMW−uPA	9.64×10^3	3.98×10^{-3}	4.13×10^{-7}	6.33
	LMW−uPA	-*	-*	-*	-*
uPAapt−02	HMW−uPA	1.28×10^6	2.77×10^{-4}	2.17×10^{-10}	1.49
	LMW−uPA	4.85×10^4	1.43×10^{-4}	2.95×10^{-9}	0.03
uPAapt−02−R	HMW−uPA	8.98×10^5	2.93×10^{-4}	3.26×10^{-10}	6.98
	LMW−uPA	6.55×10^4	3.75×10^{-4}	5.73×10^{-9}	0.02
uPAapt−02−FR	HMW−uPA	2.42×10^5	1.72×10^{-4}	7.08×10^{-10}	1.80
	LMW−uPA	2.47×10^4	5.30×10^{-4}	2.14×10^{-8}	0.02
uPAapt−03	HMW−uPA	1.94×10^5	6.50×10^{-4}	3.34×10^{-9}	0.02
	LMW−uPA	-*	-*	-*	-*
uPAapt−06	HMW−uPA	9.39×10^4	9.99×10^{-4}	1.06×10^{-8}	3.55
	LMW−uPA	-*	-*	-*	-*
uPAapt−08	HMW−uPA	2.14×10^4	8.53×10^{-4}	4.00×10^{-8}	0.20
	LMW−uPA	-*	-*	-*	-*
uPAapt−08−FR	HMW−uPA	7.77×10^2	1.57×10^{-4}	2.02×10^{-7}	0.47
	LMW−uPA	-*	-*	-*	-*
uPAapt−21	HMW−uPA	1.58×10^5	5.93×10^{-4}	3.77×10^{-9}	0.51
	LMW−uPA	4.74×10^4	2.78×10^{-3}	5.86×10^{-8}	0.05
uPAapt−26	HMW−uPA	1.90×10^5	2.46×10^{-4}	1.30×10^{-9}	0.64
	LMW−uPA	-*	-*	-*	-*
uPAapt−27	HMW−uPA	2.84×10^5	1.31×10^{-3}	4.59×10^{-9}	0.11
	LMW−uPA	-*	-*	-*	-*
uPAapt−27−FR	HMW−uPA	1.93×10^5	1.07×10^{-3}	5.54×10^{-9}	0.23
	LMW−uPA	-*	-*	-*	-*
Con	HMW−uPA	-*	-*	-*	-*
	LMW−uPA	-*	-*	-*	-*

Note: -*, no binding detected.

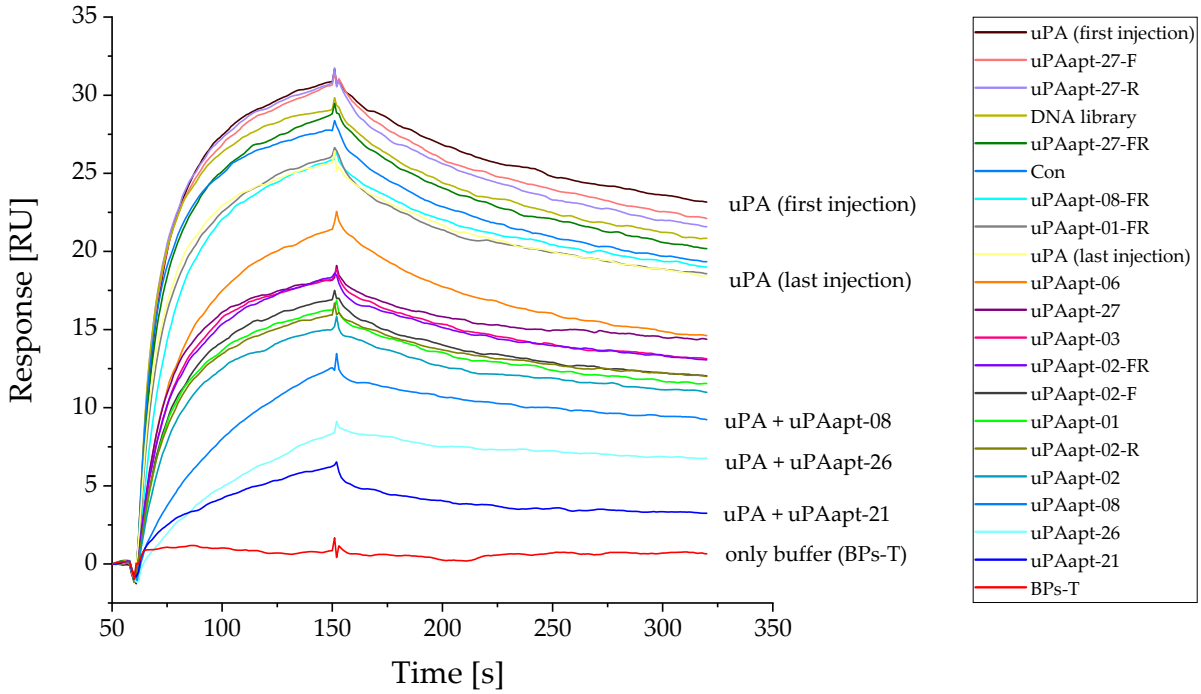

Figure A1. Screening of aptamers inhibiting uPA−uPAR binding. SPR sensograms showing each response unit (RU) over the time (s) for 20 nM human uPA alone or together with individual aptamers (500 nM) injected from 60 to 150 s on a sensor surface with immobilized human uPAR. As the ability of uPA binding to uPAR decreases due to the regeneration between each sample injection, binding of uPA alone was checked before and after aptamer injections.

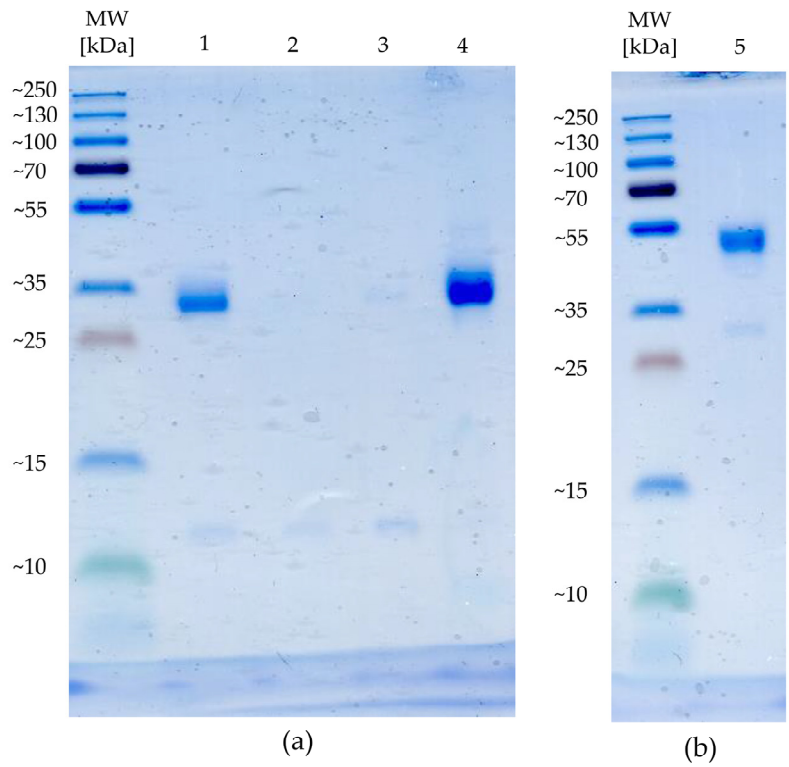

Figure A2. Analysis of the uPA forms by SDS-Page, whereby 1.5 µg of the different uPA forms was applied for analysis. (**a**) Complete conversion to LMW−uPA after incubation (1), first and second flow-through of the Nanosep® Centrifugal Device with Omega™ Membrane 30 K (2,3) and purified and concentrated LMW−uPA (4). (**b**) Analysis of HMW−uPA (5).

References

1. Mahmood, N.; Mihalcioiu, C.; Rabbani, S.A. Multifaceted Role of the Urokinase-Type Plasminogen Activator (uPA) and Its Receptor (uPAR): Diagnostic, Prognostic, and Therapeutic Applications. *Front. Oncol.* **2018**, *8*, 24. [CrossRef] [PubMed]
2. Higazi, A.; Cohen, R.L.; Henkin, J.; Kniss, D.; Schwartz, B.S.; Cines, D.B. Enhancement of the enzymatic activity of single-chain urokinase plasminogen activator by soluble urokinase receptor. *J. Biol. Chem.* **1995**, *270*, 17375–17380. [CrossRef] [PubMed]
3. Petersen, L.C.; Lund, L.R.; Nielsen, L.S.; Danø, K.; Skriver, L. One-chain urokinase-type plasminogen activator from human sarcoma cells is a proenzyme with little or no intrinsic activity. *J. Biol. Chem.* **1988**, *263*, 11189–11195. [CrossRef]
4. Mekkawy, A.H.; Pourgholami, M.H.; Morris, D.L. Involvement of urokinase-type plasminogen activator system in cancer: An overview. *Med. Res. Rev.* **2014**, *34*, 918–956. [CrossRef] [PubMed]
5. Masucci, M.T.; Minopoli, M.; Di Carluccio, G.; Motti, M.L.; Carriero, M.V. Therapeutic Strategies Targeting Urokinase and Its Receptor in Cancer. *Cancers* **2022**, *14*, 498. [CrossRef] [PubMed]
6. Dupont, D.M.; Madsen, J.B.; Kristensen, T.; Bodker, J.S.; Blouse, G.E.; Wind, T.; Andreasen, P.A. Biochemical properties of plasminogen activator inhibitor-1. *Front. Biosci.* **2009**, *14*, 1337–1361. [CrossRef]
7. Li Santi, A.; Napolitano, F.; Montuori, N.; Ragno, P. The Urokinase Receptor: A Multifunctional Receptor in Cancer Cell Biology. Therapeutic Implications. *Int. J. Mol. Sci.* **2021**, *22*, 4111. [CrossRef]
8. Su, S.-C.; Lin, C.-W.; Yang, W.-E.; Fan, W.-L.; Yang, S.-F. The urokinase-type plasminogen activator (uPA) system as a biomarker and therapeutic target in human malignancies. *Expert Opin. Ther. Targets* **2016**, *20*, 551–566. [CrossRef]
9. Dass, K.; Ahmad, A.; Azmi, A.S.; Sarkar, S.H.; Sarkar, F.H. Evolving role of uPA/uPAR system in human cancers. *Cancer Treat. Rev.* **2008**, *34*, 122–136. [CrossRef]
10. Setyono-Han, B.; Stürzebecher, J.; Schmalix, W.A.; Muehlenweg, B.; Sieuwerts, A.M.; Timmermans, M.; Magdolen, V.; Schmitt, M.; Klijn, J.G.M.; Foekens, J.A. Suppression of rat breast cancer metastasis and reduction of primary tumour growth by the small synthetic urokinase inhibitor WX-UK1. *Thromb. Haemost.* **2005**, *93*, 779–786. [CrossRef]
11. Ossowski, L.; Russo-Payne, H.; Wilson, E.L. Inhibition of urokinase-type plasminogen activator by antibodies: The effect on dissemination of a human tumor in the nude mouse. *Cancer Res.* **1991**, *51*, 274–281. [PubMed]
12. Ma, D.; Gerard, R.D.; Li, X.Y.; Alizadeh, H.; Niederkorn, J.Y. Inhibition of metastasis of intraocular melanomas by adenovirus-mediated gene transfer of plasminogen activator inhibitor type 1 (PAI-1) in an athymic mouse model. *Blood* **1997**, *90*, 2738–2746. [CrossRef] [PubMed]
13. Muehlenweg, B.; Sperl, S.; Magdolen, V.; Schmitt, M.; Harbeck, N. Interference with the urokinase plasminogen activator system: A promising therapy concept for solid tumours. *Expert Opin. Biol. Ther.* **2001**, *1*, 683–691. [CrossRef]
14. Schmitt, M.; Harbeck, N.; Brünner, N.; Jänicke, F.; Meisner, C.; Mühlenweg, B.; Jansen, H.; Dorn, J.; Nitz, U.; Kantelhardt, E.J.; et al. Cancer therapy trials employing level-of-evidence-1 disease forecast cancer biomarkers uPA and its inhibitor PAI-1. *Expert Rev. Mol. Diagn.* **2011**, *11*, 617–634. [CrossRef]
15. Zhu, F.; Jia, S.; Xing, G.; Gao, L.; Zhang, L.; He, F. cDNA transfection of amino-terminal fragment of urokinase efficiently inhibits cancer cell invasion and metastasis. *DNA Cell Biol.* **2001**, *20*, 297–305. [CrossRef]
16. Sato, S.; Kopitz, C.; Schmalix, W.A.; Muehlenweg, B.; Kessler, H.; Schmitt, M.; Krüger, A.; Magdolen, V. High-affinity urokinase-derived cyclic peptides inhibiting urokinase/urokinase receptor-interaction: Effects on tumor growth and spread. *FEBS Lett.* **2002**, *528*, 212–216. [CrossRef]
17. Dupont, D.M.; Andersen, L.M.; Botkjaer, K.A.; Andreasen, P.A. Nucleic acid aptamers against proteases. *Curr. Med. Chem.* **2011**, *18*, 4139–4151. [CrossRef]
18. Liu, M.; Zaman, K.; Fortenberry, Y.M. Overview of the Therapeutic Potential of Aptamers Targeting Coagulation Factors. *Int. J. Mol. Sci.* **2021**, *22*, 3897. [CrossRef]
19. Dupont, D.M.; Madsen, J.B.; Hartmann, R.K.; Tavitian, B.; Ducongé, F.; Kjems, J.; Andreasen, P.A. Serum-stable RNA aptamers to urokinase-type plasminogen activator blocking receptor binding. *RNA* **2010**, *16*, 2360–2369. [CrossRef]
20. Botkjaer, K.A.; Deryugina, E.I.; Dupont, D.M.; Gårdsvoll, H.; Bekes, E.M.; Thuesen, C.K.; Chen, Z.; Ploug, M.; Quigley, J.P.; Andreasen, P.A. Targeting Tumor Cell Invasion and Dissemination In Vivo by an Aptamer That Inhibits Urokinase-type Plasminogen Activator through a Novel Multifunctional Mechanism. *Mol. Cancer Res.* **2012**, *10*, 1532–1543. [CrossRef]
21. Skrypina, N.A.; Savochkina, L.P.; Beabealashvilli, R.S. In Vitro Selection of Single-Stranded DNA Aptamers that Bind Human Pro-Urokinase. *Nucleosides Nucleotides Nucleic Acids* **2004**, *23*, 891–893. [CrossRef] [PubMed]
22. Zhou, J.; Rossi, J. Aptamers as targeted therapeutics: Current potential and challenges. *Nat. Rev. Drug Discov.* **2017**, *16*, 181–202. [CrossRef] [PubMed]
23. Thevendran, R.; Citartan, M. Assays to Estimate the Binding Affinity of Aptamers. *Talanta* **2022**, *238*, 122971. [CrossRef] [PubMed]
24. Dupont, D.M.; Thuesen, C.K.; Bøtkjær, K.A.; Behrens, M.A.; Dam, K.; Sørensen, H.P.; Pedersen, J.S.; Ploug, M.; Jensen, J.K.; Andreasen, P.A. Protein-binding RNA aptamers affect molecular interactions distantly from their binding sites. *PLoS ONE* **2015**, *10*, e0119207. [CrossRef]
25. Dupont, D.M.; Madsen, J.B.; Hartmann, R.K.; Tavitian, B.; Ducongé, F.; Kjems, J.; Andreasen, P.A. Protein-binding RNA aptamers affect molecular interactions distantly from their binding sites. *PLoS ONE* **2015**, *10*, e0119207, Correction in *PLoS ONE* **2015**, *10*, e0126782. [CrossRef]
26. Schmidt, C.; Perbandt, M.; Klussmann, S.; Betzel, C. Molecular characterization of a ghrelin-l-aptamer complex. *J. Mol. Struct.* **2020**, *1204*, 127510. [CrossRef]

27. Wang, R.E.; Wu, H.; Niu, Y.; Cai, J. Improving the stability of aptamers by chemical modification. *Curr. Med. Chem.* **2011**, *18*, 4126–4138. [CrossRef]
28. Nobuhara, M.; Sakamaki, M.; Ohnishi, H.; Suzuki, Y. A comparative study of high molecular weight urokinase and low molecular weight urokinase. *J. Biochem.* **1981**, *90*, 225–232. [CrossRef]
29. Gallagher, S.R. One-dimensional SDS gel electrophoresis of proteins. *Curr. Protoc. Mol. Biol.* **2006**, *10*. [CrossRef]
30. Wochner, A.; Cech, B.; Menger, M.; Erdmann, V.A.; Glökler, J. Semi-automated selection of DNA aptamers using magnetic particle handling. *Biotechniques* **2007**, *43*, 346–348. [CrossRef]
31. Garner, M.M.; Revzin, A. A gel electrophoresis method for quantifying the binding of proteins to specific DNA regions: Application to components of the Escherichia coli lactose operon regulatory system. *Nucleic Acids Res.* **1981**, *9*, 3047–3060. [CrossRef] [PubMed]
32. Wochner, A.; Glökler, J. Nonradioactive fluorescence microtiter plate assay monitoring aptamer selections. *Biotechniques* **2007**, *42*, 578–582. [CrossRef] [PubMed]
33. Sass, S.; Stöcklein, W.F.M.; Klevesath, A.; Hurpin, J.; Menger, M.; Hille, C. Binding affinity data of DNA aptamers for therapeutic anthracyclines from microscale thermophoresis and surface plasmon resonance spectroscopy. *Analyst* **2019**, *144*, 6064–6073. [CrossRef] [PubMed]
34. Breitsprecher, D.; Schlinck, N.; Witte, D.; Duhr, S.; Baaske, P.; Schubert, T. Aptamer Binding Studies Using MicroScale Thermophoresis. *Methods Mol. Biol.* **2016**, *1380*, 99–111. [CrossRef] [PubMed]

3.2 Manuscript II

Label-Free Determination of the Kinetic Parameters of Protein-Aptamer Interaction by Surface Plasmon Resonance

Nico Dreymann [1,2], Anja Möller [1] and Marcus M. Menger [1]

[1] Fraunhofer Institute for Cell Therapy and Immunology (IZI), Branch Bioanalytics and Bioprocesses (IZI-BB), D-14476 Potsdam, Germany
[2] Institute for Biochemistry and Biology, University of Potsdam, D-14476 Potsdam, Germany

Contributions:

- Designed the project supervised by Marcus M. Menger
- Designed and conducted parts of the experiments
- Interpreted and analyzed the data
- Designed all figures in this manuscript
- Wrote the manuscript

Published in Nucleic Acid Aptamers: Selection, Characterization, and Application

(Part of Methods in Molecular Biology, vol. 2570),

September 27, 2022

DOI: 10.1007/978-1-0716-2695-5_11

Chapter 11

Label-Free Determination of the Kinetic Parameters of Protein-Aptamer Interaction by Surface Plasmon Resonance

Nico Dreymann, Anja Möller, and Marcus M. Menger

Abstract

Due to their high specificity and affinity to target molecules, aptamers can be used as powerful tools in diagnostics, therapeutics, and environmental or food analytics. For the use in various applications, the detailed characterization of their binding behavior is an important step after selection to determine the interaction strength between the aptamer and its target and to find the best kinetics depending on the field of application. The surface plasmon resonance (SPR) spectroscopy is a powerful technology to investigate important parameters in molecular interaction, for example, kinetics, affinity, and specificity. The most-used system is the Biacore™ SPR system which comprises an optical biosensor for label-free monitoring of binding events in real time based on SPR. This biophysical phenomenon describes the changes in refractive index on a sensor surface which can be used to measure binding events and to determine kinetic constants. In this chapter, a detailed protocol for the determination of kinetic constants for protein-aptamer interaction is provided. An 82-nt long ssDNA aptamer which are targeted against human urokinase is used as a model system for determination of binding and dissociation constants using Biacore™ SPR technology. A detailed note section provides useful tips and pitfalls at the end of this chapter.

Key words Aptamer, Protein-aptamer interaction, Surface plasmon resonance, SPR, Binding constant, Dissociation constant, K_D, Kinetics, Urokinase-type plasminogen activator

1 Introduction

Urokinase-type plasminogen activator (uPA) is a serine protease which plays a key role in cancer progression by converting plasminogen to plasmin on cell surfaces [1]. This promotes several different pathways for tumorigenesis [2]. Therefore, uPA is widely discussed as a potential therapeutic target as well as a prognostic and diagnostic marker for human malignancies [3]. In the past, several nucleic acid aptamers were selected against serine proteases not only to use them for the detection of proteases in diagnostics but also to use them as protease inhibitors by targeting the proteolytic

Günter Mayer and Marcus M. Menger (eds.), *Nucleic Acid Aptamers: Selection, Characterization, and Application*, Methods in Molecular Biology, vol. 2570, https://doi.org/10.1007/978-1-0716-2695-5_11,
© The Author(s), under exclusive license to Springer Science+Business Media, LLC, part of Springer Nature 2023

Reproduced with permission from Springer Nature

activity [4]. The analysis of basic binding parameters is essential for the development of potential diagnostic or therapeutic aptamer candidates. The surface plasmon resonance (SPR) spectroscopy is a powerful technology for the quantification of the affinities of aptamer-target interaction. The most-used Biacore™ SPR system is a label-free technique to monitor non-covalent molecular interaction in real time [5]. This biophysical phenomenon occurs when polarized light strikes the gold surface of a biosensor chip. At a specific angle, light energy is transferred to the electrons on the gold film which causes the intensity of the reflected light to be reduced at a different angle, the so-called SPR-angle. As molecules bind to the sensor surface, there is a change in refractive index close to the sensor surface which causes a change in the SPR angle [6]. The Biacore™ SPR technology utilizes the change in SPR angle which is directly proportional to mass concentration of the material bound at the sensor surface. The change of SPR-angle is then plotted in real time in a sensogram with the SPR response given in response units (RU) against the time, whereas one RU indicates approximately 1 pg of protein per mm^2 on a Biacore™ CM5 biosensor chip. For the measurement of binding events between two molecules, one interacting partner (the ligand) is attached to the surface of a sensor chip, while the other interacting partner (the analyte) is injected with a constant flow and concentration over the sensor surface. If the analyte binds to the immobilized ligand, the mass on the surface changes, and a SPR response is recorded. After the analyte sample injection, running buffer flows over the surface of the sensor chip to allow monitoring of the dissociation of the analyte from the ligand. Low volume reagents (in microliter range) are required as the Biacore™ SPR system works with a microfluidic system and an integrated and automated liquid handling. Since SPR is highly sensitive, it can be used to determine equilibrium constants, such as the dissociation constant K_D. For this, a defined level of ligand is immobilized on the gold layer of a sensor chip, and the analyte is injected in a serial dilution over the surface. After each injection, the surface is regenerated to remove bound analyte completely, while the activity of the surface must be unaffected. The recorded SPR response for each injection is used to derive the binding constant by fitting the sensogram to a specific binding model [7]. Here we provide a detailed protocol for Biacore™ SPR system-based analysis of aptamer binding: An 82-nucleotide (nt) long ssDNA aptamer selected against human urokinase-type plasminogen activator was used for the determination of kinetic parameters [8, 9]. Therefore, the aptamer was immobilized as the ligand on the biosensor surface, while the protein was injected as the analyte to the sensor surface at different concentrations. Afterward, the data was fitted to a 1:1 *Langmuir* binding model to determine kinetic parameters, and a K_D of 6.19 nM could be calculated.

Reproduced with permission from Springer Nature

2 Materials

Unless indicated otherwise, prepare all solutions in ultrapure water and use analytical grade reagents (*see* **Note 1**). All reagents should be brought to room temperature before starting the experiment.

2.1 SPR Instrumentation

A variety of SPR instruments are on the market today [9]. The principle of all these optical biosensors is the same; one binding partner is immobilized on the sensor surface (ligand), and the other binding partner (analyte) is injected in a continuous flow of solution. A common instrument is the Biacore™ T200 SPR system (Cytiva, formerly GE Healthcare Life Sciences, Marlborough, United States) which is a versatile and precise SPR system for a wide range of high-quality molecular interaction data. The label-free monitoring of biological interaction can be measured with a high sensitivity from small compounds up to even viruses and whole cells in a fully automated process. Depending on the assay, data can be evaluated with the Biacore™ T200 Evaluation Software (version 3.2, GE Healthcare Bio-Sciences AB, Uppsala, Sweden), and parameters like kinetics, affinity, specificity, concentration, or epitope binning can be determined.

2.2 SPR Biosensor Chip

Equally to the variety of SPR instruments, there are a lot of different SPR biosensor chips based on the different instruments and fields of applications. One chip for the Biacore™ T200 SPR system consists of four flow channels, whereby each channel can be controlled individually. All chips consisting of a thin glass slide with a layer of gold. Different surface chemistries on the gold layer serves as the sensor surface. Various sensor surfaces are provided for different applications and to immobilize or capture a specific ligand (see manufacturer's instructions). In our experiment we are using the SPR biosensor chip HC200M (XanTec bioanalytics GmbH, Duesseldorf, Germany). This biosensor chip is suitable for Biacore™ T200 and has a medium density of a hydrogel layer of 200 nm linear polycarboxylates, therefore recommended for protein-DNA interaction analysis (*see* **Note 2**). Before use, SPR biosensor chips were stored at −20 °C.

2.3 Immobilization of Capture Molecule

1. 0.2 M EDC (1-Ethyl-3-(3-dimethylaminopropyl) carbodiimide).
2. 0.1 M NHS (N-Hydroxysuccinimide).
3. 1 M ethanolamine.
4. NaAc/HAc (sodium acetate) (pH 5.5).
5. 50 mM MES pH 5.0 (2-(N-morpholino) ethanesulfonic acid).
6. Neutravidin.
7. Ultrapure water.

Reproduced with permission from Springer Nature

2.4 Running Buffer and Reaction Partners

1. Aptamer binding buffer (BPs-T): 50 mM Bis-Tris-HCl (pH 6.5), 110 mM NaCl, 5 mM $MgCl_2$, 1 mM $CaCl_2$, 1 mM KCl, 0.005% v/v Tween20 (*see* **Note 1**).
2. 82 nucleotide long ssDNA chemically modified with a biotin molecule at 5′-end. The biotin-labeled aptamer was dissolved in water to a final concentration of 100 μM and stored at −20 °C.
3. Human urokinase (ProSpec-Tany TechnoGene Ltd., Ness-Ziona, Israel) was dissolved according to manufacturer's specification and stored at −20 °C upon use.

3 Methods

Prior to each experiment, you must ensure that the device is cleaned according to the manufactures protocol. To ensure that there are no residues from the cleaning procedure, the instrument must be primed with ultrapure water before starting the experiment. This also ensures that the microfluidic system is rinsed with fresh pure water. Before starting the experiment, the biosensor chip must be inserted into the instrument (*see* **Note 3**). All experiments were carried out at 25 °C. The temperature for the sample compartment was set to 20 °C.

3.1 Immobilization of Capture Molecule

For capturing of biotinylated DNA ligand, neutravidin was immobilized via amine coupling to the sensor surface of the HC200M chip (*see* **Note 4**). The polycarboxylates on the sensor surface are activated by EDC and NHS to form NHS ester for amine coupling of neutravidin. Afterward not coupled neutravidin is washed away with ultrapure water, and remained binding sites were blocked with 1 M ethanolamine.

1. Prepare a mixture of 0.2 M EDC and 0.1 M NHS in MES (pH 5.0) (*see* **Note 5**).
2. Dissolve neutravidin in 10 mM NaAc/HAc (pH 5.5) to a final concentration of 20 mg/mL (*see* **Note 6**).
3. Prepare ultrapure water for washing of the sensor surface and ethanolamine for blocking of remained reactive NHS ester.

All reagents should be prepared in separate tubes and afterward transferred to the given tubes for the sample rack of the instrument (*see* **Note 6**). For the immobilization of the chip, a *Wizard Template* must be created. When programming the *Wizard Template,* you must set how many channels of the chip should be loaded. To perform the immobilization of neutravidin, the *Wizard Template* for immobilization must be programmed as followed:

Reproduced with permission from Springer Nature

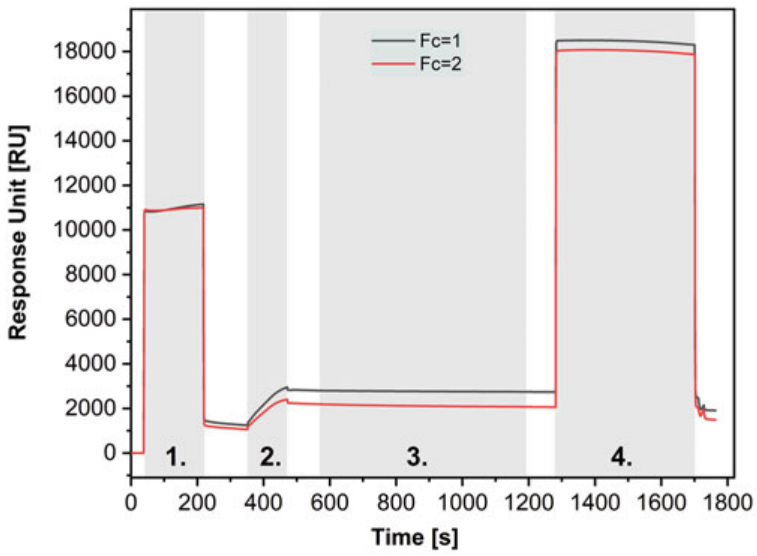

Fig. 1 Example of *Immobilization Wizard* results. The adjusted sensogram shows the injections and each response [RU] over the time [s] of the experiment. (1) Injection of 0.2 M EDC/0.1 M NHS; (2) Injection of 20 mg/mL neutravidin; (3) Injection of ultrapure water; (4) Injection of 1 M ethanolamine. Final response units (RU) for flow channel one (Fc = 1) is 1913 RU and for flow channel two (Fc = 2) 1496 RU

1. Injection of 0.2 M EDC/0.1 M NHS in MES (pH 5.0) for 180 s.
2. Injection of 20 mg/mL neutravidin in 10 mM NaAc/HAc (pH 5.5) for 120 s.
3. Injection of ultrapure water for 600 s.
4. Injection of 1 M ethanolamine for 420 s.

All injections were performed at a flow rate of 20 μL/min. For running buffer use ultrapure water (*see* **Notes 1** and **6**). Before starting the *Wizard Template*, you must determine where each sample is located in the sample rack and the device requires the minimum volume of each sample. After running the *Wizard Template*, the immobilization wizard results (final response units that has bound to the surface given in RU) are shown by the Biacore™ T200 control software. All data and sensograms can be shown in the Biacore™ T200 evaluation software (Fig. 1).

3.2 Ligand Immobilization on SPR Sensor Chip

The immobilized neutravidin on the sensor chip can then be used for capturing of biotinylated aptamer as the ligand.

1. Change running buffer of the instrument to aptamer binding buffer (BPs-T) and perform the *Prime* procedure of the instrument to ensure that all microfluidics are rinsed with binding buffer.
2. Before using the aptamer, it must be refolded in its specific binding buffer. Therefore, prepare the aptamer working stock by diluting the ligand to a concentration of 1 μM in BPs-T and

Reproduced with permission from Springer Nature

incubate at 92 °C for 3 min and slowly (for about 30 min) cool down to 25 °C (*see* **Note 7**).

3. For the injection of the aptamer, dilute the working stock further down in a 1:10 dilution to 100 nM in BPs-T.
4. Start a manual run with a flow rate of 20 μl/min.
5. Select the channel where the aptamer should be immobilized. Here, for example, flow channel two, while flow channel one is used as a reference without an immobilized aptamer (*see* **Note 8**).
6. Inject the prepared aptamer solution on flow channel two and stop by hand when the response unit reaches 100 RU (*see* **Note 9**).
7. Block remaining binding sites of neutravidin subsequently with an excess of biotin (40 μM biotin in BPs-T) for all used flow channels (for flow channel one used as reference without aptamer and for flow channel two with captured aptamer). Therefore, prepare 4 mM biotin solution in 50 mM NaOH and directly dilute it in a 1:100 dilution in BPs-T.
8. Inject the 40 μM biotin solution for 120 s on flow channel one and two.
9. To wash away excess of biotin, let the program run for a few minutes and stop the manual run.

The data of the manual run can then be viewed in the evaluation software to verify that the specified amount of biotinylated aptamer has been immobilized (Fig. 2).

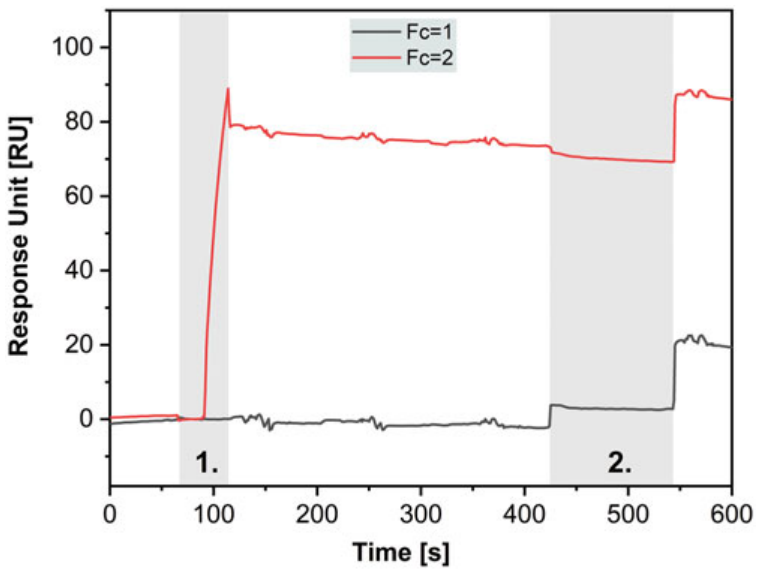

Fig. 2 Adjusted sensogram of the manual run. The sensogram shows the injections and each response [RU] over the time [s] of the experiment. (1) Injection of the aptamer solution only on flow channel two (Fc = 2). Injection was stopped after reaching 80 RU. (2) Injection of 40 μM biotin on both flow channels (Fc = 1 and Fc = 2)

Reproduced with permission from Springer Nature

3.3 Sample Preparation

For the determination of the dissociation constant (K_D) from a serial dilution, the concentration of the protein should be close to or below the expected K_D.

1. Pre-dilute the protein to 1000 nM with the aptamer binding buffer (*see* **Note 10**).
2. Prepare a 1:2 (v/v) serial dilution of the protein in the respective aptamer binding buffer up to 3.9 nM to end up in concentrations of 3.9 nM to 1000 nM.

3.4 SPR Measurement

Because the binding between aptamer and protein can usually be well resolved by high salt or change in pH value, multi-cycle kinetics is recommended for the determination of kinetics and affinity. For the multi-cycle kinetics, the sensor surface is regenerated after each analyte concentration which is injected in a separate analysis cycle. For regeneration of the surface of bound protein to aptamers, we recommend 20 mM Na_2CO_3 (*see* **Note 11**). The kinetic measurement is performed at a flow rate of 30 μL/min. For multi-cycle kinetics, it is recommended to start with a minimum of three running buffer injections to avoid buffer effects before starting with the serial dilution of the protein. Injection of running buffer will also be used as a blank in data analysis. To perform a multi-cycle kinetic, a new method must be created. Method template for the kinetic measurement must be programmed as followed:

1. Set *Data collection rate* on 1 Hz and *Detection* on dual (in case you charged all four flow channels of the chip, e.g., Channel 1 as reference and Channel 2–4 with aptamers, you need multi-detection). *Concentration unit* must be set on nM.
2. Name the assay step and change *Purpose* to *Sample*.
3. Insert a cycle type and insert two commands. One command for the different sample solutions of the analyte uPA and one for the regeneration of the sensor surface.
4. For the sample solutions set, *Type* on high performance and *sample solution* on variable. *Evaluation purpose* must set on kinetics/affinity. Enter contact time on 180 s and dissociation time on 600 s. As mentioned before, flow rate should be at 30 μL/min to avoid mass transport limitations and set flow path for the different channels.
5. For regeneration command, name the regeneration solution and set contact time on 30 s and flow rate on 10 μL/min. Here it is recommended to use Predip for the injection needle in the sample compartment and a stabilization period of 300 s.
6. Name the sample solutions and start with three times of buffer. For buffer set concentration (nM) on zero. Start then with your sample with the lowest concentration and fill table with ascending concentrations. Samples are injected in the order of the table, so it is very important to start with the lowest concentration.

Reproduced with permission from Springer Nature

7. If the method is verified by the software, you can setup the run and control the order of samples. To be sure that the system is rinsed with BPs-T as running buffer, you can choose *Prime* before run.
8. Prepare all samples in the given tubes of the sample rack and determine where each sample is located in the sample rack. The device requires the minimum volume for each sample and regeneration solution. After preparation, start the method.

3.5 Data Analysis

The kinetic parameters can be calculated using the Biacore™ T200 evaluation software provided by the manufacturer. Samples can be selected to display the different sensograms of each sample. When looking at the sensograms, it is important to check if the buffer samples do not show any binding compared to the samples. Different plots for quality control of the experiment can be viewed.

1. For determination of kinetic parameters load the acquired data and choose *Kinetic Screen*.
2. Choose data series of choice and the association and dissociation phases of the reference-subtracted sensograms are displayed. Curves are aligned at the start of injection with the baseline before injection set to zero. Include the curves for kinetic evaluation in the select curve window. Here, exclude seriously disturbed sensograms. It is recommended to include zero concentration samples as blanks which will be subtracted (*see* **Note 12**).
3. Choose fit settings and the right binding model for your binding partners. Here we are using 1:1 binding model since in most cases one ligand binds one aptamer. Nevertheless, there are other binding models available which should be considered (*see* **Note 13**).
4. After fitting the data using the standard algorithm, the quality control tab gives a brief overview of the reliability of the results. The residual plot shows the difference in RU between each data point in the experimental curves and the calculated curves. Here you can control how well the data fit to the chosen model as a first visual inspection. The residuals should be scatter randomly around zero and within the inner green limits (approximately ±1 to 2 RU). The fitted parameters like association rate, dissociation rate, and the calculated dissociation constant K_D as well as the fitted sensograms of the interaction are displayed in the report window. Several statistical parameters were calculated for the closeness of the fit between the experimental data and the fitted curve which are displayed in the parameters window. Additionally, a value for the mass transport contribution (t_c) is given in the report window which represents the flow-rate-independent component of

Reproduced with permission from Springer Nature

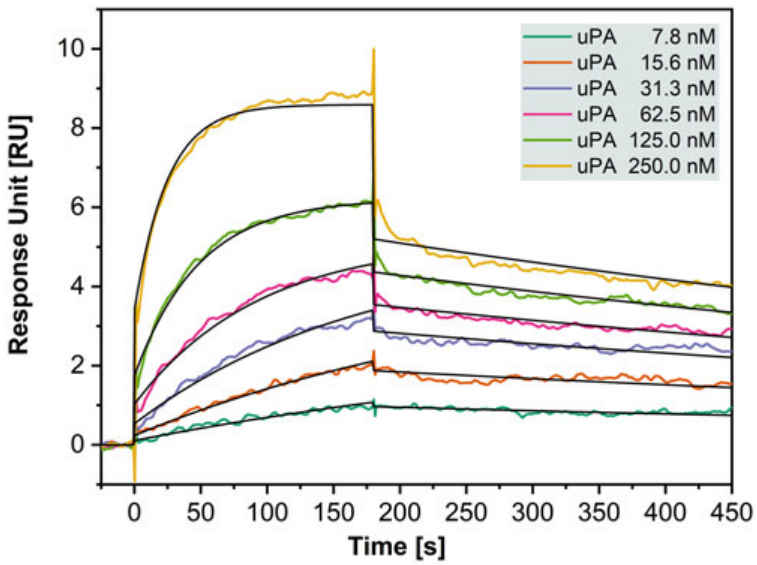

Fig. 3 SPR sensogram of aptamer-uPA interactions. The sensogram shows each response unit [RU] over the time [s] of six different urokinase concentrations (7.8, 15.6, 31.25, 62.5, 125, and 250 nM) which were overlaid and globally fitted to a 1:1 binding model to obtain values for rate and equilibrium constants

Table 1
Kinetic parameters with the respective standard error after fitting the data to the 1:1 binding model (k_a ≙ association rate constant, SE ≙ standard error, k_d ≙ dissociation rate constant, K_D ≙ dissociation constant, t_c ≙ mass transport contribution, Chi^2 ≙ chi-square, *U*-values ≙ uniqueness factor)

k_a (1/Ms)	SE(k_a)	k_d (1/s)	SE(k_d)	K_D (*M*)	t_c	SE(t_c)	Chi^2 (RU^2)	*U*-value
1,60E+05	3,00E+03	9,92E-04	1,40E-05	6,19E-09	8,09E+06	6,00E+06	0.0339	4

the mass transport coefficient (*see* **Note 14**). An example of the fitted sensograms is shown in Fig. 3 with its corresponding data shown in Table 1.

4 Notes

1. Only ultrapure water should be used for the microfluidic system of the device. Running buffer should always be filtered with a membrane filter (e.g., with a pore size of 0.2 μM) before use within the device.
2. To measure protein-aptamer interaction, it is recommended to capture the aptamer as a ligand via 5′-biotin or 3′-biotin to a neutravidin or streptavidin to the sensor surface. In our case, we load the chip surface with neutravidin by ourselves in order to determine the amount of neutravidin immobilized on the surface. However, there are also chips on the market that are already loaded with a defined amount of neutravidin or streptavidin to capture biotinylated molecules.

Reproduced with permission from Springer Nature

3. It is helpful to perform a DipCheck, to verify the biosensor chip works appropriately. To determine whether the device and the chip works sufficiently, it is advised to perform a manual run with pure water to ensure that the sensogram shows a stable signal without fluctuations.
4. It is also possible to immobilize the protein directly to the sensor surface as a ligand and using the aptamer as an analyte in solution. Here you can work, for example, with direct amine coupling of the protein to the surface. However, this is a random immobilization of the protein by its free amino groups which can be near by or a part of the binding epitope. As a result the binding epitope can be inaccessible if the protein is immobilized by these amino groups. If the protein is used as an analyte in solution, it is fully accessible, and it is more likely that the aptamer can spread its full structure by immobilization via 5′-biotin or 3′-biotin. An additional molecular spacer between the functional coupling group (here biotin) and the aptamer ligand can be helpful to avoid steric hindrance and to enable optimal binding of the analyte to the ligand.
5. Prepare the activation reagent shortly before starting the immobilization wizard to ensure reactivity.
6. If a higher level of immobilized neutravidin is needed, either a higher concentration can be used, or the injection time can be extended. For a more exact amount of immobilized neutravidin on each channel, here is also the option of selecting the *Immobilized Ligand* setting and specifying an RU value. In this case, the device automatically performs small, short injections until the specified RU number is reached. Before performing the immobilization wizard, it is recommended to perform a manual run with ultrapure water to rinse the sensor chip. We are using ultrapure water because aptamer-binding buffer contains primary amines which can interfere with the NHS ester while amine coupling of neutravidin. It is also possible to use the general purpose running buffer HBS-EP+ for use in Biacore™ T200 (Cytiva, formerly GE Healthcare Life Sciences, Marlborough, United States).
7. The binding buffer and refolding protocol can be individual for each aptamer.
8. One flow channel should always be used as a reference (negative control). Here we are using a flow channel without immobilized aptamer. However, it is also recommended to use a scrambled control DNA for the reference channel. If a protein is used as a ligand, it is also recommended to use an unrelated protein of approximately the same size for the reference channel as a control. Only channels one or three can serve as a reference, and controls on the reference channel should be immobilized with the same RU as the ligands being tested.

Reproduced with permission from Springer Nature

Kinetic measurements should always be performed with reference-subtracted data. When the ligand is captured, capturing molecule should be immobilized on both the reference and active surfaces and ligand injected over the active surface only.

9. Reaching the exact amount on each flow channel is sometimes difficult. When analyzing more than one flow channel, try to capture the same amount of RU (~100 RU). The captured aptamer should not reach over 150 RU. Low immobilization or capture levels reduce limiting effects of mass transport limitations and allows a better data interpretation.
10. To avoid bulk effects it is important that both reactants are dissolved in the same buffer as the running buffer. To remove other buffer components from the stock solutions, it is recommended to dialyze the reactants against the running buffer (BPs-T). Bulk effects can occur due to differences in the refractive index of running buffer and sample solution.
11. To remove bound analyte completely from the surface, we are using 5 μL of 20 mM Na_2CO_3. If that is not enough, other high salt solutions or solutions with low or high pH value can be used (see manufacturer's specifications). It is important to remove bound analyte completely from the surface, while the activity of the surface remains unaffected. Efficient regeneration is crucial for high-quality data. Therefore, it is important to test the regeneration of the surface after regeneration with a second injection of the same analyte which reveals whether the ligand is still fully active.
12. The first injection (buffer injection) is never reliable and should not be used for blank subtraction.
13. The simplest model is the 1:1 Langmuir binding model. For determination of association and dissociation rate constants, the experimental data is fitted to a 1:1 interaction model between analyte A and ligand B by the following equation:

$$A + B \underset{k_d}{\overset{k_a}{\rightleftharpoons}} AB$$

where k_a is the association rate constant ($M^{-1}\ s^{-1}$) and k_d is the dissociation rate constant (s^{-1}).

The equilibrium dissociation constant (K_D) is calculated by

$$K_D = \frac{k_a}{k_d}$$

14. Standard error (SE) is given for each parameter separately to show its significance. In statistics, the T-value can be calculated which is shown as the parameter value divided by the

Reproduced with permission from Springer Nature

standard error to simplify the comparison of the significance of each parameter. The T-value should at least higher than 50 (better is higher than 100). Chi-square (Chi^2) is calculated for the closeness of fit as the average square residual (the difference between the experimental data and the fitted curve) as:

$$Chi^2 = \frac{\sum_{1}^{n} (r_f - r_x)^2}{n - p}$$

where r_f is the fitted value at a given point, r_x is the experimental value at the same point, n is the number of data points, and p is the number of fitted parameters. The uniqueness factor (U-value) estimates the uniqueness of the calculated values for rate constants and should be below 15 which means that the parameter values are not significantly correlated. A high U-value (above 25) indicates that the reported kinetic constants contain no useful information. Mass transport contribution (t_c) can be ignored if the t_c-value is 100-fold higher than the reported k_a and the SE-value indicates that t_c is not significant (according to Biacore™ Application Guides).

Acknowledgments

This work was supported by the German state of Brandenburg, Ministry for Science, Research, and Culture (MWFK) within the funding program StaF (Strengthening technological and applied research in scientific institutions, grant number 85017631 to M.M.M.).

References

1. Mahmood N, Mihalcioiu C, Rabbani SA (2018) Multifaceted role of the Urokinase-Type Plasminogen Activator (uPA) and Its Receptor (uPAR): diagnostic, prognostic, and therapeutic applications. Front Oncol 8:24. https://doi.org/10.3389/fonc.2018.00024
2. Mekkawy AH, Pourgholami MH, Morris DL (2014) Involvement of urokinase-type plasminogen activator system in cancer: an overview. Med Res Rev 34(5):918–956. https://doi.org/10.1002/med.21308
3. Su SC, Lin CW, Yang WE, Fan WL, Yang SF (2016) The urokinase-type plasminogen activator (uPA) system as a biomarker and therapeutic target in human malignancies. Expert Opin Ther Targets 20(5):551–566. https://doi.org/10.1517/14728222.2016.1113260
4. Dupont DM, Andersen LM, Botkjaer KA, Andreasen PA (2011) Nucleic acid aptamers against proteases. Curr Med Chem 18(27): 4139–4151. https://doi.org/10.2174/092986711797189556
5. Jason-Moller L, Murphy M, Bruno J (2006) Overview of Biacore systems and their applications. Curr Protoc Protein Sci Chapter 19:Unit 19 13. https://doi.org/10.1002/0471140864.ps1913s45
6. Pattnaik P (2005) Surface plasmon resonance: applications in understanding receptor-ligand interaction. Appl Biochem Biotechnol 126(2): 79–92. https://doi.org/10.1385/abab:126:2:079
7. Fivash M, Towler EM, Fisher RJ (1998) BIAcore for macromolecular interaction. Curr Opin

Reproduced with permission from Springer Nature

Biotechnol 9(1):97–101. https://doi.org/10.1016/s0958-1669(98)80091-8

8. Dreymann N, Wuensche J, Sabrowski W, Moeller A, Czepluch D, Vu Van D, Fuessel S, Menger MM (2022) Inhibition of human Urokinase-Type Plasminogen Activator (uPA) enzyme activity and receptor binding by DNA aptamers as potential therapeutics through binding to the different forms of uPA. Int J Mol Sci 23(9):4890. https://doi.org/10.3390/ijms23094890
9. Schasfoort RBM, Tudos AJ (2008) Handbook of surface plasmon resonance. RSC Pub, Cambridge, UK

Reproduced with permission from Springer Nature

3.3 Manuscript III

Aptamer-based Sandwich Assay Formats for Detection and Discrimination of Human High- and Low-Molecular-Weight uPA for Cancer Prognosis and Diagnosis

Nico Dreymann [1,2], Wiebke Sabrowski [1,3], Jennifer Danso [1,4] and Marcus M. Menger [1,*]

[1] Fraunhofer Institute for Cell Therapy and Immunology (IZI), Branch Bioanalytics and Bioprocesses (IZI-BB), D-14476 Potsdam, Germany
[2] Institute for Biochemistry and Biology, University of Potsdam, D-14476 Potsdam, Germany
[3] Institute of Chemistry and Biochemistry – Biochemistry, Freie Universität Berlin, D-14195 Berlin, Germany
[4] Berliner Hochschule für Technik (BHT), D-13353 Berlin, Germany
[*] Correspondence: marcus.menger@izi-bb.fraunhofer.de (M.M.M.); Tel.: +49-331-58187-316

Contributions:

- Designed and planned the study supervised by Marcus M. Menger
- Designed and conducted most of the experiments
- Analyzed, evaluated and interpreted the data
- Designed all figures in this manuscript
- Wrote the manuscript

Published in Cancers,

October 25, 2022

DOI: 10.3390/cancers14215222

cancers

MDPI

Article

Aptamer-Based Sandwich Assay Formats for Detection and Discrimination of Human High- and Low-Molecular-Weight uPA for Cancer Prognosis and Diagnosis

Nico Dreymann [1,2], Wiebke Sabrowski [1,3], Jennifer Danso [1,4] and Marcus M. Menger [1,*]

[1] Fraunhofer Institute for Cell Therapy and Immunology (IZI), Branch Bioanalytics and Bioprocesses (IZI-BB), D-14476 Potsdam, Germany
[2] Institute for Biochemistry and Biology, University of Potsdam, D-14476 Potsdam, Germany
[3] Institute of Chemistry and Biochemistry, Freie Universität Berlin, D-14195 Berlin, Germany
[4] Berliner Hochschule für Technik (BHT), D-13353 Berlin, Germany
* Correspondence: marcus.menger@izi-bb.fraunhofer.de; Tel.: +49-331-58187-316

Simple Summary: Urokinase-type plasminogen activator (urokinase, uPA) is a widely discussed biomarker for cancer prognosis and diagnosis. The gold standard for the determination of protein biomarkers in physiological samples is the enzyme-linked immunosorbent assay (ELISA). Here, antibodies are used to detect the specific protein. In our study, recently published urokinase aptamers were tested for their use in a sandwich assay format as alternative specific recognition elements. Different aptamer combinations were used for the detection of uPA in a sandwich-assay format and a combination of aptamers and antibodies additionally allowed the differentiation of human high and low molecular weight- (HMW- and LMW-) uPA. Hence, uPA aptamers offer a valuable alternative as specific recognition elements for analytical purposes. Since aptamers are easy to synthesize and modify, they can be used as a cost-effective alternative in sandwich assay formats for the detection of uPA in physiological samples.

Abstract: Urokinase-type plasminogen activator (urokinase, uPA) is a frequently discussed biomarker for prognosis, diagnosis, and recurrence of cancer. In a previous study, we developed ssDNA aptamers that bind to different forms of human urokinase, which are therefore assumed to have different binding regions. In this study, we demonstrate the development of aptamer-based sandwich assays that use different combinations of these aptamers to detect high molecular weight- (HMW-) uPA in a micro titer plate format. By combining aptamers and antibodies, it was possible to distinguish between HMW-uPA and low molecular weight- (LMW-) uPA. For the best performing aptamer combination, we calculated the limit of detection (LOD) and limit of quantification (LOQ) in spiked buffer and urine samples with an LOD up to 50 ng/mL and 138 ng/mL, respectively. To show the specificity and sequence dependence of the reporter aptamer uPAapt−02−FR, we have identified key nucleotides within the sequence that are important for specific folding and binding to uPA using a fluorescent dye-linked aptamer assay (FLAA). Since uPA is a much-discussed marker for prognosis and diagnosis in various types of cancers, these aptamers and their use in a micro titer plate assay format represent a novel, promising tool for the detection of uPA and for possible diagnostic applications.

Keywords: ALISA; aptamer; biomarker; cancer prognosis; early stage cancer detection; ELONA; sandwich assay; uPA; urokinase

check for updates

Citation: Dreymann, N.; Sabrowski, W.; Danso, J.; Menger, M.M. Aptamer-Based Sandwich Assay Formats for Detection and Discrimination of Human High- and Low-Molecular-Weight uPA for Cancer Prognosis and Diagnosis. *Cancers* **2022**, *14*, 5222. https://doi.org/10.3390/cancers14215222

Academic Editor: Victor M. Gonzalez

Received: 21 September 2022
Accepted: 22 October 2022
Published: 25 October 2022

Publisher's Note: MDPI stays neutral with regard to jurisdictional claims in published maps and institutional affiliations.

Copyright: © 2022 by the authors. Licensee MDPI, Basel, Switzerland. This article is an open access article distributed under the terms and conditions of the Creative Commons Attribution (CC BY) license (https://creativecommons.org/licenses/by/4.0/).

1. Introduction

Early cancer detection and therapy are one of the most important tasks of today's medicine as the number of cancer incidences is increasing and, according to the World Health Organization (WHO), will rise rapidly in the next years. Many studies have focused

on the molecular level of tumor development, using aberrant expression of various proteins as potential targets for cancer therapy or biomarkers for cancer diagnosis. Compared to traditional histological characterization of tumors, they enable impressive progress as a non-invasive alternative for cancer prognosis and diagnosis [1].

Urokinase-type plasminogen activator (urokinase, uPA) is one of the many proteins involved in various processes necessary for cancer progression and is therefore widely discussed as a potential therapeutic target and a prognostic and diagnostic marker for human malignancies [2,3]. Urokinase is a serine protease consisting of 411 amino acid residues. Through cleavage of the K158-I159 bridge by several proteases, uPA is activated to the two-chain high molecular weight uPA (HMW-uPA). It is composed of the N-terminal A-chain containing the growth factor domain (GFD) and the kringle domain (KD), and the C-terminal B-chain containing the catalytically active serine protease domain (SPD), both linked by a disulfide bond. Further cleavage between Lys135 and Lys136 of HMW-uPA results in two fragments—the amino terminal fragment (ATF) with the GFD and KD, and the C-terminal catalytic domain that forms the catalytically active low molecular weight uPA (LMW-uPA) [3].

While the ATF (especially the GFD) is responsible for binding to the uPA receptor (uPAR), the catalytic domain of uPA is responsible for the conversion of plasminogen into plasmin, which promotes proteolysis of fibrinogen into fibrin and degradation of the extracellular matrix [3]. This is crucial for the early steps of tumor progression by promoting the expansion of tumor mass and release of tumor growth factors, as well as inducing tumor cell proliferation, migration, invasion, and angiogenesis [4].

Elevated expression of uPA is shown in many different types of cancer and mainly correlates with poor prognosis [3–5]. For example, high levels of uPA in breast cancer tissue extracts showed clinical significance in primary breast cancer patients and can be used as an independent prognostic biomarker of overall and relapse-free survival [6,7]. Therefore, the Tumor Marker Guideline of the American Society of Clinical Oncology (ASCO) recommended uPA biomarker testing by ELISA to assess the risk of recurrence in node negative breast cancer patients and to decide individually if adjuvant chemotherapy is beneficial after surgery [8]. In a recent study, it was shown that uPA can serve alongside other biomarkers as a prognostic marker in the blood of patients with metastatic breast cancer [9].

High levels of uPA were found in plasma of patients with prostate cancer, which is correlated with increased aggressiveness, postoperative progression, and metastasis [10,11]. Urokinase was suggested by Yang et al. [12] to be used as an independent prognostic factor for colorectal cancer patients' survival and metastasis. Herszéyi et al. [13] have proved that circulating uPA can be used as better prognostic markers than the commonly used colorectal cancer markers CEA and CA 19-9 as increased uPA levels could be detected in the blood of colorectal cancer patients. Increased uPA concentrations could also be found in the plasma of bladder cancer patients compared to healthy controls [14]. Recent studies showed that it could be used for personalized clinical decision-making. Concentrations of uPA showed the potential as a predictor for aggressiveness and worse survival outcomes in patients with urothelial carcinoma of the bladder after radical cystectomy and it was also associated with recurrence-free and cancer-specific survival [15].

Besides elevated uPA levels in different tumor tissues and blood, a higher uPA concentration was found in the urine of bladder cancer patients [16]. Shariat et al. [17] have shown that urinary uPA could be used as a diagnostic biomarker to improve the ability to predict bladder cancer besides cytology and other urinary biomarkers.

The enzyme-linked immunosorbent assay (ELISA) is the basic method for detection and determination of uPA concentrations, as it is still the gold standard for the detection of proteins in physiological samples. Commercially available kits using different antibodies in a sandwich-assay format allow the detection and determination of uPA concentrations in different samples. Besides antibodies, aptamers offer the possibility as alternative molecular recognition elements, as they recognize their targets with high specificity and

affinity comparable to antibodies. The single-stranded (ss) nucleic acid (ssDNA or RNA) molecules have the advantages that they are easy and cheap to produce, can easily be modified, are smaller in size, and are more chemically stable [18]. Therefore, aptamers are a promising tool for the detection of target molecules [19] and for in vitro detection strategies of cancer (e.g., cancer biomarkers) [20]. Hence, previously selected uPA aptamers were used to test whether they can be used as a substitute for antibodies in a sandwich assay format for analytical purpose, as they target different uPA epitopes [21].

In our study, we present the development of a novel aptamer-based sandwich assay (aptamer–target–aptamer; Figure 1a) using different aptamers for the detection of HMW-uPA. By combining different aptamers and antibodies, it was possible to detect both HMW-uPA and LMW-uPA in different sandwich assay formats (aptamer–target–antibody or antibody–target–aptamer; Figure 1b,c, respectively). For the best aptamer combination of the aptamer-based sandwich assay, the limit of detection (LOD) and limit of quantification (LOQ) was determined in buffer conditions, as well as spiked urine samples. For the best reporter aptamer uPAapt−02−FR, we have identified key nucleotides within the aptamer sequence that are important for the specific folding and binding to uPA demonstrating sequence dependence for specific detection of uPA. Since uPA is a much-discussed marker for prognosis and diagnosis in various types of cancer, the use of the aptamers in a sandwich assay format represents a novel, promising, and cost-effective tool for the detection of uPA and possibly for prognostic and diagnostic applications.

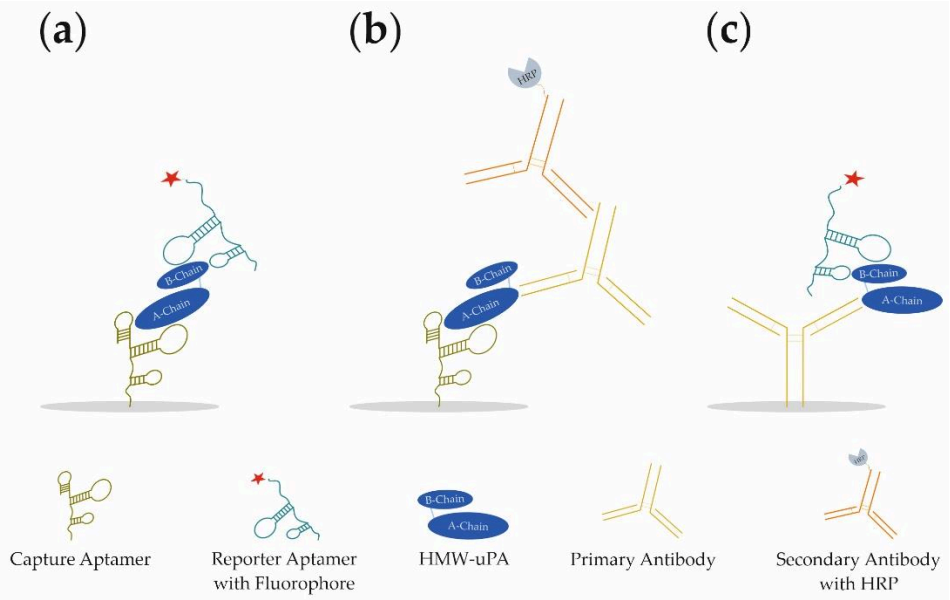

Figure 1. Schematic illustration of the three different sandwich assay formats developed for the detection of different forms of human urokinase. (**a**) Aptamer–Target–Aptamer, (**b**) Aptamer–Target–Antibody, and (**c**) Antibody–Target–Aptamer.

2. Materials and Methods

2.1. Urokinase and Aptamer Preperation

Native HMW-uPA isolated from human urine was purchased from ProSpec-Tany TechnoGene Ltd. (Ness-Ziona, Israel). LMW-uPA was prepared as previously described [21]. For the fluorescent-dye linked aptamer assays (FLAA), HMW-uPA was biotinylated using EZ-Link™ Sulfo-NHS-SS-Biotin (Thermo Fisher Scientific Inc., Waltham, MA, USA) according to the manufacturer's instructions. All chemicals were purchased from Carl Roth GmbH + Co. KG, Karlsruhe, Germany. Aptamers were obtained from three different providers (biomers.net GmbH, Ulm, Germany; IBA Lifesciences GmbH, Göttingen, Germany; Integrated DNA Technologies, Inc., Coralville, IL, USA).

All uPA aptamers [21] were tested in micro titer plate assay formats. For this purpose, 5′-biotinylated uPA aptamers were used as capture aptamers and 5′-Cyanine(Cy)-5-labled aptamers were used as reporter aptamers. Prior to use of aptamers in the respective assay formats, aptamers were refolded. Therefore, aptamers were diluted to a specific concentration in BPs-T (50 mM Bis-Tris/HCl pH 6.5, 110 mM NaCl, 5 mM $MgCl_2$, 1 mM $CaCl_2$, 1 mM KCl_2, 0.05% *v/v* Tween®20) and incubated it at 92 °C for 3 min and then slowly (for about 30 min) cooled to 25 °C. All solutions were prepared in a total volume of 100 µL if not indicated otherwise.

2.2. Aptamer-Based Sandwich Assay (Sandwich-ALISA)

For the development of an aptamer-linked immobilized sorbent assay (ALISA) in a sandwich format, 5′-biotinylated aptamers were used as capture aptamers on black Pierce™ streptavidin-coated high-capacity 96-well micro titer plates (Thermo Fisher Scientific Inc., Waltham, MA, USA). All incubation and washing steps were carried out at 23 °C and 300 rpm in a thermoshaker. Before immobilization of capture aptamers and between each incubation step, wells were washed thrice with 300 µL BPs-T for 90 s. For the immobilization of capture aptamers, 25 pmol of each refolded 5′-biotinylated aptamer in BPs-T was added to each well and incubated for 15 min. To block remaining biotin binding sites, wells were blocked subsequently with 5000 pmol biotin in BPs-T for 15 min. For binding of the two different uPA-forms, 40 pmol of HMW-uPA or LMW-uPA– either in BPs-T or human urine—was added to different wells and incubated for 30 min. Refolded 5′-Cy-5-labled aptamers were used as reporter aptamers for detection of captured uPA. Here, 32 pmol of refolded reporter aptamer in BPs-T was added to each well and incubated for 30 min. Subsequently, wells were washed thrice with BPs-T. Fluorescence was measured either by EnVision® 2105 multimode plate reader (excitation 620 nm, emission 685 nm, top mirror Cy5; PerkinElmer Inc., Waltham, MA, USA) or by multimode microplate reader Mithras^2 LB 943 (excitation 610 nm, emission 665 nm; Berthold Technologies GmbH & Co. KG, Bad Wildbad, Germany). The limit of detection and limit of quantification were calculated from three independent experiments, with each three technical replicates using a linear calibration curve. LOD and LOQ were calculated by the following formula: $3 \times \sigma/k$ and $10 \times \sigma/k$, respectively, where σ is the standard deviation of y-intercepts of regression lines and k is the slope of the calibration curve [22].

2.3. Fluorescent Dye-Linked Aptamer Assay (FLAA)

To identify relevant binding nucleotides, a fluorescence-based binding assay with the nucleotide-exchanged sequence aptamers was carried out on a black Pierce™ streptavidin-coated high-capacity 96-well micro titer plate (Thermo Fisher Scientific Inc., Waltham, MA, USA) as previously described [21]. All incubation and washing steps were carried out at 23 °C and 300 rpm in a thermoshaker. Before and between each incubation step, wells were washed thrice with 300 µL BPs-T for 90 s. Here, biotinylated HMW-uPA (35 pmol) was immobilized in 100 µL BPs-T for 60 min in different wells. Subsequently, wells were incubated with 50 µM biotin in 200 µL BPs-T for 30 min to block remaining biotin-binding residues. Biotin-blocked wells without uPA were used as a no target control (NTC). Before application, all nucleotide-exchanged sequences were refolded as previously described and 32 pmol of refolded aptamers in BPs T were added to each well and incubated for 60 min at 23 °C. After washing for 90 s at 300 rpm, 100 µL of a 1:200 dilution of Invitrogen™ Quant-iT™ OLIGREEN™ (Fisher Scientific GmbH, Schwerte, Germany) in BPs-T was added to each well. Following an incubation step of 12 min, fluorescence (excitation 485 nm, emission 535 nm) was measured by a multimode microplate reader Mithras^2 LB 943 Monochromator Multimode Reader (Berthold Technologies GmbH & Co. KG, Bad Wildbad, Germany). Binding of the nucleotide-exchanged sequence aptamers was tested using different micro titer plates. Therefore, uPAapt−02−FR was carried along in each experiment as the positive control. All new sequence aptamers as well as the positive control were tested as duplicates.

For the determination of the maximum binding capacity of capture aptamers immobilized on Pierce™ streptavidin-coated high-capacity 96-well micro titer plates, a modified version of the FLAA was used. Here, a 5′-biotinylated aptamer was incubated at different concentrations (0 pmol–100 pmol) in 100 µL BPs-T for 30 min in different wells. Subsequently, wells were washed thrice, incubated with 100 µL of a 1:200 dilution of Invitrogen™ Quant-iT™ OLIGREEN™ and measured as described above.

2.4. Aptamer–Antibody-Based Sandwich Assay

For the aptamer–antibody-based sandwich assay, 5′-biotinylated aptamers were used as capture aptamers on clear Pierce™ streptavidin-coated high-capacity plates (Thermo Fisher Scientific Inc., Waltham, MA, USA). Antibodies, binding either only HMW-uPA (binding to chain A of uPA) or binding HMW- and LMW-uPA (binding to chain B of uPA), were used for detection of different captured uPA-forms. All incubation and washing steps were carried out at 23 °C and 300 rpm in a thermoshaker. Before immobilization of capture aptamers and between each incubation step, wells were washed thrice with 300 µL BPs-T for 90 s. For the immobilization of capture aptamers, 25 pmol of each refolded 5′-biotinylated aptamer in BPs-T was added to each well and incubated for 60 min. To block remained biotin binding sites, wells were blocked with 5000 pmol biotin in 100 µL BPs-T for 60 min. For binding of the two different uPA-forms, 40 pmol of either HMW-uPA or LMW-uPA in BPs-T was added to different wells and incubated for 60 min. For the detection, two different antibodies were used. Anti-PLAU antibody (anti-PLAU antibody (AA16-115), ABIN562262, antibody-online GmbH, Aachen, Germany), which binds to Chain A of uPA, was used for detection of HMW-uPA (Ab Chain A). Anti-uPA antibody [U-16] (Anti-uPA antibody [U-16] ab131433, abcam, Cambridge, UK), which binds to Chain B of uPA, was used for detection of HMW- and LMW-uPA (Ab Chain B). Antibodies were diluted at a ratio of 1:4000 in Roti®Block (Carl Roth GmbH + Co. KG, Karlsruhe, Germany) and 100 µL of either Ab Chain A or Ab Chain B dilution was added to different wells and incubated for 30 min. A secondary polyclonal sheep anti-mouse IgG antibody labeled with horseradish peroxidase (A6782, Sigma-Aldrich, St. Louis, MO, USA) was used for detection of the primary antibodies. For this purpose, the secondary antibody was diluted at a ratio of 1:3000 in Roti®Block and 100 µL of the dilution was added to each well and incubated for another 30 min. Afterwards, each well was washed thrice with BPs-T and 100 µL of 1-Step™ Ultra TMB-ELISA Substrate Solution (Thermo Fisher Scientific Inc., Waltham, MA, USA) was added to each well. The reaction was stopped using 50 µL of 2 M H_2SO_4. Subsequently, the absorbance at 450 nm was measured by multimode microplate reader Mithras^2 LB 943.

2.5. Antibody–Aptamer-Based Sandwich Assay

For the antibody-aptamer based sandwich assay, different antibodies (binding either only HMW-uPA or binding HMW- and LMW-uPA) were used for capturing the different uPA forms on a black 96-well polystyrene micro titer plate (Fluotrac™ 600 high binding, Greiner Bio-One International GmbH, Frickenhausen, Germany). For detection of different captured uPA forms, 5′-Cy5-labled aptamers were used. All incubation and washing steps were carried out at 23 °C at 300 rpm in a thermoshaker. For immobilization, an excess of antibodies was used to achieve maximum coating of the wells. As the manufacturer specifies a maximum coating of 600 ng protein per cm^2, 800 ng of either anti PLAU antibody (Ab Chain A) or Anti-uPA antibody [U-16] (Ab Chain B) for binding of HMW- and LMW-uPA in 100 µL 1xPBS were incubated for 3 h. Before and after immobilization of antibodies, wells were washed thrice with 1xPBS for 90 s. To block remained binding sites, wells were blocked with blocking solution (1% *v/v* BSA, 10% *v/v* saccharose in 1xPBS) for another 3 h. Subsequently, wells were washed thrice with BPs-T for 90 s. Then, 40 pmol of the different uPA-forms in BPs-T were added to different wells and incubated for 60 min. After incubation, wells were washed thrice with BPs-T for 90 s. For the detection of the different uPA forms, 5′-Cy5-labled aptamers were used. Therefore, 32 pmol of refolded 5′-Cy5-

aptamers in BPs-T was added to each well and incubated for 30 min. Afterwards, wells were washed thrice with BPs-T for 90 s and fluorescence was measured by EnVision® 2105 multimode plate reader (excitation 620 nm, emission 685 nm, top mirror Cy5; PerkinElmer® Inc., Waltham, MA, USA).

3. Results

3.1. Aptamer-Based Sandwich Assay System for Detection of uPA (Sandwich-ALISA)

3.1.1. Design of the Aptamer-Based Sandwich Assay

Before testing different aptamer combinations for the aptamer-based sandwich assay, several considerations were made regarding the use of the concentrations of the capture aptamer, the target, and the reporter aptamer, and their respective ratios. To achieve a maximum immobilization of the capture aptamer, a modified FLAA was performed to obtain the maximum binding capacity of an aptamer to the streptavidin-coated wells. For this test, the smallest aptamer, uPAapt−08−FR, was used, as it was assumed that larger aptamers will also achieve the maximum coating of the wells at the same concentration. Results showed that no considerable increase of fluorescence signal was observed above 25 pmol aptamer (Figure 2).

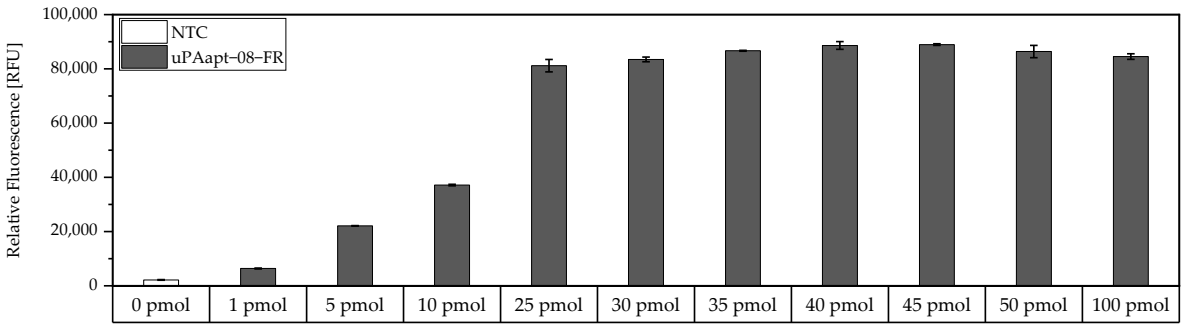

Figure 2. Binding of different amounts of 5′-biotinylated uPAapt−08−FR to the wells of the Pierce™ streptavidin coated high-capacity 96-well micro titer plate by a modified FLAA. Different amounts of uPAapt−08−FR were incubated in different concentrations (0 pmol–100 pmol in 100 µL BPs-T) to the wells to determine the maximum binding capacity for the smallest aptamer. After washing of the wells, followed by incubation with Invitrogen™ Quant-iT™ OLIGREEN™, a fluorescence signal of the immobilized aptamer could be measured. The relative fluorescence unit [RFU] for each sample is shown as the mean value of technical replicates and was measured using the multimode microplate reader Mithras^2 LB 943. Error bars represent the range of measured values. NTC = No Target Control (0 pmol). Number of records n = 2.

Therefore, 25 pmol capture aptamer were used for the micro titer plate assays to achieve an approximate maximum immobilization of capture aptamers. To add an excess of target, 40 pmol was added in each assay. However, if we assume that the complete 25 pmol of capture aptamers are immobilized and we assume a 1:1 binding model, theoretically, a maximum of 25 pmol target can be captured. In order to detect the entire amount of target, 32 pmol of reporter aptamer were used to also have an excess of the reporter aptamer. Consequently, a ratio of 1:1.6:1.3 (capture aptamer:target:reporter aptamer) was used in the following aptamer-based sandwich assay.

3.1.2. Combination of uPA-Aptamers Enabled Detection of HMW-uPA

Different combinations of uPA aptamers were tested for their functionality in an aptamer-based sandwich assay system to detect the different uPA forms. In order to find suitable aptamer pairs for the development of an aptamer-linked immobilized sorbent assay (ALISA), all full-length uPA aptamers (uPAapt−01, uPAapt−02, uPAapt−03, uPAapt−06, uPAapt−08, uPAapt−21, uPAapt−26, and uPAapt−27) were immobilized on a streptavidin coated micro titer plate via 5′-biotin modification to serve as capture aptamers. The full-

length aptamers uPAapt−02 and uPAapt−21 were selected as potential 5′-fluorescently labeled reporter aptamers due to their different binding properties [21]. Thus, selected capture and reporter aptamers were combined in a sandwich assay format using constant concentrations of HMW- or LMW-uPA. The results of the screening for possible aptamer combinations for HMW-uPA are shown in Figure 3.

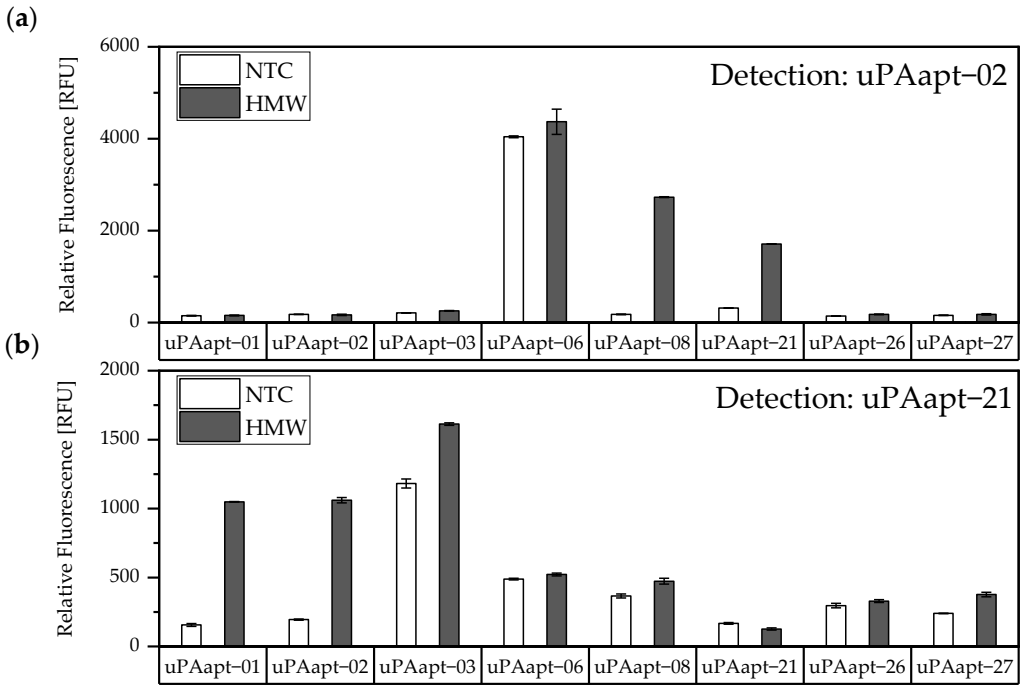

Figure 3. Screening for possible aptamer combinations for detection of HMW-uPA. All aptamers were tested for their use as capture aptamers when (**a**) uPAapt−02 or when (**b**) uPAapt−21 is used as the reporter aptamer. The relative fluorescence unit [RFU] for each sample is shown as the mean value of technical replicates and was measured using the multimode microplate reader Mithras^2 LB 943. Error bars represent the range of measured values. NTC = No Target Control, HMW = HMW-uPA. Number of records n = 2.

The results of the screening showed that different aptamer combinations were able to detect HMW-uPA. This supports the already suspected different binding sites. No signals were detected for LMW-uPA, indicating that these combinations of aptamers are not suitable to detect LMW-uPA and that tested aptamers may not have different binding sites on LMW-uPA (Figure 4).

Additionally, the aptamer combinations of uPAapt−06 and uPAapt−02, as well as uPAapt−03 and uPAapt−21, also showed high signals in the absence of uPA (NTC), which could arise from partial sequence complementarity and does not derive from an aptamer–target interaction. Consequently, these combinations were excluded from the study. Unspecific interactions between other capture and reporter aptamer combinations were not detected. No binding of uPA or the reporter aptamers to the streptavidin coated micro titer plate was detected.

Sandwich assays with suitable aptamer combinations for HMW-uPA were repeated using the EnVision® 2105 multimode plate reader and are shown in Figure 5. Suitable aptamer pairs were uPAapt−21 as a reporter aptamer and uPAapt−01 or uPAapt−02 as capture aptamers (Figure 5a) or uPAapt−02 as a reporter aptamer and uPAapt−08 or uPAapt−21 as capture aptamers (Figure 5b).

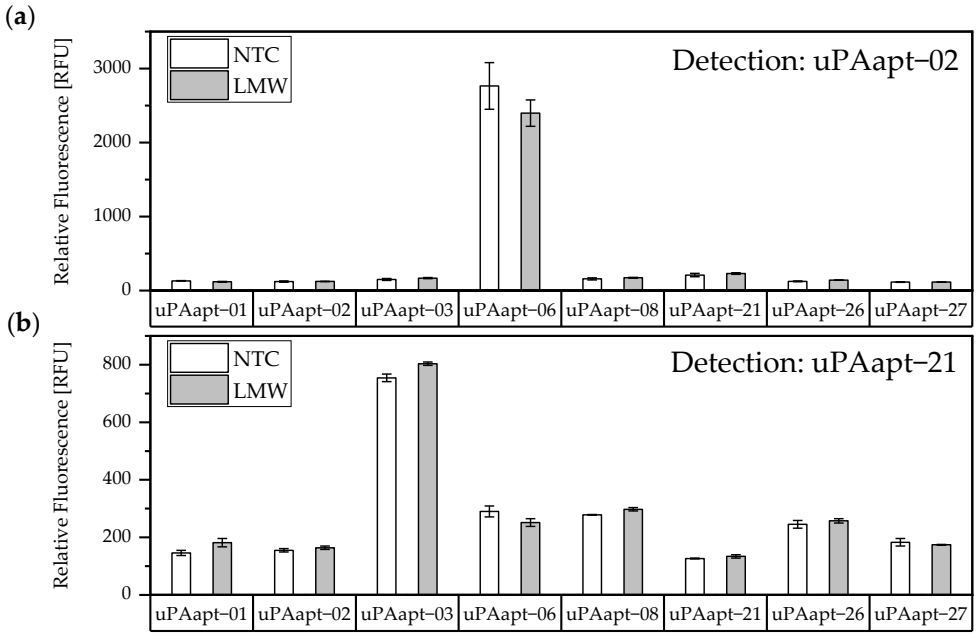

Figure 4. Screening for possible aptamer combinations for detection of LMW-uPA. All aptamers were tested for their use as capture aptamers when (**a**) uPAapt−02 or when (**b**) uPAapt−21 is used as the reporter aptamer. The relative fluorescence unit [RFU] for each sample is shown as the mean value of technical replicates and was measured using the multimode microplate reader Mithras^2 LB 943. Error bars represent the range of measured values. NTC = No Target Control, HMW = HMW-uPA. Number of records n = 2.

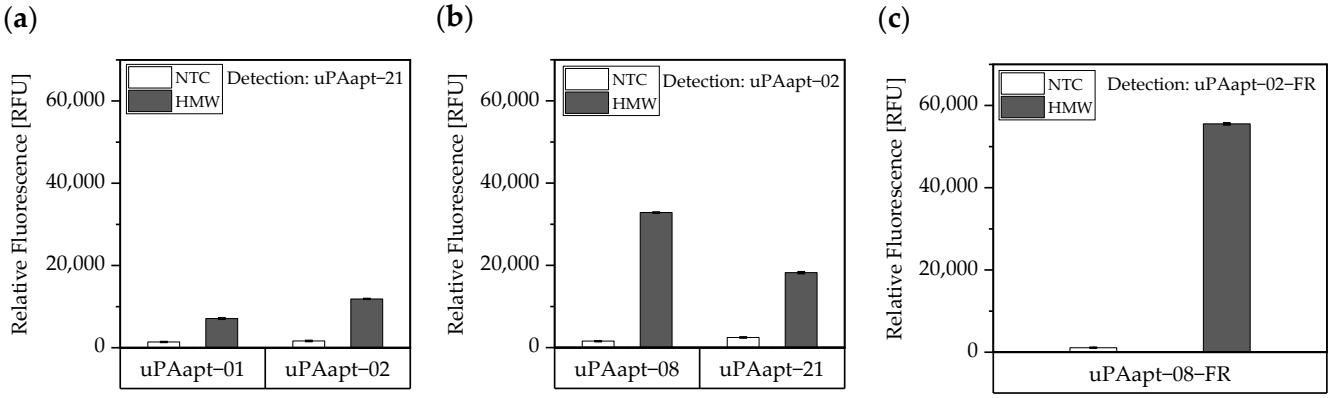

Figure 5. Aptamer-based sandwich assay for detection of HMW-uPA by different combinations of aptamers. HMW-uPA could be detected when (**a**) uPAapt−01 or uPAapt−02 are used as capture aptamers and uPAapt−21 as the reporter aptamer or when (**b**) uPAapt−08 or uPAapt−21 are used as capture aptamers and uPAapt−02 as the reporter aptamer or when (**c**) uPAapt−08−FR is used as a capture aptamer and uPAapt−02−FR as the reporter aptamer. The relative fluorescence unit [RFU] for each sample is given as the mean value of technical replicates and was measured using the EnVision® 2105 multimode plate reader. Error bars represent the range of measured values. NTC = No Target Control, HMW = HMW-uPA. Number of records n = 2.

As the combination of the full-length aptamers uPAapt−08 (capture aptamer) and uPAapt−02 (reporter aptamer) showed the highest signal for the detection of HMW-uPA, the fully truncated versions (truncated by both primer binding sites) uPAapt−08−FR and uPAapt−02−FR were tested in the aptamer-based sandwich assay. Combination of these two truncated aptamers revealed the highest signal for the detection of HMW-uPA compared to the full-length aptamers and thus serve as best performing aptamer pair for the aptamer-based sandwich assay (Figure 5c).

3.1.3. Aptamer-Based Sandwich Assay Showed a Detection Limit of 50 ng/mL in BPs-T and Still Detects up to 138 ng/mL HMW-uPA in Spiked Urine Samples

As studies have shown, elevated levels of uPA are found in urine from bladder cancer patients and uPA can serve as a diagnostic marker in human urine. Hence, it was tested whether the aptamer-based sandwich assay also works on human urine samples. For this purpose, human urine was collected on three different days and spiked with a constant concentration of 40 pmol HMW-uPA per well, individually. For comparison, the same was performed in BPs-T. Three independent experiments were performed with three technical replicates each. Results are shown in Figure 6a. Even though the signal was no longer as high as in BPs-T, it was demonstrated that the sandwich assay still showed a high signal compared to the no target control (NTC). To test its sensitivity, the LOD and the LOQ were determined by a linear calibration curve. Here, three independent experiments each with three technical replicates were performed. In each experiment a standard series ranging from 0–1.200 ng/mL HMW-uPA was prepared in BPs-T or human urine and the aptamer-based sandwich assay was performed. The calibration curves were obtained by plotting the measured relative fluorescence units (RFU) as a function of the HMW-uPA concentration. A linear dependence was found between the concentration of HMW-uPA and the measured RFU having a determination coefficient (R^2) for BPs-T and urine samples with 0.99 and 0.97, respectively. The LOD for the assay in BPs-T was calculated as 50 ng/mL and for spiked human urine as 138 ng/mL. The LOQ for BPs-T was 166 ng/mL and for spiked human urine 458 ng/mL (Figure 6b).

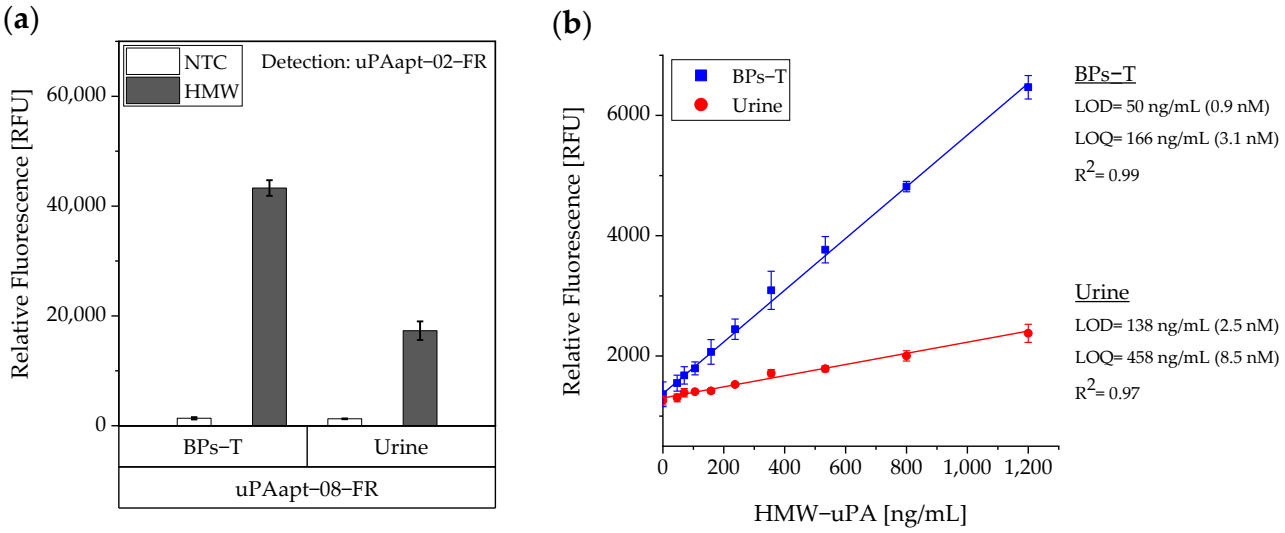

Figure 6. Sensitivity of the aptamer-based sandwich assay for detection of HMW-uPA by uPAapt−08−FR and uPAapt−02−FR in BPs-T and spiked urine samples. (**a**) Comparison of the aptamer-based sandwich assay in BPs-T and spiked urine at a constant concentration of 40 pmol HMW-uPA per well. (**b**) Determination of the sensitivity of the aptamer-based sandwich assay. Calibration curves were obtained by plotting the measured relative fluorescence unit as a function of the HMW-uPA concentration in a standard series. A linear dependence was found between the concentration of HMW-uPA and the measured relative fluorescence units [RFU]. The relative fluorescence is given as the average value of three independent experiments each with three technical replicates and was measured using the EnVision® 2105 multimode plate reader. Error bars represent the standard deviation. NTC = No Target Control, HMW = HMW-uPA. Number of records n = 3.

3.1.4. FLAA Experiments Revealed Key Nucleotides That Are Important for the Specific Folding and Binding of uPAapt−02−FR

As described above, uPAapt−02−FR served as the most promising detection aptamer. The specificity of the reporter aptamer uPAapt−02−FR for human uPA has already been described [21]. To evaluate sequence dependence and to identify key nucleotides within the

aptamer sequence, nucleotide exchange sequences were designed. Here, each nucleotide of the sequence was replaced individually (for G/C a T and for A/T a C) and all 42 new sequence aptamers (named Exchange-Sequence 1−42; Ex−S1–Ex−S42) were tested for binding to HMW-uPA by FLAA. The results of the FLAA and a table of all tested sequences are shown in Supplementary Figure S1 and Table S1, respectively. The results of the FLAAs are summarized in Figure 7. Here, the secondary structure of uPAapt−02−FR was visualized using the program mfold [23] which predicted a secondary structure containing two four-base hairpin loop motifs (tetraloops). Exchanged nucleotides for which the resulting aptamer showed a signal reduction of greater than or equal to 85% (Figure 7a), 90% (Figure 7b) or 95% (Figure 7c) compared to uPAapt−02−FR are circled in red. Using FLAA, it was shown that especially the second tetraloop within the sequence predicted by the program mfold appears to be important for the binding affinity to uPA. In conclusion, sequence dependence was shown for the formation of a specific structure that is important for the binding affinity to HMW-uPA.

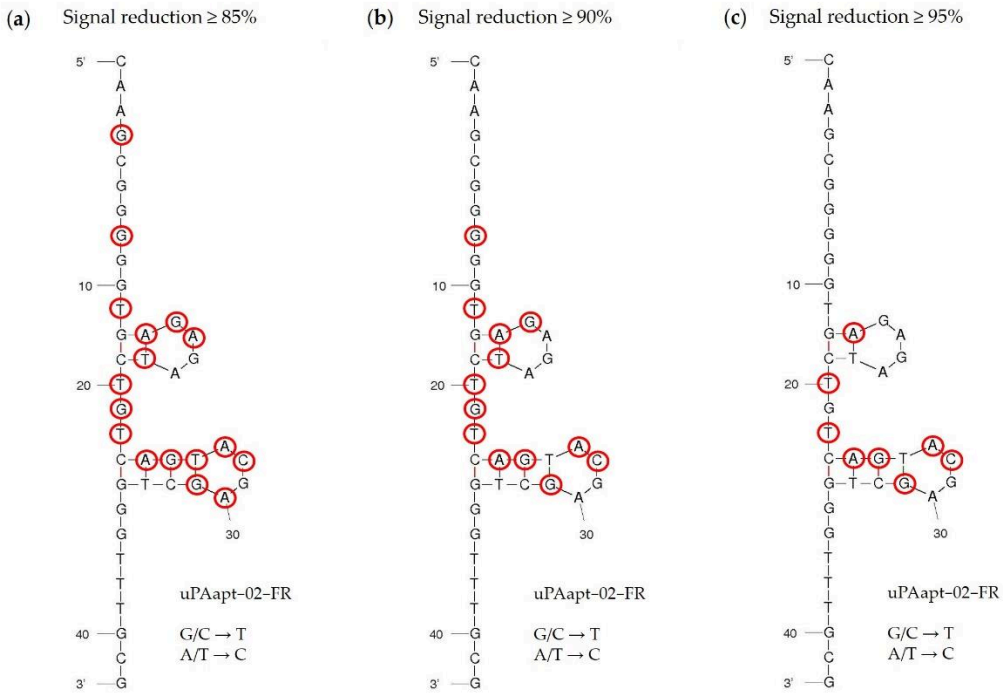

Figure 7. Secondary structure of the reporter aptamer uPAapt−02−FR predicted by mfold. All 42 nucleotides were replaced individually (for G/C a T and for A/T a C) and each sequence was analyzed for binding in FLAA. Exchanged nucleotides for which the resulting aptamer showed a signal reduction of (**a**) ≥85%, (**b**) ≥90%, or (**c**) ≥95% compared to uPAapt−02−FR are circled in red.

3.2. Combination of Aptamers and Antibodies in a Sandwich-Assay System for Detection and Discrimination of HMW- and LMW-uPA

The aptamer-based sandwich assay was developed as a tool suitable to detect HMW-uPA. However, LMW-uPA could not be detected. Therefore, different combinations of aptamers and antibodies were used to detect both forms of uPA and to distinguish between HMW-uPA and LMW-uPA. For comparability to the aptamer-based sandwich assay, the same concentrations of aptamers and targets were used.

3.2.1. Aptamer–Antibody Sandwich Assay

For the aptamer–antibody sandwich assay (sandwich ELONA—sandwich enzyme-linked oligonucleotide assay), the aptamers were used as capture molecules and the antibodies as reporter molecules. Here, all uPA aptamers and several truncated variants were used to capture HMW-uPA. Detection of captured HMW-uPA was shown by using the

Ab Chain A as a reporter molecule which only binds to HMW-uPA due to binding to the A-chain of human uPA (Figure 8). Results indicate that aptamers and Ab Chain A probably have different binding sites on HMW-uPA and that there is no steric hindrance between the aptamers and the antibody.

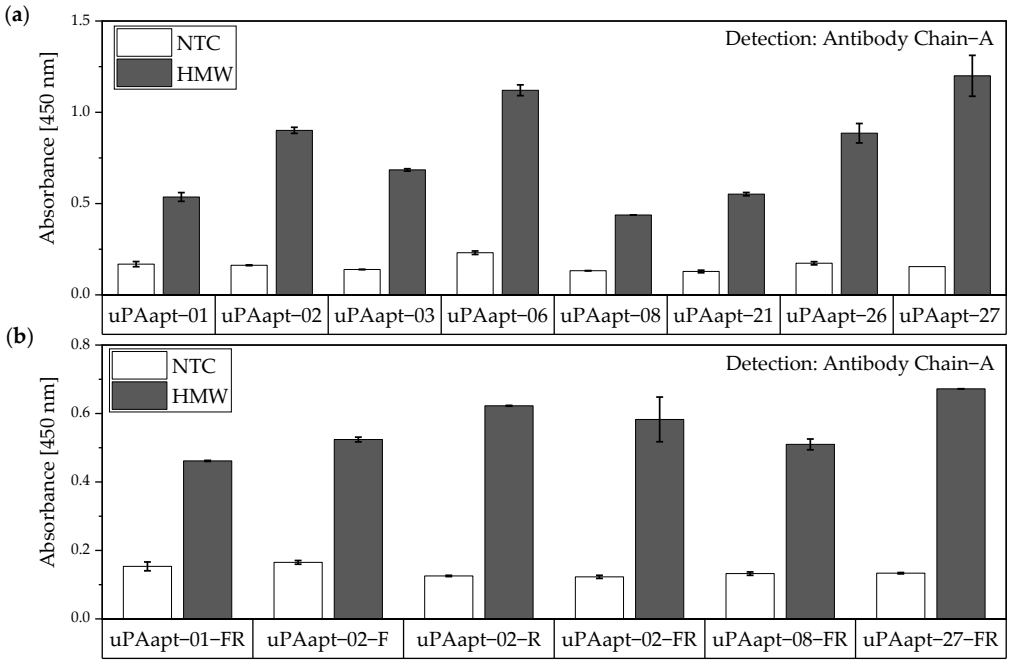

Figure 8. Aptamer–Antibody-based sandwich assay for detection of HMW-uPA by Antibody Chain A (Ab Chain A). HMW-uPA could be detected using (**a**) all uPA aptamers and (**b**) several of the truncated variants as capture aptamers when Ab Chain A is used as a reporter molecule, which only detects the HMW-uPA form due to binding to the A-chain of uPA. The absorbance for each sample is given as the mean value of technical replicates. Error bars represent the range of measured values. Number of records $n = 2$.

Detection of captured HMW-uPA could also be shown for the full-length uPA aptamers by using the Ab Chain B which can bind both uPA forms due to binding to the B-chain of uPA. Only the uPA aptamers uPAapt−02, uPAapt−03, uPAapt−06, uPAapt−26, and uPAapt−27 captured LMW-uPA and were detected by Ab Chain B (Figure 9). This indicates that these aptamers bind LMW-uPA and that these aptamers and the antibody may not have the same binding site on LMW-uPA.

The same assay was performed for the truncated versions of aptamers used as capture molecules. All truncated versions of the aptamers could be used for capturing HMW-uPA if the uPA form is detected by Ab Chain B. Only uPAapt−02−F, uPAapt−02−R, uPAapt−02−FR and uPAapt−27−FR captured LMW-uPA, and therefore could be detected by Ab Chain B (Figure 10).

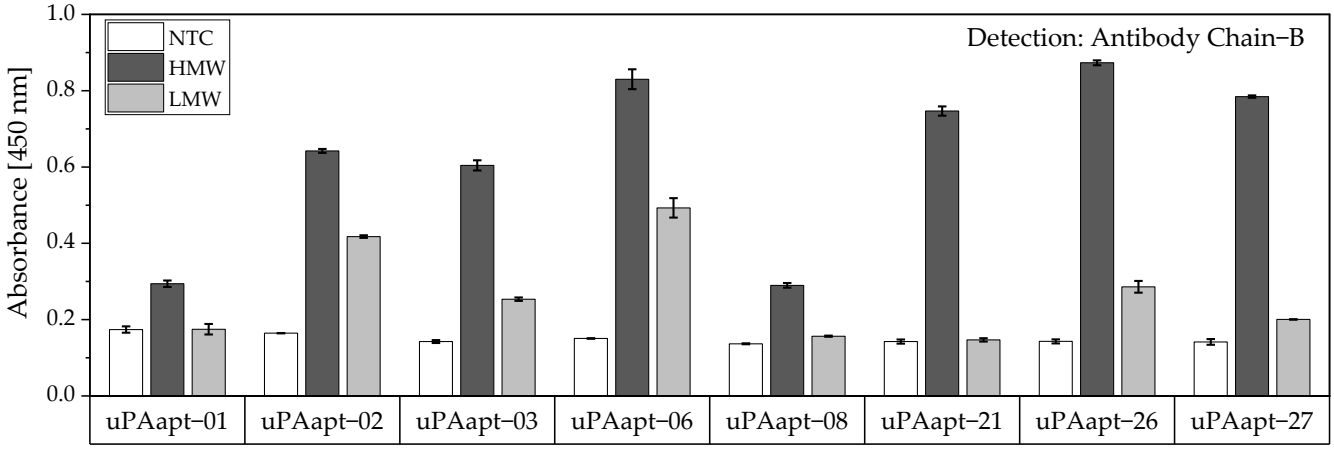

Figure 9. Aptamer–Antibody-based sandwich assay for detection of HMW- and LMW-uPA by Ab Chain B. HMW-uPA could be detected using all uPA aptamers while only uPAapt−02, uPAapt−03, uPAapt−06, uPAapt−26, and uPAapt−27 captured LMW-uPA and could therefore be detected by Ab Chain B, which bind both uPA forms due to binding to the B-Chain of uPA. The absorbance for each sample is given as the mean value of technical replicates. Error bars represent the range of measured values. Number of records n = 2.

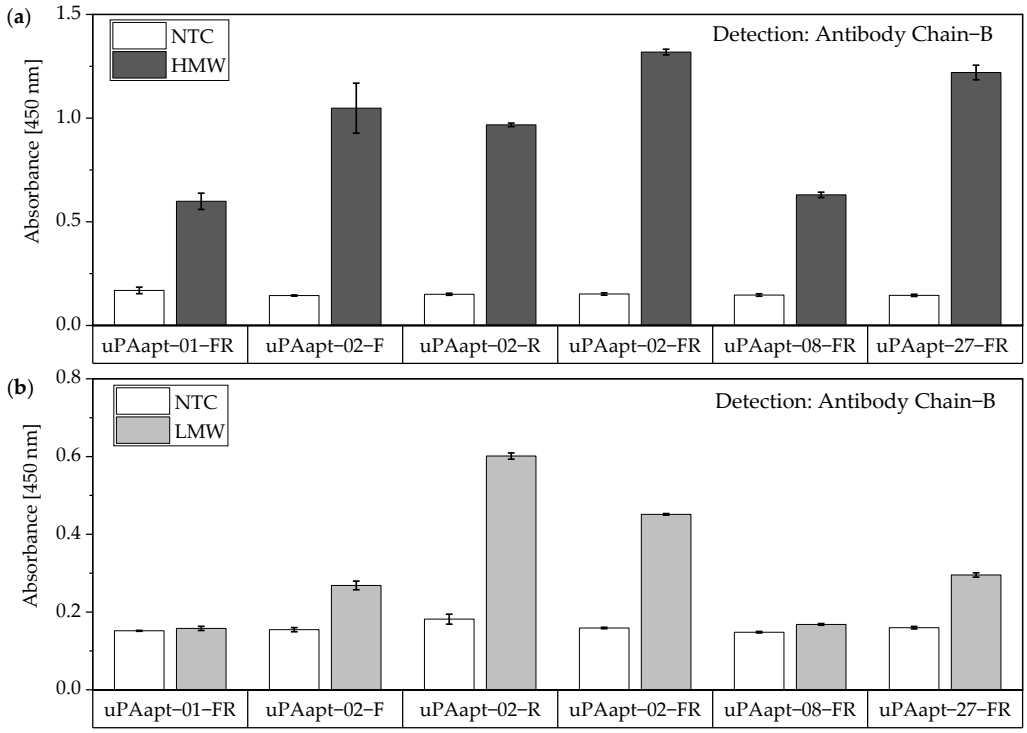

Figure 10. Aptamer–Antibody-based sandwich assay for detection of (**a**) HMW- and (**b**) LMW-uPA by Ab Chain B. HMW-uPA could be detected using all truncated uPA aptamers while only uPAapt−02−F, uPAapt−02−R, uPAapt−02−FR, and uPAapt−27−FR captured LMW-uPA and could therefore be detected by Ab Chain B, which bind both uPA forms due to binding to the B-Chain of uPA. The absorbance for each sample is given as the mean value of technical replicates. Error bars represent the range of measured values. Number of records n = 2.

3.2.2. Antibody–Aptamer Sandwich Assay

For the antibody–aptamer sandwich assay, the antibodies were used as capture molecules and the 5′-fluorescently labeled aptamers as reporter molecules. Ab Chain A captured only HMW-uPA, and therefore, uPAapt−02, or the truncated version uPAapt−02−FR,

detected the HMW-uPA form. Using the Ab Chain B, HMW- and LMW-uPA was captured and detected by uPAapt−02 or uPAapt−02−FR. Hence, uPAapt−02 and uPAapt−02−FR maintain binding to LMW-uPA despite binding of the antibody in the region of the serine protease domain. The reporter aptamer uPAapt−21 detected only HMW-uPA and showed no binding to LMW-uPA. (Figure 11).

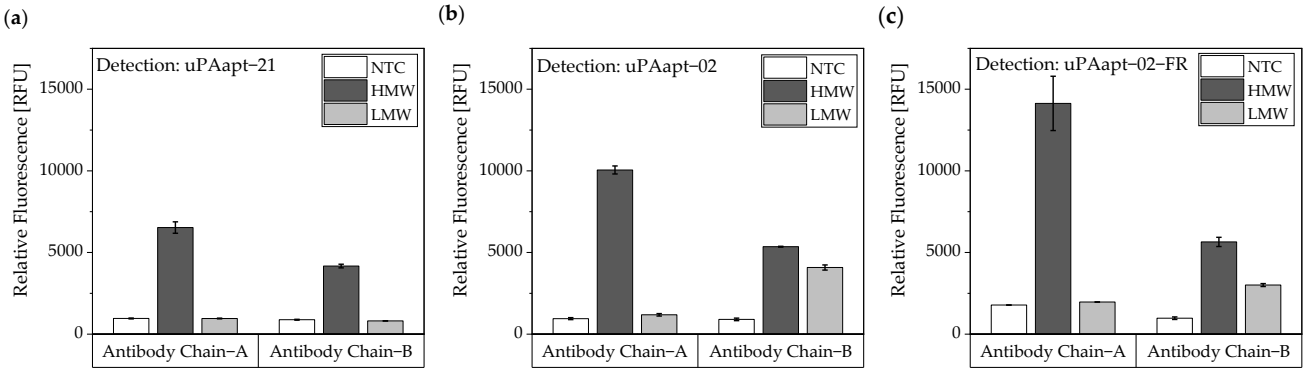

Figure 11. Antibody–Aptamer-based sandwich assay for detection and discrimination of HMW- and LMW-uPA. Antibodies (Ab Chain A or Ab Chain B) were used to capture the different forms of uPA. For detection, (**a**) uPAapt−21 (**b**) uPAapt−02 and (**c**) uPAapt−02−FR were used as reporter molecules. Whereas Ab Chain A can only capture HMW-uPA and therefore uPAapt−02 or the truncated version uPAapt−02−FR can only detect the HMW-uPA form, the Ab Chain B captured the LMW-uPA form and uPAapt−02 or uPAapt−02−FR bind LMW-uPA. The reporter aptamer uPAapt−21 detected only HMW-uPA and showed no binding to LMW-uPA. The relative fluorescence unit [RFU] for each sample is given as the mean value of two technical replicates and was measured using the EnVision® 2105 multimode plate reader. Error bars represent the range of measured values. NTC = No Target Control, HMW = HMW-uPA. Number of records $n = 2$.

4. Discussion

In this study, we present the use of recently published urokinase aptamers in sandwich assay formats for the detection of the different urokinase forms. Sandwich systems included different formats, such as aptamer–target–aptamer, aptamer–target–antibody, and antibody–target–aptamer. Compared to direct or indirect ELISA or ALISA systems, these sandwich format assays have the advantage of more accurately detecting the target molecule by using two specific detection molecules. Previously, we have shown that aptamers are very likely to target different binding sites, as they can bind either HMW-uPA or HMW- and LMW-uPA [21]. This suggested that the aptamers binding either in the region of the ATF or in the region of the SPD. Because of their different binding sites to uPA, it was possible to detect HMW-uPA in an aptamer-based sandwich assay format using different combinations of aptamers (Figure 5). Here, uPAapt−08−FR used as the capture molecule and uPAapt−02−FR used as the reporter molecule turned out to be the best aptamer combination. Differences in the relative fluorescence signal between the same experiments (Figure 5c and the first two columns of Figure 6a) are probably due to the different labeling efficiencies of different batches of capture and reporter aptamers, which can affect the relative fluorescence signal. Labeling efficiencies with biotin or a fluorescence molecule may vary during chemical synthesis depending on the manufacturer and batch, so aptamers may not be 100% labeled. Variations in the immobilization efficiency caused by differences in biotin labeling efficiency can affect the assay, because different amounts of HMW-uPA may be captured. Furthermore, the fluorescence signal of the reporter aptamer may differ, in case labeling of 5′-Cy5 differs between batches. The quality of the streptavidin-coated plates may also impact the assay.

No tested combination of aptamers was able to detect LMW-uPA in the aptamer-based sandwich assay, indicating that the LMW-uPA binding aptamers tested probably share binding sites in close proximity to each other on LMW-uPA or sterically hinder each other

from binding to LMW-uPA. However, the combination of aptamers and antibodies enabled the detection of LMW-uPA—in addition to the detection of the two-chain HMW-uPA form—by some aptamers capable of binding LMW-uPA (Figures 9–11). This allows the additional detection of the cleaved serine protease domain and possibly enables the differentiation of the two uPA forms within one sample. Yet, differentiation between the two uPA forms within one sample would have to be validated in further tests by combining different ratios of HMW- and LMW-uPA. In addition, this combination showed that the antibodies and some of the aptamers most likely have different binding sites to HMW- and LMW-uPA.

Specificity of the best performing reporter aptamer, uPAapt−02−FR, has already been shown [21]. In this study, we could also identify key nucleotides within the aptamer sequence that are important for specific folding and binding to uPA, which demonstrates the sequence dependence of the uPA reporter aptamer. Interestingly, for some sequences, the exchange of only one nucleotide was sufficient to reduce binding affinity or impede binding completely. Most of the identified key nucleotides are located near, or are part of, the two four-base hairpin structures in the secondary structure predicted by the program mfold (Figure 7). In particular, signal reduction of equal to or more than 95% compared to uPAapt−02−FR indicates that especially the second hairpin structure is probably very important for binding to uPA (Figure 7c). However, a few nucleotides also appear to be important for binding affinity, which are located outside or between the hairpins formed, as some exchanges showed a signal reduction of at least 85% (Figure 7a,b). These nucleotides may be important for the structural stability of the aptamer. Although these results support the importance of specific structure elements in aptamer–target interactions, further detailed structure analysis, e.g., NMR-spectroscopy or X-ray crystallography, is required in this case to understand the complete role of the identified key nucleotides.

Even though uPA levels are significantly increased in body fluids of cancer patients compared to healthy individuals, uPA concentrations in physiological samples are relatively low. Casella et al. showed that the highest measured concentration of uPA in the urine of bladder cancer patients was 34.1 ng/mL [16] and concentrations of uPA in blood or tissue extracts are far below this level [9,13,14,24]. In a recent study, the optimal cut-off value for serum uPA of patients with metastatic breast cancer was determined as 2.52 ng/mL [9]. Other studies in which uPA was used as a prognostic marker in breast cancer tissue extracts to decide if adjuvant chemotherapy is beneficial in patients with early breast cancer used a cutoff point of 3 ng/mg of protein [7].

For the aptamer-based sandwich assay, a detection limit of 50 ng/mL in buffer conditions was calculated (Figure 6), which is clearly above the concentrations that need to be detected and can be measured by commercially available ELISAs, which are based on antibodies [25]. However, there are several advantages to using aptamers. Aptamers are smaller and are easily produced via chemical synthesis. This is very cost- and time-effective and has less batch-to-batch variation in production [19]. They are also easy to label or modify with different reporter molecules, functional groups, or linkers [26]. Compared to antibodies, aptamers also have the advantage that they do not permanently degrade at elevated temperatures and return to their original conformation when the optimal temperature is reached again. Even if a micro titer plate-based method is normally intended for single use, the capture aptamers could be reused due to their ability to refold after denaturation by heat, high salt solutions, or other chemicals [19].

There are several different strategies to enhance aptamer affinity and specificity during the aptamer selection process and/or after selection which could enhance the overall assay sensitivity and specificity [27]. Several chemical modifications of the bases, sugar moieties, or the phosphate backbone of aptamers after selection could improve their binding affinity [28,29]. Other chemical modifications using synthetic alternatives to natural nucleic acids (DNA or RNA)—so called Xeno Nucleic Acids (XNAs), including, for example SOMAmers (slow off-rate modified aptamers) or Locked Nucleic Acids (LNAs)—could also improve aptamer affinity and thus assay sensitivity [30–32]. Using other modifications for immobilization strategies, e.g., an amino group at the 5′- or 3′-end for amine-coupling

of the aptamers, or other detection strategies, for example, by the biotin-streptavidin-HRP(Horseradish peroxidase)-system, could also be tested to improve assay sensitivity.

Although there is still some work to be done to improve the sensitivity of the aptamer-based sandwich assay, given these advantages of using aptamers and the possibilities to improve sensitivity, the use of aptamers in micro titer plate-based assays is interesting. As a future attempt, it can also be tested whether a combination of aptamer and antibody has better LOD and LOQ than a combination of aptamers and whether they can approach the concentrations measured by the commercially available ELISAs. It could also be tested how other amounts of immobilized aptamer or antibody and different ratios of capture, target, and reporter molecules might affect or even improve the assays. Furthermore, it would be interesting to test the assay on samples from cancer patients, as we have shown that the assay also works with human urine. In the case of human urine, samples could be pretreated, e.g., by centrifugation or filtration, to eliminate interfering factors (e.g., cells) and to obtain an even better detection limit. Urine samples can also be pretreated by concentrating the analyte to ensure better detection, as uPA is generally present at lower concentrations.

The use of the aptamers in electrochemical aptamer-based sensors [33,34] or lateral flow devices [35–37]—for cost-effective point-of-care testing (POCT)—could also be considered, as they also provide a high signal-to-noise ratio (low background signal), which usually improves sensitivity [27].

5. Conclusions

In conclusion, we successfully developed aptamer-based sandwich assay systems for the rapid detection of human HMW- and LMW-uPA with high specificity and sensitivity. The different sandwich assay formats are: 1. aptamer–target–aptamer, 2. aptamer–target–antibody, and 3. antibody–target–aptamer. The best combinations for detecting HMW-uPA were uPAapt−08−FR as the capture molecule and uPAapt−02−FR as the reporter molecule (format 1), uPAapt−02−FR as the capture molecule and Antibody Chain B as the reporter molecule (format 2), and Antibody Chain A as capture molecule and uPAapt−02−FR as reporter molecule (format 3). The best combinations for detecting LMW-uPA was uPAapt−02−R as capture molecule and Antibody Chain B as reporter molecule (format 2) or Antibody Chain B as capture molecule and uPAapt−02 as reporter molecule (format 3). Since uPA is a highly discussed biomarker for several types of cancer, this aptamer-based assay can be used as a cost-effective alternative to commercially available antibody-based ELISAs.

6. Patents

All aptamers used in this manuscript are protected by pending patents.

Supplementary Materials: The following supporting information can be downloaded at: https://www.mdpi.com/article/10.3390/cancers14215222/s1, Figure S1: Binding of the exchange sequences (Ex−S1–Ex−S42) to HMW-uPA by FLAA.; Table S1: Exchange sequences of uPAapt−02−FR.

Author Contributions: Conceptualization, N.D. and M.M.M.; methodology, N.D.; validation, N.D., W.S. and J.D.; formal analysis, N.D.; investigation, N.D., W.S., and J.D.; writing—original draft preparation, N.D.; writing—review and editing, N.D., W.S., J.D. and M.M.M.; visualization, N.D.; supervision, M.M.M.; project administration, M.M.M.; funding acquisition, M.M.M. All authors have read and agreed to the published version of the manuscript.

Funding: This research was funded by the German state of Brandenburg's Ministry for Science, Research and Culture (MWFK) through the funding program StaF (Strengthening Technological and Applied Research in Scientific Institutions, grant number 85017631 to M.M.M.). The APC was supported by the publishing fund of the Fraunhofer Society.

Institutional Review Board Statement: Not applicable.

Informed Consent Statement: Not applicable.

Data Availability Statement: The datasets for the current study are available from the corresponding author on request.

Conflicts of Interest: The authors declare no conflict of interest.

References

1. Zou, J.; Wang, E. Cancer biomarker discovery for precision medicine: New progress. *Curr. Med. Chem.* **2019**, *26*, 7655–7671. [CrossRef] [PubMed]
2. Su, S.-C.; Lin, C.-W.; Yang, W.-E.; Fan, W.-L.; Yang, S.-F. The urokinase-type plasminogen activator (uPA) system as a biomarker and therapeutic target in human malignancies. *Expert Opin. Ther. Targets* **2016**, *20*, 551–566. [CrossRef] [PubMed]
3. Mahmood, N.; Mihalcioiu, C.; Rabbani, S.A. Multifaceted role of the urokinase-type plasminogen activator (uPA) and its receptor (uPAR): Diagnostic, prognostic, and therapeutic applications. *Front. Oncol.* **2018**, *8*, 24. [CrossRef] [PubMed]
4. Mekkawy, A.H.; Pourgholami, M.H.; Morris, D.L. Involvement of urokinase-type plasminogen activator system in cancer: An overview. *Med. Res. Rev.* **2014**, *34*, 918–956. [CrossRef] [PubMed]
5. Dass, K.; Ahmad, A.; Azmi, A.S.; Sarkar, S.H.; Sarkar, F.H. Evolving role of uPA/uPAR system in human cancers. *Cancer Treat. Rev.* **2008**, *34*, 122–136. [CrossRef]
6. Foekens, J.A.; Peters, H.A.; Look, M.P.; Portengen, H.; Schmitt, M.; Kramer, M.D.; Brünner, N.; Jänicke, F.; Meijer-van Gelder, M.E.; Henzen-Logmans, S.C.; et al. The urokinase system of plasminogen activation and prognosis in 2780 breast cancer patients. *Cancer Res.* **2000**, *60*, 636–643. [PubMed]
7. Duffy, M.J.; McGowan, P.M.; Harbeck, N.; Thomssen, C.; Schmitt, M. uPA and PAI-1 as biomarkers in breast cancer: Validated for clinical use in level-of-evidence-1 studies. *Breast Cancer Res.* **2014**, *16*, 428. [CrossRef] [PubMed]
8. Harris, L.; Fritsche, H.; Mennel, R.; Norton, L.; Ravdin, P.; Taube, S.; Somerfield, M.R.; Hayes, D.F.; Bast, R.C. American society of clinical oncology 2007 update of recommendations for the use of tumor markers in breast cancer. *J. Clin. Oncol.* **2007**, *25*, 5287–5312. [CrossRef]
9. Banys-Paluchowski, M.; Witzel, I.; Aktas, B.; Fasching, P.A.; Hartkopf, A.; Janni, W.; Kasimir-Bauer, S.; Pantel, K.; Schön, G.; Rack, B.; et al. The prognostic relevance of urokinase-type plasminogen activator (uPA) in the blood of patients with metastatic breast cancer. *Sci. Rep.* **2019**, *9*, 2318. [CrossRef]
10. Shariat, S.F.; Roehrborn, C.G.; McConnell, J.D.; Park, S.; Alam, N.; Wheeler, T.M.; Slawin, K.M. Association of the circulating levels of the urokinase system of plasminogen activation with the presence of prostate cancer and invasion, progression, and metastasis. *J. Clin. Oncol.* **2007**, *25*, 349–355. [CrossRef]
11. Shariat, S.F.; Semjonow, A.; Lilja, H.; Savage, C.; Vickers, A.J.; Bjartell, A. Tumor markers in prostate cancer I: Blood-based markers. *Acta Oncol.* **2011**, *50* (Suppl. S1), 61–75. [CrossRef] [PubMed]
12. Yang, J.-L.; Seetoo, D.-q.; Wang, Y.; Ranson, M.; Berney, C.R.; Ham, J.M.; Russell, P.J.; Crowe, P.J. Urokinase-type plasminogen activator and its receptor in colorectal cancer: Independent prognostic factors of metastasis and cancer-specific survival and potential therapeutic targets. *Int. J. Cancer* **2000**, *89*, 431–439. [CrossRef]
13. Herszényi, L.; Farinati, F.; Cardin, R.; István, G.; Molnár, L.D.; Hritz, I.; de Paoli, M.; Plebani, M.; Tulassay, Z. Tumor marker utility and prognostic relevance of cathepsin B, cathepsin L, urokinase-type plasminogen activator, plasminogen activator inhibitor type-1, CEA and CA 19-9 in colorectal cancer. *BMC Cancer* **2008**, *8*, 194. [CrossRef] [PubMed]
14. Shariat, S.F.; Monoski, M.A.; Andrews, B.; Wheeler, T.M.; Lerner, S.P.; Slawin, K.M. Association of plasma urokinase-type plasminogen activator and its receptor with clinical outcome in patients undergoing radical cystectomy for transitional cell carcinoma of the bladder. *Urology* **2003**, *61*, 1053–1058. [CrossRef]
15. Schuettfort, V.M.; Pradere, B.; D'Andrea, D.; Grossmann, N.C.; Quhal, F.; Mostafaei, H.; Laukhtina, E.; Mori, K.; Rink, M.; Karakiewicz, P.I.; et al. Prognostic impact of preoperative plasma levels of urokinase plasminogen activator proteins on disease outcomes after radical cystectomy. *J. Urol.* **2021**, *206*, 1122–1131. [CrossRef] [PubMed]
16. Casella, R.; Shariat, S.F.; Monoski, M.A.; Lerner, S.P. Urinary levels of urokinase-type plasminogen activator and its receptor in the detection of bladder carcinoma. *Cancer* **2002**, *95*, 2494–2499. [CrossRef] [PubMed]
17. Shariat, S.F.; Casella, R.; Monoski, M.A.; Sulser, T.; Gasser, T.C.; Lerner, S.P. The addition of urinary urokinase-type plasminogen activator to urinary nuclear matrix protein 22 and cytology improves the detection of bladder cancer. *J. Urol.* **2003**, *170*, 2244–2247. [CrossRef]
18. Sabrowski, W.; Dreymann, N.; Möller, A.; Czepluch, D.; Albani, P.P.; Theodoridis, D.; Menger, M.M. The use of high-affinity polyhistidine binders as masking probes for the selection of an NDM-1 specific aptamer. *Sci. Rep.* **2022**, *12*, 7936. [CrossRef]
19. Toh, S.Y.; Citartan, M.; Gopinath, S.C.B.; Tang, T.-H. Aptamers as a replacement for antibodies in enzyme-linked immunosorbent assay. *Biosens. Bioelectron.* **2015**, *64*, 392–403. [CrossRef]
20. Bakhtiari, H.; Palizban, A.A.; Khanahmad, H.; Mofid, M.R. Aptamer-based approaches for in vitro molecular detection of cancer. *Res. Pharm. Sci.* **2020**, *15*, 107–122. [CrossRef]
21. Dreymann, N.; Wuensche, J.; Sabrowski, W.; Moeller, A.; Czepluch, D.; Vu Van, D.; Fuessel, S.; Menger, M.M. Inhibition of human urokinase-type plasminogen activator (uPA) enzyme activity and receptor binding by DNA aptamers as potential therapeutics through binding to the different forms of uPA. *IJMS* **2022**, *23*, 4890. [CrossRef] [PubMed]

22. Shrivastava, A.; Gupta, V. Methods for the determination of limit of detection and limit of quantitation of the analytical methods. *Chron. Young Sci.* **2011**, *2*, 21. [CrossRef]
23. Zuker, M. Mfold web server for nucleic acid folding and hybridization prediction. *Nucleic Acids Res.* **2003**, *31*, 3406–3415. [CrossRef]
24. Duffy, M.J.; Duggan, C.; Mulcahy, H.E.; McDermott, E.W.; O'Higgins, N.J. Urokinase plasminogen activator: A prognostic marker in breast cancer including patients with axillary node-negative disease. *Clin. Chem.* **1998**, *44*, 1177–1183. [CrossRef] [PubMed]
25. Benraad, T.J.; Geurts-moespot, J.; Grøndahl-hansen, J.; Schmitt, M.; Heuvel, J.J.T.M.; de Witte, J.H.; Foekens, J.A.; Leake, R.E.; Brünner, N.; Sweep, C.G.J. Immunoassays (ELISA) of urokinase-type plasminogen activator (uPA): Report of an EORTC/BIOMED-1 Workshop. *Eur. J. Cancer* **1996**, *32*, 1371–1381. [CrossRef]
26. Luzi, E.; Minunni, M.; Tombelli, S.; Mascini, M. New trends in affinity sensing. *TrAC Trends Anal. Chem.* **2003**, *22*, 810–818. [CrossRef]
27. Kalra, P.; Dhiman, A.; Cho, W.C.; Bruno, J.G.; Sharma, T.K. Simple methods and rational design for enhancing aptamer sensitivity and specificity. *Front. Mol. Biosci.* **2018**, *5*, 41. [CrossRef]
28. Abeydeera, N.D.; Egli, M.; Cox, N.; Mercier, K.; Conde, J.N.; Pallan, P.S.; Mizurini, D.M.; Sierant, M.; Hibti, F.-E.; Hassell, T.; et al. Evoking picomolar binding in RNA by a single phosphorodithioate linkage. *Nucleic Acids Res.* **2016**, *44*, 8052–8064. [CrossRef]
29. Lee, K.Y.; Kang, H.; Ryu, S.H.; Lee, D.S.; Lee, J.H.; Kim, S. Bioimaging of nucleolin aptamer-containing 5-(*N*-benzylcarboxyamide)-2′-deoxyuridine more capable of specific binding to targets in cancer cells. *J. Biomed. Biotechnol.* **2010**, *2010*, 168306. [CrossRef]
30. Lipi, F.; Chen, S.; Chakravarthy, M.; Rakesh, S.; Veedu, R.N. In vitro evolution of chemically-modified nucleic acid aptamers: Pros and cons, and comprehensive selection strategies. *RNA Biol.* **2016**, *13*, 1232–1245. [CrossRef]
31. Gold, L.; Ayers, D.; Bertino, J.; Bock, C.; Bock, A.; Brody, E.N.; Carter, J.; Dalby, A.B.; Eaton, B.E.; Fitzwater, T.; et al. Aptamer-based multiplexed proteomic technology for biomarker discovery. *PLoS ONE* **2010**, *5*, e15004. [CrossRef] [PubMed]
32. Hernandez, F.J.; Kalra, N.; Wengel, J.; Vester, B. Aptamers as a model for functional evaluation of LNA and 2′-amino LNA. *Bioorg. Med. Chem. Lett.* **2009**, *19*, 6585–6587. [CrossRef] [PubMed]
33. Yang, Y.; Yang, X.; Yang, Y.; Yuan, Q. Aptamer-functionalized carbon nanomaterials electrochemical sensors for detecting cancer relevant biomolecules. *Carbon* **2018**, *129*, 380–395. [CrossRef]
34. Bahner, N.; Reich, P.; Frense, D.; Menger, M.; Schieke, K.; Beckmann, D. An aptamer-based biosensor for detection of doxorubicin by electrochemical impedance spectroscopy. *Anal. Bioanal. Chem.* **2018**, *410*, 1453–1462. [CrossRef]
35. Huang, L.; Tian, S.; Zhao, W.; Liu, K.; Ma, X.; Guo, J. Aptamer-based lateral flow assay on-site biosensors. *Biosens. Bioelectron.* **2021**, *186*, 113279. [CrossRef]
36. Dalirirad, S.; Steckl, A.J. Lateral flow assay using aptamer-based sensing for on-site detection of dopamine in urine. *Anal. Biochem.* **2020**, *596*, 113637. [CrossRef]
37. Frohnmeyer, E.; Tuschel, N.; Sitz, T.; Hermann, C.; Dahl, G.T.; Schulz, F.; Baeumner, A.J.; Fischer, M. Aptamer lateral flow assays for rapid and sensitive detection of cholera toxin. *Analyst* **2019**, *144*, 1840–1849. [CrossRef]

3.4 Manuscript IV

The use of high-affinity polyhistidine binders as masking probes for the selection of an NDM-1 specific aptamer

Wiebke Sabrowski [1,2], **Nico Dreymann [1,3]**, Anja Möller [1], Denise Czepluch [1], Patricia P. Albani [4], Dimitrios Theodoridis [4] and Marcus M. Menger [1,*]

[1] Fraunhofer Institute for Cell Therapy and Immunology, Branch Bioanalytics and Bioprocesses (IZI-BB), Am Mühlenberg 13, 14476 Potsdam, Germany.
[2] Institute of Chemistry and Biochemistry – Biochemistry, Freie Universität Berlin, Takustr. 6, 14195 Berlin, Germany.
[3] Institute of Biochemistry and Biology, University of Potsdam, Karl-Liebknecht Strasse 24-25, 14476 Potsdam-Golm, Germany.
[4] nal von minden GmbH, Robert-Bosch-Breite 23, 37079 Göttingen, Germany.
[*]email: marcus.menger@IZI-BB.fraunhofer.de

Contributions:

- Contributed to design of experiments
- Conducted SPR experiments
- Analyzed and evaluated SPR experiments
- Contributed to preparation of the final manuscript

Published in Scientific Reports,

May 13, 2022

DOI: 10.1038/s41598-022-12062-2

scientific reports

Check for updates

OPEN

The use of high-affinity polyhistidine binders as masking probes for the selection of an NDM-1 specific aptamer

Wiebke Sabrowski[1,2], Nico Dreymann[1,3], Anja Möller[1], Denise Czepluch[1], Patricia P. Albani[4], Dimitrios Theodoridis[4] & Marcus M. Menger[1]✉

The emergence of carbapenemase-producing multi-drug resistant Enterobacteriaceae poses a dramatic, world-wide health risk. Limited treatment options and a lack of easy-to-use methods for the detection of infections with multi-drug resistant bacteria leave the health-care system with a fast-growing challenge. Aptamers are single stranded DNA or RNA molecules that bind to their targets with high affinity and specificity and can therefore serve as outstanding detection probes. However, an effective aptamer selection process is often hampered by non-specific binding. When selections are carried out against recombinant proteins, purification tags (e.g. polyhistidine) serve as attractive side targets, which may impede protein target binding. In this study, aptamer selection was carried out against N-terminally hexa-histidine tagged New Delhi metallo-ß-lactamase 1. After 14 selection rounds binding to polyhistidine was detected rather than to New Delhi metallo-ß-lactamase 1. Hence, the selection strategy was changed. As one aptamer candidate showed remarkable binding affinity to polyhistidine, it was used as a masking probe and selection was restarted from selection round 10. Finally, after three consecutive selection rounds, an aptamer with specific binding properties to New Delhi metallo-ß-lactamase 1 was identified. This aptamer may serve as a much-needed detection probe for New Delhi metallo-ß-lactamase 1 expressing Enterobacteriaceae.

Antibiotics are the most important line in the defense against bacterial infections. Since their discovery more than 70 years ago, antibiotics have enabled the treatment of previously life-threatening conditions[1]. However, overuse and misuse of these medications resulted in a rapid emergence of resistant bacteria[2]. In 2019, the World Health Organization (WHO) declared antimicrobial resistances as one of the top ten health threats worldwide, ranking carbapenem resistance as the most crucial concern[3]. Carbapenem antibiotics are usually considered the most effective drugs to fight infections with multi-drug resistant bacteria and therefore serve as agents of last resort[4]. Yet, carbapenem-resistant Enterobacteriaceae (CRE) and other bacterial families are on the rise leaving the health care system with very little treatment options[5]. Carbapenem resistance in CRE is mainly mediated through the expression of carbapenemases. Carbapenemases are a specialized class of ß-lactamases that harbor the ability to hydrolyze carbapenem antibiotics[6]. ß-lactamases can be classified by the Ambler classification, dividing them into for subgroups (A-D) owing to their amino acid sequence. Classes A, C and D are serine ß-lactamases, while members of class B require a bivalent metal ion for activity and are therefore described as metallo-ß-lactamases (MBLs)[7]. Prominent carbapenemases belonging to the group of serine ß-lactamases are for example Klebsiella Pneumoniae Carbapenemases (KPCs) and Oxacillinases (OXAs). KPCs are class A ß-lactamases while OXAs are members of the group of class D ß-lactamases. Another highly prevalent carbapenemase, belonging to class B of ß-lactamases, is New Delhi metallo-ß-lactamase 1 (NDM-1).

NDM-1 is a carbapenemase firstly discovered in India which has spread across the globe. The genetic element encoding NDM-1 is located on a highly transmissible plasmid allowing rapid horizontal gene transfer[8]. Even though NDM-1 belongs to the family of class B ß-lactamases, it shares very little identity with other MBLs. Verona-Integron-Metallo-ß-lactamases (VIM1/2) are the most closely related MBLs with only 32.4% consensus[9].

[1]Fraunhofer Institute for Cell Therapy and Immunology, Branch Bioanalytics and Bioprocesses (IZI-BB), Am Mühlenberg 13, 14476 Potsdam, Germany. [2]Institute of Chemistry and Biochemistry – Biochemistry, Freie Universität Berlin, Takustr. 6, 14195 Berlin, Germany. [3]Institute of Biochemistry and Biology, University of Potsdam, Karl-Liebknecht Strasse 24-25, 14476 Potsdam-Golm, Germany. [4]nal von minden GmbH, Robert-Bosch-Breite 23, 37079 Göttingen, Germany. ✉email: marcus.menger@IZI-BB.fraunhofer.de

NDM-1 can hydrolyze all ß-lactam antibiotics except for Aztreonam. In contrast to other carbapenemases, NDM-1 is not susceptible to the ß-lactamase inhibitor Avibactam[10]. Hence, treatment options are very limited. Therefore, fast, affordable and comprehensive detection of NDM-1-harboring bacteria is important for both limitation of further spread of carbapenem resistant bacteria and for effective treatment. However, detection methods used to date exhibit certain limitations, such as time-consuming workflows, the need for well-trained personal or the inability to discriminate between different carbapenemase types[11]. Here, a possible solution is the development of detection systems based on highly specific and robust aptamers.

Aptamers are short single-stranded (ss) nucleic acids (ssDNA or RNA) molecules with the ability to bind their target molecule with high specificity and selectivity. Binding is mediated via their three-dimensional structure[12]. Aptamer development is based on an iterative in vitro selection process called SELEX (Systematic Evolution of Ligands by Exponential enrichment) including repeated rounds of DNA-target incubation[13,14]. Aptamers display a range of desirable features, such as high stability over a great range of conditions, regenerative target binding, and chemical synthesis that is free of batch-to-batch variations. Chemical synthesis is low in production costs and allows a broad range of facile chemical modification[15]. Therefore, aptamers serve as excellent detection probes for incorporation into analytical devices like biosensors[16].

However, the selection of aptamers harbors certain pitfalls. Enrichment of non-specific binders happens frequently throughout the in vitro selection process. Especially, when selecting against recombinant proteins, target purification often requires the incorporation of affinity tags. Furthermore, separation of binding sequences from non-binding sequences regularly necessitates target immobilization. Both, affinity tags as well as the immobilization matrix may serve as additional aptamer binding epitopes[17]. Negative selections with other proteins harboring the same affinity tag as well as the immobilization matrix alone can be used to reduce the enrichment of non-specific binders[18]. However, negative selections may not always be sufficient to eliminate non-specific binders completely.

In this study, we describe how selection against N-terminally hexa-histidine tagged New Delhi metallo-ß-lactamase 1 (HIS-NDM-1) initially resulted in polyhistidine tag (HIS-tag) binding. The identified, HIS-tag binding DNA aptamer and its truncated derivate were found to bind to polyhistidine tagged proteins with up to picomolar affinity. The aptamers truncated derivate NDM1-H14-01-FR was further utilized to reverse HIS-tag binding and facilitate specific target binding. Finally, we introduce a DNA aptamer that binds to HIS-NDM-1 but neither to the N-terminally HIS-tagged carbapenemase OXA-23 (HIS-OXA-23) nor to a synthetic hexa-HIS peptide. Scramble control ConSc as well as unrelated control aptamer Con1 did not show binding to HIS-NDM-1, highlighting sequence dependence of the binding event. Other DNA aptamers, targeting either NDM-1 or NDM-1 and VIM-2 simultaneously, were patented in 2012 and 2018[19,20]. Here, affinity to NDM-1 or to NDM-1 and VIM-2 was quantified using surface plasmon resonance spectroscopy (SPR), while specificity and sequence dependence of the binding event were not assessed. Based on the comprehensive characterization of our aptamer by different methods and controls, we believe it can serve as a valuable binding probe for the detection of NDM-1. The development of new detection systems for NDM-1 provides the opportunity to prevent the further spread of carbapenem-resistant bacteria and the mismanagement of infections caused by antibiotic-resistant bacteria.

Results

First selection rounds resulted in the selection of HIS-tag binding aptamers. Eleven selection rounds (SR) were performed against HIS-NDM-1 covalently coupled to tosylactivated magnetic beads. Varying numbers of negative selections against beads only were carried out prior to target incubation in every selection round (Supplementary Table S1). Additionally, for SR5.1–7.2, negative selection was performed against N-terminally HIS-tagged KPC-2 (HIS-KPC-2) and for SR8.1–11.1 with both HIS-KPC-2 and HIS-OXA-23. To monitor enrichment of matrix binders, control selections with tosylactivated beads only were carried out frequently throughout the selection process (SRX.X_Control). After SR11.1, enriched DNA-pools from SR10.1, 11.1, and 11.1_Control were analyzed utilizing next generation sequencing (NGS) and bioinformatics. Pool enrichment was rather low with 71.4% unique sequences for SR10.1, and 65.3% for SR11.1. Enrichment of control selection 11.1_Control was also low with 75.6% unique sequences. For SR11.1, the most enriched pattern accounted for only 0.4% of total sequences and analysis of the 50 most enriched sequences revealed only little homology. Yet, 9 clones were screened for binding to NDM-1. Clone selection was performed based on two criteria. First, overall enrichment after SR11.1 was considered, and second, clones were selected and synthesized on the condition that the percentage of total sequences was higher for SR11.1 than for SR11.1_Control, since stronger enrichment in control selections indicates matrix binding. Selected clones were screened for binding to HIS-NDM-1 using fluorescent dye-linked aptamer assay (FLAA) and SPR. No binding was detected (Supplementary Fig. S1). To lower selection pressure and thereby possibly facilitate target binding, three more selection rounds were conducted in which negative selections were limited to tosylactivated magnetic beads only. After 14 selection rounds, enriched DNA-pools from selection rounds 13.1, 14.1, and 14.1_Control were sequenced by NGS and analyzed bioinformatically. Here, enrichment for target selections was still low with 75.3% unique sequences for SR13.1, and 64.8% for SR 14.1, whereas SR14.1_Control was strongly enriched with only 38.8% unique sequences. However, for SR14.1, the most enriched pattern accounted for 4.72% of total sequences and analysis of the 50 most enriched clones revealed five distinct motives that were present in a high number of sequences. Sequences bearing the same motive were clustered as four sequence families. Representatives from each family were selected and synthesized on the condition that the percentage of total sequences was higher for SR14.1 than for SR14.1_Control.

To test binding properties, aptamer candidates were screened for binding to HIS-NDM-1 by FLAA using Greiner FLUOTRAC™ 600 microplates. High binding signals were obtained for the aptamer candidate NDM1-H14-01, clearly exceeding signals obtained from incubation with the initial library used as a negative control.

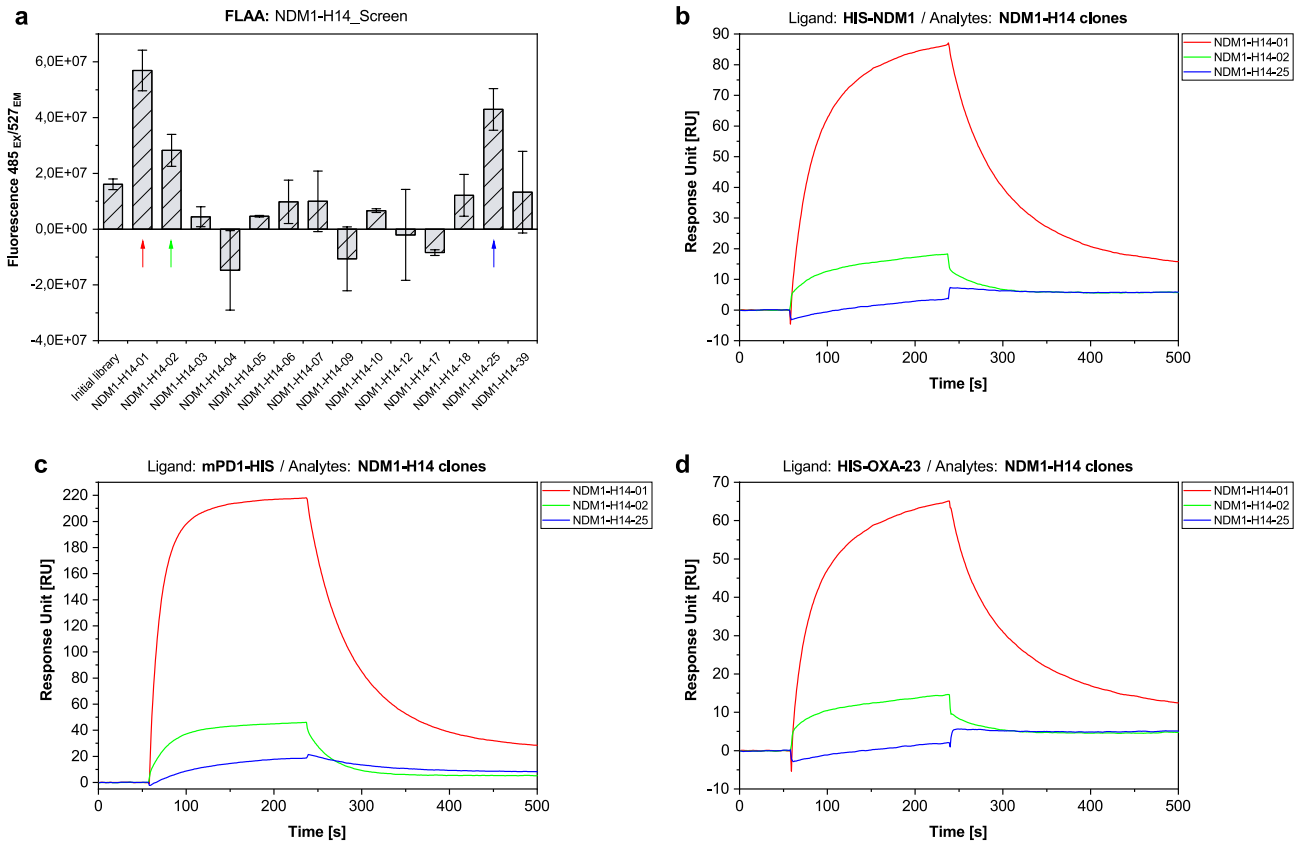

Figure 1. Aptamer candidate screening after SR14.1. HIS-NDM-1 was immobilized on a micro titer plate and incubated with aptamer candidates for FLAA (**a**). For further characterization of promising clones NDM1-H14-01, NDM1-H14-02, and NDM1-H14-25, HIS-NDM1, HIS-OXA-23, and mPD1-HIS were immobilized on an SPR sensor chip and aptamer candidates were injected (**b**–**d**). Binding signals were obtained for clones NDM1-H14-01 and NDM1-H14-02 for all three proteins with strong binding signals for NDM1-H14-01 and weaker binding signals NDM1-H14-02. For NDM1-H14-25, binding was only detected when injected into the mPD1-HIS-channel (**c**). Buffer signals were subtracted. Error bars reflect the range of signals from two different target-coated wells plus the range of two negative control wells in FLAA.

Furthermore, clones NDM1-H14-02 and NDM1-H14-25 also showed signals exceeding that of the initial library. Binding screening for these three aptamer candidates was also performed using SPR. Here, HIS-NDM-1, HIS-OXA-23 (carbapenemase negative control), as well as an unrelated C-terminally HIS-tagged protein—mouse Programmed cell Death protein 1 (mPD1-HIS; HIS-tag negative control), were immobilized as ligands and aptamer candidates were injected as analytes. Surprisingly, binding of clones NDM1-H14-01 and NDM1-H14-02 was detected for all three proteins, while clone NDM1-H14-25 only bound to mPD1. Binding to all three HIS-tagged proteins or to only one, unrelated HIS-tagged protein indicates polyhistidine binding rather than binding to NDM-1 (Fig. 1).

As the highest binding signals in both SPR and FLAA were obtained for NDM1-H14-01, it was chosen for further characterization of potential HIS-tag binding. 5′-biotinylated NDM1-H14-01 was immobilized on an SPR sensor chip as a ligand and varying concentrations of HIS-NDM-1, as well as two unrelated C-terminally HIS-tagged proteins, mPD1-HIS and Complement factor H-related protein 1 (CFHR1-HIS), were injected as analytes. Determined dissociation constants (K_D) varied between 4.49×10^{-11} and 4.43×10^{-9} M for the three different proteins (Table 1). Hence, highly affine binding to three HIS-tagged proteins was shown. However, to exclude binding to a common protein motive and to demonstrate HIS-tag binding, aptamers were tested for binding to a synthetic, 840 Da hexa-HIS peptide. Due to its low molecular size, hexa-HIS peptide was neither suitable for SPR injection, nor for immobilization-based methods, as immobilization can lead to false negative results. Hence, binding was characterized via immobilization-free Microscale Thermophoresis (MST). Here, 5′-Cy5-labelled NDM1-H14-01, as well as an unrelated control aptamer (Con1) were incubated with varying concentrations of the hexa-HIS peptide. A K_D of $2.81 \pm 0.39 \times 10^{-8}$ M was calculated for NDM1-H14-01, while Con1 did not show binding. Thus, the highly affine HIS-tag binding indicated by SPR was confirmed by MST (Fig. 2).

Masking approach to prevent enrichment of HIS-tag binding sequences. To avoid HIS-tag binding, negative selections are commonly used. However, in our initial approach, seven selection rounds with negative selections against either one or two related N-terminally HIS-tagged proteins were not sufficient to remove all HIS-tag binding sequences. After only three consecutive rounds without negative selections, HIS-tag binding

Method	Ligand	Analyte	k_a (1/Ms)	k_d (1/s)	K_D (M)	Chi² (RU²)	K_D confidence (M)
SPR	Bio-NDM1-H14-01	HIS-NDM-1	1.30E+06	5.62E−03	4.34E−09	6.47	–
		mPD1-HIS	1.40E+06	1.38E−04	9.86E−11	0.20	–
		CFHR1-HIS	2.79E+06	1.25E−04	4.49E−11	6.97	–
MST	Cy5-NDM1-H14-01	Hexa-HIS-peptide	–	–	2.81E−08	–	3.90E−09
SPR	Bio-NDM1-H14-01-FR	HIS-NDM-1	1.20E+06	7.11E−03	5.91E−09	9.68	–
		mPD1-HIS	1.02E+06	1.28E−04	1.25E−10	0.20	–
		CFHR1-HIS	4.28E+06	1.22E−04	2.86E−11	9.22	–

Table 1. Quantitative characterization of binding parameters of NDM1-H14-01 and NDM1-H14-01-FR using SPR and MST.

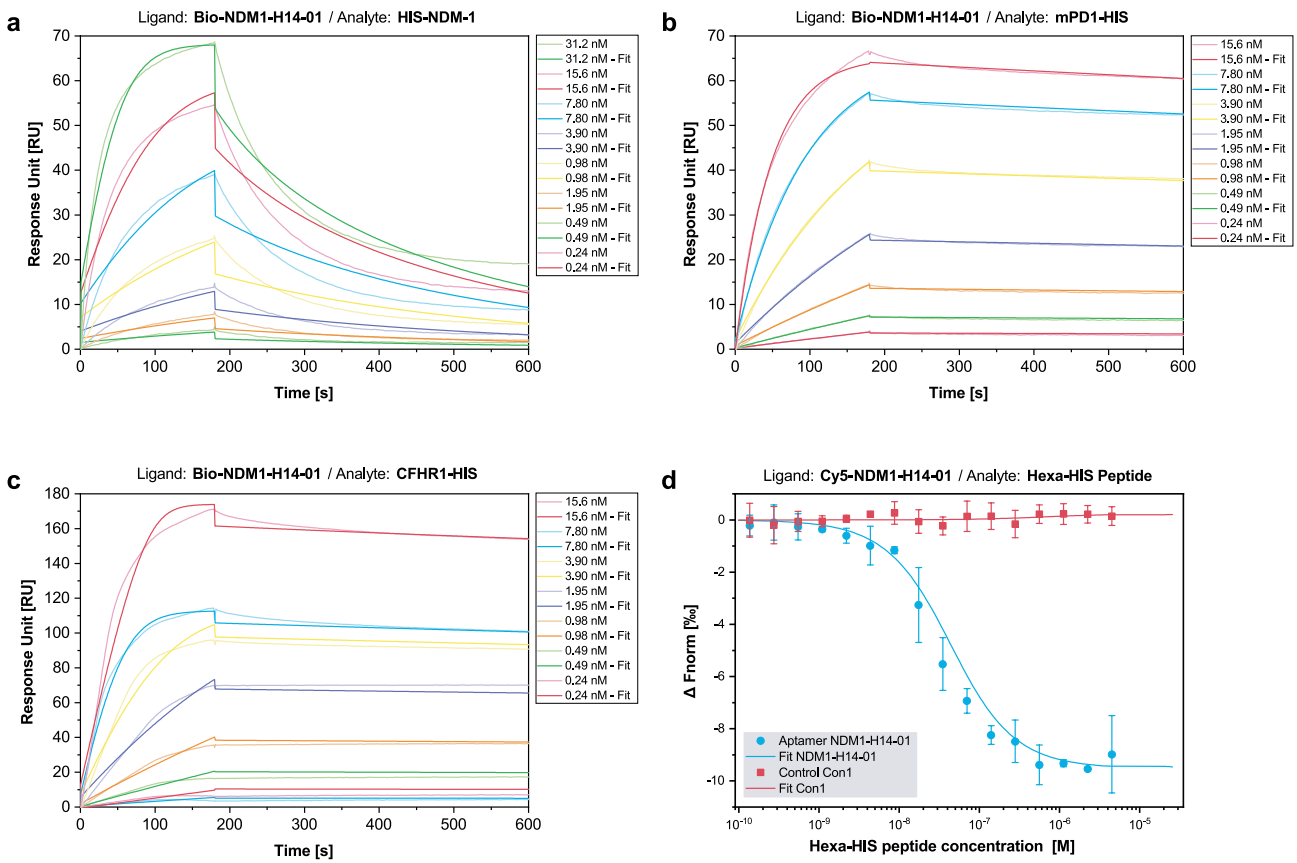

Figure 2. Characterization of NDM1-H14-01 binding to polyhistidine. Binding was analyzed using SPR (**a**–**c**) and MST (**d**). Binding was confirmed for HIS-NDM-1 (**a**), mPD1-HIS (**b**), CFHR1-HIS (**c**), and the hexa-HIS peptide (**d**). K_D-values ranged from the mid-picomolar to the mid-nanomolar range (Table 1). Error bars reflect the standard deviation from three independent experiments in MST.

sequences were strongly enriched and sequences binding specifically to NDM-1 could not be identified. Therefore, we went back to the ssDNA pool from selection round 10.1 and designed a new selection strategy. The ssDNA pool from selection round 10.1 was chosen as sequencing data did not show enrichment of identified HIS-tag binding sequences.

To facilitate NDM-1 binding while preventing HIS-tag binding, a combinatorial approach of negative selection against unrelated HIS-tagged proteins and masking of the HIS-tag was chosen. Here, NDM1-H14-01 was already shown to bind the HIS-tag of various proteins with high affinity and therefore served as an excellent masking aptamer. However, using aptamers from the same selection bears a risk, as both the ssDNA pool and the masking aptamer have the same primer binding sites. PCR amplification after the selection step may lead to high rates of HIS-tag binder amplification and bears the risk of losing specific NDM-1 binders. Hence, to prevent distortion of the selection process by enrichment of NDM1-H14-01 copies, a truncated derivative of the aptamer, lacking both primer binding sites, was designed (NDM1-H14-01-FR). To assess whether HIS-tag binding was retained, SPR-based kinetic measurements were performed as previously described for the full-length aptamer. Binding to all three proteins was preserved and binding was even more affine with binding constants of 5.91×10^{-9} M for

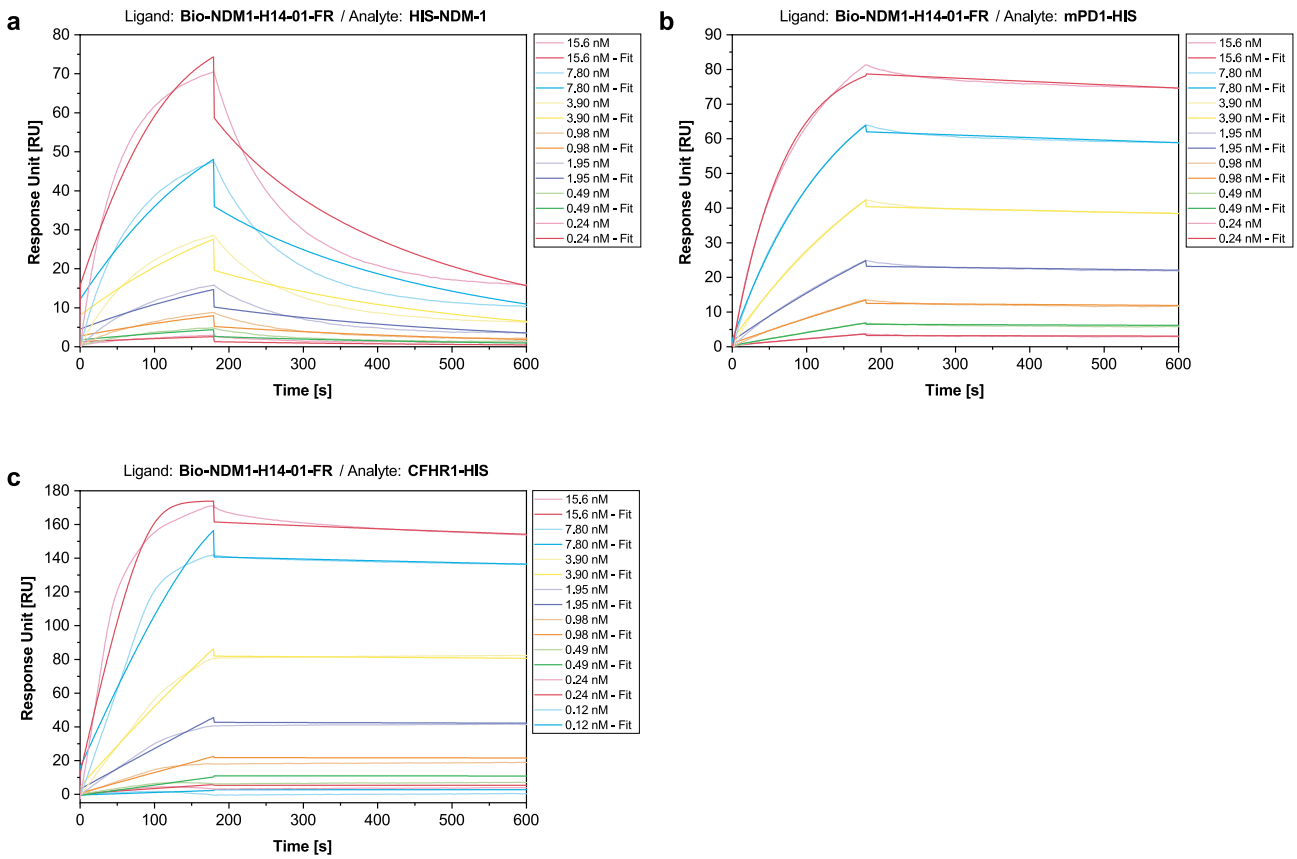

Figure 3. Characterization of NDM1-H14-01-FR binding to polyhistidine. Binding was analyzed using SPR. Binding was confirmed for HIS-NDM-1 (**a**), mPD1-HIS (**b**), and CFHR1-HIS (**c**). K_D-values were ranging from the mid-picomolar to the mid-nanomolar range (Table 1).

HIS-NDM-1, 1.25×10^{-10} M for mPD1-HIS, and 2.86×10^{-11} M for CHFR1-HIS (Fig. 3). K_D-values and kinetic parameters of these HIS-tag binding aptamers that showed strongest binding parameters are summarized in Table 1. As highly affine binding was retained, NDM1-H14-01-FR was used to mask the HIS-tag of HIS-NDM-1 in further selection rounds.

Selection against HIS-NDM-1 with masking approach and negative selections. Three selection rounds (SR11.2_Mask–14.2_Mask) were conducted with negative selections against unrelated mPD1-HIS or with unrelated mPD1-HIS and CFHR1-HIS prior to target incubation. Furthermore, HIS-NDM-1-coupled beads were pre-incubated with NDM1-H14-01-FR to mask the HIS-tag. Subsequently, enriched DNA-pools from SR 14.2_Mask and 14.2_Mask_Control were sequenced by NGS and analyzed bioinformatically. Enrichment was higher than for SR11.1 and 14.1, with 57.1% unique sequences for SR14.2_Mask. SR14.2_Mask_Control was also enriched, with 50.9% unique sequences. For SR14.2_Mask, the most enriched pattern accounted for 3.52% of total sequences. Six sequence families were identified, and 20 representatives were selected and synthesized for characterization of binding properties. The 20 representatives included members of each sequence family, as well as the most enriched clones on the condition that their percentage of total sequences was higher for SR14.2_Mask than for SR14.2_Mask_Control.

Identification of NDM1-H14.2_43 as an NDM-1 specific aptamer. As a first screening approach, aptamer candidates were tested for binding to HIS-NDM-1 and mPD1-HIS by FLAA using Greiner FLUOTRAC™ 600 microplates (Supplementary Fig. S2). Compared to SR14.1, binding signals were magnitudes lower. Hence, the combinatorial approach of negative selection with unrelated proteins and aptamer masking of the HIS-tag was sufficient to prevent prominent HIS-tag binding for all tested sequences. For sequences NDM1-H14.2_16, _19, _39, _42, and _43, binding signals were detected that were higher for HIS-NDM-1 than for mPD1-HIS, exceeded the signal of the initial library, and were therefore chosen for further characterization. To reduce HIS-tag accessibility, in FLAA HIS-NDM-1 was immobilized on a Ni-NTA-coated MTP via its HIS-tag and incubated with promising aptamer candidates (Fig. 4a). Here, a stable fluorescence signal, exceeding that of the initial library, used as a negative control, was detected for NDM1-H14.2_43. Therefore, this clone was chosen for quantitative characterization by MST and SPR (Fig. 4b–d). Specificity of the binding event was assessed using MST. 5′-Cy5 labeled NDM1-H14.2_43 was tested for binding to HIS-NDM-1, HIS-OXA-23, and the hexa-HIS peptide. In addition, an unrelated, 5′-Cy5-labelled DNA sequence (Con1) was used to evaluate non-specific DNA-binding to HIS-NDM-1. NDM1-H14.2_43, showed no binding to HIS-OXA-23 and hexa-HIS peptide,

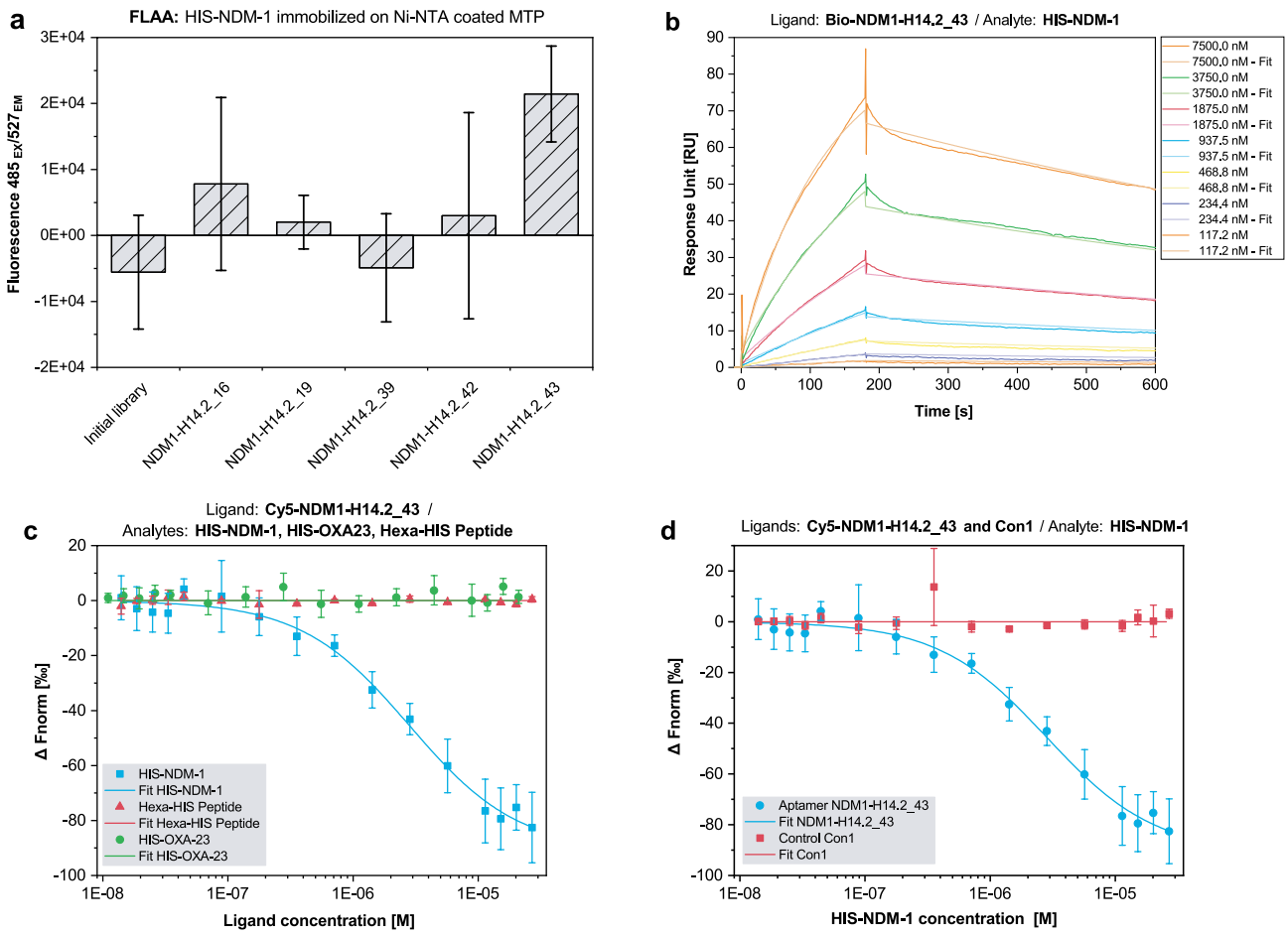

Figure 4. Characterization of NDM1-H14.2_43 binding to NDM-1 by FLAA, SPR and MST. HIS-NDM-1 was immobilized on a Ni-NTA-coated micro titer plate to reduce HIS-tag accessibility and incubated with promising aptamer candidates (**a**). Binding to NDM-1 was retained for the aptamer candidate NDM-1-H14.2_43. Immobilization of 5′-biotinylated NDM1-H14.2_43 on an SPR sensor chip and subsequent incubation with varying HIS-NDM-1 concentrations resulted in a K_D of 7.45×10^{-7} M (**b**). Cross-reactivity with HIS-OXA-23 and the hexa-HIS peptide, as well as non-specific binding of Con1, was tested using MST (**c**, **d**) whereby sequence-dependent, specific binding to NDM-1 could be confirmed. Error bars reflect the standard deviation of signals from three different target-coated wells plus the standard deviation from three negative controls wells in FLAA and the standard deviation from three different, independent experiments in MST.

but to HIS-NDM-1 with a K_D of 2.82×10^{-6} M. The unrelated control aptamer Con1, did not bind to HIS-NDM-1. For SPR measurement, 5′-biotinylated NDM1-H14.2_43 was immobilized on an SPR sensor chip as a ligand and increasing concentrations of HIS-NDM-1 were injected as analytes. Binding parameters were calculated as $K_D = 7.45 \times 10^{-7}$ M, $k_a = 1.00 \times 10^3$ M^{-1} s^{-1}, and $k_d = 7.48 \times 10^{-4}$ s^{-1}. To further investigate sequence dependence of binding, 5′-biotinylated scramble control ConSc was used as a negative control aptamer in SPR (Supplementary Fig. S3). When compared to NDM1-H14.2_43, response units upon injection of HIS-NDM-1 were strongly decreased for ConSc. Kinetic parameters could not be determined as k_a was outside of the measurable range. Thus, sequence-dependent binding, specifically to HIS-NDM-1, could be validated. K_D-values and kinetic parameters of the NDM-1 binding aptamer NDM1-H14.2_43 and controls are summarized in Table 2.

Discussion

Selection was performed against HIS-NDM-1, with negative selections against up to two other HIS-tagged carbapenemases. After eleven selection rounds, slight pool enrichment was detected, but selected aptamer candidates did not show binding to HIS-NDM-1. Negative selections against closely related molecules exert a strong selection pressure on the ssDNA pool[21]. Therefore, selection was progressed for three rounds without negative selections against other carbapenemases. After 14 SR, HIS-tag binding was indicated by SPR and confirmed by MST. The most promising aptamer candidate, NDM1-H14-01, and its truncated version, NDM1-H14-01-FR, were chosen for quantitative binding studies. Binding constants of both aptamers varied from the picomolar to the low nanomolar range for different proteins and different methods. Aptamers that bind to HIS-tags with high affinity have already been selected and published. Tsuji et al. published RNA aptamers that bind to polyhistidine, where the best binder, Shot47, had a K_D of 3.78×10^{-12} M when incubated with various concentrations of HIS-tagged macrophage migration inhibitory factor (HIS-MIF)[22]. In addition, Doyle et al. obtained a U.S.

Method	Ligand	Analyte	k_a (1/Ms)	k_d (1/s)	K_D (M)	Chi^2 (RU^2)	K_D confidence (M)
SPR	Bio-NDM1-H14.2_43	HIS-NDM-1	1.00E+03	7.48E−04	7.45E−07	0.70	–
	Bio-ConSc		–	–	–	–	–
MST	Cy5-Con1	HIS-NDM-1	–	–	–	–	–
	Cy5-NDM1-H14.2_43	HIS-NDM-1			2.82E−06	–	3.77E−07
		HIS-OXA-23			–	–	–
		Hexa-HIS-peptide			–	–	–

Table 2. Quantitative characterization of binding parameters of NDM1-H14.2_43 and control aptamers ConSc and Con1 using SPR and MST.

patent covering three DNA aptamers (6H1, 6H5, 6H7) characterized for binding to various HIS-tagged proteins that exhibited K_Ds of 8.00×10^{-11}–1.76×10^{-7} M[23]. Like NDM1-H14-01 and NDM1-H14-01-FR, all published aptamers were characterized by SPR and the K_Ds are in a comparable range to those of our aptamers. However, as with NDM1-H14-01 and NDM1-H14-01-FR, the K_Ds of 6H1, 6H5, and 6H7 varied for different HIS-tagged proteins. Hence, for masking the HIS-tag of NDM-1, it seemed advisable to use the HIS-tag binding aptamer that was selected against and characterized for binding to HIS-NDM-1. For other HIS-tagged proteins, an evaluation of the binding properties of different, potential masking aptamers may be useful before starting a new aptamer selection. Variations in K_D-values for different HIS-tagged proteins are well in line with differences in HIS-tag accessibility[24]. The discrepancy in K_D-values calculated from SPR and MST may be explained by two factors. On the one hand, a synthetic hexa-HIS peptide was used for MST, whereas HIS-tagged proteins were chosen as analytes for SPR. Here, the protein scaffold surrounding the HIS-tag may have had a positive effect on aptamer binding. On the other hand, differences in the methods themselves may be explanatory. For SPR, the aptamer is immobilized on a chip and the analyte is free in solution, while both ligands and analytes are free in solution for MST. Furthermore, different labels were used. For SPR, the aptamer was 5′-biotinylated, while for MST, 5′-Cy5 labels were used. Despite the difference in K_D values obtained by the two methods, highly affine binding of the NDM1-H14-01 aptamer and its truncated version to HIS-tags was shown.

Since selection was initially aimed at enriching binders against NDM-1 rather than polyhistidine tags, a new selection strategy was designed, in which NDM1-H14-01-FR was used to mask the N-terminal HIS-tag of NDM-1. Another possible approach to avoid selection of HIS-tag binding aptamers is tag removal prior to selection. Proteases such as enterokinase, thrombin, and factor Xa can be used to remove affinity tags via specific cleavage sites that can be inserted between the protein of interest and its respective affinity tag[25]. However, unwanted, non-specific cleavage sites can compromise protein integrity. Viral proteases such as human rhinovirus 3C protease (3CP or PreScission) and tobacco etch virus (TEV) protease are known to be more specific. However, some fusion proteins are inherently poor substrates for the TEV protease, which poses the risk of incomplete cleavage[26]. In addition, the need for purification after cleavage can lead to a reduction in yield. If the desired protein is commercially available, cleavage sites may not be included, and custom synthesis may increase acquisition costs. Therefore, tag masking, for some proteins of interest, may be a more appropriate approach to avoid selecting aptamers that bind to tags. Masking of dominant epitopes in proteins with existing aptamers is known in the aptamer community but has, to the best of our knowledge, not been applied to HIS-tags yet[27]. In this study, we demonstrate the selection of an NDM-1-specific aptamer by masking the HIS-tag of the target molecule. The applicability of our approach to other affinity tags would need further investigation. In particular, masking might be difficult for tags with higher molecular size, such as glutathione S-transferase tag or F_c-tag, because high molecular weight tags may have multiple aptamer binding sites.

After three rounds of selection with the masking approach in combination with negative selections against one or two unrelated HIS-tagged proteins, the aptamer candidate NDM1-H14.2_43 was identified to specifically bind to HIS-NDM-1 but not to HIS-OXA-23, nor to the hexa-HIS peptide. The dissociation constant, calculated for non-HIS mediated NDM-1 binding, was in the moderate range and may allow detection of this prevalent and health-hazardous carbapenemase. Here, SPR-based K_D calculation resulted in higher affinity values than MST-based K_D calculation. Thus, immobilization of the aptamer may be expedient for future detection assay formats. To date, detection of NDM-1 can be done mainly by genotypic, phenotypic, or lateral flow assays. Genotype-based tests such as PCR are highly sensitive and accurate, but require well-trained personnel and usually cannot detect mutant genes. Phenotypic assays detect the in vitro enzyme activity of carbapenemases, not necessarily distinguishing between different carbapenemase types. Detection of carbapenemases, which also allows discrimination between different enzyme types and does not require trained technicians, can be accomplished with antibody-based lateral flow devices (LFD) such as the NG-Test® CARBA 5[28]. Antibody-based LFDs are valuable tools for simple and effective point-of-care detection of carbapenemases. However, aptamer-based LFDs have certain advantages over antibody-based systems. Their long shelf life and stability, as well as chemical synthesis that allows for easy chemical modification and enables low-cost production with extremely low batch-to-batch variability, make aptamers ideal candidates for implementation in LFDs[29]. Therefore, NDM1-H14.2_43 may serve as a valuable detection probe when used in a competitive LFD assay format. In addition, an aptamer-antibody sandwich assay format can be developed if the aptamer and antibody have different binding sites. Sandwich assay formats are known for their high specificity and sensitivity[30].

In conclusion, we presented a strategy to prevent and reverse selection of HIS-tag binding sequences during aptamer selection. We further introduce an aptamer with specific binding properties to the highly prevalent

carbapenemase NDM-1 and its potential for future use as a detection probe. Carbapenem resistance in Enterobacteriaceae poses a worldwide health risk. Specific detection of resistance markers is a prerequisite for containing transmission and to facilitate appropriate treatment. Our NDM1-H14.2_43 aptamer may be used for the development of specific, cost efficient, and easy-to-use detection methods and thereby prevent unnecessary spread of carbapenem resistant bacteria and to help avoid medical malpractice.

Methods

Target preparation. N-terminally hexa-HIS-tagged carbapenemases NDM-1 (derived from *E. coli*), OXA-23 (derived from *A. baumannii*), and KPC-2 (derived from *K. pneumonia*) were purchased from Hölzel Diagnostica Handels GmbH (Köln, Germany). HIS-NDM-1 and HIS-OXA-23 were supplied as a filtered solutions in PBS, while HIS-KPC-2 was supplied as filtered solution in 100 mM NaH_2PO_4, 0.3 M NaCl, and 4 M Urea. For negative selections with unrelated proteins, C-terminally HIS-tagged mPD1 and CFHR1 were purchased from Abcam plc (Cambridge, US) and Hölzel Diagnostica Handels GmbH (Köln, Germany). The hexa-HIS peptide was purchased from BIOTREND Chemikalien GmbH (Köln, Germany). For selection, 10 µg of all proteins were covalently coupled to 1 mg of magnetic beads (Dynabeads™ M-280 Tosylactivated, Thermo Fisher Scientific Inc, Waltham, USA) for 16 h at 37 °C using a rotator. Coupling efficiency was determined by protein quantification in the supernatant prior to and after bead incubation using the Micro BCA™ Protein-Assay-Kit (Thermo Fisher Scientific Inc, Waltham, USA).

Nucleic acid preparation. The initial library (DSB-44) was composed of a 44 nt randomized sequence, flanked by two 18 nt constant primer regions (GTATCTGGTGGTCTATGG–N(44)–GCATAGACGACGAAG AAC) and purchased from Ella Biotech GmbH (Fürstenfeldbruck, Germany). Primers were purchased from TIB Molbiol Syntheselabor GmbH (Berlin, Germany) and aptamers including modifications from biomers.net GmbH (Ulm, Germany) and Integrated DNA Technologies Inc (Coralville, USA). Oligonucleotides were synthesized by standard solid-phase DNA synthesis and purified either by HPLC or standard desalting. Sequences of nucleic acids used in this work can be found in Supplementary Table S2.

Semiautomatic in vitro selection. Aptamers were selected using a semiautomatic selection procedure as previously described[31,32]. Prior to every selection round, ssDNA pools were activated by denaturation at 92 °C for 3 min followed by slowly cooling down to room temperature (RT) for approximately 30 min (refolding step) in binding buffer BP-T (20 mM Tris–HCl [pH 7.4], 140 mM NaCl, 5 mM $MgCl_2$, 1 mM $CaCl_2$, 1 mM KCl, 0.1% BSA, and 0.05% [v/v] Tween® 20). Subsequently, ssDNA libraries and enriched ssDNA pools were incubated with uncoupled tosylactivated magnetic beads as a negative selection step to reduce matrix binders. Negative selection steps with other HIS-tagged carbapenemases or the unrelated, HIS-tagged proteins mPD1-HIS and CFHR1-HIS were introduced and varied over the course of selection. For SR 11.2_Mask–14.2_Mask, HIS-NDM-1-coated beads were pre-incubated with HIS-tag binding aptamer NDM1-H14-01-FR for 1 h in BP-T at RT using a rotator (for further information on negative selections and the masking approach, see section below and Supplementary Table S1). As a selection step, ssDNA pools were either incubated with the HIS-NDM-1-coated beads (target selection) or tosylactivated magnetic beads (control selection) for 1 h at RT in BP-T. Non-binding sequences were removed by extensive washing steps in BP-T. Washing was performed for 3–30 min in volumes up to 2.5 × incubation volume. Remaining sequences were eluted with 8 M urea in BP-T for 30 min at 65 °C and 900 rpm using a thermo shaker and precipitated with 2-propanol at − 20 °C overnight. Eluted ssDNA was amplified by PCR with phosphorylated reverse primers and analyzed by gel electrophoresis. Subsequent purification of the single stranded forward (aptamer) strand was enabled by lambda exonuclease digestion (1.5 U/µg dsDNA)[33].

Negative selections and masking approach. From SR1 onwards, pre-incubation with varying amounts of tosylactivated beads was used as a negative selection step to reduce matrix binding sequences (Supplementary Table S1). Further negative selections were introduced for SR5.1–11.1 (pre-incubation with HIS-KPC-2-coated beads) and SR8.1–11.1 (pre-incubation with HIS-OXA-23-coated beads). Negative selection against carbapenemase-coated beads was stopped for SR11.1–14.1. Here, only uncoated magnetic beads were used to reduce matrix binders. After SR14.1, the selection strategy was changed and SR11.2_Mask–14.2_Mask were conducted with negative selections against tosylactivated beads and mPD1-HIS-coated beads. For SR13.2_Mask and SR14.2_Mask, negative selection was additionally performed against CFHR1-HIS-coated beads. Moreover, for SR11.2_Mask–14.2_Mask, prior to the selection step, HIS-NDM-1-coated beads were pre-incubated with the HIS-tag binding sequence NDM1-H14.1-01-FR to mask the HIS-tag. Detailed information on negative selection and masking of the HIS-tag can be found in Supplementary Table S1.

Next generation sequencing and bioinformatic analysis of enriched ssDNA pools. Enriched pools were sequenced after selection rounds 10.1, 11.1, 11.1_Control, 13.1, 14.1, 14.1_Control, as well as 14.2_Mask and 14.2_Mask_Control. Enriched ssDNA pools were prepared for sequencing using the TruSeq® Nano DNA Library Prep Kit (Illumina, Inc, San Diego, USA). Sequencing was performed using the Mini Seq Mid Output Kit on a Miniseq sequencing platform (Illumina, Inc, San Diego, USA). Paired end mode was chosen with 150 reads per direction and data was bioinformatically analyzed using AptaAnalyzer™-SELEX (AptaIT GmbH, Martinsried, Germany).

Fluorescence dye-linked aptamer assay (FLAA). As a first screening of potential aptamers, FLAAs were performed as previously described[34] using an EnVision® 2105 multimode plate reader (PerkinElmer Inc., Waltham, USA). All reagents were diluted to their final concentrations in BP-T. Targets were immobilized either on Greiner FLUOTRAC™ 600 microplates (Merck KGaA, Darmstadt, Germany) for three hours at RT and 300 rpm followed by 14 h at 18 °C, or on Pierce™ Nickel Coated Plates (Thermo Fisher Scientific, Waltham, USA) for one hour at RT and 300 rpm. Wells were incubated with either 0.6 µg protein in PBS or with PBS only (negative control). Subsequently, wells were washed thrice with BP-T and incubated with 60–100 pmol of activated ssDNA for one hour at RT and 300 rpm. Micro titer plates (MTP) were washed thrice with BP-T and incubated with a 1:200 dilution of Quant-iT™ OliGreen™ ssDNA reagent (Thermo Fisher Scientific, Waltham, USA) for up to 20 min. Fluorescence was measured thrice (excitation 485 nm, emission 527 nm) after 12 min of dye incubation for clones from SR11.1 and 14.1 and after 20 min of dye incubation for clones from SR14.2_Mask. Measurements were performed in duplicate or triplicate. Fluorescence values were averaged, and negative control values were subtracted.

Surface plasmon resonance spectroscopy (SPR). SPR was performed using a BIAcore T200 facility (GE healthcare, Chicago, USA). The system was operating at 25 °C at flow rates of 10–30 µl/min. BP-T* (20 mM Tris–HCl [pH 7.4], 140 mM NaCl, 5 mM $MgCl_2$, 1 mM $CaCl_2$, 1 mM KCl, and 0.005% [v/v] Tween® 20) was used as the running buffer. HC200M sensor chips (XanTec bioanalytics GmbH, Düsseldorf, Germany) were primed twice with ddH_2O and activated with 0.2 M EDC and 0.1 M NHS for 180 s. Regenerations were performed with 20 mM Na_2CO_3.

For aptamer candidate screenings, protein ligands were immobilized via amine coupling for 180 s and the chip was blocked with 1 M ethanolamine for 420 s at a flow rate of 20 µl/min. Aptamer candidates were activated, diluted to 1 µM and injected with 180 s association and 300 s dissociation at a flow rate of 30 µl/min.

For kinetic measurements, 20 µg/ml NeutrAvidin was immobilized via amine coupling for 120 s and the chip was blocked with 1 M ethanolamine for 420 s at a flow rate of 20 µl/min. 5′-biotinylated aptamers were activated, diluted to 0.1 µM in BP-T*, and immobilized at a flow rate of 10 µl/min to approximately 100 RU. NeutrAvidin blocking was performed with 40 µM biotin for 120 s at a flow rate of 20 µl/min. Analytes were diluted in BP-T* and injected to both the ligand-bound and the reference channel with 180 s association and 600 s dissociation at a flow rate of 30 µl/min. Kinetic parameters were calculated using BIAevaluation software (version 3.1, BIAcore). SPR scramble control aptamer ConSc was designed using The Sequence Manipulation Suite®[35].

MicroScale Thermophoresis (MST). MST experiments were conducted using constant concentrations of the 5′-Cy5-labelled aptamers NDM1-H14-01, NDM1-H14.2_43, and Con1, and varying concentrations of HIS-NDM-1, HIS-OXA-23, and the hexa-HIS peptide. For characterization of NDM1-H14-01 binding to the hexa-HIS peptide, NDM1-H14-01 and Con1 were diluted to 20 nM in BP-T. A serial dilution of the hexa-HIS peptide (8960–2.72 nM) was prepared in BP-T and 10 µl of each aptamer and target solution were mixed. For characterization of selective binding of NDM1-H14.2_43 to HIS-NDM-1, aptamers NDM1-H14.2_43 and Con1 were diluted to 42 nM in BP-T and activated as described above. Serial dilutions of HIS-NDM-1, the hexa-HIS peptide (32.3–0.017 µM), and HIS-OXA-23 (25.3–0.013 µM) were prepared in BP-T, and 1 µl of each aptamer was mixed with 5 µl of ligand solution. Binding experiments were performed on a Monolith NT.115 (NanoTemper Technologies, Munich, Germany) with 40–70% excitation power and 40–60% MST power using standard capillaries. The recorded fluorescence was normalised to ΔF_{norm} in per mill and fitted utilizing the K_D formula derived from the law of mass action by MO.*Affinity Analysis* software as previously described[36]. All measurements were performed in triplicate.

Data availability

All datasets generated during and/or analyzed during the current study are available from the corresponding author. Next generation sequencing data is available in the Sequence Read Archive (SRA) repository, Accession number PRJNA830749.

Received: 10 February 2022; Accepted: 4 May 2022
Published online: 13 May 2022

References

1. Laws, M., Shaaban, A. & Rahman, K. M. Antibiotic resistance breakers: Current approaches and future directions. *Fems Microbiol. Rev.* **43**, 490–516. https://doi.org/10.1093/femsre/fuz014 (2019).
2. Ventola, C. L. The antibiotic resistance crisis: part 1: Causes and threats. *P T* **40**, 277–283 (2015).
3. Global Antimicrobial Resistance and Use Surveillance System (GLASS) Report: 2021. (World Health Organization, 2021).
4. Doi, Y. Treatment options for carbapenem-resistant gram-negative bacterial infections. *Clin. Infect. Dis.* **69**, S565–S575. https://doi.org/10.1093/cid/ciz830 (2019).
5. Potter, R. F., D'Souza, A. W. & Dantas, G. The rapid spread of carbapenem-resistant Enterobacteriaceae. *Drug Resist. Update* **29**, 30–46. https://doi.org/10.1016/j.drup.2016.09.002 (2016).
6. Cui, X., Zhang, H. & Du, H. Carbapenemases in Enterobacteriaceae: Detection and antimicrobial therapy. *Front. Microbiol.* **10**, 1823. https://doi.org/10.3389/fmicb.2019.01823 (2019).
7. Hall, B. G. & Barlow, M. Revised Ambler classification of {beta}-lactamases. *J. Antimicrob. Chemother.* **55**, 1050–1051. https://doi.org/10.1093/jac/dki130 (2005).
8. Sun, D., Jeannot, K., Xiao, Y. & Knapp, C. W. Editorial: Horizontal gene transfer mediated bacterial antibiotic resistance. *Front. Microbiol.* **10**, 1933. https://doi.org/10.3389/fmicb.2019.01933 (2019).

9. Yong, D. *et al.* Characterization of a new metallo-beta-lactamase gene, bla(NDM-1), and a novel erythromycin esterase gene carried on a unique genetic structure in Klebsiella pneumoniae sequence type 14 from India. *Antimicrob. Agents Chemother.* **53**, 5046–5054. https://doi.org/10.1128/AAC.00774-09 (2009).
10. Lagace-Wiens, P., Walkty, A. & Karlowsky, J. A. Ceftazidime-avibactam: An evidence-based review of its pharmacology and potential use in the treatment of Gram-negative bacterial infections. *Core Evid.* **9**, 13–25. https://doi.org/10.2147/CE.S40698 (2014).
11. Osei Sekyere, J., Govinden, U. & Essack, S. Y. Review of established and innovative detection methods for carbapenemase-producing Gram-negative bacteria. *J. Appl. Microbiol.* **119**, 1219–1233. https://doi.org/10.1111/jam.12918 (2015).
12. Menger, M. *et al.* MIPs and aptamers for recognition of proteins in biomimetic sensing. *Biosensors* https://doi.org/10.3390/bios6030035 (2016).
13. Ellington, A. D. & Szostak, J. W. Invitro selection of rna molecules that bind specific ligands. *Nature* **346**, 818–822. https://doi.org/10.1038/346818a0 (1990).
14. Tuerk, C. & Gold, L. Systematic evolution of ligands by exponential enrichment: RNA ligands to bacteriophage T4 DNA polymerase. *Science* **249**, 505–510. https://doi.org/10.1126/science.2200121 (1990).
15. McKenzie, L. K., El-Khoury, R., Thorpe, J. D., Damha, M. J. & Hollenstein, M. Recent progress in non-native nucleic acid modifications. *Chem. Soc. Rev.* **50**, 5126–5164. https://doi.org/10.1039/d0cs01430c (2021).
16. Strehlitz, B., Nikolaus, N. & Stoltenburg, R. Protein detection with aptamer biosensors. *Sensors (Basel)* **8**, 4296–4307. https://doi.org/10.3390/s8074296 (2008).
17. Darmostuk, M., Rimpelova, S., Gbelcova, H. & Ruml, T. Current approaches in SELEX: An update to aptamer selection technology. *Biotechnol. Adv.* **33**, 1141–1161. https://doi.org/10.1016/j.biotechadv.2015.02.008 (2015).
18. Shamah, S. M., Healy, J. M. & Cload, S. T. Complex target SELEX. *Acc. Chem. Res.* **41**, 130–138. https://doi.org/10.1021/ar700142z (2008).
19. Zuguo, Z. *et al.* New Delhi metallo-beta-lactamase-1 aptamer, its screening method and application. Chinese Patent. 2012 Aug 30.
20. Zuguo, Z. A kind of aptamer that can identify NDM-1 and VIM-2 simultaneously. Chinese Patent. 2018 Jun 25.
21. Tian, H., Duan, N., Wu, S. & Wang, Z. Selection and application of ssDNA aptamers against spermine based on Capture-SELEX. *Anal. Chim. Acta* **1081**, 168–175. https://doi.org/10.1016/j.aca.2019.07.031 (2019).
22. Tsuji, S. *et al.* RNA aptamer binding to polyhistidine-tag. *Biochem. Biophys. Res. Commun.* **386**, 227–231. https://doi.org/10.1016/j.bbrc.2009.06.014 (2009).
23. Doyle, S. A., Murphy, M. B. Aptamers and methods for their in vitro selection and uses thereof. United States Patent US10,934,856. 2005 Jun 30.
24. Eschenfeldt, W. H. *et al.* Cleavable C-terminal His-tag vectors for structure determination. *J. Struct. Funct. Genomics* **11**, 31–39. https://doi.org/10.1007/s10969-010-9082-y (2010).
25. Wu, X. *et al.* A novel method for high-level production of TEV protease by superfolder GFP tag. *J. Biomed. Biotechnol.* **2009**, 591923. https://doi.org/10.1155/2009/591923 (2009).
26. Raran-Kurussi, S., Cherry, S., Zhang, D. & Waugh, D. S. Removal of affinity tags with TEV protease. *Methods Mol. Biol.* **1586**, 221–230. https://doi.org/10.1007/978-1-4939-6887-9_14 (2017).
27. Kulbachinskiy, A. V. Methods for selection of aptamers to protein targets. *Biochemistry (Mosc)* **72**, 1505–1518. https://doi.org/10.1134/s000629790713007x (2007).
28. Kon, H. *et al.* Multiplex lateral flow immunochromatographic assay is an effective method to detect carbapenemases without risk of OXA-48-like cross reactivity. *Ann. Clin. Microbiol. Antimicrob.* **20**, 61. https://doi.org/10.1186/s12941-021-00469-0 (2021).
29. Kaiser, L., Weisser, J., Kohl, M. & Deigner, H. P. Small molecule detection with aptamer based lateral flow assays: Applying aptamer-C-reactive protein cross-recognition for ampicillin detection. *Sci. Rep.* **8**, 5628. https://doi.org/10.1038/s41598-018-23963-6 (2018).
30. Pei, X. *et al.* Sandwich-type immunosensors and immunoassays exploiting nanostructure labels: A review. *Anal. Chim. Acta* **758**, 1–18. https://doi.org/10.1016/j.aca.2012.10.060 (2013).
31. Wochner, A. *et al.* A DNA aptamer with high affinity and specificity for therapeutic anthracyclines. *Anal. Biochem.* **373**, 34–42. https://doi.org/10.1016/j.ab.2007.09.007 (2008).
32. Wochner, A., Cech, B., Menger, M., Erdmann, V. A. & Glokler, J. Semi-automated selection of DNA aptamers using magnetic particle handling. *Biotechniques* **43**, 344. https://doi.org/10.2144/000112532 (2007).
33. Avci-Adali, M., Paul, A., Wilhelm, N., Ziemer, G. & Wendel, H. P. Upgrading SELEX technology by using lambda exonuclease digestion for single-stranded DNA generation. *Molecules* **15**, 1–11. https://doi.org/10.3390/molecules15010001 (2009).
34. Wochner, A. & Glokler, J. Nonradioactive fluorescence microtiter plate assay monitoring aptamer selections. *Biotechniques* **42**, 578. https://doi.org/10.2144/000112472 (2007).
35. Stothard, P. The Sequence Manipulation Suite: JavaScript programs for analyzing and formatting protein and DNA sequences. *Biotechniques* **28,** 1102–1104. https://doi.org/10.2144/00286ir01 (2000)
36. Sass, S. *et al.* Binding affinity data of DNA aptamers for therapeutic anthracyclines from microscale thermophoresis and surface plasmon resonance spectroscopy. *Analyst* **144**, 6064–6073. https://doi.org/10.1039/c9an01247h (2019).

Acknowledgements
This work was supported by German Federal Ministry of Education and Research (BMBF) within the funding program SME innovative—medical technology (Grant Number 13GW0287A to D.T. and Grant Number 13GW0287C to M.M.M.). Figures were created by W.S. using OriginPro 2021, https://www.originlab.com/.

Author contributions
W.S. designed and performed experiments, analyzed data and wrote the manuscript. N.D. and A.M. designed and performed experiments and analyzed data. DC planned and performed experiments. M.M.M. supervised the practical and theoretical work, provided some of the equipment and materials. All authors, including P.P.A and D.T. contributed to the preparation of the final manuscript, carefully revised the manuscript, and gave approval for publication.

Funding
Open Access funding enabled and organized by Projekt DEAL.

Competing interests
The author declares no competing interests.

Additional information
Supplementary Information The online version contains supplementary material available at https://doi.org/10.1038/s41598-022-12062-2.

Correspondence and requests for materials should be addressed to M.M.M.

Reprints and permissions information is available at www.nature.com/reprints.

Publisher's note Springer Nature remains neutral with regard to jurisdictional claims in published maps and institutional affiliations.

Open Access This article is licensed under a Creative Commons Attribution 4.0 International License, which permits use, sharing, adaptation, distribution and reproduction in any medium or format, as long as you give appropriate credit to the original author(s) and the source, provide a link to the Creative Commons licence, and indicate if changes were made. The images or other third party material in this article are included in the article's Creative Commons licence, unless indicated otherwise in a credit line to the material. If material is not included in the article's Creative Commons licence and your intended use is not permitted by statutory regulation or exceeds the permitted use, you will need to obtain permission directly from the copyright holder. To view a copy of this licence, visit http://creativecommons.org/licenses/by/4.0/.

© The Author(s) 2022

4. General Discussion

Aptamers were discovered more than 30 years ago and a variety of aptamers against different targets have been developed in the meantime. However, aptamer research is still at an early stage of understanding their structures, interactions with the target and their pharmacokinetics (Haßel and Mayer 2019). Until the early 2000s, mostly RNA aptamers were selected because RNA can perform many other functions besides converting genetic information into proteins and RNA was thought to be structurally more diverse compared to ssDNA (Pfeiffer and Mayer 2016; Lakhin et al. 2013). Due to their higher stability and lower synthesis costs, DNA aptamers are now much more common as they show similar or even higher affinity and specificity (Huang and Liu 2022; Wang et al. 2019).

In this work, the first ssDNA aptamers known today with different binding sites for human urokinase were presented. After 11 rounds of selection for HMW-uPA and 12 rounds of selection for LMW-uPA, sequencing was performed to select aptamers against HMW- and LMW-uPA, respectively. Here, eight ssDNA aptamers were identified as highly affine binders to human urokinase. Binding to different uPA forms was tested and binding affinity and specificity was determined. The identification of highly affine binders with different binding sites served as the basis for the functional characterization of the aptamers for their potential use in diagnostic and therapeutic applications. Based on binding to the different uPA forms (HMW-uPA and/or LMW-uPA), approximate binding sites of the aptamers were assumed. Aptamers that showed binding to both uPA forms were assumed to bind near or at the serine protease domain (SPD) whereas aptamers that showed binding only to HMW-uPA were assumed to bind to the amino-terminal fragment (ATF) of uPA, which consists of the kringle domain (KD) and the growth factor domain (GFD). While the SPD is responsible for the conversion of plasminogen to plasmin, the GFD serves as the receptor binding interface to bind uPA to the glycolipid-anchored uPA receptor (uPAR) on cell surfaces, making plasmin activation a specific, localized event on cell surfaces and thus leading to pericellular proteolysis and extracellular degradation (Su et al. 2016). In addition, binding of uPA to uPAR plays an important role in signal transduction by interacting with adhesion molecules including integrins and vitronectin, cellular receptors and extracellular matrix proteins, to control cell proliferation, apoptosis, chemotaxis, adhesion, and migration (Mekkawy et al. 2014). This provides two target-specific binding sites for inhibition of its function. Firstly, uPA activity can be influenced by the inhibition of its proteolytic activity and secondly by inhibiting the uPA-uPAR interaction. Because aptamers were assumed to bind either in the region of the SPD or in the region of the ATF, aptamers were tested for their function as uPA-inhibitors. Based on their binding site, the aptamers exhibited inhibitory properties by either blocking the uPA-uPAR interaction or the catalytic activity of uPA, with some aptamers being able to block both.

In addition to its therapeutic value, uPA is widely discussed as a biomarker for prognosis, diagnosis and recurrence of cancer, as studies have shown an elevated uPA expression in cancer patients (Mahmood et al. 2018). Therefore, aptamers were evaluated for their use in an immunoassay for detection of uPA. Here, various sandwich assay formats were established using aptamers as capture and detection probes. Different sandwich assay combinations were developed for the detection of HMW- and LMW-uPA. Due to binding to the different regions of uPA, a sandwich assay with different aptamer combinations was established for detection of HMW-uPA. Combining aptamers and antibodies, detection of LMW-uPA was also facilitated. These sandwich assay systems were composed of some of the established aptamers and an antibody capable of binding to LMW-uPA.

Before aptamers can be used in specific applications, a detailed analysis is required in advance. In this work, aptamers were used that were selected against different uPA forms. Upon enrichment, ssDNA pools were sequenced by NGS. A high number of relevant sequences were analyzed looking at the most enriched sequences. These were compared and clustered by alignment of specific sequence motifs. After analysis and comparison of the sequences and possible motifs, aptamer candidates were selected to be tested for target binding. The characterization of binding properties is an important step in the aptamer generation process as is allows the identification of highly affine and specific aptamers with respect to the requirements of the planned application. Therefore, aptamers were evaluated by different analytical methods to determine their specific binding and affinity to the target.

This was also the case in another study in which an NDM-1 specific DNA aptamer was identified. Here, SELEX was carried out against commercially available N-terminally His-tagged NDM-1. After 14 rounds of selection, characterization of aptamer candidates resulted in the identification of highly affine His-tag binding aptamers instead of NDM-1 specific aptamers. To circumvent His-tag binding and facilitate carbapenemase binding, a strategy was developed using a truncated version of the His-tag binding aptamer as a masking probe in the *in vitro* selection process. After 3 consecutive rounds of selection with this new selection strategie, a NDM-1 specific aptamers was identified. The binding was characterized, sequenced dependence of the binding event was shown and cross reactivity to another His-tagged carbapenemase as well as to a synthetic hexa-His peptide was excluded by analytical methods. Hence, this aptamer may serve as a potential detection probe in analytical or diagnostic applications.

4.1 Aptamer Characterization for Identification of Aptamers with Therapeutic and Diagnostic Potential

A detailed aptamer characterization is essential to test whether aptamers are suitable for the intended applications. Several methods have been used to identify and characterize the binding properties of the aptamers. Since all bioanalytical methods have their advantages and disadvantages, it is advisable to test aptamer-target binding using different methods and to determine binding affinity by more than one method. An electrophoretic mobility shift assay (EMSA) and a fluorescent dye-linked aptamer assay (FLAA) were used as cost effective and fast screening methods for potential aptamer candidates. Besides their potential to screen a variety of potentially binding sequences without the need for costly equipment, these methods do not require direct labeling, which is also expensive and can interfere with the binding properties of the aptamers (German et al. 1998). In the case of the uPA aptamers, EMSA and FLAA were used to test the binding of the aptamers to the different uPA forms in order to predict potential different binding sites. However, these methods were used only for the qualitative determination of binding. The EMSA revealed potential aptamer candidates for HMW- and LMW-uPA, although it was not always easy to identify a distinct shift in the native PAGE. Rapid dissociation in the gel prevents detection of the DNA-protein complex and only high-affinity binders show a significant shift (Hellman and Fried 2007). Additionally, ethidium bromide, as a nucleic acid intercalating dye, is not as sensitive as for example radioisotope-labeled DNA which would make the detection of DNA-protein complexes much more sensitive (Hellman and Fried 2007). However, it is harmful and involves high disposal costs, which is why other detection methods are increasingly being used (Green et al. 2001). The FLAA was used as another method for identification of binding sequences. This assay also works with a DNA-intercalating fluorescent dye specific for ssDNA. Invitrogen™ Quant-iT™ OLIGREEN™ only shows fluorescence when bound to ssDNA. However, this dye is known to have considerable base selectivity, and the amount of intercalating fluorescent dye, and thus the relative fluorescence signal, may depend on the sequence and the length of an aptamer. In this context, the specific aptamer structure can also influence the incorporation of the dye. Since no calibration curve was used for each aptamer, this also serves only as a qualitative evidence of binding (Wochner and Glökler 2007).

After screening of the aptamer candidates, target-binding sequences were identified. These aptamer candidates were then analyzed using quantitative methods such as SPR and MST to determine binding affinities. Identified uPA aptamers showed dissociation constants in the low nanomolar to picomolar range, which is comparable to monoclonal antibodies specific for human urokinase (Sgier et al. 2010). In SPR experiments, the best binding uPA aptamer uPAapt-02 and its truncated variants showed binding affinities up to a K_D of 0.2 nM. Here, the

binding affinities of the aptamers were evaluated for both uPA forms to obtain dissociation constants for HMW- and LMW-uPA and to provide additional evidence for potential different binding sites. However, these results were only partially consistent with those obtained from the screening of aptamers for LMW-uPA using FLAA and EMSA. In FLAA, the target molecules are coupled to the surface of a microtiter plate. The aptamers are then incubated freely in solution and detected with a fluorescent dye. Aptamers that do not bind or bind poorly to the target molecule are washed away not detected. In SPR, preferably, the aptamers are immobilized as ligands on the sensor surface and the target is free in solution as the analyte. This ensures complete accessibility of the targets potential binding sites. However, coupling positions, e.g., at the 5'-, 3'-end or any internal positions, may have an influence on the specific folding of the aptamer and thus may be important for binding.

MST was used for determination of dissociations constants in solution. Here, both binding partners are free in solution while one of the binding partners must be fluorescently labeled. This technique was used both to confirm the dissociation constants for the best binding aptamers and to test cross-reactivity to related targets to evaluate the specificity of the aptamers. In the case of uPA aptamers, specificity of the truncated aptamer uPAapt-02-FR was tested using MST, as this aptamer showed the best binding affinity for both uPA forms (HMW- and LMW-uPA) in SPR experiments, which also indicated binding near or at the serine protease domain. For this purpose, binding to pro-uPA, tPA and mouse-uPA was tested. Here, uPAapt-02-FR showed binding not only to HMW- and LMW-uPA but also to the single-chain precursor pro-uPA. Especially for serine proteases, cross-reactivity with highly related targets can often be a major problem, as the topology of the active site of proteases is highly conserved (Botkjaer et al. 2012). However, no binding was observed for human tPA as a representative of a human serine protease and plasminogen activator, and for mouse uPA. Since mouse uPA has the highest homology compared to any human homologous protease (Botkjaer et al. 2012), high specificity was observed for uPAapt-02-FR.

Selection of an NDM-1 specific aptamer was performed with recombinantly produced NDM-1 containing an N-terminal polyhistidine as a purification tag. First selection rounds resulted in a His-tag binding aptamer NDM1-H14-01. K_D-values for different His-tagged proteins were determined using SPR. NDM1H14-01 showed high affinity for His-tagged proteins with K_D-values in the low nanomolar to mid picomolar range and a K_D of 28 nM for a hexa-his-peptide in MST. Using a truncated version of this aptamer for masking approaches, further selection rounds were conducted to obtain an NDM-1 specific aptamer and to prevent the selection of His-tag-binding aptamers. Specificity of NDM-1-H14.2_43 was tested using MST. The NDM-1 specific aptamer did not bind to His-Oxa-23, a representative of another His-tagged carbapenemase, nor to the synthetic hexa-His peptide, demonstrating specific binding

to NDM-1. The use of highly purified targets is crucial for aptamer selection to ensure direct selection for the desired target. However, many recombinantly expressed proteins include a purification tag to isolate them from cell lysates. As shown in manuscript IV, this can poses a challenge in aptamer selection, as it can serve as an additional undesired binding epitope, which should be considered when selecting aptamers against recombinantly expressed proteins. Since the commercially available uPA, which was used in this work, was isolated from human urine without the need of a purification tag, this could be neglected for the uPA aptamers.

To underline the specificity of the uPA aptamer uPAapt-02-FR and to demonstrate sequence-specific folding and binding to uPA, key nucleotides were identified within the aptamer sequence. For some exchange sequences, the exchange of only one nucleotide resulted in a reduction or loss of the binding signal in FLAA. Using the secondary structure prediction program mfold (Zuker 2003) it was shown that identified key nucleotides that were required to measure a binding signal were located near or were part of the two four-base hairpin structures. Here, the second hairpin structure was suggested to be important for specific folding and uPA binding. Other nucleotides, which are not within these strucutres according to the mfold prediction, were also identified to may have an effect on structure and/or stability of the aptamer. Here, FLAA was used for the identification of key nucleotides for a fast and cost-effective screening of the nucleotide exchange sequences. As already discussed before, without the use of calibration curves, FLAA can only serve as a qualitative but not a quantitative measure of binding events. Here, sequence and structure dependence of the intercalation of Invitrogen™ Quant-iT™ OLIGREEN™ should be taken into account. Although the original aptamer sequence uPAapt-02-FR was included in each experiment as a control, allowing comparison of the signals from the different sequences, the substitution of a single nucleotide can cause a change in structure and thus in fluorescence signal. However, as the exchange of single nucleotides in certain positions of the aptamer sequence was sufficient to reduce the signal by more than 95%, their importance for uPA binding was strongly indicated.

As these results support the importance of specific structure elements in aptamer-target-interactions, detailed structure analysis such as nuclear magnetic resonance (NMR), circular dichroism (CD) spectroscopy or X-ray crystallography could provide structural information on the aptamers and aptamer-target-complexes (Cai et al. 2018). In particular, this could be used to understand the interaction and the role of the identified key nucleotides, since mfold is only a prediction of the secondary structure. In addition, this could provide information about the exact binding sites and the interaction of uPA with its uPA specific aptamers, as they revealed different binding sites with different effects on uPA.

4.2 Use of Aptamers Targeting uPA for Therapeutic Purposes in Cancer

To date, several therapeutic strategies have been developed targeting the uPA system in cancer. Here, monoclonal antibodies, peptides or small molecules have shown inhibition of uPA catalytic activity, inhibition of uPA-uPAR binding, or uPA triggered signaling activity, with some of them have already shown positive results in cancer treatment in phase 1 and 2 clinical trials (Masucci et al. 2022). Aptamers targeting proteases are considered as promising therapeutic alternatives as they have shown inhibitory effects on enzymatic and regulatory mechanisms (Dupont et al. 2011). Due to their several advantages over protein-based therapeutics, they are widely discussed for the treatment of various diseases including cancer. Aptamers that bind to uPA with high affinity and specificity and thereby have an inhibitory effect on uPA function are of great interest, as they have an advantage over the already known small molecule inhibitors. These were not specific for human uPA and showed also inhibition of other homogenous proteases (Xu et al. 2017)

Dupont et al. identified the first uPA-specific aptamers in 2010. They described thirteen 79 nt long 2'-F-pyrimidine-modified RNA aptamers that were able to inhibit uPA-uPAR binding at low nanomolar concentrations with IC_{50} values ranging from 4.6-85.4 nM. No binding to mouse uPA was detected, demonstrating high specificity for human uPA. Using one of the aptamers - upanap-12 - as a representative, they were able to demonstrate binding to pro-uPA and HMW-uPA, but not to LMW-uPA or a mutated variant of HMW-uPA, which was lacking the GFD. Thus, they were able to show that the GFD was required for binding and assumed that the aptamer binding site was near the GFD. As the GFD is known to mediate receptor binding, this explains the functional effect on uPA-uPAR interaction. Using radioactively labeled ATF, binding of ^{125}I-labled ATF to U937 cells was inhibited by upanap-12 at low nanomolar concentrations, confirming the inhibitory effect on uPA-uPAR interaction cell culture experiments. However, none of their selected aptamers were able to bind to LMW-uPA and/or inhibit the catalytic activity of uPA (Dupont et al. 2010). Two years later, Botkjaer et al. identified pro-uPA specific 2'-fluoro-pyrimidine RNA aptamers through a selection against pro-uPA lacking the GFD and KD as a target. They identified two aptamers, upanap-126 and upanap-231, inhibiting the activation of pro-uPA to the active two-chain HMW-uPA and thereby inhibiting the subsequent generation of plasmin. However, plasminogen activation mediated by already active uPA was not inhibited. Both aptamers were able to bind to pro-uPA as well as active uPA (HMW-uPA) with half-maximal binding at approximately 50 – 100 nM. SPR experiments showed that the aptamers did not bind to the ATF, confirming that the binding site is near or at the SPD of uPA. Upanap-126 was also highly specific for human uPA, as no binding to mouse uPA was detected. In addition, upanap-126 was able to inhibit binding of

pro-uPA to uPAR and uPA to uPAR with IC_{50}-values of 19.2 and 306 nM respectively. Finally, they demonstrated that upanap-126 reduced uPA-dependent human tumor cell invasion and dissemination in *in vitro* and in an *in vivo* chicken embryo model of tumor dissemination (Botkjaer et al. 2012). Skrypina et al. were the first who described a selection of DNA aptamers against pro-uPA. After 12 selection rounds, sequencing data revealed a similar group of sequences with increased affinity to pro-uPA compared to the initial library pool. No further binding analysis or analysis of the therapeutic potential was described (Skrypina et al. 2004).

In this work, the first DNA aptamers known today with different binding sites for human uPA were presented and functionally characterized with respect to their inhibitory properties on uPA. The functional characterization was performed with focus on the inhibition of the proteolytic activity and the inhibition of uPA-uPAR binding, which may provide further information about the relationship between aptamer binding sites and their functional activities. Putative binding sites and their functional activity are comparable to those found in the literature about the existing RNA aptamers (Dupont et al. 2010; Botkjaer et al. 2012). However, this thesis describes the first aptamers capable of inhibiting the proteolytic activity of uPA. Aptamers that showed a significant inhibition of the catalytic activity were able to bind to LMW-uPA and are therefore very likely to have access to the active site of uPA. Hence, it is very likely that aptamers sterically block the access to the active site due to binding to the SPD. This mechanism is already known for other protease-binding aptamers that were able to inhibit the enzymatic activity (Dupont et al. 2011). To confirm this hypothesis, it could be tested whether aptamers are able to inhibit PAI-1 binding, which requires access to the active site of uPA (Dupont et al. 2015). However, it should be noted that aptamers do not bind covalently and the catalytic inhibition is reversible. A competitive inhibition due to steric hindrance at the active site was assumed, as the turnover rate of the enzyme was reduced and complete inactivation of the enzyme did not occur. In contrast, complete inactivation of the enzyme is known for PAI-1, as it binds covalently to the active site of uPA and thereby irreversibly inactivates the enzyme (Dupont et al. 2009). In contrast to the RNA aptamers, uPAapt-02-FR also bound to the zymogen pro-uPA with similarly high affinity. Therefore, it would be of future interest to test if not only the catalytic activity of uPA but also the activation of pro-uPA to the active two-chain HMW-uPA can be inhibited.

In addition to inhibition of the proteolytic activity, DNA aptamers identified in this work were also able to inhibit uPA-uPAR binding. IC_{50}-values were determined for three aptamers (uPAapt-08, uPAapt-21, and uPAapt-26) that showed the best inhibitory effect in a range of 87 – 298 nM. These values are in between the values of previously published modified RNA aptamers (Botkjaer et al. 2012; Dupont et al. 2010). Dupont et al. (2010) showed that the uPA-uPAR inhibitory effect of RNA aptamers with low nanomolar IC_{50}-values was mediated by

binding to the ATF of uPA. The aptamers from this thesis - uPAapt-26 and uPAapt-08 - are in good agreement with this hypothesis, as they showed only binding to HMW-uPA and were therefore assumed to bind to the ATF. However, aptamers could also have inhibitory properties distant from the binding site (Dupont et al. 2015). Even with binding sites distant from the ATF, aptamers could have inhibitory properties on uPA-uPAR binding (Botkjaer et al. 2012). Interestingly, the in this work identified aptamer uPAapt-21, which showed binding to HMW- and LMW-uPA, was the aptamer with the best inhibitory effect on uPA-uPAR interaction. Because binding to LMW-uPA was also observed but no inhibition of the proteolytic activity of uPA was detected, it was assumed that uPAapt-21 binding may occur to the linker region or the SPD but distant from the active site. Therefore, the inhibitory impact of aptamers cannot always be immediately attributable to their binding site. Even though aptamers are relatively low in mass compared to antibodies, they have relatively large dimensions compared to the target protein. As described by Dupont et al. (2015) this could be due to two structural effects. First, because of their size and shape, aptamers can sterically interfere with binding events in the protein that are distant from their own binding site. And second, functional sites of the protein can be brought into close proximity to the aptamer binding site by the general domain organization of the protein (Dupont et al. 2015). Interestingly, all aptamers that showed an inhibitory effect on uPA activity, showed also inhibition of the uPA-uPAR interaction, underlining the pleiotropic effect due to overlapping inhibitory profiles.

In this study, the inhibitory effect on uPA-uPAR interaction was analyzed by SPR experiments and inhibition of uPA activity was tested in a microtiter plate format using an artificial chromogenic substrate (a tripeptide with a p-nitroaniline (pNA) group), which can be hydrolyzed by uPA. It is of great, future interest, to test whether the aptamers that were suitable to inhibit uPAs proteolytic activity also prevent plasminogen activation in solution, as well as cell surface associated plasminogen activation. Furthermore, it is of interest to determine whether aptamers that were suitable to inhibit uPA-uPAR interaction in SPR, maintain their inhibitory potential in cell culture experiments, with cells carrying the uPAR receptor on their surface. Further it should be investigated, if aptamers can bind to the uPA-uPAR complex and thereby prevent binding to adhesion molecules like integrins and vitronectin. Moreover, inhibition of human tumor cell invasion and dissemination are to be tested in *in vitro* and in *in vivo* models in future experiments (Botkjaer et al. 2012).

None of the reported uPA-aptamers have been or are currently being tested in clinical trials. Using aptamers as therapeutic agents usually requires stabilization or modification of the aptamers as they often show short serum half-life's and are susceptible for nuclease degradation (Morita et al. 2018). Modifications, such as, 2'-fluoro-pyrimidine or 2'-NH_2 substitution on riboses, the use of locked nucleic acids (LNAs) or Spiegelmers® can serve to

reduce nuclease-mediated degradation (Ni et al. 2021). The described 2'-flouro-pyrimidine modified RNA aptamer for uPA showed resistance against nucleases in cell culture experiments (Dupont et al. 2010). Additionally, small aptamers are rapidly excreted through renal clearance. For applications that require prolonged circulation times, aptamers can be enlarged by, for example, polyethylene glycol (Turecek et al. 2016), liposomes (Willis et al. 1998), proteins (Heo et al. 2016), cholesterol (Lee et al. 2015) or other nanomaterials (Zhou et al. 2009).

Since uPA is a protein target with more than one function that can be interfered, aptamer-aptamer conjugates with different aptamers targeting different binding sites and thereby different functions could be of great interest. As it was shown in this thesis that two different aptamers can bind to uPA simultaneously in the aptamer-based sandwich assay, this could potentially also work for therapeutic purposes with a combination of two different aptamers selected in this work. It was demonstrated in a previous study that a conjugation of two different RNA aptamers and a peptide that inhibits uPA activity combined inhibition of enzyme activity, receptor binding and enzyme activation (Dupont et al. 2016).

4.3 Use of Aptamers in Immunoassays for Detection of uPA

Due to their various desirable features, aptamers rival antibodies as alternative recognition molecules in immunoassays. Antibody-based ELISAs have been the basic diagnostic immunoassay technique for a variety of antigens since their development in 1971 (Toh et al. 2015). This assay can be used in different configurations. In the direct ELISA, the antigen is immobilized on a surface of a microtiter plate and directly detected by a labeled antibody. In an indirect ELISA, the antigen is detected via an unlabeled primary and a labeled secondary antibody that binds the primary antigen-specific antibody (Crowther 2008). Direct methods have the advantage that the antigen can be detected rapidly, but the primary antibody must be labeled individually for each antigen beforehand, which is time consuming and costly. Furthermore the signal intensity is usually lower than for indirect methods. The use of secondary antibodies to detect the antigen in the indirect ELISA method has the advantage that the primary antibody can be used unlabeled. The use of polyclonal, labeled secondary antibodies allows amplification of the measured signal to detect even small amounts of antigens due to multiple secondary antibodies bound to the primary antibody (Koivunen and Krogsrud 2006). Multiple detection of the primary antibody and the fact that the primary antibody does not need to be labeled offer greater flexibility compared to the direct method. However, the probability of a non-specific background signal is higher. The use of sandwich assay formats offer great advantage. Here, recognition of the antigen by two different

antibodies is required for detection, providing high specificity (Shah and Maghsoudlou 2016). However, the antigen must have two different binding sites, which is often the case with larger macromolecules such as proteins. This type of ELISA allows specific detection of antigens in a sample.

Due to the high specificity of a sandwich ELISA and the fact that aptamers showed binding either to HMW or HMW- and LMW-uPA and thus likely have different binding sites, an aptamer-based sandwich assay system was developed for the detection of HMW-uPA by different aptamer combinations. Aptamers were used as capture and detection probes, with a fluorescently labeled reporter aptamer for detection. None of the combinations tested were able to detect LMW-uPA, suggesting that the aptamers tested likely have the same binding sites on LMW-uPA or are in close proximity to each other, and thereby preventing each other from binding. Therefore, combinations of aptamers and antibodies were tested for the detection of HMW- and LMW-uPA. In this regard, some combinations of aptamers that can bind to LMW-uPA and an antibody specific for LMW-uPA allowed the detection of LMW-uPA in addition to the detection of HMW-uPA. The results showed that the antibodies and some of the aptamers most likely have different binding sites.

To evaluate the sandwich assay which consists solely of aptamers, the limit of detection (LOD) and limit of quantification (LOQ) were determined. A detection limit of 50 ng/mL uPA in a buffer conditions was calculated. However, this value is far above that of conventional antibody-based sandwich ELISAs that can detect up to 2 pg/mL (Benraad et al. 1996). A low detection limit is required to detect the low uPA concentrations present in urine, blood or tissue from cancer patients. Here, the highest concentration that was measured in urine was 34.1 ng/mL (Casella et al. 2002). Concentration levels of uPA in serum are far below that level with concentrations around 2.52 ng/mL (Banys-Paluchowski et al. 2019). The higher detection limit of the aptamer-based sandwich assay compared to the antibody-based ELISA is probably due to the signal amplifying effect by the secondary antibody. Even though affinity of aptamers can play a major role here, which could be improved by various modifications of the aptamers to enhance the limit of detection (Kalra et al. 2018), a signal amplification is needed for sensitivity and a lower detection limit. This could be achieved by using enzymes for signal amplification or by implementation of the aptamer in electrochemical biosensors (Yang et al. 2018). A study by Jarczewska et al. (2015) demonstrated the use of an RNA aptamer specific for uPA in an electrochemical aptasensor allowed detection of 10^{-12} - 10^{-9} M uPA. They also detected uPA in serum, which can be useful for clinical applications. Other detection methods like lateral flow devices (LFD) that usually have high signal-to-noise ratios could also improve sensitivity (Kalra et al. 2018).

4.4 Conclusion and Outlook

In this work, novel ssDNA aptamers were developed for human urokinase and NDM-1. Affinity and specificity of the aptamers were determined by different methods, with uPA aptamers showing K_D-values in the low nanomolar range. Aptamers targeting uPA were found to likely have different binding sites because binding was shown for different uPA forms. The potential therapeutic value of uPA aptamers was proven by *in vitro* experiments. Inhibition of uPA-uPAR interaction by different aptamers was determined using SPR revealing IC_{50}-values of up to 87 nM. Significant inhibition of uPA activity was determined for aptamers that were assumed to bind to or near the SPD. While uPA-uPAR inhibition has already been shown with other RNA aptamers (Dupont et al. 2010), inhibition of the uPA catalytic activity by uPA-specific aptamers has not yet been reported in the literature, which opens up new possibilities for the use of aptamers in uPA inhibition. Here, initial characterizations were carried out while further investigations are needed to prove the aptamers potential as therapeutics. Aptamers have to be tested for plasminogen activation in solution, as well as cell surface-associated plasminogen activation in cell culture experiments. Inhibition of uPA-uPAR binding on cell surfaces for suppression of downstream processes has to be investigated as well. Further *in vivo* studies and the effect of aptamers on cancer progression and metastasis would also be of future interest.

The applicability of aptamers for diagnostic purposes has been demonstrated by the development of microtiter plate-based sandwich assays. Different binding sites on uPA opened up the possibility for the development of an aptamer-based sandwich assay using different combinations of aptamers. For the best aptamer combination, a detection limit of 50 ng/mL was determined for HMW-uPA. LMW-uPA could be detected using a combination of aptamers and antibodies. However, the sensitivity required to detect uPA, for example, in urine or blood samples of cancer patients was not achieved in the aptamer-based microtiter plate assay. An increase in sensitivity may be achieved by implementation of the aptamers in different biosensors. Modifications on aptamers may be tested to increase the aptamer affinity and thereby the assay sensitivity. Furthermore, evaluation of the detection limit of the aptamer-antibody-based sandwich assay systems compared to antibody-based ELISA is of future interest. By combining aptamers with antibodies, the detection limit may be improved.

Selection against His-NDM-1 initially resulted in the identification of His-tag binding aptamers. High affinity was demonstrated for the His-tag binding aptamer NDM-1-H14-01 by SPR using different His-tagged proteins as analytes with K_D-values up to 29 pM. Further selections were carried out using a truncated version of this aptamer as a masking probe to prevent His-tag binding and facilitate carbapenemase binding. Characterization of aptamer candidates revealed an aptamer specific for NDM-1 with a K_D up to 745 nM. This aptamer has

the potential to be used as a detection probe in various applications, e.g., microtiter plate-based assays, lateral flow devices or biosensors, to facilitate detection of the prevalent and health-hazardous carbapenemase NDM-1. Here, detection is required to facilitate appropriate treatment of patients with multidrug resistant infections and to control their transmission. Functional effects of aptamer binding on the catalytic activity of NDM-1 may also be tested in the future.

5. Literature

Banys-Paluchowski, Malgorzata; Witzel, Isabell; Aktas, Bahriye; Fasching, Peter A.; Hartkopf, Andreas; Janni, Wolfgang; Kasimir-Bauer, Sabine; Pantel, Klaus; Schön, Gerhard; Rack, Brigitte; Riethdorf, Sabine; Solomayer, Erich-Franz; Fehm, Tanja; Müller, Volkmar (2019): The prognostic relevance of urokinase-type plasminogen activator (uPA) in the blood of patients with metastatic breast cancer. In *Scientific Reports* 9. DOI: 10.1038/s41598-018-37259-2.

Benraad, T. J.; Geurts-Moespot, J.; Grøndahl-Hansen, J.; Schmitt, M.; Heuvel, J. J. T. M.; de Witte, J. H.; Foekens, J.A.; Leake, R.E.; Brünner, N.; Sweep, C.G.J. (1996): Immunoassays (ELISA) of urokinase-type plasminogen activator (uPA): report of an EORTC/BIOMED-1 workshop. In *European Journal of Cancer* 32A (8), pp. 1371–1381. DOI: 10.1016/0959-8049(96)00118-9.

Blank, Michael; Blind, Michael (2005): Aptamers as tools for target validation. In *Current Opinion in Chemical Biology* 9 (4), pp. 336–342. DOI: 10.1016/j.cbpa.2005.06.011.

Botkjaer, Kenneth A.; Deryugina, Elena I.; Dupont, Daniel M.; Gårdsvoll, Henrik; Bekes, Erin M.; Thuesen, Cathrine K.; Chen, Zhuo; Ploug, Michael; Quigley, James; Andreasen, Peter A. (2012): Targeting tumor cell invasion and dissemination in vivo by an aptamer that inhibits urokinase-type plasminogen activator through a novel multifunctional mechanism. In *Molecular Cancer Research* 10 (12), pp. 1532–1543. DOI: 10.1158/1541-7786.MCR-12-0349.

Boutal, Hervé; Naas, Thierry; Devilliers, Karine; Oueslati, Saoussen; Dortet, Laurent; Bernabeu, Sandrine; Simon, Stéphanie; Volland, Hervé (2017): Development and validation of a lateral flow immunoassay for rapid detection of NDM-producing enterobacteriaceae. In *Journal of Clinical Microbiology* 55 (7), pp. 2018–2029. DOI: 10.1128/JCM.00248-17.

Cai, Shundong; Yan, Jianhua; Xiong, Hongjie; Liu, Yanfei; Peng, Dongming; Liu, Zhenbao (2018): Investigations on the interface of nucleic acid aptamers and binding targets. In *The Analyst* 143 (22), pp. 5317–5338. DOI: 10.1039/c8an01467a.

Casella, Roberto; Shariat, Shahrokh F.; Monoski, Mara A.; Lerner, Seth P. (2002): Urinary levels of urokinase-type plasminogen activator and its receptor in the detection of bladder carcinoma. In *Cancer* 95 (12), pp. 2494–2499. DOI: 10.1002/cncr.10989.

Cesarman-Maus, Gabriela; Hajjar, Katherine A. (2005): Molecular mechanisms of fibrinolysis. In *British Journal of Haematology* 129 (3), pp. 307–321. DOI: 10.1111/j.1365-2141.2005.05444.x.

Chan, Kwing Yeung; Kinghorn, Andrew Brian; Hollenstein, Marcel; Tanner, Julian Alexander (2022): Chemical modifications for a next generation of nucleic acid aptamers. In *ChemBioChem* 23 (15), e202200006. DOI: 10.1002/cbic.202200006.

Crowther, John (2008): Enzyme Linked Immunosorbent Assay (ELISA). In *John M. Walker, Ralph Rapley (Eds.): Molecular Biomethods Handbook*, vol. 262, pp. 657–682.

Danø, Keld; Behrendt, Niels; Høyer-Hansen, Gunilla; Johnsen, Morten; Lund, Leif R.; Ploug, Michael; Rømer, John (2005): Plasminogen activation and cancer. In *Thrombosis and Haemostasis* 93 (4), pp. 676–681. DOI: 10.1160/TH05-01-0054.

Darmostuk, Mariia; Rimpelova, Silvie; Gbelcova, Helena; Ruml, Tomas (2015): Current approaches in SELEX: An update to aptamer selection technology. In *Biotechnology Advances* 33 (6 Pt 2), pp. 1141–1161. DOI: 10.1016/j.biotechadv.2015.02.008.

Dreymann, Nico; Sabrowski, Wiebke; Danso, Jennifer; Menger, Marcus M. (2022): Aptamer-based sandwich assay formats for detection and discrimination of human high- and low-molecular-weight uPA for cancer prognosis and diagnosis. In *Cancers* 14 (21). DOI: 10.3390/cancers14215222.

Duffy, Michael J.; O'siorain, Liam; O'grady, Pauline; Devaney, Deirdre; Fennelly, James J.; Lijnen, Henri J. (1988): Urokinase-plasminogen activator, a marker for aggressive breast carcinomas. Preliminary report. In *Cancer* 62 (3), pp. 531–533. DOI: 10.1002/1097-0142(19880801)62:3<531::AID-CNCR2820620315>3.0.CO;2-B.

Dunn, Matthew R.; Jimenez, Randi M.; Chaput, John C. (2017): Analysis of aptamer discovery and technology. In *Nature Reviews Chemistry* 1 (10), p. 1304. DOI: 10.1038/s41570-017-0076.

Dupont, D. M.; Andersen, L. M.; Botkjaer, K. A.; Andreasen, P. A. (2011): Nucleic acid aptamers against proteases. In *Current Medicinal Chemistry* 18 (27), pp. 4139–4151. DOI: 10.2174/092986711797189556.

Dupont, Daniel M.; Bjerregaard, Nils; Verpaalen, Ben; Andreasen, Peter A.; Jensen, Jan K. (2016): Building a molecular trap for a serine protease from aptamer and peptide modules. In *Bioconjugate Chemistry* 27 (4), pp. 918–926. DOI: 10.1021/acs.bioconjchem.6b00007.

Dupont, Daniel M.; Thuesen, Cathrine K.; Bøtkjær, Kenneth A.; Behrens, Manja A.; Dam, Karen; Sørensen, Hans P.; Pedersen, Jan S.; Ploug, Michael; Jensen, Jan K.; Andreasen, Peter A. (2015): Protein-binding RNA aptamers affect molecular interactions distantly from their binding sites. In *PloS One* 10 (3), e0119207. DOI: 10.1371/journal.pone.0119207.

Dupont, Daniel Miotto; Madsen, Jeppe Buur; Hartmann, Roland Karl; Tavitian, Bertrand; Ducongé, Frédéric; Kjems, Jørgen; Andreasen, Peter André (2010): Serum-stable RNA aptamers to urokinase-type plasminogen activator blocking receptor binding. In *RNA* 16 (12), pp. 2360–2369. DOI: 10.1261/rna.2338210.

Dupont, Daniel Miotto; Madsen, Jeppe Buur; Kristensen, Thomas; Bodker, Julie Stove; Blouse, Grant Ellsworth; Wind, Troels; Andreasen, Peter Andre (2009): Biochemical properties of plasminogen activator inhibitor-1. In *Frontiers in Bioscience (Landmark edition)* 14 (4), pp. 1337–1361. DOI: 10.2741/3312.

Ellington, Andrew D.; Szostak, Jack W. (1990): In vitro selection of RNA molecules that bind specific ligands. In *Nature* 346 (6287), pp. 818–822. DOI: 10.1038/346818a0.

Favaloro, Emmanuel J.; Lippi, Giuseppe (2012): The new oral anticoagulants and the future of haemostasis laboratory testing. In *Biochemia Medica* 22 (3), pp. 329–341. DOI: 10.11613/bm.2012.035.

Foekens, J. A.; Peters, H. A.; Look, M. P.; Portengen, H.; Schmitt, M.; Kramer, M. D.; Brünner, N.; Jänicke, F.; Meijer-van Gelder, M. E.; Henzen-Logmans, S. C.; van Putten, W. L.; Klijn, J. G. (2000): The urokinase system of plasminogen activation and prognosis in 2780 breast cancer patients. In *Cancer Research* 60 (3), pp. 636–643.

Gelinas, Amy D.; Davies, Douglas R.; Janjic, Nebojsa (2016): Embracing proteins: structural themes in aptamer-protein complexes. In *Current Opinion in Structural Biology* 36, pp. 122–132. DOI: 10.1016/j.sbi.2016.01.009.

German, Igor; Buchanan, Danielle D.; Kennedy, Robert T. (1998): Aptamers as ligands in affinity probe capillary electrophoresis. In *Analytical Chemistry* 70 (21), pp. 4540–4545. DOI: 10.1021/ac980638h.

Green, Louis. S.; Bell, Carol.; Janjic, Nebojsa (2001): Aptamers as reagents for high-throughput screening. In *BioTechniques* 30 (5), 1094–1100. DOI: 10.2144/01305dd02.

Guo, Wenfei; Zhang, Chuanxiang; Ma, Tingting; Liu, Xueying; Chen, Zhu; Li, Song; Deng, Yan (2021): Advances in aptamer screening and aptasensors' detection of heavy metal ions. In *Journal of Nanobiotechnology* 19 (1), p. 166. DOI: 10.1186/s12951-021-00914-4.

Hammerum, Anette M.; Hansen, Frank; Nielsen, Hans Linde; Jakobsen, Lotte; Stegger, Marc; Andersen, Paal S.; Jensen, Paw; Nielsen, Tue Kjaergaard; Hansen, Lars Hestbjerg; Hasman, Henrik; Fuglsang-Damgaard, David (2016): Use of WGS data for investigation of a long-term NDM-1-producing Citrobacter freundii outbreak and secondary in vivo spread of blaNDM-1 to Escherichia coli, Klebsiella pneumoniae and Klebsiella oxytoca. In *The Journal of Antimicrobial Chemotherapy* 71 (11), pp. 3117–3124. DOI: 10.1093/jac/dkw289.

Harris, Lyndsay; Fritsche, Herbert; Mennel, Robert; Norton, Larry; Ravdin, Peter; Taube, Sheila; Sommerfield, Mark R.; Hayes, Daniel; Bast Jr., Robert C. (2007): American Society of Clinical Oncology 2007 update of recommendations for the use of tumor markers in breast cancer. In *Journal of Clinical Oncology* 25 (33), pp. 5287–5312. DOI: 10.1200/jco.2007.14.2364.

Haßel, S. K.; Mayer, G. (2019): Aptamers as therapeutic agents: Has the initial euphoria subsided? In *Molecular Diagnosis and Therapy* 23 (3), pp. 301–309. DOI: 10.1007/s40291-019-00400-6.

Hellman, Lance M.; Fried, Michael G. (2007): Electrophoretic mobility shift assay (EMSA) for detecting protein-nucleic acid interactions. In *Nature Protocols* 2 (8), pp. 1849–1861. DOI: 10.1038/nprot.2007.249.

Heo, Kyun; Min, Sung-Won; Sung, Ho Jin; Kim, Han Gyul; Kim, Hyun Jung; Kim, Yun Hee; Choi, Beom Kyu; Han, Sewoon; Chung, Seok; Lee, Eun Sook; Chung, Junho; Kim, In-Hoo (2016): An aptamer-antibody complex (oligobody) as a novel delivery platform for targeted cancer therapies. In *Journal of Controlled Release* 229, pp. 1–9. DOI: 10.1016/j.jconrel.2016.03.006.

Herman, Rod A.; Scherer, Peter N.; Shan, Guomin (2008): Evaluation of logistic and polynomial models for fitting sandwich-ELISA calibration curves. In *Journal of Immunological Methods* 339 (2), pp. 245–258. DOI: 10.1016/j.jim.2008.09.001.

Herszényi, László; Farinati, Fabio; Cardin, Romilda; István, Gábor; Molnár, László D.; Hritz, István; De Paoli, Massimo; Plebani, Mario; Tulassay, Zsolt (2008): Tumor marker utility and prognostic relevance of cathepsin B, cathepsin L, urokinase-type plasminogen activator, plasminogen activator inhibitor type-1, CEA and CA 19-9 in colorectal cancer. In *BMC Cancer* 8, p. 194. DOI: 10.1186/1471-2407-8-194.

Hianik, T. (2018): Aptamer-based biosensors. In *Encyclopedia of Interfacial Chemistry*, vol. 344: Elsevier, pp. 11–19. DOI: 10.1016/B978-0-12-409547-2.13492-4

Huang, Po-Jung Jimmy; Liu, Juewen (2022): A DNA aptamer for theophylline with ultrahigh selectivity reminiscent of the classic RNA aptamer. In *ACS Chemical Biology* 17 (8), pp. 2121–2129. DOI: 10.1021/acschembio.2c00179.

Irigoyen, J. P.; Muñoz-Cánoves, P.; Montero, L.; Koziczak, M.; Nagamine, Y. (1999): The plasminogen activator system: biology and regulation. In *Cellular and Molecular Life Sciences* 56 (1-2), pp. 104–132. DOI: 10.1007/pl00000615.

Jarczewska, Marta; Kékedy-Nagy, László; Nielsen, Jesper S.; Campos, Rui; Kjems, Jørgen; Malinowska, Elżbieta; Ferapontova, Elena E. (2015): Electroanalysis of pM-levels of urokinase plasminogen activator in serum by phosphorothioated RNA aptamer. In *The Analyst* 140 (11), pp. 3794–3802. DOI: 10.1039/C4AN02354D.

Jerabek-Willemsen, Moran; Wienken, Chistoph J.; Braun, Dieter; Baaske, Philipp; Duhr, Stefan (2011): Molecular interaction studies using microscale thermophoresis. In *Assay and Drug Development Technologies* 9 (4), pp. 342–353. DOI: 10.1089/adt.2011.0380.

Kalra, Priya; Dhiman, Abhijeet; Cho, William C.; Bruno, John G.; Sharma, Tarun K. (2018): Simple methods and rational design for enhancing aptamer sensitivity and specificity. In *Frontiers in Molecular Biosciences* 5, p. 41. DOI: 10.3389/fmolb.2018.00041.

Kanwar, Jagat R.; Roy, Kislay; Maremanda, Nihal G.; Subramanian, Krishnakumar; Veedu, Rakesh N.; Bawa, Raj; Kanwar, Rupinder K. (2015): Nucleic acid-based aptamers: applications, development and clinical trials. In *Current Medicinal Chemistry* 22 (21), pp. 2539–2557. DOI: 10.2174/0929867322666150227144909.

Keefe, Anthony D.; Pai, Supriya; Ellington, Andrew (2010): Aptamers as therapeutics. In *Nature Reviews Drug Discovery* 9 (7), pp. 537–550. DOI: 10.1038/nrd3141.

Kelly, Ana M.; Mathema, Barun; Larson, Elaine L. (2017): Carbapenem-resistant Enterobacteriaceae in the community: a scoping review. In *International Journal of Antimicrobial Agents* 50 (2), pp. 127–134. DOI: 10.1016/j.ijantimicag.2017.03.012.

Klug, Stefanie J.; Famulok, Michael (1994): All you wanted to know about SELEX. In *Molecular Biology Reports* 20 (2), pp. 97–107. DOI: 10.1007/BF00996358.

Kobayashi, Hiroshi; Fujishiro, Suguru; Terao, Toshihiko (1994): Impact of urokinase-type plasminogen activator and its inhibitor type 1 on prognosis in cervical cancer of the uterus. In *Cancer Research* 54 (24), pp. 6539–6548.

Koelbl, H.; Kirchheimer, J. C.; Tatra, G.; Christ, G.; Binder, B. R. (1988): Increased plasma levels of urokinase-type plasminogen activator with endometrial and cervical cancer. In *Obstetrics and Gynecology* 72 (2), pp. 252–256.

Koivunen, Marja E.; Krogsrud, Richard L. (2006): Principles of immunochemical techniques used in clinical laboratories. In *Laboratory Medicine* 37 (8), pp. 490–497. DOI: 10.1309/MV9RM1FDLWAUWQ3F.

Kumari, G. Lakshmi; Dhir, Ravindra N. (2003): Comparative studies with penicillinase, horseradish peroxidase, and alkaline phosphatase as enzyme labels in developing enzyme immunoassay of cortisol. In *Journal of Immunoassay and Immunochemistry* 24 (2), pp. 173–190. DOI: 10.1081/IAS-120020083.

Lakhin, A. V.; Tarantul, V. Z.; Gening, L. V. (2013): Aptamers: problems, solutions and prospects. In *Acta Naturae* 5 (4), pp. 34–43.

Lee, Chang Ho; Lee, Soo-Han; Kim, Ji Hyun; Noh, Yook-Hwan; Noh, Gyu-Jeong; Lee, Seong-Wook (2015): Pharmacokinetics of a cholesterol-conjugated aptamer against the hepatitis C virus (HCV) NS5B protein. In *Molecular Therapy–Nucleic Acids* 4 (10), e254. DOI: 10.1038/mtna.2015.30.

Li Santi, Anna; Napolitano, Filomena; Montuori, Nunzia; Ragno, Pia (2021): The urokinase receptor: A multifunctional receptor in cancer cell biology. Therapeutic Implications. In *International Journal of Molecular Sciences* 22 (8), p. 4111. DOI: 10.3390/ijms22084111.

Liu, Zheng; Gurlo, Tatyana; von Grafenstein, Hermann (2000): Cell-ELISA using beta-galactosidase conjugated antibodies. In *Journal of Immunological Methods* 234 (1-2), pp. 153–67. DOI: 10.1016/S0022-1759(99)00216-1.

Lutgring, Joseph D.; Limbago, Brandi M. (2016): The problem of carbapenemase-producing-carbapenem-resistant-enterobacteriaceae detection. In *Journal of Clinical Microbiology* 54 (3), pp. 529–534. DOI: 10.1128/jcm.02771-15.

MacFarlane, R. G.; Pilling, J. (1947): Fibrinolytic activity of normal urine. In *Nature* 159 (4049), p. 779. DOI: 10.1038/159779a0.

Madunić, Josip (2018): The urokinase plasminogen activator system in human cancers: An overview of its prognostic and predictive role. In *Thrombosis and Haemostasis* 118 (12), pp. 2020–2036. DOI: 10.1055/s-0038-1675399.

Mahmood, Niaz; Mihalcioiu, Catalin; Rabbani, Shafaat A. (2018): Multifaceted role of the urokinase-type plasminogen activator (uPA) and its receptor (uPAR): Diagnostic, prognostic, and therapeutic applications. In *Frontiers in Oncology* 8, p. 24. DOI: 10.3389/fonc.2018.00024.

Marimuthu, Citartan; Tang, Thean-Hock; Tominaga, Junji; Tan, Soo-Choon; Gopinath, Subash C. B. (2012): Single-stranded DNA (ssDNA) production in DNA aptamer generation. In *The Analyst* 137 (6), p. 1307. DOI: 10.1039/C2AN15905H.

Marshall, Kristin A.; Ellington, Andrew D. (2000): [14] In vitro selection of RNA aptamers. In : RNA-Ligand Interactions Part B, vol. 318: Elsevier (Methods in Enzymology), pp. 193–214.

Masucci, Maria Teresa; Minopoli, Michele; Di Carluccio, Gioconda; Motti, Maria Letizia; Carriero, Maria Vincenza (2022): Therapeutic strategies targeting urokinase and its receptor in cancer. In *Cancers* 14 (3). DOI: 10.3390/cancers14030498.

Mekkawy, Ahmed H.; Pourgholami, Mohammad H.; Morris, David L. (2014): Involvement of urokinase-type plasminogen activator system in cancer: an overview. In *Medicinal Research Reviews* 34 (5), pp. 918–956. DOI: 10.1002/med.21308.

Mencin, Nina; Šmuc, Tina; Vraničar, Marko; Mavri, Jan; Hren, Matjaž; Galeša, Katja; Kroč, Peter; Ulrich, Henning; Šolar, Borut (2014): Optimization of SELEX: comparison of different methods for monitoring the progress of in vitro selection of aptamers. In *Journal of Pharmaceutical and Biomedical Analysis* 91, pp. 151–159. DOI: 10.1016/j.jpba.2013.12.031.

Moellering, Robert C. (2010): NDM-1--a cause for worldwide concern. In *The New England Journal of Medicine* 363 (25), pp. 2377–2379. DOI: 10.1056/NEJMp1011715.

Morita, Yoshihiro; Leslie, Macall; Kameyama, Hiroyasu; Volk, David E.; Tanaka, Takemi (2018): Aptamer therapeutics in cancer: Current and future. In *Cancers* 10 (3). DOI: 10.3390/cancers10030080.

Nagatoishi, Satoru; Isono, Noburu; Tsumoto, Kouhei; Sugimoto, Naoki (2011): Loop residues of thrombin-binding DNA aptamer impact G-quadruplex stability and thrombin binding. In *Biochimie* 93 (8), pp. 1231–1238. DOI: 10.1016/j.biochi.2011.03.013.

Nguyen, Hoang Hiep; Park, Jeho; Kang, Sebyung; Kim, Moonil (2015): Surface plasmon resonance: a versatile technique for biosensor applications. In *Sensors* 15 (5), pp. 10481–10510. DOI: 10.3390/s150510481.

Ni, Shuaijian; Zhuo, Zhenjian; Pan, Yufei; Yu, Yuanyuan; Li, Fangfei; Liu, Jin; Wang, Luyao; Wu, Xiaoqiu; Li, Dijie; Wan, Youyang; Zhang, Lihe; Yang, Zhenjun; Zhang, Bao-Ting; Lu, Aiping; Zhang, Ge (2021): Recent progress in aptamer discoveries and modifications for therapeutic applications. In *ACS Applied Materials & Interfaces* 13 (8), pp. 9500–9519. DOI: 10.1021/acsami.0c05750.

Niazi, Javed H.; Lee, Su Jin; Kim, Yeon Seok; Gu, Man Bock (2008): ssDNA aptamers that selectively bind oxytetracycline. In *Bioorganic and Medicinal Chemistry* 16 (3), pp. 1254–1261. DOI: 10.1016/j.bmc.2007.10.073.

Null, Allison P.; Hannis, James C.; Muddiman, David C. (2000): Preparation of single-stranded PCR products for electrospray ionization mass spectrometry using the DNA repair enzyme lambda exonuclease. In *The Analyst* 125 (4), pp. 619–626. DOI: 10.1039/A908022H.

O'Grady, P.; Lijnen, H. R.; Duffy, M. J. (1985): Multiple forms of plasminogen activator in human breast tumors. In *Cancer Research* 45 (12 Pt 1), pp. 6216–6218.

Ospina-Villa, Juan David; López-Camarillo, César; Castañón-Sánchez, Carlos A.; Soto-Sánchez, Jacqueline; Ramírez-Moreno, Esther; Marchat, Laurence A. (2018): Advances on aptamers against protozoan parasites. In *Genes* 9 (12). DOI: 10.3390/genes9120584.

Petersen, Lars C.; Lund, Leif R.; Nielsen, Lars S.; Danø, Keld; Skriver, Lars (1988): One-chain urokinase-type plasminogen activator from human sarcoma cells is a proenzyme with little or no intrinsic activity. In *The Journal of Biological Chemistry* 263 (23), pp. 11189–11195.

Pfeiffer, Franziska; Mayer, Günter (2016): Selection and Biosensor Application of Aptamers for Small Molecules. In *Frontiers in Chemistry* 4, p. 25. DOI: 10.3389/fchem.2016.00025.

Plach, Maximilian; Schubert, Thomas (2020): Biophysical characterization of aptamer-target interactions. In *Advances in Biochemical Engineering/Biotechnology* 174, pp. 1–15. DOI: 10.1007/10_2019_103.

Poon, Terence C.; Johnson, Philip J. (2001): Proteome analysis and its impact on the discovery of serological tumor markers. In *Clinica Chimica Acta* 313 (1-2), pp. 231–239. DOI: 10.1016/S0009-8981(01)00677-5.

Röthlisberger, Pascal; Hollenstein, Marcel (2018): Aptamer chemistry. In *Advanced Drug Delivery Reviews* 134, pp. 3–21. DOI: 10.1016/j.addr.2018.04.007.

Ruckman, Judy; Green, Louis S.; Beeson, Jim; Waugh, Sheela; Gillette, Wwendy L.; Henninger, Dwight D.; Claesson-Welsh, Lena; Janjic, Nebojsa (1998): 2'-Fluoropyrimidine RNA-based aptamers to the 165-amino acid form of vascular endothelial growth factor (VEGF165). Inhibition of receptor binding and VEGF-induced vascular permeability through interactions requiring the exon 7-encoded domain. In *The Journal of Biological Chemistry* 273 (32), pp. 20556–20567. DOI: 10.1074/jbc.273.32.20556.

Salden, M.; Splinter, T. A.; Peters, H. A.; Look, M. P.; Timmermans, M.; van Meerbeeck, J. P.; Foekens, J. A. (2000): The urokinase-type plasminogen activator system in resected non-small-cell lung cancer. In *Annals of Oncology* 11 (3), pp. 327–332. DOI: 10.1023/a:1008312801800.

Sánchez-Báscones, Elena; Parra, Francisco; Lobo-Castañón, María Jesús (2021): Aptamers against viruses: Selection strategies and bioanalytical applications. In *Trends in Analytical Chemistry* 143, p. 116349. DOI: 10.1016/j.trac.2021.116349.

Schmitt, M.; Goretzki, L.; Jänicke, F.; Calvete, J.; Eulitz, M.; Kobayashi, H. et al. (1991): Biological and clinical relevance of the urokinase-type plasminogen activator (uPA) in breast cancer. In *Biomedica Biochimica Acta* 50 (4-6), pp. 731–741.

Schuettfort, Victor M.; Pradere, Benjamin; D'Andrea, David; Grossmann, Nico C.; Quhal, Fahad; Mostafaei, Hadi; Laukhtina, Ekaterina; Mori, Keiichiro; Rink, Michael; Karakiewicz, Pierre I.; Motlagh, Reza Sari; Katayama, Satoshi; Lotan, Yair; Scherr, Doaglas; Abufaraj, Mohammad; Fajkovica, Harun; Compérat, Eva; Enikeev, Dmitry; Shariat, Shahrok F. (2021): Prognostic impact of preoperative plasma levels of urokinase plasminogen activator proteins on disease outcomes after radical cystectomy. In *The Journal of Urology* 206 (5), pp. 1122–1131. DOI: 10.1097/JU.0000000000001936.

Schütze, Tatjana; Wilhelm, Barbara; Greiner, Nicole; Braun, Hannsjörg; Peter, Franziska; Mörl, Mario; Erdmann, Volker A.; Lehrbach, Hans; Konthur, Zoltán; Menger, Marcus; Arndt, Peter F.; Glökler, Jörn (2011): Probing the SELEX process with next-generation sequencing. In *PloS One* 6 (12), e29604. DOI: 10.1371/journal.pone.0029604.

Sgier, David; Zuberbuehler, Kathrin; Pfaffen, Stefanie; Neri, Dario (2010): Isolation and characterization of an inhibitory human monoclonal antibody specific to the urokinase-type plasminogen activator, uPA. In *Protein Engineering, Design and Selection* 23 (4), pp. 261–269. DOI: 10.1093/protein/gzp089.

Shah, Karishma; Maghsoudlou, Panagiotis (2016): Enzyme-linked immunosorbent assay (ELISA): the basics. In *British Journal of Hospital Medicine* 77 (7), pp. 98–101. DOI: 10.12968/hmed.2016.77.7.C98.

Shakil, S.; Azhar, E. I.; Tabrez, S.; Kamal, M. A.; Jabir, N. R.; Abuzenadah, A. M. et al. (2011): New Delhi metallo-β-lactamase (NDM-1): an update. In *Journal of Chemotherapy* 23 (5), pp. 263–265. DOI: 10.1179/joc.2011.23.5.263.

Shariat, Shahrokh F.; Casella, Roberto; Monoski, Mara A.; Sulser, Tullio; Gasser, Thomas C.; Lerner, Seth P. (2003a): The addition of urinary urokinase-type plasminogen activator to urinary nuclear matrix protein 22 and cytology improves the detection of bladder cancer. In *The Journal of Urology* 170 (6 Pt 1), pp. 2244–2247. DOI: 10.1097/01.ju.0000090965.71697.37.

Shariat, Shahrokh F.; Monoski, Mara A.; Andrews, Ben; Wheeler, Thomas M.; Lerner, Seth P.; Slawin, Kevin M. (2003b): Association of plasma urokinase-type plasminogen activator and its receptor with clinical outcome in patients undergoing radical cystectomy for transitional cell carcinoma of the bladder. In *Urology* 61 (5), pp. 1053–1058. DOI: 10.1016/s0090-4295(02)02522-0.

Shariat, Shahrokh F.; Roehrborn, Claus G.; McConnell, John D.; Park, Sangtae; Alam, Nina; Wheeler, Thomas M.; Slawin, Kevin M. (2007): Association of the circulating levels of the urokinase system of plasminogen activation with the presence of prostate cancer and invasion, progression, and metastasis. In *Journal of Clinical Oncology* 25 (4), pp. 349–355. DOI: 10.1200/jco.2006.05.6853.

Shariat, Shahrokh F.; Semjonow, Axel; Lilja, Hans; Savage, Caroline; Vickers, Andrew J.; Bjartell, Anders (2011): Tumor markers in prostate cancer I: blood-based markers. In *Acta Oncologica* 50, pp. 61–75. DOI: 10.3109/0284186X.2010.542174.

Shigdar, Sarah; Qian, Christine; Lv, Li; Pu, Chunwen; Li, Yong; Li, Lianhong; Marappan, Manju; Lin, Jia; Wang, Lifen; Duan, Wei (2013): The use of sensitive chemical antibodies for diagnosis: detection of low levels of EpCAM in breast cancer. In *PloS One* 8 (2), e57613. DOI: 10.1371/journal.pone.0057613.

Skrypina, Natalia A.; Savochkina, Larissa P.; Beabealashvilli, Robert Sh. (2004): In vitro selection of single-stranded DNA aptamers that bind human pro-urokinase. In *Nucleosides, Nucleotides and Nucleic Acids* 23 (6-7), pp. 891–893. DOI: 10.1081/NCN-200026037.

Song, Kyung-Mi; Lee, Seonghwan; Ban, Changill (2012): Aptamers and their biological applications. In *Sensors* 12 (1), pp. 612–631. DOI: 10.3390/s120100612.

Span, Paul N.; Witjes, Johannes A.; Grebenchtchikov, Nicolai; Geurts-Moespot, Anneke; Moonen, Paula M. J.; Aalders, Tilly W.; Vriesema, Jessica L.J.; Kiemeney, Lambertus A.L.M.; Schalken, Jack A.; Sweep, Fred C.G.J. (2008): Components of the plasminogen activator system and their complexes in renal cell and bladder cancer: comparison between normal and matched cancerous tissues. In *BJU International* 102 (2), pp. 177–182. DOI: 10.1111/j.1464-410x.2008.07568.x.

Stoltenburg, Regina; Reinemann, Christine; Strehlitz, Beate (2005): FluMag-SELEX as an advantageous method for DNA aptamer selection. In *Analytical and Bioanalytical Chemistry* 383 (1), pp. 83–91. DOI: 10.1007/s00216-005-3388-9.

Stoltenburg, Regina; Reinemann, Christine; Strehlitz, Beate (2007): SELEX–a (r)evolutionary method to generate high-affinity nucleic acid ligands. In *Biomolecular Engineering* 24 (4), pp. 381–403. DOI: 10.1016/j.bioeng.2007.06.001.

Su, Shih-Chi; Lin, Chiao-Wen; Yang, Wei-En; Fan, Wen-Lang; Yang, Shun-Fa (2016): The urokinase-type plasminogen activator (uPA) system as a biomarker and therapeutic target in human malignancies. In *Expert Opinion on Therapeutic Targets* 20 (5), pp. 551–566. DOI: 10.1517/14728222.2016.1113260.

Tabarzad, Maryam; Jafari, Marzieh (2016): Trends in the design and development of specific aptamers against peptides and proteins. In *The Protein Journal* 35 (2), pp. 81–99. DOI: 10.1007/s10930-016-9653-2.

Talebi Bezmin Abadi, Amin; Rizvanov, Albert A.; Haertlé, Thomas; Blatt, Nataliya L. (2019): World Health Organization report: Current crisis of antibiotic resistance. In *BioNanoScience* 9, pp. 778–788. DOI: 10.1007/s12668-019-00658-4.

Toh, Saw Yi; Citartan, Marimuthu; Gopinath, Subash C. B.; Tang, Thean-Hock (2015): Aptamers as a replacement for antibodies in enzyme-linked immunosorbent assay. In *Biosensors and Bioelectronics* 64, pp. 392–403. DOI: 10.1016/j.bios.2014.09.026.

Trunzo, Nevina E.; Hong, Ka Lok (2020): Recent progress in the identification of aptamers against bacterial origins and their diagnostic applications. In *International Journal of Molecular Sciences* 21 (14), p. 5074. DOI: 10.3390/ijms21145074.

Tuerk, Craig; Gold, Larry (1990): Systematic evolution of ligands by exponential enrichment: RNA ligands to bacteriophage T4 DNA polymerase. In *Science* 249 (4968), pp. 505–510. DOI: 10.1126/science.2200121.

Turecek, Peter L.; Bossard, Mary J.; Schoetens, Freddy; Ivens, Inge A. (2016): PEGylation of biopharmaceuticals: A review of chemistry and nonclinical safety information of approved drugs. In *Journal of Pharmaceutical Sciences* 105 (2), pp. 460–475. DOI: 10.1016/j.xphs.2015.11.015.

Ulisse, Salvatore; Baldini, Enke; Sorrenti, Salvatore; D'Armiento, Massimino (2009): The urokinase plasminogen activator system: a target for anti-cancer therapy. In *Current Cancer Drug Targets* 9 (1), pp. 32–71. DOI: 10.2174/156800909787314002.

Ünlü, Betül; Versteeg, Henri H. (2014): Effects of tumor-expressed coagulation factors on cancer progression and venous thrombosis: is there a key factor? In *Thrombosis Research* 133, pp. 76–84. DOI: 10.1016/S0049-3848(14)50013-8.

Vassalli, Jean-Dominique; Sappino, André-Pascal; Belin, Dominique (1991): The plasminogen activator/plasmin system. In *The Journal of Clinical Investigation* 88 (4), pp. 1067–1072. DOI: 10.1172/JCI115405.

Wang, Tao; Chen, Changying; Larcher, Leon M.; Barrero, Roberto A.; Veedu, Rakesh N. (2019): Three decades of nucleic acid aptamer technologies: Lessons learned, progress and opportunities on aptamer development. In *Biotechnology Advances* 37 (1), pp. 28–50. DOI: 10.1016/j.biotechadv.2018.11.001.

Willis, Michael. C.; Collins, Brian; Zhang, Tong; Green, Louis S.; Sebesta, David P.; Bell, Carol; Kellogg, Elizabeth; Gill, Stanley C.; Magallanez, Anna; Knauer, Susan; Bendele, Ray A.; Gill, Parkash S.; Janjic, Nebojsa (1998): Liposome-anchored vascular endothelial growth factor aptamers. In *Bioconjugate Chemistry* 9 (5), pp. 573–582. DOI: 10.1021/bc980002x.

Wing Fen, Yap; Mahmood Mat Yunus, W. (2013): Surface plasmon resonance spectroscopy as an alternative for sensing heavy metal ions: a review. In *Sensor Review* 33 (4), pp. 305–314. DOI: 10.1108/SR-01-2012-604.

Wochner, Aniela; Cech, Birgit; Menger, Marcus; Erdmann, Volker A.; Glökler, Jörn (2007): Semi-automated selection of DNA aptamers using magnetic particle handling. In *BioTechniques* 43 (3), pp. 344–353. DOI: 10.2144/000112532.

Wochner, Aniela; Glökler, Jörn (2007): Nonradioactive fluorescence microtiter plate assay monitoring aptamer selections. In *BioTechniques* 42 (5), pp. 578–582. DOI: 10.2144/000112472.

Wu, Jie; Fu, Zhifeng; Yan, Feng; Ju, Huangxian (2007): Biomedical and clinical applications of immunoassays and immunosensors for tumor markers. In *Trends in Analytical Chemistry* 26 (7), pp. 679–688. DOI: 10.1016/j.trac.2007.05.007.

Xu, Peng; Andreasen, Peter A.; Huang, Mingdong (2017): Structural principles in the development of cyclic peptidic enzyme inhibitors. In *International Journal of Biological Sciences* 13 (10), pp. 1222–1233. DOI: 10.7150/ijbs.21597.

Yang, Jia-Lin; Seetoo, Da-qiang; Wang, Yao; Ranson, Marie; Berney, Christophe R.; Ham, John M.; Russel, Pamela J.; Crowe, Philip J. (2000): Urokinase-type plasminogen activator and its receptor in colorectal cancer: Independent prognostic factors of metastasis and cancer-specific survival and potential therapeutic targets. In *International Journal of Cancer* 89 (5), pp. 431–439. DOI: 10.1002/1097-0215(20000920)89:5<431::aid-ijc6>3.0.co;2-v.

Yang, Yanbing; Yang, Xiangdong; Yang, Yujie; Yuan, Quan (2018): Aptamer-functionalized carbon nanomaterials electrochemical sensors for detecting cancer relevant biomolecules. In *Carbon* 129 (3), pp. 380–395. DOI: 10.1016/j.carbon.2017.12.013.

Yin, Yongmei; Cao, Ya; Xu, Yuanyuan; Li, Genxi (2010): Colorimetric immunoassay for detection of tumor markers. In *International Journal of Molecular Sciences* 11 (12), pp. 5077–5094. DOI: 10.3390/ijms11125077.

Yong, Dongeun; Toleman, Mark A.; Giske, Christian G.; Cho, Hyun S.; Sundman, Kristina; Lee, Kyungwon; Walsh, Timothy R. (2009): Characterization of a new metallo-beta-lactamase gene, bla(NDM-1), and a novel erythromycin esterase gene carried on a unique genetic structure in Klebsiella pneumoniae sequence type 14 from India. In *Antimicrobial Agents and Chemotherapy* 53 (12), pp. 5046–5054. DOI: 10.1128/AAC.00774-09.

Zhou, Jing; Soontornworajit, Boonchoy; Martin, Jacob; Sullenger, Bruce A.; Gilboa, Eli; Wang, Yong (2009): A hybrid DNA aptamer-dendrimer nanomaterial for targeted cell labeling. In *Macromolecular Bioscience* 9 (9), pp. 831–835. DOI: 10.1002/mabi.200900046.

Zhuo, Zhenjian; Yu, Yuanyuan; Wang, Maolin; Li, Jie; Zhang, Zongkang; Liu, Jin; Wu, Xiaohao; Lu, Aiping; Zhang, Ge; Zhang, Boating (2017): Recent advances in SELEX technology and aptamer applications in biomedicine. In *International Journal of Molecular Sciences* 18 (10), p. 2142. DOI: 10.3390/ijms18102142.

Zuker, Michael (2003): Mfold web server for nucleic acid folding and hybridization prediction. In *Nucleic Acids Research* 31 (13), pp. 3406–3415. DOI: 10.1093/nar/gkg595.

6. List of Figures

Figure 1: Schematic illustration of the SELEX process with a ssDNA library 4

Figure 2: Domain structure of pro-uPA and uPA.....11

Figure 3: Schematic illustration of the three different sandwich assay formats developed for the detection of human urokinase.....14

7. Eidesstattliche Erklärung

Hiermit versichere ich an Eides statt, dass ich die vorliegende Arbeit selbständig und nur mit den angegebenen Quellen und Hilfsmitteln angefertigt habe. Alle Stellen der Arbeit, die ich aus diesen Quellen und Hilfsmitteln dem Wortlaut oder dem Sinne nach entnommen habe, sind kenntlich gemacht und im Literaturverzeichnis aufgeführt. Weiterhin versichere ich, dass die eingereichte Arbeit oder wesentliche Teile dieser Arbeit in keinem anderen Verfahren zur Erlangung eines akademischen Grades vorgelegt wurden.

Potsdam-Golm, 18.04.2023

Ort, Datum

Unterschrift

8. Appendix

8.1 Supplementary Information to Manuscript III

Dreymann, Nico; Sabrowski, Wiebke; Danso, Jennifer; Menger, Marcus M. (2022): Aptamer-Based Sandwich Assay Formats for Detection and Discrimination of Human High- and Low-Molecular-Weight uPA for Cancer Prognosis and Diagnosis. In *Cancers* 14 (21). DOI: 10.3390/cancers14215222.

Supplementary Materials: Aptamer-based Sandwich Assay Formats for Detection and Discrimination of High- and Low-Molecular-Weight uPA for Cancer Prognosis and Diagnosis

Nico Dreymann [1,2], Wiebke Sabrowski [1,3], Jennifer Danso [1,4] and Marcus M. Menger [1,*]

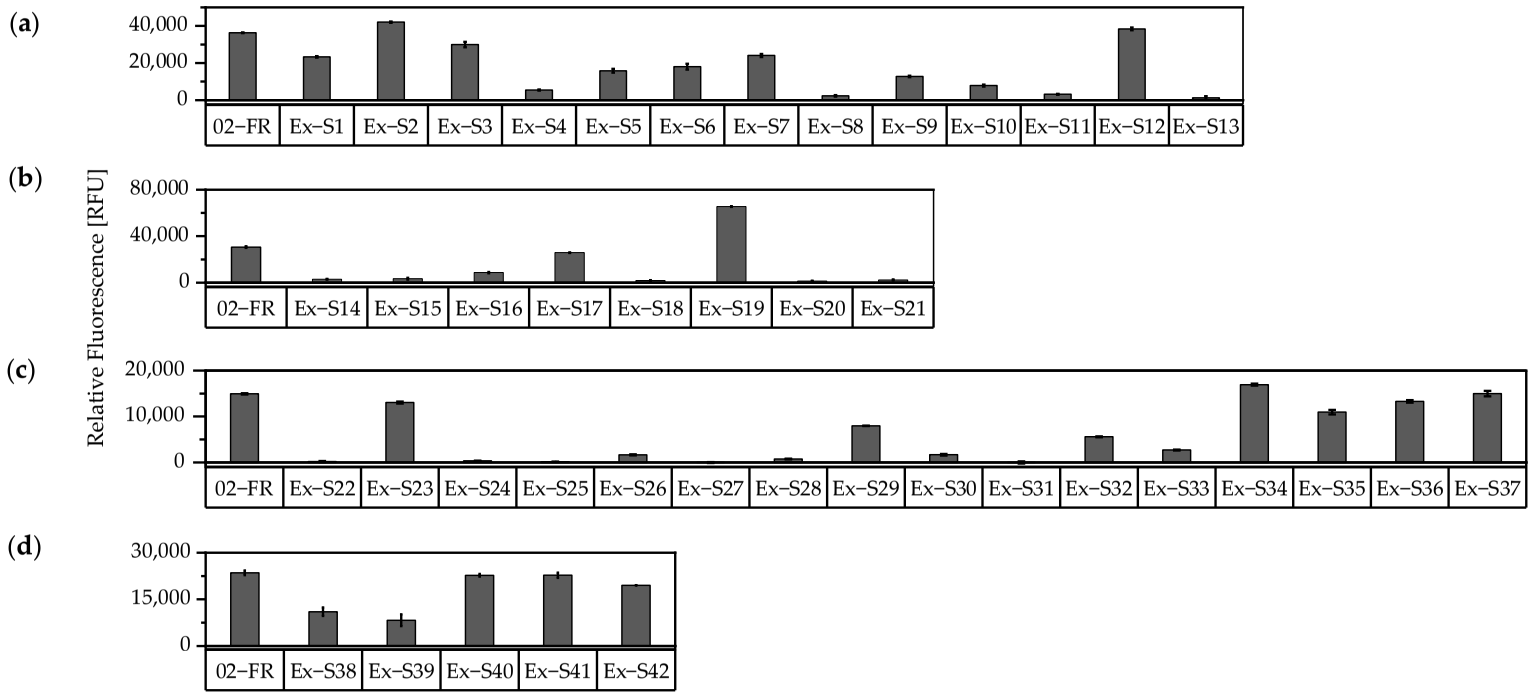

Figure S1. Binding of the exchange sequences (Ex–S1 – Ex–S42) to HMW-uPA by FLAA. Binding experiments were performed on different micro titer plates and are therefore shown as individual diagrams with the respective positive control uPAapt–02–FR (02–FR). (**a**) Ex–S1 – Ex–S13 (**b**) Ex–S14 – Ex–S21 (**c**) Ex–S22 – Ex–S37 (**d**) Ex–S38 – Ex–S42. The relative fluorescence unit [RFU] for each sample is given as the mean value of technical replicates and was measured using the multimode microplate reader Mithras² LB943. Negative control values were subtracted. Error bars represent the range of measured values of signals from the two target-coated wells plus the range of the measured values of the two negative control wells. Number of records n=2.

Table S1. Exchange sequences of uPAapt−02−FR. Each nucleotide of the sequence of uPAapt−02−FR was replaced individually (for G/C a T and for A/T a C). All 42 new sequence aptamers (Ex−S1 – Ex−S42) were tested for binding to HMW-uPA by FLAA. The reduction in fluorescence signal compared to the control uPAapt−02−FR is given as a percentage for each sequence. Exchanged nucleotides in each sequence are shown in red.

Name	Sequence	Signal reduction compared to control (uPAapt−02−FR)
Ex−S1	TAAGCGGGGGTGAGAGATCTGTCAGTACGAGCTGGGTTTGCG	36%
Ex−S2	CCAGCGGGGGTGAGAGATCTGTCAGTACGAGCTGGGTTTGCG	n.r.*
Ex−S3	CACGCGGGGGTGAGAGATCTGTCAGTACGAGCTGGGTTTGCG	18%
Ex−S4	CAATCGGGGGTGAGAGATCTGTCAGTACGAGCTGGGTTTGCG	85%
Ex−S5	CAAGTGGGGGTGAGAGATCTGTCAGTACGAGCTGGGTTTGCG	56%
Ex−S6	CAAGCTGGGGTGAGAGATCTGTCAGTACGAGCTGGGTTTGCG	50%
Ex−S7	CAAGCGTGGGTGAGAGATCTGTCAGTACGAGCTGGGTTTGCG	34%
Ex−S8	CAAGCGGTGGTGAGAGATCTGTCAGTACGAGCTGGGTTTGCG	94%
Ex−S9	CAAGCGGGTGTGAGAGATCTGTCAGTACGAGCTGGGTTTGCG	65%
Ex−S10	CAAGCGGGGTTGAGAGATCTGTCAGTACGAGCTGGGTTTGCG	78%
Ex−S11	CAAGCGGGGGCGAGAGATCTGTCAGTACGAGCTGGGTTTGCG	91%
Ex−S12	CAAGCGGGGGTTAGAGATCTGTCAGTACGAGCTGGGTTTGCG	n.r.*
Ex−S13	CAAGCGGGGGTGCGAGATCTGTCAGTACGAGCTGGGTTTGCG	97%
Ex−S14	CAAGCGGGGGTGATAGATCTGTCAGTACGAGCTGGGTTTGCG	91%
Ex−S15	CAAGCGGGGGTGAGCGATCTGTCAGTACGAGCTGGGTTTGCG	89%
Ex−S16	CAAGCGGGGGTGAGATATCTGTCAGTACGAGCTGGGTTTGCG	72%
Ex−S17	CAAGCGGGGGTGAGAGCTCTGTCAGTACGAGCTGGGTTTGCG	16%
Ex−S18	CAAGCGGGGGTGAGAGACCTGTCAGTACGAGCTGGGTTTGCG	94%
Ex−S19	CAAGCGGGGGTGAGAGATTTGTCAGTACGAGCTGGGTTTGCG	0%*
Ex−S20	CAAGCGGGGGTGAGAGATCCGTCAGTACGAGCTGGGTTTGCG	95%
Ex−S21	CAAGCGGGGGTGAGAGATCTTTCAGTACGAGCTGGGTTTGCG	92%
Ex−S22	CAAGCGGGGGTGAGAGATCTGCCAGTACGAGCTGGGTTTGCG	99%
Ex−S23	CAAGCGGGGGTGAGAGATCTGTTAGTACGAGCTGGGTTTGCG	13%
Ex−S24	CAAGCGGGGGTGAGAGATCTGTCCGTACGAGCTGGGTTTGCG	98%
Ex−S25	CAAGCGGGGGTGAGAGATCTGTCATTACGAGCTGGGTTTGCG	99%
Ex−S26	CAAGCGGGGGTGAGAGATCTGTCAGCACGAGCTGGGTTTGCG	89%
Ex−S27	CAAGCGGGGGTGAGAGATCTGTCAGTCCGAGCTGGGTTTGCG	100%
Ex−S28	CAAGCGGGGGTGAGAGATCTGTCAGTATGAGCTGGGTTTGCG	95%
Ex−S29	CAAGCGGGGGTGAGAGATCTGTCAGTACTAGCTGGGTTTGCG	47%
Ex−S30	CAAGCGGGGGTGAGAGATCTGTCAGTACGCGCTGGGTTTGCG	89%
Ex−S31	CAAGCGGGGGTGAGAGATCTGTCAGTACGATCTGGGTTTGCG	100%
Ex−S32	CAAGCGGGGGTGAGAGATCTGTCAGTACGAGTTGGGTTTGCG	63%
Ex−S33	CAAGCGGGGGTGAGAGATCTGTCAGTACGAGCCGGGTTTGCG	82%
Ex−S34	CAAGCGGGGGTGAGAGATCTGTCAGTACGAGCTTGGTTTGCG	0%*
Ex−S35	CAAGCGGGGGTGAGAGATCTGTCAGTACGAGCTGTGTTTGCG	27%
Ex−S36	CAAGCGGGGGTGAGAGATCTGTCAGTACGAGCTGGTTTTGCG	11%
Ex−S37	CAAGCGGGGGTGAGAGATCTGTCAGTACGAGCTGGGCTTGCG	n.r.*
Ex−S38	CAAGCGGGGGTGAGAGATCTGTCAGTACGAGCTGGGTCTGCG	53%
Ex−S39	CAAGCGGGGGTGAGAGATCTGTCAGTACGAGCTGGGTTCGCG	65%
Ex−S40	CAAGCGGGGGTGAGAGATCTGTCAGTACGAGCTGGGTTTTCG	3%
Ex−S41	CAAGCGGGGGTGAGAGATCTGTCAGTACGAGCTGGGTTTGTG	3%
Ex−S42	CAAGCGGGGGTGAGAGATCTGTCAGTACGAGCTGGGTTTGCT	17%

Note: n.r.*, no reduction (equal or higher signal compared to control uPAapt−02−FR).

8.2 Supplementary Information to Manuscript IV

Sabrowski, Wiebke; **Dreymann, Nico**; Möller, Anja; Czepluch, Denise; Albani, Patricia P.; Theodoridis, Dimitrios; Menger, Marcus M. (2022): The use of high-affinity polyhistidine binders as masking probes for the selection of an NDM-1 specific aptamer. In *Scientific reports* 12 (1), p. 7936. DOI: 10.1038/s41598-022-12062-2.

Supplementary Figures and Tables

The use of high-affinity polyhistidine binders as masking probes for the selection of an NDM-1 specific aptamer

Wiebke Sabrowski [1, 2], Nico Dreymann [1, 3], Anja Möller [1], Denise Czepluch [1], Patricia P. Albani [4], Dimitrios Theodoridis [4] and Marcus M. Menger [1*]

[1] Fraunhofer Institute for Cell Therapy and Immunology, Branch Bioanalytics and Bioprocesses (IZI-BB), Am Mühlenberg 13, 14476 Potsdam, Germany

[2] Institute of Chemistry and Biochemistry – Biochemistry, Freie Universität Berlin, Takustr. 6, 14195, Berlin, Germany

[3] Institute of Biochemistry and Biology, University of Potsdam, Karl-Liebknecht Strasse 24-25, 14476, Potsdam-Golm, Germany

[4] nal von minden GmbH, Robert-Bosch-Breite 23, 37079 Göttingen, Germany

*marcus.menger@IZI-BB.fraunhofer.de

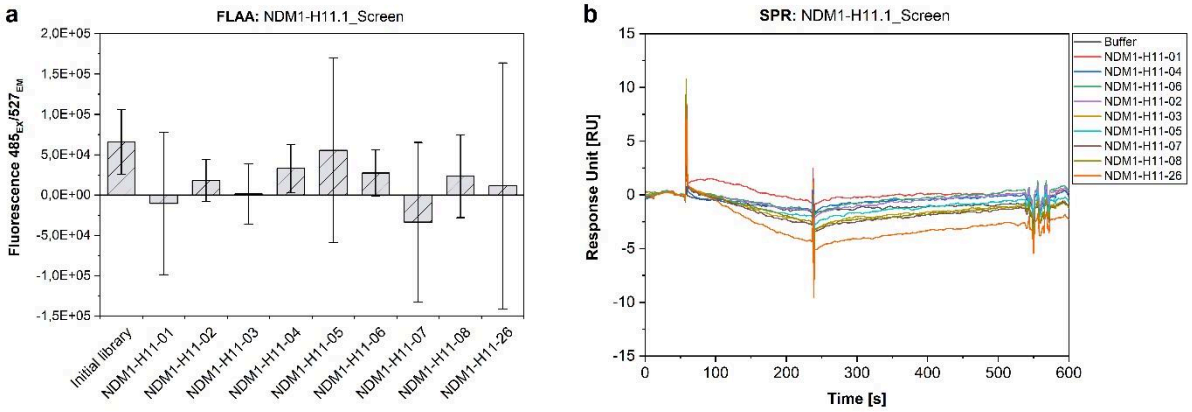

Supplementary Figure S1: FLAA and SPR Screen after SR11.1. HIS-NDM-1 was immobilized on either a FLUOTRAC™ 600 microplate and incubated with initial library and aptamer candidates (a) or on a SPR sensor chip and aptamer candidates were injected as analytes (b). No binding was detected. Error bars reflect the standard deviation of signals from three target-coated wells plus the standard deviation from three negative controll wells in FLAA.

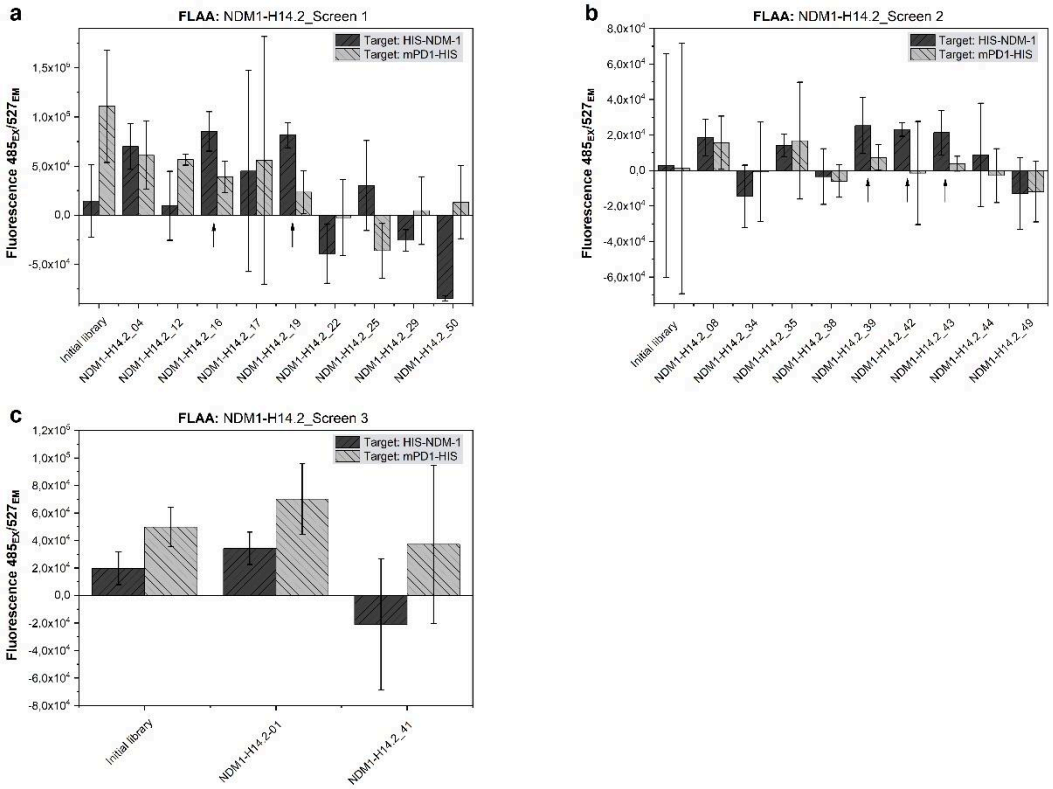

Supplementary Figure S2: FLAA screening after SR14.2. HIS-NDM-1 and mPD1-HIS were immobilized on a FLUOTRAC™ 600 microplate and incubated with initial library and aptamer candidates. Aptamer candidates for which binding signals for HIS-NDM-1 exceeded that for mPD1-HIS were chosen for further characterization. Error bars reflect the standard deviation of signals from three target-coated wells plus the standard deviation from three negative controll wells in FLAA.

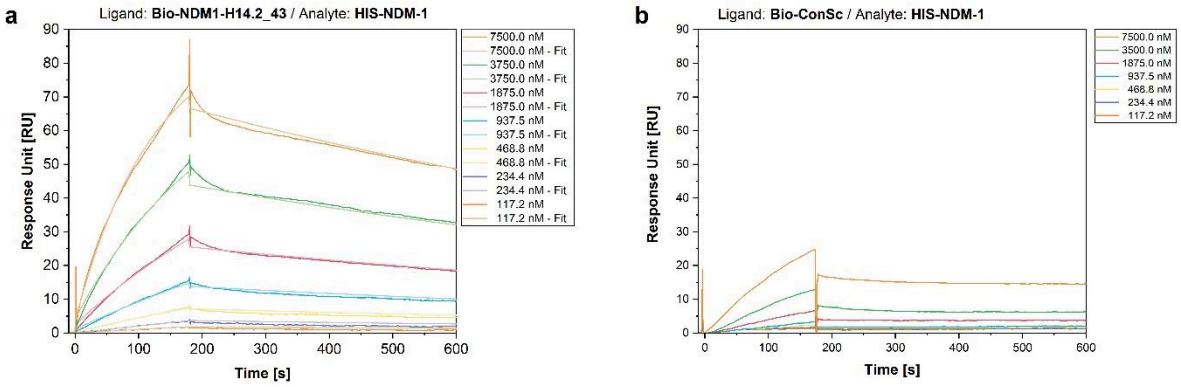

Supplementary Figure S3: SPR measurement for ConSc (b) in comparison to NDM1-H14.2_43 (a). Response units upon injection of increasing concentrations of HIS-NDM-1 were strongly reduced for ConSc. Kinetic parameters could not be determined.

Supplementary Table S1: Selection against HIS-NDM-1: Negative selections and masking approach.

SR	ssDNA [pmol]	NDM-1-coated beads [pmol]	NDM-1-coated beads [µl]	Beads only [µl]	KPC-2-coated beads [pmol]	OXA-23-coated beads [pmol]	mPD1-coated beads [pmol]	CFHR1-coated beads [pmol]	NDM1-H14-01-FR (masking) [pmol]
1.1	1000	100	13.2	1x 13.2	-	-	-	-	-
1.2	1000	100	13.2	1x 13.2					
2.1	200	40	5.6	2x 5.6					
3.1	200	40	5.3	2x 5.3 + 1x 10.6					
3.1_ Control	200	-	-	2x 5.3 + 1x 10.6, selection step with 5.3					
4.1	120	40	5.3	2x 5.3 + 1x 10.6					
5.1	120	40	3.8	1x 3.8 + 1x 7.6	40				
5.1_ Control	120	-	-	1x 3.8 + 1x 7.6, selection step with with 3.8	40				
6.1	120	40	3.8	1x 3.8 + 1x 7.6	40				
6.1_ Control	120	-	-	1x 3.8 + 1x 7.6, selection step with 3.8	40				
7.1	120	40	3.8	1x 3.8 + 1x 7.6	40				
6.2	120	40	5.1	1x 5.1 + 1x 10.2	40				
6.2_ Control	120	-	-	1x 5.1 + 1x 10.2, selection step with 5.3	40				
7.2	120	40	5.1	1x 5.1 + 1x 10.2	40				
7.2_ Control	120	-	-	1x 5.1 + 1x 10.2, selection step with 5.3	40				
8.1	80	40	5.1	1x 5.1 + 1x 10.2 + 1x 15.3	40	40			
8.1_ Control	80	-	-	1x 5.1 + 1x 10.2 + 1x 15.3, selection step with 5.3	40	40			
9.1	80	40	3.4	1x 3.4 + 1x 6.8 + 1x 10.2	40	40			
10.1	80	40	8.5	1x 8.5 + 1x 17 + 1x 25.5	80	80			
10.1_ Control	80	40	-	1x 8.5 + 1x 17 + 1x 25.5, selection step with 8.5	80	80			
11.1	80	40	3.4	1x 3.4 + 1x 6.8 + 1x 10.2, selection step with 3.4	80	80			
11.1_ Control	80	40	-	1x 3.4 + 1x 6.8 + 1x 10.2, selection step with 3.4	80	80			
12.1	80	40	3.8	1x 3.8 + 1x 7.6 + 1x 11.4	-	-			
12.1_ Control	80	-	-	1x 3.8 + 1x 7.6 + 1x 11.4, selection step with 3.8					
13.1	80	40	5.3	1x 15.9 + 1x 10.6 + 1x 5.3					
13.1_ Control	80	-	-	1x 15.9 + 1x 10.6 + 1x 5.3, selection step with 5.3					
14.1	80	40	5.3	1x 15.9 + 1x 10.6 + 1x 5.3					
14.1_ Control	80	40	-	1x 15.9 + 1x 10.6 + 1x 5.3, selection step with 5.3					
11.2_Mask	80	40	4.0	1x 8 + 1x 4			40		400
12.2_Mask	80	40	4.0	1x 8 + 1x 4			80		400
12.2_Mask_ Control	80	-	-	1x 8 + 1x 4, selection step with 4			80		400
13.2_Mask	80	40	4.0	1x 8 + 1x 4			40	40	400
14.2_Mask	80	20	2.0	1x 4 + 1x 2			40	20	200
14.2_Mask_ Control	80	-	-	1x 4 + 1x 2, selection step with 2			40	20	200

Supplementary Table S2: Aptamer candidate sequences used in this work.

NDM1-H11-01	GTATCTGGTGGTCTATGGCCCGGGTCAACCGTTCTTCTCGTTTCCGTTATTTTGTCTTCTATGTTCTTCGTCGTCTATGC
NDM1-H11-02	GTATCTGGTGGTCTATGGCATAGACGACGAAGAACAGGACATTTTTGGTTTTTGGGTACTCCTCCGTTCTTCGTCGTCTATGC
NDM1-H11-03	GTATCTGGTGGTCTATGGCGGAGGTGTTCTGAGTAGTCAGTTCAAGTCGCTTAATTTTCGGGGTTCTTCGTCGTCTATGC
NDM1-H11-04	GTATCTGGTGGTCTATGGCACAGTGAAAATTCTTCGTCCCAATCTCTCTCTTCGACTCATATGTTCTTCGTCGTCTATGC
NDM1-H11-05	GTATCTGGTGGTCTATGGGTCGTCTCTTTTTTGTTGTTTTTTTTTGGTTTCCCGTGTTCTTCGTCGTCTATGC
NDM1-H11-06	GTATCTGGTGGTCTATGGCCCCGGAACCTTCGTCGATAGTTCTTCTCAACAGATACATTCCGGTTCTTCGTCGTCTATGC
NDM1-H11-07	GTATCTGGTGGTCTATGGCGGGACGTCGTCTAACGGTTCTTCTCTTGTCCTTTTTTGTGTGTGTTCTTCGTCGTCTATGC
NDM1-H11-08	GTATCTGGTGGTCTATGGCGGCGATAACAAAAAAAAAAACAAATTTGCTGTATCTGGTGGTCTATGGTTCTTCGTCGTCTATGC
NDM1-H11-26	GTATCTGGTGGTCTATGGCGAGGGGTGAGCTAAAAAAAAAAAAAAAATGTCCACGTCGTGGGGGGTTCTTCGTCGTCTATGC
NDM1-H14-01	GTATCTGGTGGTCTATGGCGTCATAGGTACCATGGGGGACTGCTCGGGATTGCGGATTCATGGCATAGACGACGAAGAAC
NDM1-H14-01-FR	CGTCATAGGTACCATGGGGGACTGCTCGGGATTGCGGATTCATG
NDM1-H14-02	GTATCTGGTGGTCTATGGCCAGTATGGCTGTTCAAGTCTTCAGAGGGTCTGCTCGGGATTGCGCATAGACGACGAAGAAC
NDM1-H14-03	GTATCTGGTGGTCTATGGCATAGACGACGAAGAACAGGACATTTTTGGTTTTTGGGTACTCCTCCGCATAGACGACGAAGAAC
NDM1-H14-04	GTATCTGGTGGTCTATGGCATAGACGACGAAGAACAGCCGCAAAAAATAAAAGCCTAACGAGGGGCATAGACGACGAAGAAC
NDM1-H14-05	GTATCTGGTGGTCTATGGCCCCGGAACCTTCGTCGATAGTTCTTCTCAACAGATACATTCCGGCATAGACGACGAAGAAC
NDM1-H14-06	GTATCTGGTGGTCTATGGCATAGACGACGAAGAACAACAAAAAGAGCGAACAAATCGGGGCTGGTGGGCATAGACGACGAAGAAC
NDM1-H14-07	GTATCTGGTGGTCTATGGCATAGACGACGAAGAACAGGCGGGCATAGACGACGAAGAACAGGCGGGCATAGACGACGAAGAAC
NDM1-H14-09	GTATCTGGTGGTCTATGGCATAGACGACGAAGAACACTAACACGTTTTTTTACCTTATACTTGCGGGCATAGACGACGAAGAAC
NDM1-H14-10	GTATCTGGTGGTCTATGGCGGCGATAACAAAAAAAAAACAAATTTGCTGTATCTGGTGGTCTATGGCATAGACGACGAAGAAC
NDM1-H14-12	GTATCTGGTGGTCTATGGCATAGACGACGAAGAACAGTGTATCTGGTGGTCTATGGCATAGACGACGAAGAAC
NDM1-H14-17	GTATCTGGTGGTCTATGGCGGAGGTGTTCTGAGTAGTCAGTTCAAGTCGCTTAATTTTCGGGGCATAGACGACGAAGAAC
NDM1-H14-18	GTATCTGGTGGTCTATGG CCCGGGTCAACCGTTCTTCTCGTTTCCGTTATTTTGTCTTCTATGCATAGACGACGAAGAAC
NDM1-H14-25	GTATCTGGTGGTCTATGGCAAACGTTCTGAGTTAGGCTTATTTTTCTCTCTTCCCTTCGCCGCATAGACGACGAAGAAC
NDM1-H14-39	GTATCTGGTGGTCTATGGCATAGACGACGAAGAACAATAAGGGGCAAATCTATTTAATTGGGGAGAGCATAGACGACGAAGAAC
NDM1-H14.2_04	GTATCTGGTGGTCTATGGCATAGACGACGAAGAACAATGAAACCCAATCCCTCTCCCCTTCGCCGCATAGACGACGAAGAAC
NDM1-H14.2_08	GTATCTGGTGGTCTATGGCCCCGGAACCTTCGTCGATAGTTCTTCTCAACAGATACATTCCGGCATAGACGACGAAGAAC
NDM1-H14.2_12	GTATCTGGTGGTCTATGGCCCCGTACCTATGACGCGCTTTTCTTTTTCTTATCTTTCCTTGTGCATAGACGACGAAGAAC
NDM1-H14.2_16	GTATCTGGTGGTCTATGGCCAACGAGAATCGGCAATCCTTAAACTGTGTATCTGGTGGTCTATGGCATAGACGACGAAGAAC

NDM1-H14.2_17	GTATCTGGTGGTCTATGGCATAGACGACGAAGAACAACCTTGAATCCAATTATCCCCAGCATAGACGACGAAGAAC
NDM1-H14.2_19	GTATCTGGTGGTCTATGGCCAAAATCCATCAATCCCGTTTTCATGTGCTCCGCTTACTCTTCGCATAGACGACGAAGAAC
NDM1-H14.2_22	GTATCTGGTGGTCTATGGCATAGACGACGAAGAACAGACCACTTATTTAATCCCACCCAGGCATAGACGACGAAGAAC
NDM1-H14.2_25	GTATCTGGTGGTCTATGGCCAGACTACTTTCAAAAACCAGACCATTTCATTTTAGTAAATCCGCATAGACGACGAAGAAC
NDM1-H14.2_29	GTATCTGGTGGTCTATGGCCAACAAATACAATTAACATGAAGCCGCCCTGTTTTTTCCTTCCGCATAGACGACGAAGAAC
NDM1-H14.2_34	GTATCTGGTGGTCTATGGCCAAGAATCCATCATATCTCCAATCCCAAGCTTTTATTTACTCAGCATAGACGACGAAGAAC
NDM1-H14.2_35	GTATCTGGTGGTCTATGGCCACAACATGAATCCGTTTCTAATTCCTTTTACCTTTTCTCTCAGCATAGACGACGAAGAAC
NDM1-H14.2_38	GTATCTGGTGGTCTATGGCAAGGGCGTTCTTCATCGGTTCTTCTCACATTTTCCTCCCACCAGCATAGACGACGAAGAAC
NDM1-H14.2_39	GTATCTGGTGGTCTATGGCGGAGGTCTAAAAAAAAAAAAAACGCAATCCTATCTCATAATCCGCATAGACGACGAAGAAC
NDM1-H14.2_41	GTATCTGGTGGTCTATGGCGCTAGTTCTTCGCATCATTCCGCTTCCTTTCTTCTCCTTCTCCGCATAGACGACGAAGAAC
NDM1-H14.2_42	GTATCTGGTGGTCTATGGCATAGACGACGAAGAACACTACCCGCAAATTTTCACTGTAATCCGCATAGACGACGAAGAAC
NDM1-H14.2_43	GTATCTGGTGGTCTATGGCCGCTATCCGCAATCTGTCTCTTTTCTTTATTCTTTTACTCACCGCATAGACGACGAAGAAC
NDM1-H14.2_44	GTATCTGGTGGTCTATGGCATAGACGACGAAGAACATGAATGATCAACTAAGGGATAGCAATCTCGGCATAGACGACGAAGAAC
NDM1-H14.2_49	GTATCTGGTGGTCTATGGGCCCGGACTAAAAATCAAAATCATATCGACCGCAATCCCTTTCCGCATAGACGACGAAGAAC
NDM1-H14.2_50	GTATCTGGTGGTCTATGGCGCATCCCTATCCCGTCTCTTTTTGTATTTTTATTTTTGTTTCCGCATAGACGACGAAGAAC
Bio-NDM1-H14-01-FR	/5BiotinTEG/CGTCATAGGTACCATGGGGGACTGCTCGGGATTGCGGATTCATG
Bio-NDM1-H14-01	/5BiotinTEG/GTATCTGGTGGTCTATGGCGTCATAGGTACCATGGGGGACTGCTCGGGATTGCGGATTCATGGCATAGACGACGAAGAAC
Cy5-NDM1-H14-01	/5Cy5/GTATCTGGTGGTCTATGGCGTCATAGGTACCATGGGGGACTGCTCGGGATTGCGGATTCATGGCATAGACGACGAAGAAC
Bio-NDM1-H14.2_43	/5BiotinTEG/GTATCTGGTGGTCTATGGCCGCTATCCGCAATCTGTCTCTTTTCTTTATTCTTTTACTCACCGCATAGACGACGAAGAAC
Cy5-NDM1-H14.2_43	/5Cy5/GTATCTGGTGGTCTATGGCCGCTATCCGCAATCTGTCTCTTTTCTTTATTCTTTTACTCACCGCATAGACGACGAAGAAC
Cy5-Con1	/5Cy5/GGGAATTCGAGCTCGGTACCGGCTGCTTTGCTGCAGATTTGTGGGTGGGTGGGTGGTGATCTGCAGGCATGCAAGCTTGG
Bio-ConSc	/5BiotinTEG/TTATAACCGGTTATACTGGTTGTTCCTAGATGCTTCATGATGCCCAACCTTTGTCCCTGGCCCTGACATGTTTCGACTAA

8.3 Parameters of the SELEX for HMW-uPA

Appendix Table 1: Parameters of the SELEX for HMW-uPA

Selection Round	ssDNA [pmol]	Selection step		Pre-selection steps		Washing steps (number x duration [min])
		HMW-uPA [pmol]	SA-beads [µl]	uncoupled SA-beads (number x volume [µl])	Biotin coupled SA-beads (number x volume [µl])	
1	1600	200	200	-	-	3x 3
2	240	48	48	1x 48	-	4x 3
3	200	50	50	2x 50	-	6x 3, 1x 5, 1x 10
4	160	53	53	2x 106	-	6x 3, 1x 20, 1x 40
5	120	40	40	2x 80	-	6x 3, 1x 30, 1x 60
6	80			2x 80	1x 80	
7				3x 80	-	
8				3x80	1x 80	5x 3, 1x 15, 1x 30, 1x 60
9				4x 80	-	
10				4x 80	-	4x 3, 2x 15, 1x 30, 1x 60
11				4x 80	-	

8.4 Parameters of the SELEX for LMW-uPA

Appendix Table 2: Parameters of the SELEX for LMW-uPA

<table>
<tr><th rowspan="2">Selection Round</th><th rowspan="2">ssDNA [pmol]</th><th colspan="2">Selection step</th><th colspan="2">Pre-selection steps</th><th rowspan="2">Washing steps (number x duration [min])</th></tr>
<tr><th>LMW-uPA [pmol]</th><th>SA-beads [µl]</th><th>uncoupled SA-beads (number x volume [µl])</th><th>Biotin coupled SA-beads (number x volume [µl])</th></tr>
<tr><td>1</td><td>1600</td><td>200</td><td>120</td><td>-</td><td>-</td><td>3x 3</td></tr>
<tr><td>2</td><td>240</td><td>48</td><td>29</td><td>1x 29</td><td>-</td><td>4x 3</td></tr>
<tr><td>3</td><td>200</td><td>50</td><td>30</td><td>2x 30</td><td>-</td><td>6x 3, 1x 5, 1x 10</td></tr>
<tr><td>4</td><td>160</td><td>53</td><td>32</td><td>2x 64</td><td>-</td><td>6x 3, 1x 20, 1x 40</td></tr>
<tr><td>5</td><td>120</td><td rowspan="3">40</td><td rowspan="3">24</td><td>2x 48</td><td></td><td rowspan="3">6x 3, 1x 30, 1x 60</td></tr>
<tr><td>6</td><td rowspan="7">80</td><td>2x 48</td><td>1x 48</td></tr>
<tr><td>7</td><td>3x 48</td><td>-</td></tr>
<tr><td>8</td><td>46</td><td>30</td><td>3x 48</td><td>1x 48</td><td rowspan="2">5x 3, 1x 15, 1x 30, 1x 60</td></tr>
<tr><td>9</td><td rowspan="4">40</td><td rowspan="4">24</td><td>4x 48</td><td>-</td></tr>
<tr><td>10</td><td>4x 48</td><td>-</td><td rowspan="3">4x 3, 2x 15, 1x 30, 1x 60</td></tr>
<tr><td>11</td><td>4x 48</td><td>-</td></tr>
<tr><td>12</td><td>4x 48</td><td>-</td></tr>
</table>

8.5 Overview of the Different Sandwich Assay Combinations for Detection of HMW- and/or LMW-uPA

Appendix Table 3: Overview of different sandwich assays formats for detection and discrimination of HMW- and LMW-uPA

Sandwich Assay Format	Capture molecule*	Detection molecule**	Capable to detect HMW uPA	Capable to detect LMW-uPA
Aptamer-Target-Aptamer	uPAapt-08	uPAapt-02	+	-
Aptamer-Target-Aptamer	uPAapt-21		+	-
Aptamer-Target-Aptamer	uPAapt-08-FR	uPAapt-02-FR	+	-
Aptamer-Target-Aptamer	uPAapt-01	uPAapt-21	+	-
Aptamer-Target-Aptamer	uPAapt-02		+	-
Aptamer-Target-Aptamer	uPAapt-02-F		+	-
Aptamer-Target-Aptamer	uPAapt-02-R		+	-
Aptamer-Target-Aptamer	uPAapt-02-FR		+	-
Aptamer-Target-Antibody	uPAapt-01	Ab Chain A	+	-
Aptamer-Target-Antibody	uPAapt-02		+	-
Aptamer-Target-Antibody	uPAapt-03		+	-
Aptamer-Target-Antibody	uPAapt-06		+	-
Aptamer-Target-Antibody	uPAapt-08		+	-
Aptamer-Target-Antibody	uPAapt-21		+	-
Aptamer-Target-Antibody	uPAapt-26		+	-
Aptamer-Target-Antibody	uPAapt-27		+	-
Aptamer-Target-Antibody	uPAapt-01-FR		+	-
Aptamer-Target-Antibody	uPAapt-02-F		+	-
Aptamer-Target-Antibody	uPAapt-02-R		+	-
Aptamer-Target-Antibody	uPAapt-02-FR		+	-
Aptamer-Target-Antibody	uPAapt-08-F		+	-

Sandwich Assay Format	Capture molecule*	Detection molecule**	Capable to detect HMW uPA	Capable to detect LMW-uPA
Aptamer-Target-Antibody	uPAapt-08-FR	Ab Chain A	+	-
Aptamer-Target-Antibody	uPAapt-27-FR		+	-
Aptamer-Target-Antibody	uPAapt-01	Ab Chain B	+	-
Aptamer-Target-Antibody	uPAapt-02		+	+
Aptamer-Target-Antibody	uPAapt-03		+	+
Aptamer-Target-Antibody	uPAapt-06		+	+
Aptamer-Target-Antibody	uPAapt-08		+	-
Aptamer-Target-Antibody	uPAapt-21		+	-
Aptamer-Target-Antibody	uPAapt-26		+	+
Aptamer-Target-Antibody	uPAapt-27		+	+
Aptamer-Target-Antibody	uPAapt-01-FR		+	-
Aptamer-Target-Antibody	uPAapt-02-F		+	+
Aptamer-Target-Antibody	uPAapt-02-R		+	+
Aptamer-Target-Antibody	uPAapt-02-FR		+	+
Aptamer-Target-Antibody	uPAapt-08-F		+	-
Aptamer-Target-Antibody	uPAapt-08-FR		+	-
Aptamer-Target-Antibody	uPAapt-27-FR		+	+
Antibody-Target-Aptamer	Ab Chain A	uPAapt-02	+	-
Antibody-Target-Aptamer		uPAapt-02-FR	+	-
Antibody-Target-Aptamer		uPAapt-21	+	-
Antibody-Target-Aptamer	Ab Chain B	uPAapt-02	+	+
Antibody-Target-Aptamer		uPAapt-02-FR	+	+
Antibody-Target-Aptamer		uPAapt-21	+	-

+ = binding detected; - = no binding detected

* In case of aptamers as a capture molecule capture via 5'-biotin modification on streptavidin-coated microtiter plates, in case of antibodies as a capture molecule capture directly on polystyrene microtiter plate

** In case of aptamers as a detection molecule detection via 5'-Cy5 modification, in case of antibodies as a detection molecule detection via secondary polyclonal sheep anti-mouse IgG antibody labeled with HRP antibody anti-PLAU antibody is capable to bind to the A chain of HMW-uPA, anti uPA antibody is capable to bind the B chain of HMW-uPA and LMW-uPA

8.6 Individual Author Contributions to the Publications

The individual contributions of the authors to the manuscripts can be assigned according to the Contributor Roles Taxonomy (CRediT) as follows:

Manuscript I

Inhibition of Human Urokinase-Type Plasminogen Activator (uPA) Enzyme Activity and Receptor Binding by DNA Aptamers as Potential Therapeutics through Binding to the Different Forms of uPA

Conceptualization, **N.D.** and M.M.M.; validation, **N.D.**, J.W., W.S. and A.M.; formal analysis, **N.D.**; investigation, **N.D.**, J.W., W.S., A.M. and D.V.V.; writing—original draft preparation, **N.D.**; writing—review and editing, **N.D.**, W.S., A.M., D.C., S.F. and M.M.M.; visualization, **N.D.**; supervision, M.M.M.; project administration, M.M.M.; funding acquisition, S.F. and M.M.M.

Manuscript II

Label-Free Determination of the Kinetic Parameters of Protein-Aptamer Interaction by Surface Plasmon Resonance

Conceptualization, **N.D.** and M.M.M.; investigation, **N.D.** and A.M.; methodology, **N.D.** and A.M.; formal analysis, **N.D.**; writing—original draft preparation, **N.D.**; writing—review and editing, **N.D.**, A.M. and M.M.M.; visualization, **N.D.**; supervision, M.M.M.; project administration, M.M.M.; funding acquisition, M.M.M.

Manuscript III

Aptamer-based Sandwich Assay Formats for Detection and Discrimination of Human High- and Low-Molecular-Weight uPA for Cancer Prognosis and Diagnosis

Conceptualization, **N.D.** and M.M.M.; methodology, **N.D.**; validation, **N.D.**, W.S. and J.D.; formal analysis, **N.D.**; investigation, **N.D.**, W.S., and J.D.; writing—original draft preparation, **N.D.**; writing—review and editing, **N.D.**, W.S., J.D. and M.M.M.; visualization, **N.D.**; supervision, M.M.M.; project administration, M.M.M.; funding acquisition, M.M.M.

Manuscript IV

The use of high-affinity polyhistidine binders as masking probes for the selection of an NDM-1 specific aptamer

Conceptualization, W.S. and M.M.M.; validation, W.S., **N.D.**, and A.M.; formal analysis, W.S. and **N.D.**; investigation, W.S., **N.D.**, A.M. and D.C.; writing—original draft preparation, W.S.; writing—review and editing, W.S., **N.D.**, A.M., D.C., P.P.A., D.T. and M.M.M.; visualization, W.S.; supervision, M.M.M.; project administration, M.M.M.; funding acquisition, D.T. and M.M.M.

8.7 Patent Descriptions

8.7.1 DNA Aptamers and their use in (pre)diagnosis of cancer

Abstract

The present invention relates in a first aspect to a DNA aptamer selected from the group consisting of

A) a polynucleotide comprising a first nucleotide sequence having at least 70% identity to a sequence selected from the group consisting of SEQ ID NO:1 to SEQ ID NO:8, and
B) a polynucleotide comprising a first nucleotide sequence having at least 70 % identity to a sequence selected from the group consisting of SEQ ID NO:1 to SEQ ID NO: 8, a second nucleotide sequence, which is at least 70% identical to SEQ ID NO:9, and/or a third nucleotide sequence, which is at least 70% identical to SEQ ID NO:10.

In a second aspect, the invention is related to an *in vitro* method for pre-diagnosing or diagnosing in a subject cancer, the method comprising the step of detecting the binding of an aptamer according to the first aspect in a sample of said subject. The *in vitro* method is also of use for discriminating in a sample between high molecular weight uPA (HMW-uPA) and low molecular weight uPA (LMW-uPA).

A third aspect of the invention is directed to a kit comprising a DNA aptamer according to the first aspect comprised in a housing.

Patentsteckbrief: 2021F64339 (F64339) IZI-BB 10.01.2023

Organistationseinheit: 375 IZI-BB

Erfinder: Dreymann, Nico [redacted]; Menger, Marcus [redacted]; Wünsche, Julia [redacted]

Erfindungstitel: DNA-Aptamers against human Urokinase-Typ Plasminogen Aktivator (uPA)

Anmeldetitel: DNA Aptamers and their use in (pre)diagnosis of cancer

Anmelder: Fraunhofer-Gesellschaft zur Förderung der angewandten Forschung e.V.

Patentanwalt: Altmann Stößel Dick Patentanwälte PartG mbB (Berlin)

Priorität: 03.09.2021 **IPC-Hauptklasse:**

Abstract:

Art	Land	Anmelde Tag	Anmelde Nr.	Erteilung am	Patent Nr.	geschlossen/ Erlöschensdatum
P	EP	03.09.2021	21194714.8			
P	WO	02.09.2022	PCT/EP2022/074491			

8.7.2 DNA aptamers inhibiting binding of Urokinase type plasminogen activator (uPA) with Urokinase type plasminogen activator receptor (uPAR) and inhibiting uPA activity

Abstract

In a first aspect, the invention relates to a DNA aptamer comprising a polynucleotide sequence having at least 70% identity to a sequence selected from the group consisting of SEQ ID NO:1, SEQ ID NO:2, SEQ ID NO:3, SEQ ID NO:4, SEQ ID NO:5, SEQ ID NO:6, SEQ ID NO:7, SEQ ID NO:8, SEQ ID NO:9, SEQ ID NO:10 and SEQ ID NO:11 for use as a medicament, especially for use in treatment of cancer and/or prevention of cancer in a subject. The DNA aptamers are able to inhibit binding of Urokinase type plasminogen activator (uPA) with Urokinase type plasminogen activator receptor (uPAR) and are also able to inhibit activity of Urokinase type plasminogen activator (uPA). A second aspect of the invention relates to the DNA aptamer, used according to the first aspect, itself. A third aspect of the invention is related to a method for identifying a subject benefiting from cancer treatment with a DNA aptamer according to the first aspect and of the second aspect respectively. In a fourth aspect, the invention relates to a kit comprising a DNA aptamer according to the first aspect and of the second aspect respectively.

Patentsteckbrief: 2021F64442 (F64442) IZI-BB 10.01.2023

Organistationseinheit: 375 IZI-BB

Erfinder: Dreymann, Nico [redacted]; Menger, Marcus [redacted]; Wünsche, Julia [redacted]

Erfindungstitel: DNA-Aptamers agajnst human Urokjnase-Typ Plasmjnogen Aktivator (uPA) as potential therapeutic agents

Anmeldetitel: DNA aptamers inhibiting binding of Urokinase type plasminogen activator (uPA) with Urokinase
type plasminogen activator receptor (uPAR) and inhibiting uPA activity

Anmelder: Fraunhofer-Gesellschaft zur Förderung der angewandten Forschung e.V.

Patentanwalt: Altmann Stößel Dick Patentanwälte PartG mbB (Berlin)

Priorität: 09.12.2021 **IPC-Hauptklasse:**

Abstract:

Art	Land	Anmelde Tag	Anmelde Nr.	Erteilung am	Patent Nr.	geschlossen/ Erlöschensdatum
P	EP	09.12.2021	EP21213412.6			
P	WO	08.12.2022	PCT/EP2022/084996			